Conceptual Design of Oxygen-Based PC Boiler

Final Report

Andrew Seltzer
Zhen Fan

September 2005

DE-FC26-03NT41736

Foster Wheeler Power Group, Inc.
12 Peach Tree Hill Road
Livingston, New Jersey 07039

DISCLAIMER

This report was prepared as an account of work sponsored by an agency of the United States Government. Neither the United States Government nor any agency thereof, nor any of their employees, makes any warranty, express or implied, or assumes any legal liability or responsibility for the accuracy, completeness, or usefulness of any information, apparatus, product, or process disclosed, or represents that its use would not infringe privately owned rights. Reference herein to any specific commercial product, process, or service by trade name, trademark, manufacturer, or otherwise does not necessarily constitute or imply its endorsement, recommendation, or favoring by the United States Government or any agency thereof. The views and opinions of authors expressed herein do not necessarily state or reflect those of the United States Government or any agency thereof.

ABSTRACT

Coal is presently the world's primary fuel for generating electrical power and, being more abundant and less expensive than oil or natural gas, is expected to continue its dominance into the future. Coal, however, is more carbon intensive than natural gas and oil and consequently coal-fired power plants are large point source emitters of carbon dioxide (CO_2). Since CO_2 is a greenhouse gas, which may have an adverse impact on the world's climate/weather patterns, studies have been conducted to determine the feasibility and economic impact of capturing power plant CO_2 emissions for pipeline transport to a sequestration/storage site.

The stack gas that exhausts from a modern coal-fired power plant typically contains about 15 per cent CO_2 on a dry volume basis. Although there are numerous processes available for removing CO_2 from gas streams, gas scrubbing with amine solvent is best suited for this application because of the large gas volumes and low CO_2 concentrations involved. Unfortunately the energy required to regenerate the solvent for continued use as a capturing agent is large and imposes a severe energy penalty on the plant. In addition this "back end" or post combustion cleanup requires the addition of large vessels, which, in retrofit applications, are difficult to accommodate.

As an alternative to post combustion scrubbing, Foster Wheeler (FW) has proposed that the combustion process be accomplished with oxygen rather than air. With all air nitrogen eliminated, a CO_2-water vapor rich flue gas will be generated. After condensation of the water vapor, a portion of the flue gas will be recirculated back to the boiler to control the combustion temperature and the balance of the CO_2 will be processed for pipeline transport. This proposed oxygen-carbon dioxide (O_2/CO_2) combustion process eliminates the need for CO_2 removal/separation and reduces the cost of supplying a CO_2 rich stream for sequestration.

Under DOE Contract No DE-FC26-03NT41736 FW has developed a conceptual design of an O_2 fired boiler to determine overall plant performance and economics. Five subtasks were conducted: 1) a literature review, 2) a system design and analysis, 3) a low NOx burner design and analysis, 4) a furnace and heat recovery area design analysis, and 5) an economic analysis.

The objective of the literature search is to locate any data/information relevant to the Oxygen-Based PC Boiler conceptual design.

The objective of the system design and analysis task is to optimize the PC boiler plant by maximizing system efficiency within practical considerations. Simulations of the oxygen-fired plant with CO_2 sequestration were conducted using Aspen Plus and were compared to a reference air-fired 460 MW plant. Flue gas recycle is used in the O_2-fired PC to control the flame temperature. Parametric runs were made to determine the effect of flame temperature on system efficiency and required waterwall material and thickness. The degree of improvement on system efficiency of various modifications including hot gas recycle, purge gas recycle, flue gas feedwater recuperation, and

recycle purge gas expansion were investigated. The selected O_2-fired design case has a system efficiency of 30.6% compared to the air-fired system efficiency of 36.7%. The design O_2-fired case requires T91 waterwall material and has a waterwall surface area of only 65% of the air-fired reference case.

The objective of the low NOx burner design and analysis task is to optimize the burner design to ensure stable ignition, to provide safe operation, and to minimize pollutant formation. The burners were designed and analyzed using the Fluent CFD computer program. Four burner designs were developed: 1) with no OFG and 65% flue gas recycle, 2) with 20% OFG and 65% flue gas recycle, 3) with no OFG and 56% flue gas recycle and 4) with 20% OFG and 56% flue gas recycle. A 3-D Fluent simulation was made of a single wall-fired burner and horizontal portion of the furnace from the wall to the center. Without primary gas swirl, coal burnout was relatively small, due to the low oxygen content of the primary gas. Consequently, the burners were modified to include primary gas swirl to bring the coal particles in contact with the secondary gas. An optimal primary gas swirl was chosen to achieve sufficient burnout.

The objective of the furnace and heat recovery area design and analysis task is to optimize the location and design of the furnace, burners, over-fire gas ports, and internal radiant surfaces. The furnace is designed with opposed wall-firing burners and over-fire air ports. Water is circulated in the furnace by natural circulation to the waterwalls and divisional wall panels. Compared to the air-fired furnace, the oxygen-fired furnace requires only 65% of the surface area and 45% of the volume. Two oxygen-fired designs were simulated: 1) without over-fire air and 2) with 20% over-fire air. The maximum wall heat flux in the oxygen-fired furnace is more than double that of the air-fired furnace due to the higher flame temperature and higher H_2O and CO_2 concentrations. The coal burnout for the oxygen-fired case is 100% due to a 500°F higher furnace temperature and higher concentration of O_2. Because of the higher furnace wall temperature of the oxygen-fired case compared to the air-fired case, furnace water wall material was upgraded from carbon steel to T91. The total heat transfer surface required in the oxygen-fired heat recovery area is 25% less than the air-fired HRA due to more heat being absorbed in the oxygen-fired furnace and the greater molecular weight of the oxygen-fired flue gas.

The objective of the economic analysis is to prepare a budgetary estimate of capital and operating costs of the O_2-fired PC power plant as well as for the equivalent conventional PC-fired power plant. Capital and operating costs of conventional steam generation, steam heating, and power generation equipment are estimated based on Foster Wheeler's experience and database. Capital and operating costs of equipment, such as oxygen separation and CO_2 liquefaction, are based on vendor supplied data and FW process plant experience. The levelized cost of electricity is determined for both the air-fired and O_2-fired power plants as well as the CO_2 mitigation cost. An economic comparison between the O_2-fired PC and other alternate technologies is presented. The levelized COE was calculated to be 4.61 ¢/kWh for the reference air-fired plant and 6.41¢/kWh for the O_2 PC plant. The CO_2 mitigation cost of the O_2-PC plant was calculated at 21.4 $/tonne.

Table of Contents

ABSTRACT 3
1.0 Introduction 11
2.0 Executive Summary 14
3.0 Experimental 21
4.0 Results and Discussion 22
4.1 Literature Review 22
4.1.1 Combustion With Partial Oxygen Enhancement 22
4.1.2 O_2/CO_2 Combustion 25
4.1.3 Impact of CO_2 Removal on New Plants 32
4.1.3.1 International Energy Agency Study 32
4.1.3.2 Parsons Study 35
4.1.3.3 American Air Liquide Study 40
4.1.3.4 Summary of New Plant Studies 42
4.1.4 Impact of CO_2 Removal On Existing Plants 44
4.1.5 Oxygen Supply Systems 45
4.2 System Design and Analysis 47
4.2.1 Reference Site and Fuel Conditions 47
4.2.2 Air-Fired Reference Case 47
4.2.3 Oxygen-Based PC Plant 49
4.2.3.1 Boiler Plant Modifications 49
4.2.3.2 Air Separation Unit 49
4.2.4 Parametric Cases 50
4.2.5 Hot Recycle 51
4.2.6 CO_2 Compression 52
4.2.7 Vent Gas Recycle 53
4.2.8 Case 12 54
4.2.9 Design Case: Case 13 55
4.2.10 Furnace Waterwall Temperature 55
4.2.11 Comparison With Post CO_2 Capture 57
4.3 Low NOx Burner Design and Analysis 93
4.3.1 Model Geometry 93
4.3.2 Sub Models 93
4.3.3 Boundary Conditions 93
4.3.4 65% Recycle Case With No OFG 94
4.3.4.1 No Primary Gas Swirl 94
4.3.4.2 Primary Gas Swirl Ratio = 0.5 94
4.3.5 65% Recycle Case With 20% OFG 94
4.3.5.1 No Primary Gas Swirl 95
4.3.5.2 Primary Gas Swirl Ratio = 0.5 95
4.3.6 56% Recycle Case With No OFG 95
4.3.6.1 No Primary Gas Swirl 95
4.3.6.2 Primary Gas Swirl Ratio = 0.5 95
4.3.7 56% Recycle Case With 20% OFG 96
4.3.7.1 No Primary Gas Swirl 96

4.3.7.2 Primary Gas Swirl Ratio = 0.5 96
4.4 Furnace and HRA Design and Analysis 144
4.4.1 Furnace Design and Analysis 144
4.4.1.1 FW-FIRE Computer Program Description 144
4.4.1.2 Model Geometry 145
4.4.1.3 Boundary Conditions 146
4.4.1.4 Air-Fired Reference Case 146
4.4.1.5 Oxygen-Fired Design Case 147
4.4.1.5.1 No OFG Case 148
4.4.1.5.2 20% OFG Case 149
4.4.2 Heat Recovery Area Design and Analysis 150
4.4.2.1 HEATEX Program Description 150
4.4.2.2 Air-Fired Reference Case 150
4.4.2.3 Oxygen-Fired Case 150
4.5 Economic Analysis 190
4.5.1 Main Assumptions 190
4.5.2 Plant Cost Basis 190
4.5.3 Total Plant Investment (TPI) 193
4.5.4 Total Capital Requirement (TCR) 193
4.5.5 Operating Costs And Expenses 194
4.5.6 Cost Of Electricity (COE) 195
4.5.7 Comparison with Other Technologies 196
5.0 Conclusion 205
6.0 References 209
7.0 Bibliography 212
8.0 List of Acronyms and Abbreviations 213

LIST OF GRAPHICAL MATERIALS

Tables

Table 4.1.1 CANMET Burner Operating Conditions 28
Table 4.1.2 CANMET Burner Test Flow Rates 28
Table 4.1.3 CANMET Burner Performance 29
Table 4.1.4 Performance of Nominal 500 MWe Power Generating Technologies 34
Table 4.1.5 Effect of CO_2 Capture Technologies on a Nominal 500 MWe PC Fired Plant 35
Table 4.1.6 Effect of CO_2 Absorption on Alternative Power Generating Technologies.. 35
Table 4.1.7 Illinois No 6 Coal Analysis 36
Table 4.1.8 Natural Gas Analysis 37
Table 4.1.9 NGCC and Illinois No 6 PC Plants Without CO_2 Capture 38
Table 4.1.10 NGCC and Illinois No 6 PC Plants with 90 Per Cent CO_2 Capture 39
Table 4.1.11 PRB Fueled PC Plant Performance With and Without CO_2 Capture 41
Table 4.1.12 Summary of Plant CO_2 Removal Studies 43
Table 4.1.13 CO_2 Removal Incorporated Into An Existing PC Plant 45
Table 4.2.1 – Site Conditions and Coal Properties 59
Table 4.2.2 – Case 1 (Air-Fired Reference) Boundary Conditions and Results 61
Table 4.2.3 – Auxiliary Power Requirements for Case 1 62
Table 4.2.4 – Parametric Cases Summary (Without CO_2 Compression) 71
Table 4.2.5 – Parametric Cases Summary (With CO_2 Compression) 82
Table 4.2.6 – Radiation Heat Flux and Water Wall Temperature 86
Table 4.3.1 – Coal Properties 99
Table 4.3.2 –Model Boundary Conditions 100
Table 4.3.3 – Summary of Fluent Burner Modeling Results 101
Table 4.4.1 – Air-Fired Boundary Conditions 155
Table 4.4.2 – Oxygen-Fired Boundary Conditions 156
Table 4.4.3 – Summary of FW-FIRE Furnace Modeling Results 158
Table 4.4.4 – HRA Tube Bank Design 188
Table 4.4.5 – HRA Tube Bank Performance 189
Table 4.5.1 – Oxygen-Fired PC Plant Capital Cost Estimate 192
Table 4.5.2 - Operating, Maintenance and Fuel Costs for the O_2 PC and the Air-fired Reference 198
Table 4.5.3 - Estimate Basis/Financial Criteria for Revenue Requirement Calculations: Air-fired Reference Plant 199
Table 4.5.4 - Estimate Basis/Financial Criteria for Revenue Requirement Calculations: O_2-fired Reference Plant 200
Table 4.5.5 - Capital Investment and Revenue Requirement Summary: Air-fired Reference Plant 201
Table 4.5.6 - Capital Investment and Revenue Requirement Summary: O_2-fired Plant 202

Figures

Figure 4.1.1 Effect of OEC on Class C Bituminous Coal NOx Emissions 24
Figure 4.1.2 Effect of OEC on Class A Bituminous Coal NOx Emissions..... 24
Figure 4.1.3 Effect of Oxygen Ratio on Burner Combustion Efficiency 26
Figure 4.1.4 Effect of Primary to Secondary O_2 Ratio on Burner Combustion Efficiency 26
Figure 4.1.5 CANMET Burner 27
Figure 4.1.6 Centerline Temperatures Downstream of Burner..... 30
Figure 4.1.7 Centerline NOx Emission Rates..... 30
Figure 4.1.8 Centerline SO_2 Emission Rates 31
Figure 4.1.9 PRB Fired PC Plant Capital Costs With and Without CO_2 Capture..... 42
Figure 4.1.10 PRB Fired PC Plant COE and CO_2 Avoided Costs 42
Figure 4.2.1 – Cycle Analysis of Case 1 (Air-Fired Reference Case)..... 60
Figure 4.2.2 – Air Separation Unit 63
Figure 4.2.3 – ASPEN ASU Model..... 64
Figure 4.2.4 – Case 2 Cycle Diagram 65
Figure 4.2.5 – Case 3 Cycle Diagram 66
Figure 4.2.6 – Case 4 Cycle Diagram 67
Figure 4.2.7 – Case 5 Cycle Diagram 68
Figure 4.2.8 – Case 6 Cycle Diagram 69
Figure 4.2.9 – Case 7 Cycle Diagram 70
Figure 4.2.10 – Net Efficiency (without CO_2 compression) Versus Adiabatic Temperature 72
Figure 4.2.11 - ASU and Auxiliary Power Requirements Versus Adiabatic Temperature 73
Figure 4.2.12 – Recycled Gas Mass Flow Rate Versus Adiabatic Temperature 74
Figure 4.2.13 – Recycled Gas Volumetric Flow Rate Versus Adiabatic Temperature... 75
Figure 4.2.14 – Flue Gas Cooling Curve 76
Figure 4.2.15 – Case 8 Cycle Diagram 77
Figure 4.2.16 – Case 9 Cycle Diagram 78
Figure 4.2.17 – Net Cycle Efficiency Vs. Flue Gas Recycle Flow 79
Figure 4.2.18 – Case 10 Cycle Diagram 80
Figure 4.2.19 – Case 11 Cycle Diagram 81
Figure 4.2.20 – Vapor Pressure of CO_2..... 83
Figure 4.2.21 – Equilibrium CO and CO2 Versus Flue Gas Recycle Flow 84
Figure 4.2.22 – Adiabatic and Equilibrium Temperatures Versus Flue Gas Recycle Flow 85
Figure 4.2.23 – Case 12 Cycle Diagram 87
Figure 4.2.24 – Wet End Economizer Temperature Vs. Heat Duty 88
Figure 4.2.25 – Case 13 Cycle Diagram 89
Figure 4.2.26 – Efficiency of Saved Extraction Steam Versus Stage 90
Figure 4.2.27 – Comparison of Power Consumption of CO_2 Removal of Different Technologies..... 91
Figure 4.2.28 – Comparison of Overall Cycle Efficiency Point of CO_2 Removal of Different Technologies 92

Figure 4.3.1 – Oxygen-Fired Burner Geometry 97
Figure 4.3.2 – Computational Model of Oxygen-Fired Burner 98
Figure 4.3.3 – Burnout and NOx/burnout vs. Primary gas Swirl for 65% Recycle, No OFG 102
Figure 4.3.4 – Gas Velocity for 65% Recycle, No OFG, 0.0 PG Swirl 103
Figure 4.3.5 – Gas Temperature for 65% Recycle, No OFG, 0.0 PG Swirl 104
Figure 4.3.6 – O_2 Mole Fraction for 65% Recycle, No OFG, 0.0 PG Swirl 105
Figure 4.3.7 – Burnout of 69μ Particles for 65% Recycle, No OFG, 0.0 PG Swirl..... 106
Figure 4.3.8 – Burnout of 169μ Particles for 65% Recycle, No OFG, 0 PG Swirl..... 107
Figure 4.3.9 – Gas Velocity for 65% Recycle, No OFG, 0.5 PG Swirl 108
Figure 4.3.10 – Gas Temperature for 65% Recycle, No OFG, 0.5 PG Swirl 109
Figure 4.3.11 – O_2 Mole Fraction for 65% Recycle, No OFG, 0.5 PG Swirl 110
Figure 4.3.12 – Velocity Vectors Colored by Axial Velocity (ft/sec) for 65% Recycle, No OFG, 0.5 PG Swirl 111
Figure 4.3.13 – Burnout of 69μ Particles for 65% Recycle, No OFG, 0.0 PG Swirl..... 112
Figure 4.3.14 – Burnout of 169μ Particles for 65% Recycle, No OFG, 0 PG Swirl..... 113
Figure 4.3.15 – Gas Velocity for 65% Recycle, 20% OFG, 0.0 PG Swirl 114
Figure 4.3.16 – Gas Temperature for 65% Recycle, 20% OFG, 0.0 PG Swirl 115
Figure 4.3.17 – O2 Mole Fraction for 65% Recycle, 20% OFG, 0.0PG Swirl 116
Figure 4.3.18 – Burnout of 69μ Particles for 65% Recycle, 20% OFG, 0 PG Swirl 117
Figure 4.3.19 – Burnout of 169μ Particles for 65% Recycle, 20% OFG, 0 PG Swirl ... 118
Figure 4.3.20 – Gas Velocity for 65% Recycle, 20% OFG, 0.5 PG Swirl 119
Figure 4.3.21 – Gas Temperature for 65% Recycle, 20% OFG, 0.5 PG Swirl 120
Figure 4.3.22 – O2 Mole Fraction for 65% Recycle, 20% OFG, 0.5 PG Swirl 121
Figure 4.3.23 – Burnout of 69μ Particles for 65% Recycle, 20% OFG, 0.5 PG Swirl .. 122
Figure 4.3.24 – Burnout of 169μ Particles for 65% Recycle, 20% OFG, 0.5 PG Swirl 123
Figure 4.3.25 – Gas Velocity for 56% Recycle, 0% OFG, 0.0 PG Swirl 124
Figure 4.3.26 – Gas Temperature for 56% Recycle, 0% OFG, 0.0 PG Swirl 125
Figure 4.3.27 – O2 Mole Fraction for 56% Recycle, 0% OFG, 0.0 PG Swirl 126
Figure 4.3.28 – Burnout of 69μ Particles for 56% Recycle, 0% OFG, 0 PG Swirl 127
Figure 4.3.29 – Burnout of 169μ Particles for 56% Recycle, 0% OFG, 0 PG Swirl 128
Figure 4.3.30 – Gas Velocity for 56% Recycle, 0% OFG, 0.5 PG Swirl 129
Figure 4.3.31 – Gas Temperature for 56% Recycle, 0% OFG, 0.5 PG Swirl 130
Figure 4.3.32 – O2 Mole Fraction for 56% Recycle, 0% OFG, 0.5 PG Swirl 131
Figure 4.3.33 – Burnout of 69μ Particles for 56% Recycle, 0% OFG, 0.5 PG Swirl 132
Figure 4.3.34 – Burnout of 169μ Particles for 56% Recycle, 0% OFG, 0.5 PG Swirl .. 133
Figure 4.3.35 – Gas Velocity for 56% Recycle, 20% OFG, 0. PG Swirl 134
Figure 4.3.36 – Gas Temperature for 56% Recycle, 20% OFG, 0. PG Swirl 135
Figure 4.3.37 – O2 Mole Fraction for 56% Recycle, 20% OFG, 0. PG Swirl 136
Figure 4.3.38 – Burnout of 69μ Particles for 56% Recycle, 20% OFG, 0. PG Swirl 137
Figure 4.3.39 – Burnout of 169μ Particles for 56% Recycle, 20% OFG, 0. PG Swirl .. 138
Figure 4.3.40 – Gas Velocity for 56% Recycle, 20% OFG, 0.5 PG Swirl 139
Figure 4.3.41 – Gas Temperature for 56% Recycle, 20% OFG, 0.5 PG Swirl 140
Figure 4.3.42 – O2 Mole Fraction for 56% Recycle, 20% OFG, 0.5 PG Swirl 141
Figure 4.3.43 – Burnout of 69μ Particles for 56% Recycle, 20% OFG, 0.5 PG Swirl .. 142
Figure 4.3.44 – Burnout of 169μ Particles for 56% Recycle, 20% OFG, 0.5 PG Swirl 143

Figure 4.4.1– Computational Model of Air-Fired Furnace (with right side wall removed) 152
Figure 4.4.2 – Computational Model of Oxygen-Fired Furnace Without OFG 153
Figure 4.4.3 – Computational Model of Oxygen-Fired Furnace With OFG 154
Figure 4.4.4 – Air-Fired Boiler Design 157
Figure 4.4.5 – Gas Velocity for Air-Fired Case 159
Figure 4.4.6 – Gas Temperature for Air-Fired Case 160
Figure 4.4.7 – O_2 Mole Fraction for Air-Fired Case 161
Figure 4.4.8 – Wall Heat Flux for Air-Fired Case 162
Figure 4.4.9 – Wall Temperature for Air-Fired Case 163
Figure 4.4.10 – Wall CO for Air-Fired Case 164
Figure 4.4.11 – Char Mass Fraction (72 microns) for Air-Fired Case 165
Figure 4.4.12 – Char Mass Fraction (176 microns) for Air-Fired Case 166
Figure 4.4.13 – Outlet NOx Versus OFA Flow Rate for Air-Fired Furnace 167
Figure 4.4.14 – Coal Burnout Versus OFA Flow Rate for Air-Fired Furnace 167
Figure 4.4.15 – Air-Fired and Oxygen-Fired Boiler Outlines 168
Figure 4.4.16 – Oxygen-Fired Boiler Design 169
Figure 4.4.17 – Gas Velocity for O_2-Fired Case Without OFG 170
Figure 4.4.18 – Gas Temperature for O_2-Fired Case Without OFG 171
Figure 4.4.19 – O_2 Mole Fraction for O_2-Fired Case Without OFG 172
Figure 4.4.20 – Wall Heat Flux for O_2-Fired Case Without OFG 173
Figure 4.4.21 – Wall Temperature for O_2-Fired Case Without OFG 174
Figure 4.4.22 – Wall CO for O_2-Fired Case Without OFG 175
Figure 4.4.23 – Char Mass Fraction (69 micron) for O_2-Fired Case, No OFG 176
Figure 4.4.24 – Char Mass Fraction (169 micron) for O_2-Fired Case, No OFG 177
Figure 4.4.25 – Char Mass Fraction (169 micron) for O_2-Fired Case, No OFG, Without Primary gas Swirl 178
Figure 4.4.26 – Gas Velocity for O_2-Fired Case With 20% OFG 179
Figure 4.4.27 – Gas Temperature for O_2-Fired Case With 20% OFG 180
Figure 4.4.28 – O_2 Mole Fraction for O_2-Fired Case With 20% OFG 181
Figure 4.4.29 – Wall Heat Flux for O_2-Fired Case With 20% OFG 182
Figure 4.4.30 – Wall Temperature for O_2-Fired Case With 20% OFG 183
Figure 4.4.31 – Wall CO for O_2-Fired Case With 20% OFG 184
Figure 4.4.32 – Char Mass Fraction (69 micron) for O_2-Fired Case, 20% OFG 185
Figure 4.4.33 – Char Mass Fraction (169 micron) for O_2-Fired Case, 20% OFG 186
Figure 4.4.34 – Char Mass Fraction (169 micron) for O_2-Fired Case, 20% OFG, Without Primary gas Swirl 187
Figure 4.5.1- Comparison of Levelized Cost of Electricity Among Alternative Technologies (O_2 PC with 65% CF) 203
Figure 4.5.2 - Comparison of Mitigation Costs Among Alternative Technologies (O_2 PC with 65% CF) 203
Figure 4.5.3 - Comparison of Levelized Cost of Electricity Among Alternative Technologies (O_2 PC with 85% CF) 204
Figure 4.5.4 - Comparison of Mitigation Costs Among Alternative Technologies (O_2 PC with 85% CF) 204

1.0 Introduction

The carbon dioxide (CO_2) content of the earth's atmosphere has increased by approximately 35 per cent since the early 1800s [1]. In the last 50 years, however, the rate of accumulation of CO_2 has increased relatively rapidly going from about 310 ppmv in 1950 to about 370 ppmv in 2000. Since CO_2 is a greenhouse gas, there is increasing concern that its accumulation in the atmosphere will adversely impact the world's climate/weather patterns. Desiring that actions be taken, representatives from more than 160 countries met in Kyoto Japan in December 1997 and established goals for reducing greenhouse gas emissions.

Coal is presently the world's primary fuel for generating electrical power. In 2001 coal generated approximately 39 per cent of the world's electricity compared with 18 and 8 per cent for natural gas and oil, respectively [2]. Compared with natural gas and oil, coal also represents the world's largest reserve of energy and those reserves are more widely distributed throughout the world. Unfortunately coal is also the more carbon intensive fuel releasing roughly 70 and 30 per cent more CO_2 per unit of heat release than natural gas and oil respectively.

In the United States (U.S.) coal generates more than half of the nation's electric power (approximately 55 per cent in 2002 [3]); it is much less expensive than oil or natural gas and domestic reserves are large enough to meet the nation's energy needs for the next 300 years. Because of its relatively low cost and strategic security, coal is expected to continue to be a major source of future U.S. electric power generation; it is estimated that it will also generate approximately 55 per cent of the nation's power in 2025 [3]. To address growing CO_2 greenhouse gas concerns several states have passed legislation requiring their electric utilities to reduce CO_2 emissions; New Hampshire is requiring generators to reduce their CO_2 emissions to 1990 values by 2010, Massachusetts is requiring their six largest generators to reduce CO_2 emission rates to 1,800 lbs/MWh by 2006, etc. [4]. As a result advanced concepts are being proposed and studies undertaken to determine the performance and economic impacts of capturing power plant CO_2 emissions for sequestration/storage. The captured CO_2 could be transported by pipeline to a variety of sites for alternative uses some of which are:

1.) Injection into depleted oil fields for enhanced oil recovery (EOR)
2.) Injection into old coal mines to release/produce methane
3.) Injection into underground geologic formations and aquifers for storage
4.) Injection into the ocean for storage

Since coal-fired power plants are large point source emitters of CO_2, their centralized location and "economy of scale" make them a focal point for controlling CO_2 emissions. There are numerous, commercially proven processes for removing CO_2 from gas streams. Some are best suited for streams containing relatively low CO_2 concentrations whereas others require high CO_2 partial pressures (>75 psig). The stack gas that exhausts from coal-fired power plants is typically at atmospheric pressure, has a temperature of less than 300°F, and contains approximately 15 per cent CO_2 on a dry

volume basis. The low concentration of CO_2 in the flue gas is best suited for chemical absorption. The chemical absorption process occurs in a conventional packed bed tower wherein the gas, after being cooled to approximately 100°F, is admitted at the bottom, flows vertically up to the exit at the top, while it is contacted/scrubbed by a counter flowing liquid solvent such as monoethanolamine (MEA). The solvent chemically reacts (chemical absorption) with the CO_2 and, after exiting the absorption tower, is fed to the stripping tower, and heated with steam to approximately 250°F to drive off the CO_2 (steam stripping); the steam stripped or regenerated solvent is then, after cooling, recirculated back to the absorption tower for CO_2 capture. The released CO_2 is cooled, dried, and compressed to about 1200 psig or higher for pipeline transport.

Unfortunately the energy required to break the CO_2-solvent chemical bond and to strip out the CO_2 is large (typically 2,000 Btu/lb_{CO2}). As a result a large amount of steam must be extracted from the steam turbine to the stripping tower thereby causing a significant loss in steam turbine power output. In addition the flue gas contains impurities, i.e. SOx, NOx, O_2, hydrocarbons, etc. that can dissolve in the solvent and cause a reduction in the solvent absorption capability, lead to operating difficulties (corrosion, deposits, etc.), and require the addition of "inhibitors", cleaning steps, and continuous feed of fresh solvent. Although this "back end" or post combustion CO_2 removal approach requires no modifications to the boiler, it requires the addition of adsorption-regeneration system with large vessels and imposes harsh performance and economic penalties.

Aside from compression to pipeline pressure, the bulk of the penalties associated with CO_2 sequestration are due to selectively removing CO_2 from the nitrogen rich flue gas and releasing it by steam stripping. As an alternative, Foster Wheeler (FW) has proposed that the coal be burned with oxygen rather than air. With air nitrogen eliminated, a CO_2 rich flue gas is generated that does not require CO_2 capture and stripping. Instead, the flue gas can be fed directly to the CO_2 processing unit for cooling/water condensation, drying, and compression. Elimination of air nitrogen from the coal combustion zone can result in excessively high flame temperatures that can be detrimental to a conventional boiler. To limit flame temperatures and thereby enable commercial boiler design practices to be used, a portion of the CO_2 rich flue gas is recirculated back to the boiler yielding an O_2/CO_2 combustion medium.

It is anticipated that the oxygen required by the O_2/CO_2 combustion process would be supplied by a conventional cryogenic air separation unit (ASU). Although ASU system costs and power requirements are significant, they are expected to be less than those associated with chemical absorption and stripping. Under DOE Contract Number, DE-FC26-03NT41736, FW is:

1.) Preparing a conceptual design of a pulverized coal (PC) fired O_2 boiler
2.) Determining the performance and economics of the O_2 power plant
3.) Evaluating the commercial viability of the plant by comparison to similar sized plants incorporating other CO_2 sequestration technologies

As part of the above, FW has conducted a review of published literature to locate data that is relevant to the conceptual design of the O_2-fired PC power plant. Included in this review is identification of the performance and economics of plants incorporating other CO_2 sequestering technologies.

The system design and analysis task, which was performed using the Aspen Plus computer program, is aimed at optimizing the PC boiler plant operating parameters to minimize the overall power plant heat rate. The flow rates and other properties of individual streams of the power plant were calculated as the results of the Aspen Plus simulations. The required performance characteristics of such operating components as pulverized coal-fired furnace, heat recovery area, flue gas recuperator, and economizer were determined. Two plant configurations were simulated: 1) a conventional air-fired PC power plant and 2) the proposed oxygen-based PC plant. In order to compare the performance of the oxygen-based plant with that of the conventional plant, the power output of the steam turbine in both plants was kept constant.

The low NOx burner design and analysis, which was performed using the Fluent CFD computer program, is aimed at optimizing the burner design to ensure stable ignition, to provide safe operation, and to minimize pollutant formation. Design conditions were based on the results of the system analysis and design task. Four burner designs were developed: 1) with no OFG and 65% flue gas recycle, 2) with 20% OFG and 65% flue gas recycle, 3) with no OFG and 56% flue gas recycle, and 4) with 20% OFG and 56% flue gas recycle.

The furnace and heat recovery area design and analysis task, which was performed using the FW-FIRE and HEATEX computer programs, is aimed at optimizing the location and design of the furnace, burners, over-fire gas ports, and internal radiant surfaces. Design conditions were based on the results of the system analysis and design task. Burner design was based on the burner design task. Two furnace and HRA designs were developed: 1) a conventional air-fired PC power plant and 2) the proposed oxygen-based PC plant.

The economic analysis is based on the results of the system analysis and design task and the furnace design and analysis task. The basis of the economic analysis is a conventional air-fired power plant that Foster Wheeler is currently designing and constructing.

2.0 Executive Summary

Coal is presently the primary fuel for generating electrical power in the U.S. and the world. Even though coal is relatively inexpensive and abundant in the U.S. there is growing concern over its continued use. Compared with oil and natural gas, coal is carbon intensive, releasing roughly 70 and 30 per cent more CO_2 per unit of heat release. Since CO_2 is a greenhouse gas, there is increasing concern that its accumulation in the atmosphere will adversely impact the world's climate/weather patterns.

Coal-fired power plants are large point source emitters of CO_2 and studies have been conducted to determine the impact of capturing their CO_2 for pipeline transport to a sequestration/storage site. Although there are numerous processes available for removing CO_2 from gas streams, the large gas volumes and dilute CO_2 concentrations involved are best suited for a liquid-gas scrubbing process. In this process the gas is scrubbed with a liquid solvent designed to remove a specific gaseous component. Some solvents are best suited for streams containing relatively low CO_2 concentrations (chemical absorption) whereas others (physical absorption) require high CO_2 partial pressures (>75 psig). Since power plant flue gas CO_2 concentrations are relatively low, a chemical absorption type solvent is best suited for this application. After being cooled to about 100°F, the flue gas enters the bottom of a conventional packed bed tower, flows vertically up to exit from the top, while it is contacted by a counter flowing liquid solvent such as monoethanolamine (MEA). The solvent chemically reacts with/absorbs the CO_2 in the absorption tower, and, after exiting, the solvent is fed to stripping tower, and heated with steam to approximately 250°F; this heating releases the CO_2 (steam stripping) and allows the regenerated solvent to be returned, after cooling, to the absorber tower for CO_2 capture. The CO_2 released from the solvent is cooled, dried, and compressed for pipeline transport.

Unfortunately the energy required to break the CO_2-solvent chemical bond and to strip out the CO_2 is large (typically 2,000 Btu/lb_{CO2}). As a result a large amount of steam must be extracted from the steam turbine to the stripping tower thereby causing a significant loss in steam turbine power output. In addition, the flue gas contains impurities, i.e. SOx, NOx, O_2, hydrocarbons, etc. that can dissolve in the solvent and cause a reduction in the solvent absorption capability, lead to operating difficulties (corrosion, deposits, etc.), and require the addition of "inhibitors", cleaning steps, and continuous feed of fresh solvent. Although this "back end" or post combustion CO_2 removal approach requires no modifications to the boiler, it requires the addition of large vessels and imposes harsh performance and economic penalties; CO_2 capture by chemical absorption, excluding CO_2 cooling, drying, and compression to pipeline pressure, has been estimated to decrease the plant efficiency by approximately 8 percentage points and increase the cost of electricity by 59 per cent [9].

As an alternative to post combustion scrubbing, FW has proposed that the combustion process be accomplished with oxygen rather than air. With air nitrogen eliminated, a

CO_2-water vapor rich flue gas will be generated. After partial removal of the water vapor, a portion of the flue gas is recirculated back to the boiler to control the combustion temperature and the balance of the CO_2 is processed for pipeline transport. This proposed oxygen-carbon dioxide (O_2/CO_2) combustion process eliminates the need for the CO_2 removal/separation process and, despite the expense and power consumption of cryogenic air separation, reduces the cost of CO_2 capture. Excluding CO_2 cooling, drying, and compression to pipeline pressure, the O_2/CO_2 process increases the cost of electricity of a PC plant by 27 per cent but yields a value that is 20 per cent less than that of a plant incorporating amine scrubbing [9].

Under DOE Contract No DE-FC26-03NT41736, FW is developing a conceptual design of an O_2 fired boiler to determine overall plant performance and economics. In support of this effort a literature search was undertaken to locate any data/information relevant to this effort. This search has revealed that:

1.) Pilot scale O_2/CO_2 combustion tests have been conducted by two different investigators/teams. One used eastern bituminous coal in a 0.2 MWt test unit whereas the other used subbituminous coal in a 1.5 MWt unit. Both test programs showed that by the use of O_2 with flue gas/CO_2 recirculation:

    a. Flame temperatures can be kept within safe limits.
    b. Flue gas can be produced with a 90 to 95 per cent CO_2 content.
    c. Air-fired boiler temperature profiles and flow patterns can be maintained.
    d. Flame stability and combustion efficiency can be enhanced.
    e. NOx emissions can be reduced significantly.

2.) Several studies have been conducted on pulverized coal-fired plants to determine the performance and economic impact of capturing 90 per cent of their CO_2 for pipeline transport to a sequestration site. An International Energy Agency (IEA) study analyzed several different technologies for this separation/providing a CO_2 rich gas for pipeline transport and found the two most cost effective approaches to be: a) scrubbing post combustion flue gas with an amine solvent and b) using O_2 combustion. For a new plant, scrubbing with Monoethanolamine (MEA) to supply an uncompressed, concentrated CO_2 stream can reduce the plant efficiency by 8 to 11 percentage points and increase its cost of electricity by about 50 to 60 per cent. O_2 combustion, in contrast, has a smaller effect in that it is projected to reduce the plant efficiency by 6 to 7 percentage points and increase its cost of electricity by 27 to 58 per cent. Furthermore, for application to an existing plant, O_2 combustion retrofit also offers a lower loss in plant efficiency.

Based on the published literature it is possible to design a pulverized coal burner to operate with an oxygen-carbon dioxide gas mixture rather than air; a properly designed O_2/CO_2 burner can yield flame temperatures and thermal profiles similar to those of an air–fired boiler while also providing improved flame stability, increased combustion efficiency, and reduced NOx emissions. Plant conceptual designs and cost estimates,

although differing in absolute values, indicate an O_2 combustion based plant should be technically feasible and, when compared to alternative commercial technologies, appears to be the lowest cost way of providing a concentrated CO_2 stream for sequestration. It is also expected that when applied to a new plant, O_2 combustion can result in a more compact, less expensive boiler. Depending upon the SO_2 and NOx levels that can be recirculated back to the boiler, as well as tolerated at the sequestration site, O_2 combustion can result in reduced flue gas cleanup costs. Since O_2 combustion eliminates the need for large, back-end, amine based scrubbers and, in essence, "saves the boiler" (requires minimal if any boiler modification), it is especially attractive for retrofit applications.

O_2 based PC plants require large amounts of oxygen and cryogenic air separation is presently the best available oxygen supply technology for large-scale applications. Cryogenic units, however, are expensive and consume large amounts of power. It is noted that ceramic membranes are under development that are projected to be a lower cost, lower power consuming way to produce large quantities of oxygen. When commercial, those membranes should further enhance the performance and cost effectiveness of O_2 based plants.

The objective of the Conceptual Design of Oxygen-Based PC Boiler study is to develop a conceptual pulverized coal-fired power plant, which facilitates the practical capture of carbon dioxide capture for subsequent sequestration.

The system design and analysis task, which was performed using the Aspen Plus computer program, is aimed at optimizing the PC boiler plant operating parameters to minimize the overall power plant heat rate. The reference plant is a subcritical pressure, natural circulation boiler firing high-volatile bituminous coal (Illinois #6) generating 460 MWe (gross). A conventional air-fired case was simulated as the comparison basis. The air-fired plant has a boiler efficiency of 88.2% and a net plant efficiency of 36.7%.

The oxygen-based plant system model contains all the components in the conventional plant model (with the exception of the FGD) plus the addition of an air separation unit and a flue gas cooler. Flue gas is recycled to control the flame temperature inside the PC-fired boiler to minimize NOx formation, minimize ash slagging in the furnace combustion zone, and avoid the application of exotic materials.

Parametric runs were made varying the amount of recycled flue gas (which directly affects the flame temperature) while maintaining the same boiler outlet O_2 concentration as the air-fired case. The results show that by reducing the recycled flue gas flow rate by 33%, the adiabatic temperature increases from 3574ºF to 4337ºF, increasing the system efficiency (without CO_2 compression) from 31.2% to 31.9%. The system efficiency was further increased to 32.1% by raising the temperature of the recycled flue gas from 96ºF to 148ºF.

Equipment to compress and liquefy the CO_2 effluent to 2000 psia and to reduce the moisture to 50 ppm (to avoid transport pipe corrosion) was added to the system model. This equipment reduces the system efficiency of the 3574ºF adiabatic temperature case from 31.2% to 27.9%. Recycling the residual O_2 before CO_2 compression increases the system efficiency with CO_2 compression to 28.3%. For the high temperature case (3574ºF) recycling of the purge gases results in a system efficiency of 29.5%. A further enhancement of this high adiabatic temperature case was simulated by adding a flue gas feedwater heater prior to CO_2 separation and a turbine expander to recover power from the recycled purge gas pressure reduction. The addition of this equipment raised the system efficiency to 29.8% with a conservative 1% unburned carbon loss and an efficiency of 30.1% with negligible unburned carbon loss. To further reduce the required furnace surface area while increase the net cycle efficiency the flue gas recycle flow rate was reduced from 65% to 56% raising the net cycle efficiency to 30.6%.

Calculations were made using the computer program, EMISS, to determine the furnace waterwall temperature and required material and tube wall thickness for the various cases run. For the air-fired reference case, the waterwalls are carbon steel with a 0.285" wall thickness. For the maximum temperature O_2-fired case, the maximum wall temperature is 961ºF for which 0.24" thick T91 material is required. Furthermore, due to the greater temperature and greater concentrations of radiating gas species (H_2O and CO_2), the required waterwall surface area is only 65% of the air-fired reference case.

The efficiency of carbon sequestration in oxygen-firing boilers even can rival competing gasification plants**.** The power consumption of CO_2 removal for O_2-fired PC plants is about one-third of natural gas combined cycles, about one-half of post CO_2 removal PCs and slightly less than integrated gasification combined cycles. The reduction in power plant efficiency of CO_2 removal for O_2-fired PC plants is nearly half of either natural gas combined cycles or post CO_2 removal PCs and nearly the same as integrated gasification combined cycles.

The oxygen-based PC boiler incorporates cryogenic O_2 separation, which can produce very pure oxygen; but it requires substantial capital and operating costs. Membrane separation of O_2 has been demonstrated at small scale employing very thin membrane fibers, which preferentially allow O_2 to permeate, but not N_2. Although the purity of O_2 from membranes may not be as high as in the cryogenic separation, lower purity oxygen may be sufficient for the oxygen-based PC boiler power cycle. Membrane separation has the potential to use less power at a lower capital cost.

The low NOx burner design and analysis, which was performed using the 3-D Fluent computer program, is aimed at optimizing the burner design to ensure stable ignition, to provide safe operation, and to minimize pollutant formation.

Four burner designs were developed: 1) with no OFG and 65% flue gas recycle, 2) with 20% OFG and 65% flue gas recycle, 3) with no OFG and 56% flue gas recycle, and 4) with 20% OFG and 56% flue gas recycle. Boundary conditions are based on ASPEN simulations of the power plant. A 3-D Fluent simulation was made of a single wall-fired

burner and horizontal portion of the furnace from the wall to the center. Burner geometry is based upon FW low NOx burner experience adapted for O_2 firing.

Without primary gas swirl, coal burnout was relatively small, due to the low oxygen content of the primary gas. Consequently, the burners were modified to include primary gas swirl to bring the coal particles in contact with the secondary gas. An optimal primary gas swirl was chosen to achieve sufficient burnout (>70% by the center of the furnace), but not to produce substantial NOx.

The wall-fired burner design conditions selected were as follows:

1. 100 ft/sec primary gas exit axial velocity with a tangential swirl ratio of 0.5.

2. 60-70 ft/sec inner secondary gas exit velocity for combustion air staging to minimize NOx formation.

3. 120-135 ft/sec outer secondary gas exit axial velocity with a tangential swirl ratio of 1.0 to induce hot flue gas recirculation to the flame ignition point.

The furnace and heat recovery area design and analysis task, which was performed using the FW-FIRE and HEATEX computer programs, is aimed at optimizing the location and design of the furnace, burners, over-fire gas ports, and internal radiant surfaces.

A simulation was made for both the reference air-fired case and for the oxygen-fired case. Two oxygen-fired models were constructed: one with no OFA ports and the second with OFA ports. Boundary conditions are based on ASPEN simulations of the power plant.

The furnace is designed with opposed wall-firing burners and over-fire ports located at one burner pitch above the top burner row. Water is circulated in the furnace by natural circulation to the waterwalls at the periphery and divisional wall panels within the furnace.

For the air-fired furnace simulation, the maximum flue gas temperature is approximately 3300°F. The maximum heat flux is approximately 70,000 Btu/hr-ft^2 and is located on the side wall at the top of the burner zone. The total heat absorbed by the furnace walls before the furnace exit is 1880 MM Btu/hr. The maximum temperature of the waterwalls is approximately 800°F and of the division walls is approximately 875°F. Total burnout of all particle sizes is 99.7%. Average NOx concentration at the furnace outlet is 227 ppmvw (0.34 lb/MMBtu).

Compared to the air-fired furnace, the oxygen furnace requires only 65% of the surface area and 45% of the volume. Two oxygen-fired designs were simulated: 1) without over-fire air and 2) with 20% over-fire air. The mixed primary/secondary gas O_2 content (before combustion) is 42%.

In the oxygen-fired furnace, the maximum flue gas temperature is approximately 3900°F for 0% OFG and 3750°F for 20% OFG. The maximum heat flux is 175,000 Btu/hr-ft^2 (top of the burner zone on the side wall) for 0% OFG and 165,000 Btu/hr-ft^2 (above the over-fire ports on the side wall) for 20% OFG. The maximum wall heat flux in the oxygen-fired furnace is more than double that of the air-fired furnace due to the higher flame temperature and higher H_2O and CO_2 concentrations. The total heat absorbed by the furnace walls before the furnace exit is approximately 2200 MM Btu/hr. The coal burnout for the oxygen-fired case is 100% due to the high furnace temperature and high concentration of O_2. NOx concentration at the furnace outlet is 333 ppmvw for the 0% OFG case and 257 ppmvw for the 20% OFG case. Although the average NOx concentration at the furnace outlet is similar on a volume basis for both air-fired and O_2-fired PC, it is substantially less on a mass basis for the O_2-fired PC due to the substantially lower volumetric flue gas flow rate of the O_2-fired PC.

The maximum temperature of the oxygen-fired furnace waterwalls is approximately 935°F and of the division walls is approximately 945°F. Because of the higher temperature of the oxygen-fired case compared to the air-fired case, furnace water wall material was upgraded from carbon steel to T91.

HEATEX was used to determine the heat recovery area (HRA) design of the convective tube banks between the furnace exit and the SCR/air heater. These tube banks include the finishing superheater, finishing reheater, primary superheater, primary reheater, upper economizer, and lower economizer.

For the air-fired design, total surface area of all convective banks is 294,111 ft^2. The total heat transferred to the water/steam is 1354 MM Btu/hr as 3.88 MM lb/hr of flue gas is cooled from 2135ºF to 720ºF.

For the oxygen-fired design, total surface area of all convective banks is 215,700 ft^2. The total heat transferred to the water/steam is 1096 MM Btu/hr as 2.20 MM lb/hr of flue gas is cooled from 2350ºF to 650ºF. The total heat transfer surface required in the oxygen-fired HRA is 25% less than the air-fired HRA due to more heat being absorbed in the oxygen-fired furnace, the greater molecular weight of the oxygen-fired flue gas, and lower flue gas mass flow rate in the HRA.

The HRA tube materials and wall thickness are practically the same for the air-fired and oxygen-fired design since the flue gas and water/steam temperature profiles encountered by the heat transfer banks are very similar.

The objective of the economic analysis is to prepare a budgetary estimate of capital and operating costs of the O_2-fired PC power plant as well as for the equivalent conventional PC-fired power plant.

The reference plant is a subcritical pressure, natural circulation boiler firing high-volatile bituminous coal generating 450 MWe. A conventional air-fired case was simulated as the comparison basis.

The economic analysis was performed based on the EPRI Technical Assessment Guide (TAG) methodology. Plant capital costs were compiled under the Code of Accounts developed by EPRI. The estimate basis is 2004 dollars, 20-year life, and 85% capacity factor.

The major changes to the reference plant were boiler redesign, SCR system removal, FGD removal, ASU addition, and CO_2 compression addition. The estimated cost of the reference plant is $585,000,000 (1300 $/kW) and of the O_2-fired plant is $668,673,700 (2106 $/kW). A substantial part of this cost increase is caused by CO_2 compression equipment, which must be included for any CO_2 removal systems. Note that he energy stored in the compressed CO_2 fluid is a net loss of energy to the power plant, which is about 8% of gross power, or 3.0 points in efficiency percentage.

The levelized cost of electricity (COE) was calculated for both the reference plant and the O_2-fired plant. The COE value is made up of contributions from the capital cost, operating and maintenance costs, consumables, and fuel costs. The levelized COE was calculated to be 4.61 ¢/kWh for the reference plant and 6.41¢/kWh for the O_2 PC plant. The CO_2 mitigation cost (MC) of the O_2-PC plant was calculated at 21.4 $/tonne.

Compared to the COE of the O_2 PC, the COE for the other technologies is 45% higher for Air PC, 40% higher for NGCC, and 6% higher for IGCC. Compared to the MC of the O_2 PC, the MC for the other technologies is 250% higher for NGCC, 160% higher for Air PC, and 17% higher for IGCC.

3.0 Experimental

This work performed for this report was performed utilizing computer program simulations. No experimental equipment was used.

4.0 Results and Discussion

4.1 Literature Review

A review was conducted of published literature to locate data/information relevant to the design and cost estimating of O_2 based coal-fired power generating plants. The collected material has been divided into four sections and leads to the conclusion that O_2 combustion should be feasible and should have a CO_2 avoided cost that is lower than that of competing commercially available systems. The four sections are:

a.) coal combustion with air-oxygen mixtures (oxygen enhanced combustion)
b.) coal combustion with pure oxygen or oxygen-CO_2 mixtures
c.) impact of CO_2 removal on new coal-fired plant performance and economics
d.) impact of CO_2 removal on existing coal-fired plant performance
e.) oxygen supply systems

Sections 4.1.1 to 4.1.5 identify/summarize the findings of the literature on each of the above topics.

4.1.1 Combustion With Partial Oxygen Enhancement

Nitrous oxides (NOx) are nitrogen-containing compounds that react in the atmosphere to cause acid rain and smog (ground level ozone). Since acid rain and smog can damage the environment and public health, environmental regulations have been established at both the Federal and state level that limit, among other things, power plant NOx emissions. In a typical pulverized coal-fired boiler approximately 70 to 80 per cent of the NOx emitted comes from the fuel itself (from the nitrogen species contained in the volatile matter released during the heating of the fuel and from the remaining char residue that is eventually combusted). The conversion of fuel bound nitrogen (especially volatiles) to NOx involves numerous reactions and intermediate species that compete to form either NOx or nitrogen (N_2). Reducing or fuel rich conditions favor the transformation of fuel bound nitrogen to N_2, whereas, oxidizing or fuel lean conditions favor transformations to NOx.

Numerous techniques have been developed to reduce the NOx emissions from coal-fired boilers. One of them is the use of low NOx burners that stage the introduction and mixing of the combustion air with the coal. By limiting the amount of air (primary air) that first contacts the coal, a fuel rich zone is created close to the burner. Coal exiting the burner, enters this region, undergoes devolatilization and, because of the reducing conditions, the conversion of volatile nitrogen species to N_2 is favored. The balance of the combustion air can be admitted via an outer concentric annulus and the streams mix to form a downstream oxidizing zone wherein the combustion process is completed. By staging the introduction and mixing of the air and coal, the flame can be stretched out, a lower flame temperature can be achieved, and the formation of both fuel bound and

thermal NOx can be minimized. However, there are limits to combustion staging. If the flame temperature is too low, devolatilization may continue into the oxidizing zone and the combustion process may not go to completion, thus resulting in higher levels of NOx and higher levels of unburned carbon in the coal ash. Experience has shown that an optimized low NOx burner can reduce NOx emissions to approximately 30 to 50 per cent of the “unstaged” values.

Another method of NOx reduction that is a generally less expensive than low NOx burners, is to divert air flow from the burner to an over-fire air (OFA) port above it. Typically flame stability considerations limit the burner stoichiometry to a minimum of about 0.8 resulting in an over fire arrangement which produces about a 10 to 30 per cent reduction in NOx emissions from “unstaged” values.

A recent approach to improving the performance of low NOx burners is to enrich the combustion air with a small amount of oxygen. This approach, named oxygen enhanced combustion (OEC), typically introduces less than 10 per cent of the stoichiometric oxygen requirement and raises the overall combustion air oxygen level from 21 per cent to 22 to 23 per cent. By replacing a portion of the primary air with this oxygen, less nitrogen is present and the flame temperature can be increased without changing the combustion stoichiometry. The higher temperature increases the coal devolatilization rate and yield and drives transformations/reactions to produce N_2 rather than NOx. With devolatilization increased, less carbon is left in the char, and unburned carbon levels are reduced. This approach can also be applied to the burners of an over fire air arrangement or even a combined low NOx burner-over fire air arrangement.

Praxair Inc. has taken OEC from bench scale to commercial scale demonstrations [5]. Their first demonstration of OEC was performed in a 44 MWe wall fired boiler at City Utilities in Springfield, Missouri. The demonstration successfully reduced NOx emissions by up to 40 per cent and work proceeded to a larger scale at the 125 MWe Mt. Tom Generation Station in Holyoke, Massachusetts. The latter possesses 16 burners in a 4 by 4 wall arrangement and 6 over fire air ports are provided in a single row above the topmost row of burners. Although oxygen was injected into each of the burners, the authors do not reveal the actual amount used or the unit operating condition; they do indicate, however, that the maximum operating load was 24 per cent over the name plate rating and that the resulting higher gas temperatures and reduced gas residence times limited the potential of the demonstration. Tests were conducted with three different bituminous coals: two were Class C the other was Class A. The NOx data presented in Figure 4.1.1 and Figure 4.1.2 show that the reductions provided by OEC varied with load; the reduction was about 17 per cent at maximum load versus about 35 per cent at minimum load. With the load points not being identified, the inference is made that the minimum load test points are more representative of a normal boiler and that OEC can reduce NOx emissions to less than 0.15 lbs/MMBtu. In addition flame stability was improved and unburned carbon losses were reduced.

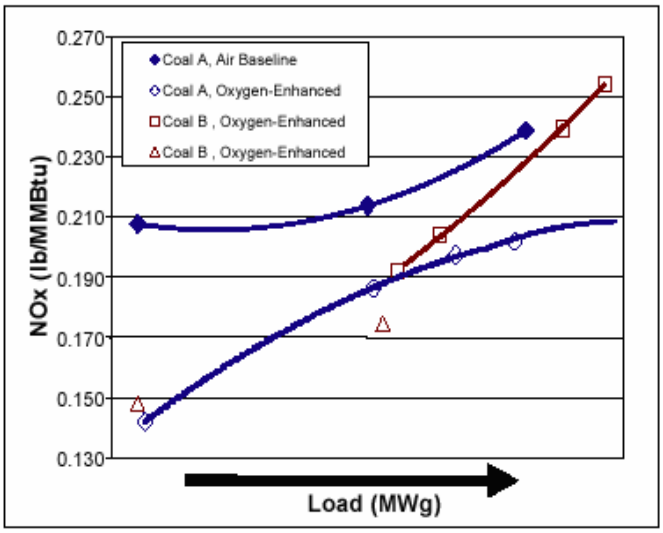

Figure 4.1.1 Effect of OEC on Class C Bituminous Coal NOx Emissions

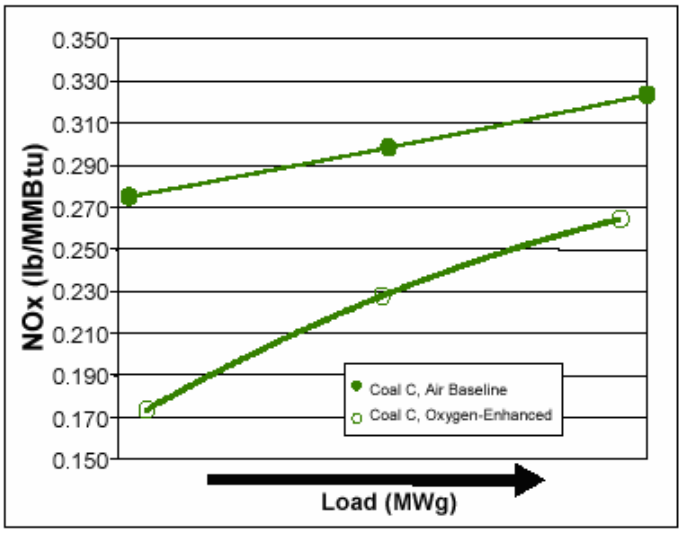

Figure 4.1.2 Effect of OEC on Class A Bituminous Coal NOx Emissions

The tests performed by Praxair show that a relatively small amount of oxygen can be safely injected into pulverized coal-fired burners for reductions in both NOx emission and unburned carbon losses. For plants designed to remove and sequester CO_2, much

higher levels of oxygen injection are envisioned and Section 4.1.2 reports on experimental work in this area.

4.1.2 O_2/CO_2 Combustion

The electric utility tests discussed in Section 4.1.1 indicate that the addition of small amounts of oxygen to the combustion air can improve plant performance, i.e. reduce NOx emissions, reduce unburned carbon, increase ash utilization, and may also improve economics. Further increases in oxygen injection can reach the extreme at which all air flow can be eliminated. At this condition the flue gas is virtually nitrogen-free and it can be cooled, dried, and compressed for pipeline transport to a sequestering site without the need for CO_2 capture or stripping. Since the nitrogen in the combustion air absorbs heat, flame temperatures will increase causing concern that metal temperatures may reach unacceptably high levels and slagging problems may develop.

Two teams of experimenters have conducted pulverized coal combustion tests using oxygen instead of air. In [6] the tests were conducted in a bench scale, down-fired, cylindrical, 145 KW furnace. The furnace roof and walls were water cooled and covered by a 50 mm thick layer of refractory that yielded a 100 mm diameter and a 2300 mm length. A total of five burner configurations were tested with Indonesian subbituminous coal pulverized to a minus 63 micron size. To protect the unit from high temperature flame impingement, testing began without any swirl; the coal and oxygen were admitted as a downward flowing mixture on the centerline. Three different configurations were tested and despite high flame temperatures, combustion efficiencies were less than expected; with Reynolds Numbers being low it was hypothesized that a CO_2 layer was forming on the surface of the coal particles that was preventing oxygen from reaching the coal surface. In the fourth and fifth burner configurations a portion of the oxygen was moved to an outer annulus that surrounded the central primary stream and CO_2 was added to the latter. Vanes located in the annulus imparted 60 degree and 75 degree swirl angles respectively. The authors report the fifth or strong swirl burner did not achieve a stable flame and the fourth burner with its weaker level of swirl was selected for more extensive testing over the following conditions:

Coal Flow Rate, kg/h	6.7
Primary O_2 Flow Rate, m^3/h	3.6
Secondary O_2 Flow Rate, m^3/h	4.8-7.2
Diluting CO_2 Flow Rate, m^3/h	1.5

Figure 4.1.3 shows that a peak combustion efficiency of 99.5 per cent was achieved at an excess oxygen level of 12.5 per cent. The ratio of primary oxygen (O2-1) to secondary oxygen (O2-2) was also varied and the referenced peak efficiency was achieved at a ratio of 0.63 (see Figure 4.1.4) along with a furnace exit CO_2 concentration of 90.4 per cent.

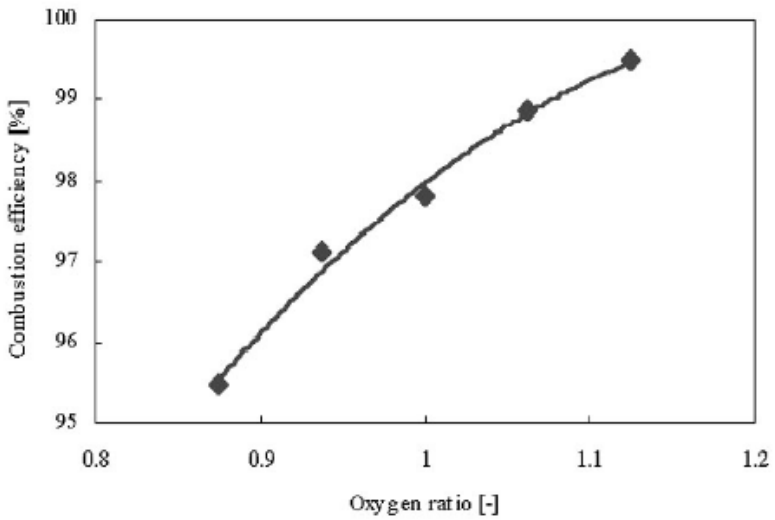

Figure 4.1.3 Effect of Oxygen Ratio on Burner Combustion Efficiency

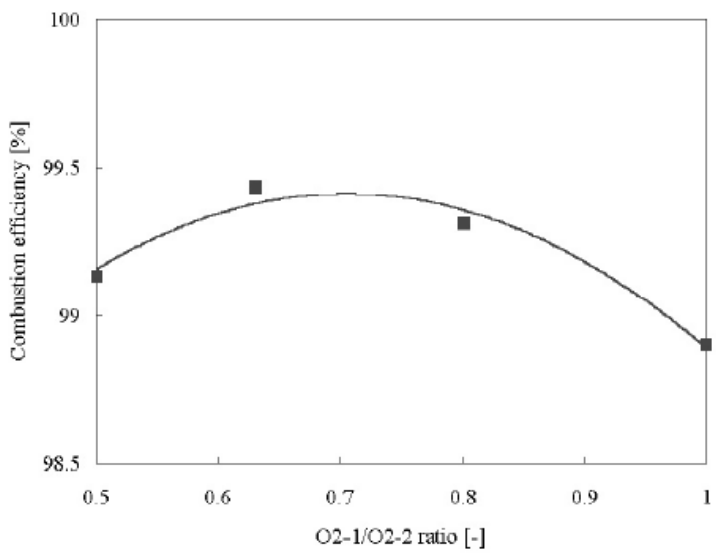

Figure 4.1.4 Effect of Primary to Secondary O_2 Ratio on Burner Combustion Efficiency

Oxygen combustion tests were also conducted at the CANMET Vertical Combustor Research Facility in an 8.3 m tall, down-fired unit possessing a 0.3 MWt maximum heat input rating [7]. The unit was refractory lined to a 600 mm diameter and, together with water-cooled panels, provided a realistic time-temperature history for burning coal particles. A single register, swirl stabilized burner developed by CANMET was located on the centerline of the unit. As shown in Figure 4.1.5 the burner possessed a centrally located natural gas-fired igniter surrounded by four concentric flow annuli. During the tests a variety of secondary gases, e.g. air, oxygen, CO_2, N_2, and recycled flue gas, were admitted through the swirl inducing outermost annulus. This outermost annulus enclosed the primary coal-air-oxygen stream annulus, which in turn enclosed an annulus that injected oxygen into the primary stream via radial holes. The oxygen annulus in turn enclosed a small tertiary stream that admitted air, N_2, and/or O_2 for the natural gas igniter and also served as a buffer that protected the burner front from excessive flame temperatures.

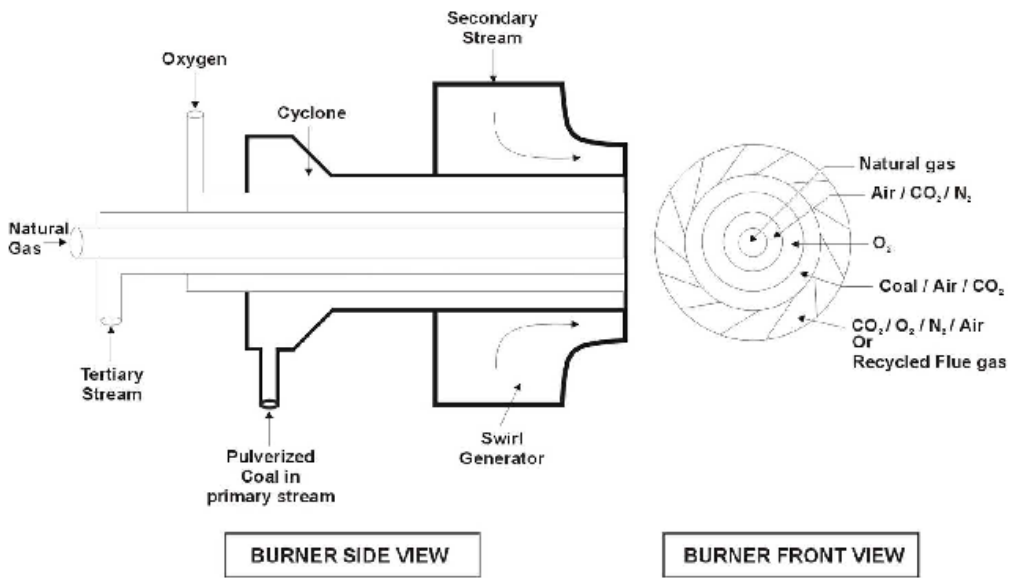

Figure 4.1.5 CANMET Burner

Table 4.1.1 and Table 4.1.2 summarize the burner test conditions. Each test was conducted with pulverized subbituminous coal using a target value of 2 per cent excess oxygen (dry volume basis) and secondary swirl set at 8 for a calculated swirl number of approximately 1.05. Test WS-1 was conducted with air to establish a performance baseline, WS-4 added oxygen to the secondary stream to demonstrate oxygen enriched combustion, and in WS-5, 7, and 3 the air was gradually backed out and replaced with CO_2 and recycled flue gas that had been cooled in a condensing heat exchanger. By using the CO_2 and recycled flue gas the flame temperature was controlled (approximated the air baseline value -- see Table 4.1.3) and a CO_2 rich flue gas was produced that was amenable, after moisture removal, for sequestration. As expected,

with the CO_2 specific heat being higher than that of nitrogen, Test WS-3 required a slightly larger oxygen flow than WS-7 to achieve the same flame temperature. Similarly as the CO_2 or recycled flue gas flow is increased, the nitrogen transported to the flame zone by air is reduced and the NOx emission is reduced. The recycled flue gas also contains NOx, which can potentially be reduced to N_2 in the fuel rich regions of the flame. Although the authors present no direct combustion efficiency data, the CO emissions are observed to be relatively low.

Table 4.1.1 CANMET Burner Operating Conditions

Trial Ref	Target Flue Gas CO_2 Content (dry vol. %)	Primary Gas	Secondary Gas	Excess CO_2 (1) (wt. %)	Total Flue Gas (2) (kg/hr)	Target Feed Gas (3) Composition (dry vol. %)		
						O_2	N_2	CO_2
WS-1	17	Air	Air	0	292	21	79	0
WS-4	25	Air	Air + O_2	0	224	28	72	0
WS-5	30	Air	Air + O_2 + CO_2	22	229	28	66	5
WS-7	70	Air	Air + O_2 + CO_2	184	271	28	27	45
WS-3	98	CO_2	Flue gas + O_2	211	238	35	0	65

Notes:
1) "excess CO_2" is defined as the mass of excess CO_2 leaving the combustion process relative to the mass of CO_2 produced in the combustion process.
2) "total flue gas" is defined as the total mass of flue gas exiting the combustion process.
3) "target feed gas" composition refers to the bulk gas mixture entering the burner.

Table 4.1.2 CANMET Burner Test Flow Rates

Trial Ref	Coal Flow (kg/hr)	Pri. Gas (kg/hr)		Direct O_2 (kg/hr)	Secondary Gas (kg/hr)			
		Air	CO_2		O_2	Air	CO_2	Flue Gas
WS-1	35.5	59.0	-	-	-	209.5	-	-
WS-4	35.5	59.3		6.4	10.4	123.6	-	-
WS-5	35.5	59.0	-	9.6	11.9	107.8	16.3	-
WS-7	35.5	60.3	-	10.9	32.8	17.9	133.2	-
WS-3	35.5	-	59.0	32.5	24.4	-	20(1)	94.9

Notes:
1) This CO_2 was used for sealing/purging and was not injected through the burner

Table 4.1.3 CANMET Burner Performance

Trial ID	Calculated Adiabatic Flame Temperature (1) (°C)	Measured Peak Flame Temperature (2) (°C)	Measured Emissions (3) (ppm, dry basis)		Estimated Emissions (4) (ng/J)
			CO	NO	NO
WS-1	2100	1380	<10	710	236
WS-4	>2750	1565	35	1750	482
WS-5	2650	1565	35	1550	352
WS-7	2120	1440	60	1100	144
WS-3	2230	1440	75	1090	78

Notes:
1) calculated using HYSYS
2) measured using a proprietary shielded high velocity thermocouple probe
3) values shown are the average taken over the duration of each experiment and were measured in the flue gas leaving the combustion process.
4) values show were corrected to account for the reduced gas flow to the stack assuming that the "excess CO_2" would be provided by recycling flue gases

The CANMET Vertical Combustor was also tested with an eastern bituminous coal [8]. The tests were conducted at a 0.2 MWt firing rate with 5 per cent excess oxygen (5 per cent dry volume basis O_2 in the flue gas). During these tests the combustion air was enriched to 28 and 35 per cent oxygen by varying amounts of oxygen and or recycled dry flue gas. Flame temperatures were measured starting from about 75 cm from the burner and, as expected, they increased (see Figure 4.1.6) when the oxygen concentration in the feed gas increased both with and without flue gas recycle. Since the specific heat of CO_2 is greater than that of N_2, the gas temperatures observed with dry flue gas recycle were lower than those observed with air at equivalent oxygen concentrations. NOx measurements were also taken and, as shown in Figure 4.1.7, oxygen enrichment reduced the NOx emission and values observed with dry flue gas recycle were lower than those observed without recycle at the same equivalent oxygen concentrations; the lower values were possibly caused by part of the recycled NOx reducing to N_2 in the flame zone and or part of the NOx dissolving in the water condensed out of the recycled flue gas. Figure 4.1.8 shows no effect of O_2 or CO_2 concentration on SO_2 emissions over the range tested but dry flue gas recycle yields lower values, again, possibly caused by SO_2 dissolving in the water condensed out of the recycle flue gas.

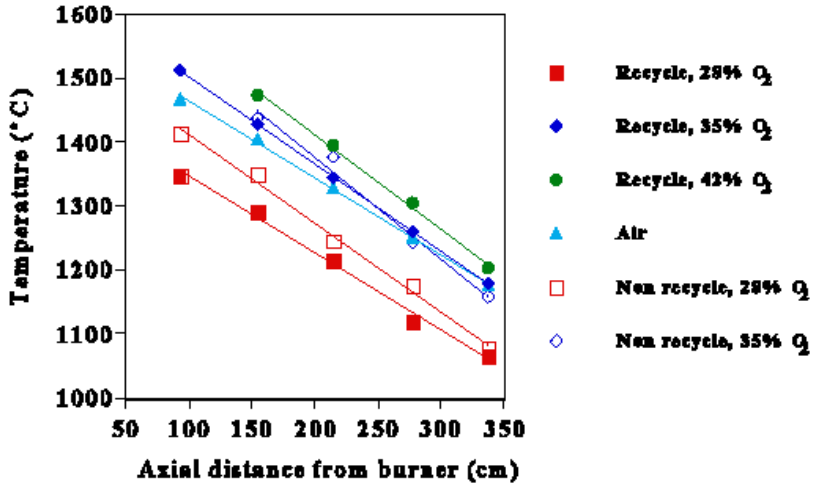

Figure 4.1.6 Centerline Temperatures Downstream of Burner

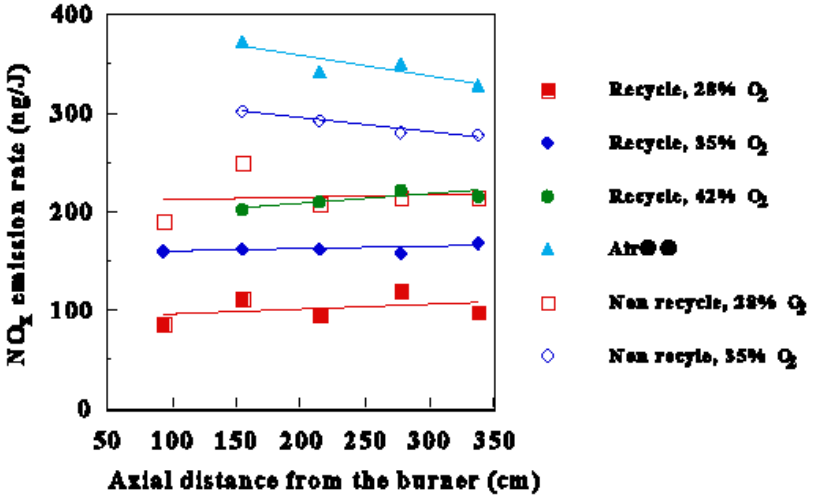

Figure 4.1.7 Centerline NOx Emission Rates

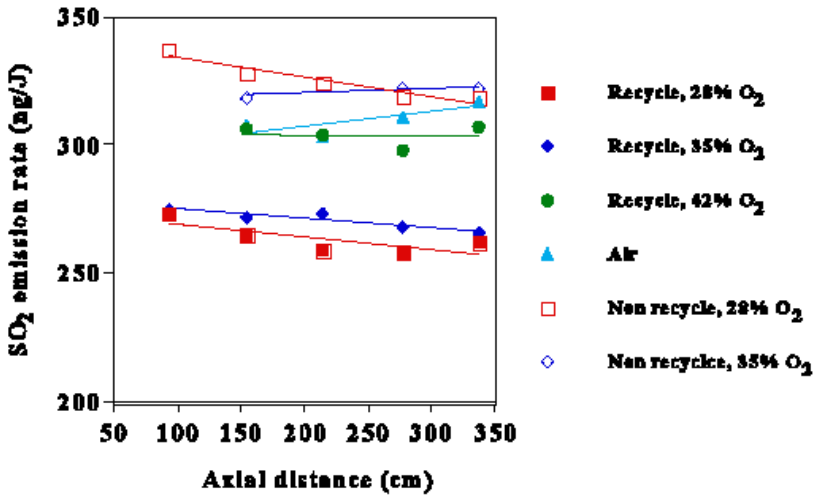

Figure 4.1.8 Centerline SO_2 Emission Rates

O_2 combustion tests were also conducted by The Babcock and Wilcox Company in a 1.5 MWt pilot scale, small boiler simulator test rig [9]. The tests were conducted with subbituminous coal and, by recirculating 75 to 80 per cent of the CO_2 rich flue gas back to the unit, the flow rates, fluid dynamics, and temperature profiles observed were similar to those experienced with air-only operation. The flue gas volumetric flow exiting the stack was about 80 per cent lower than air-fired operation and the gas volumetric concentration was about 80 per cent CO_2, 3 per cent O_2, and 17 per cent nitrogen, the latter was attributed to air infiltration into the system most probably at the scrubber, baghouse, and induced draft fan. Although overall combustion characteristics were similar to air-fired operation, NOx emissions were about 70 per cent lower; rather than 0.22 to 0.26, the NOx level dropped to 0.07 to 0.08 lbs/MMBtu.

The data collected by the above investigators show that by replacing combustion air with O_2 and by using flue gas recycle, flue gases containing 90 to 95 per cent CO_2 can be produced without excessively high flame temperatures. In addition flame stability and combustion efficiency can be enhanced and NOx emissions can be reduced significantly.

4.1.3 Impact of CO_2 Removal on New Plants

4.1.3.1 International Energy Agency Study

Under the IEA Greenhouse Gas R&D Program the performance and cost impacts of incorporating CO_2 removal on four different power generation options was studied. The options covered the spectrum of fossil fueled power generation and for each plant attempts were made to apply the following four different technologies to remove/separate their CO_2 for eventual sequestration:

a.) absorption
b.) adsorption
c.) cryogenics
d.) membranes

The study was conducted in two phases. In the first phase [10] a baseline plant configuration/conceptual design was established for each power generation option to identify performance, emissions, and economics, and then limited sensitivity studies were performed. In the second phase [11] the four CO_2 capturing options were applied separately to each baseline plant. The studies involved the participation of four different organizations in Phase 1 (each developed one of the baseline plant designs) and seven different organizations in Phase 2. Since the objective of the studies was to provide a relative ranking of technologies, attempts were made to design the plants for the same conditions and to estimate their costs using a consistent set of criteria. The plants were assumed to be located at a coastal western European site where 59°F (15°C) sea water cooling was available. Each plant was designed for a 500 MWe net output and a 35 year operating life, and costs were determined in 1992 U.S. dollars. Although attempts were made to apply a consistent set of design and economic criteria, because so many different organizations were involved, it is suggested that results be viewed on a relative basis rather than based on absolute values. The fuels used were 0.86 per cent sulfur (as received) Australian bituminous coal or North Sea “Brent” natural gas.

The four different power generation options studied, together with identification of their designer and a brief description of their base line plant, are as follows:

<u>Pulverized Coal-Fired Boiler with Wet Flue Gas Desulfurization (PC+FGD)</u>
This plant was conceptually designed by the Coal Research Establishment of British Coal Corporation. The plant utilized a conventional subcritical pressure steam cycle and a natural circulation boiler with conventional burners, an electrostatic precipitator, and wet flue gas desulfurization for 90 per cent SO_2 capture.

<u>Natural Gas-Fired Combined Cycle (NGCC)</u>
This plant was conceptually designed by the Norwegian Institute of Technology. The plant was conventional in configuration and used conventional components, i.e. two combustion turbines, two heat recovery steam generators (HRSGs), one steam turbine,

etc. The combustion turbines utilized pre-mix/hybrid burners to achieve a NOx level of 25 ppmv.

Integrated Gasification Combined Cycle (IGCC)
This plant was conceptually designed by the Netherlands Research Foundation. The plant incorporated two high pressure Texaco gasifiers with syngas cooling, two expanders, two combustion turbines (Siemens Model V94.2), one heat recovery steam generator, one steam turbine, and two elevated pressure air separation units with their nitrogen being used for combustion turbine NOx control. Selexol cold gas cleanup, together with tail gas incineration, enabled the plant to operate with 99 per cent sulfur capture efficiency.

Oxygen Fired PC with CO_2 recycle (O_2 Combustion)
This plant was conceptually designed by the Centre for Energy Research in Northern Ireland. The plant incorporated cryogenic air separation, a pulverized coal-fired boiler with low NOx burners, an electrostatic precipitator, and an air heater; the plant was not provided with an FGD or selective catalytic reduction (SCR) system to minimize flue gas SO_2 and NOx levels. Oxygen from the air separation unit served as the boiler oxidant and produced a CO_2 rich flue gas. After particulate removal and cooling, a portion of the CO_2 flue gas was recycled back to the furnace for temperature control and the balance was exhausted to atmosphere. According to the authors the beneficial feature of this plant is that, compared to a normal air fired plant, the CO_2 content of the flue gas is increased from 14 to 63 mole per cent (the majority of the balance is moisture) and the stack gas flow rate is reduced by approximately 67 per cent. Hence this plant is more amenable to sequestration.

Table 4.1.4 summarizes the performance, economics, and CO_2 emissions of the four plants. The NGCC plant is the most efficient and, with natural gas being primarily a hydrogen-based fuel, it has the lowest CO_2 emission per unit of power output—hence, the reason for interest in fuel switching. The NGCC plant, however, operates with high excess air and, as a result, it has one of the highest flue gas flow rates and the lowest CO_2 volume contents (4 per cent versus 14 per cent for the PC plant, on a dry volume basis); high volume flows and low CO_2 contents increase the cost of CO_2 removal. The O_2 PC plant, in contrast, has the lowest flue gas flow rate and, with its CO_2 content already at 91 per cent on a dry volume basis, does not require a CO_2 capture step. Depending upon the amount of SO_2 and NOx that can be tolerated by the sequestration site and the transport pipeline, the CO_2 rich flue gas may need further cleanup before it is dried and compressed to pipeline pressure.

In [11] a team of seven organizations conducted analyses to determine the impact of applying the above CO_2 capturing options to each baseline plant to remove/capture 90 per cent of its CO_2. Each of the processes had an associated parasitic power loss that reduced the plant output and, after integration into the plant, each plant was scaled up in size to maintain a 500 MWe net output. Table 4.1.5 shows the effects of the different

CO_2 separation technologies on the conventional PC plant with FGD. Of the technologies shown, absorption/amine stack gas scrubbing resulted in both the lowest power cost and the lowest CO_2 avoided cost. The plant efficiency, however, reduced from 40 per cent (LHV basis) to 29 per cent and the cost of power increased by approximately 50 per cent. Since amine scrubbing is commercially proven and is the technology most frequently used for large-scale applications, only the absorption results are presented in Table 4.1.6 for the other plants; for information on the alternative processes the reader is referred to [11].

In the CO_2 absorption process the gas is washed with a liquid solvent whose selection depends, among other things, on the CO_2 concentration level. When CO_2 levels are relatively low, chemical absorption type solvents are used (CO_2 chemically reacts with the solvent) and steam stripping is employed to release the CO_2/regenerate the solvent. When CO_2 concentrations are relatively high, physical absorption type solvents are used (CO_2 dissolves in the solvent) and depressuring/flashing is employed to release the CO_2/regenerate the solvent. The air based plants (PC+FGD and NGCC) used chemical absorption applied after combustion, whereas the oxygen-blown IGCC pressurized plant used physical absorption. In the O_2/CO_2 PC plant the CO_2 removal occurred after combustion and raised the CO_2 removal level to 99 per cent. For the IGCC plant its coal-derived syngas was water gas shifted and the CO_2 was removed prior to combustion (the combustion turbine, in essence, became fueled with hydrogen).

Recognizing that the data presented in Table 4.1.4 through Table 4.1.6 were prepared by several different organizations and, even though attempts were made to assure a consistent set of design and economic assumptions (costing accuracy is estimated to be plus or minus 30 per cent), it is suggested the data only be used for relative comparison. It is noted the O_2/CO_2 PC plant with scrubbing added to it can provide up to 99 per cent CO_2 removal and when designed for 91 per cent removal (no scrubbing) its cost of electricity is similar to that of a PC plant with 90 per cent CO_2 removal via amine scrubbing (78 versus 74 mills/kWh).

Table 4.1.4 Performance of Nominal 500 MWe Power Generating Technologies

	PC+FGD	NGCC	IGCC	PC with O2/CO2
Plant Efficiency, % (LHV)	40	52	42	33
Specific Plant Cost, $/KW	1058	702	1561	2044
COE, mills/kWh	49	35	53	78
CO2				
kg/sec/MWh	0.23	0.11	0.21	0.28
mole % wet	13	3	7	63
mole % dry	14	4	7	91

Table 4.1.5 Effect of CO_2 Capture Technologies on a Nominal 500 MWe PC Fired Plant

	Plant Efficiency % (LHV basis)	Power Cost mills/kWh	CO2 Avoided Cost $/tonne	CO2 Emission Rate g/kWh
Baseline Plant	40	49		829
Plant with CO2 Capture by:				
Absorption	29	74	35	116
Adsorption with PSA	28	114	84	57
Adsorption with TSA	29	179	264	335
Membrane	31	83	47	194
Membrane with MEA	30	81	45	222

Table 4.1.6 Effect of CO_2 Absorption on Alternative Power Generating Technologies

	PC+FGD	NGCC	IGCC	PC with O2/CO2
Baseline Plant				
Plant Efficiency, % (LHV)	40	52	42	33
Specific Plant Cost, $/KW	1058	702	1561	2044
COE, mills/kWh	49	35	53	78
CO2				
kg/sec/MWh	0.23	0.11	0.21	0.28
mole % wet	13	3	7	63
mole % dry	14	4	7	91
Plant with Absorption CO2 Removal				
CO2 Capture Efficiency, %	90	85	82	99
Plant Efficiency, % (LHV)	29	42	36	30
Specific Plant Cost, $/KW	1842	1367	2400	3102
COE, mills/kWh	74	53	63	94
CO2 Avoided Cost, $/tonne	35	55	23	16

4.1.3.2 Parsons Study

Parsons Energy and Chemical Group Inc. [12], working under a contract jointly funded by the Electric Power Research Institute and the U.S. DOE, determined the performance and cost impacts of applying CO_2 removal via amine scrubbing on three different power generation technologies. The power plants studied were:

1.) Pulverized Coal-Fired with Wet Flue Gas Desulfurization
2.) Natural Gas Combined Cycle
3.) Integrated Coal Gasification Combined Cycle

In the PC and NGCC cases CO_2 removal was performed after combustion at the back end of the plant where gas temperatures are a minimum. Since these cycles use air as their oxidant their flue gas CO_2 concentration is relatively low and a chemical absorption type solvent (MEA) was used. In the IGCC plant oxygen is used as the oxidant and the syngas is cooled to approximately 100°F to allow acid gas removal prior to combustion. With the syngas at elevated pressure at this point and CO_2 partial pressures relatively high, physical absorption was utilized.

The plants were fueled with either Illinois No 6 coal costing $1.26/MMBtu or natural gas costing $2.70/MMBtu (both on HHV basis); the compositions of these fuels are given in Table 4.1.7 and Table 4.1.8. A mid-western site with a 63°F (dry bulb) and 14.4 psia ambient was assumed and each plant separated and compressed their CO_2 to 1200 psig for pipeline transport to a sequestering site. The CO_2 specification called for a -40°F dew point, a hydrogen limit of 1.25 per cent, and sulfur limits of 100 and 50 ppm for SO_2 and H_2S respectively. All plants operated with a 1 psia steam condenser back pressure and utilized mechanical draft evaporative cooling towers. The following is a brief description of the plants (more detailed information is presented in [12]):

Table 4.1.7 Illinois No 6 Coal Analysis

	Per Cent by Weight (As Received)
Ultimate Analysis	
Moisture	11.12
Carbon	63.75
Hydrogen	4.5
Nitrogen	1.25
Chlorine	0.29
Sulfur	2.52
Ash	9.7
Oxygen (by difference)	6.88
Total	100.00
Higher Heating Value	
Btu/lb	11,666
MJ/kg	27.12

Table 4.1.8 Natural Gas Analysis

Component	Per Cent by Volume
CH4	90
C2H6	5
Inerts/N2	5
Total	100

Higher Heating Value	
Btu/lb	21,824
Btu/SCF	1,002
MJ/kg	50.75

Pulverized Coal-Fired Plant

The PC plant was conventional in configuration incorporating a PC fired boiler with low NOx burners, air staging, and SCR to minimize NOx emissions. An electrostatic precipitator was provided for particulate control and a wet limestone flue gas desulfurization system controlled SO_2 emissions. A regenerative feedwater heating system was utilized and two different steam pressures were investigated. The first utilized a supercritical pressure (SC) double reheat steam cycle with steam turbine conditions of 3500psig/1050°F/1050°F/1050°F. In the second case ultra super critical pressure, double reheat steam conditions of 5000 psig/1200°F/1200°F/1200°F were utilized and both cases were investigated with and without CO_2 capture. For CO_2 capture inhibited aqueous MEA was used for chemical absorption.

Natural Gas Combined Cycle Plant

Two NGCC plant configurations were investigated. The first utilized two General Electric (GE) Company 7FA combustion turbines, each with its own heat recovery steam generator (HRSG) that supplied steam to a single steam turbine, whereas, the second case utilized a single GE H Class combustion turbine with one HRSG and one steam turbine. Both cases utilized a triple pressure HRSG, an 1800 psig/1050°F/1050°F steam turbine, a 1 psia steam condenser back pressure, dry low NOx burners, and were investigated with and without CO_2 capture. For CO_2 capture, inhibited aqueous MEA was used for chemical absorption and only the H Class data is presented herein.

Integrated Coal Gasification Combined Cycle Plant

The IGCC plant utilized E-Gas™ type gasification technology to produce a syngas that was cooled in a fire-tube type boiler and cleaned of particulate via a porous metal candle filter. When operated without CO_2 capture, gasification occurred at approximately 500 psig and the filtered syngas underwent further cooling, water scrubbing, reheating, COS hydrolysis, cooling, removal of H_2S in absorption tower using Selexol solvent, reheating, and humidification for delivery to the combustion turbine burners. When designed for CO_2 capture, gasification occurred at approximately 800 psig (increases CO_2 partial pressure) and the filtered syngas underwent two stages of sour gas shifting, cooling, removal of H_2S in a first absorption stage tower, removal of CO_2 in a second

absorption stage tower, reheating, humidification, and expansion to 385 psia in a turbine expander. The gas was then reheated and delivered to the combustion turbine burners. Selexol solvent was used in both absorption stages. H_2S was stripped from the first stage solvent by flashing and processed by a Claus Plant with a tail gas treating unit for recovery of elemental sulfur. CO_2 was stripped from the second stage solvent by flashing and was cooled, dried, and compressed to 1200 psig yielding a virtually moisture-free, supercritical pressure CO_2 stream for pipeline transport.

Both the F and H Class plants utilized two 50 per cent capacity, cryogenic air separation units, and three 50 per cent capacity, 65 per cent coal/35 per cent water slurry preparation/feeding systems that fed their gasifiers with oxygen and fuel. The F Class plant incorporated two 50 per cent capacity gasifier equipment trains with each delivering syngas to its dedicated combustion turbine. The H Class plant incorporated three 33 per cent capacity gasifier equipment trains that delivered their syngas to the plant's single expander and single combustion turbine.

Table 4.1.9 presents the performance, economics, and emissions of the plants operating without CO_2 capture and assuming an 80 per cent plant capacity factor. The plant net power outputs ranged from 384 MWe for the NGCC to 506 MWe for the USC PC plant. With the H Class NGCC plant fueled with natural gas (essentially a hydrogen based fuel) and operating with a 53.6 per cent efficiency (HHV basis), it has the lowest total plant cost (TPC), the lowest cost of electricity (COE), and the lowest CO_2 emission rate of 0.75 lbs/kWh. The IGCC and USC PC plants both have efficiencies of about 43 per cent and CO_2 emissions of about 1.6 lbs/kWh, a value more than double that of the NGCC plant.

Table 4.1.9 NGCC and Illinois No 6 PC Plants Without CO_2 Capture

Plant Type	NGCC-H	IGCC-H	SC-PC	USC-PC
Parsons Case Number	1D	3B	7C	7D
Fuel	Nat. Gas	Illinois No 6	Illinois No 6	Illinois No 6
Fuel Cost, $/MMBtu (HHV)	2.7	1.26	1.26	1.26
Plant Net Output, MWe	384.4	424.5	462.1	506.2
Plant Efficiency, % (HHV)	53.6	43.1	40.5	42.7
Total Plant Cost, $/KW*	496	1263	1143	1161
COE, mills/kWh**	30.7	45.1	45.0	44.3
CO2 Emission				
lb/kWh	0.745	1.582	1.707	1.618
kg/kWh	0.338	0.718	0.774	0.734

*Year 2000 U.S. Dollars **20 year levelized values with 80 % capacity factor

Table 4.1.10 shows the impact of 90 per cent CO_2 removal on the H Class combustion turbine and the supercritical pressure PC plants (for the lower performing F Class plants the reader is referred to [12]). With the NGCC and PC plants using chemical absorption to remove CO_2 after combustion, they experience about a 10 to 12 percentage point drop in efficiency; the IGCC plant, which removes CO_2 from its shifted syngas before combustion and at about 800 psig, experiences about half the efficiency loss (6 percentage points). In summary 90 per cent CO_2 removal:

a.) USC PC: decreases efficiency by 12 points and increases COE by 62 per cent to 71.6 mills/kWh
b.) IGCC H: decreases efficiency by 6 points and increases COE by 25 per cent to 56.4 mills/kWh
c.) NGCC H: decreases efficiency by 10 points and increases COE by 59 per cent to 48.8 mills/kWh

The cost of CO_2 removed or the CO_2 avoided cost can be calculated by a comparison of plants with and without removal; the CO_2 avoided cost is defined as the difference in plant COE in mills/kWh divided by the difference in plant CO_2 emissions in lbs/kWh. With NGCC plants operating at high excess air and low stack gas CO_2 concentrations, Table 4.1.10 shows that the NGCC plant has the highest CO_2 avoided cost of $66.9/ton versus about $48/ton for the super critical pressure PC plants.

Recognizing that the NGCC plant both starts with and ends with a much lower CO_2 emission rate than the coal based plants, its 90 per cent CO_2 removal requirement could be relaxed and the plants compared on an equal emission rate basis. For such an analysis the reader is referred to [12].

Table 4.1.10 NGCC and Illinois No 6 PC Plants with 90 Per Cent CO_2 Capture

Plant Type+	NGCC-H	IGCC-H	SC-PC	USC-PC
Parsons Case Number	1B	3A	7A	7B
Fuel	Nat. Gas	Illinois No 6	Illinois No 6	Illinois No 6
Fuel Cost, $/MMBtu (HHV)	2.7	1.26	1.26	1.26
Plant Net Output, MWe	310.8	403.5	329.3	367.4
Plant Efficiency, % (HHV)	43.3	37	28.9	31.0
Total Plant Cost, $/KW*	943	1642	1981	1943
COE, mills/kWh**	48.8	56.4	74.4	71.6
CO2 Removal Location	Post Combustion	Pre-Combustion	Post Combustion	Post Combustion
Plant CO2 Emission				
lb/kWh	0.088	0.162	0.238	0.222
kg/kWh	0.040	0.073	0.108	0.101
CO2 Avoided Cost, $/ton	66.9	19.3	48.6	47.5

+ All plants include CO2 processing and compression to 1200 psig pipeline pressure
*Year 2000 U.S. Dollars **20 year levelized value with 80% capacity factor

The changes in plant efficiency and COE reported by Parsons are similar to those identified in the IEA Table 4.1.6. From the standpoint of absolute values, Parsons work is recommended as the IEA work is a compilation of work performed by different organizations. Parsons economic analyses was based on a natural gas price of $2.70/MMBtu; they report that with CO_2 capture the NGCC and IGCC COEs become equal at a gas price of $3.72/MMBtu and that NGCC and USC PC COEs become equal at a gas price of $5.75/MMBtu.

During the 1994 to 1997 time period, four coal fueled, power producing IGCC demonstration plants were commissioned (Buggenum, Wabash, Polk County, and Puertollano). Each had a single, high temperature, entrained flow gasifier supplied by a different manufacturer. Despite several years of operation, modifications, and improvements, the availability of these units, when fueled with coal, remains disappointingly low (in the 70s) and there is a growing consensus that future plants will require at least a spare gasifier, if not a spare gasification equipment train, to achieve high availability [13 and 14]. The IGCC demonstration plants conceptually designed by Parsons and the Netherlands Research Foundation, however, do not include spares. As a result their IGCC plant costs can be expected to increase.

4.1.3.3 American Air Liquide Study

In [9] the impact of incorporating 90 per cent CO_2 removal on a new PC plant via two different technologies/approaches was studied. Although the removed CO_2 was to be sequestered at a distant site, no pipeline conditions were identified and so the study did not include the effects of CO_2 cooling, drying, and compression to pipeline pressure. The plant was fueled with Powder River Basin (PRB) subbituminous coal and, in its baseline configuration (no CO_2 capture), it produced 501 MWe of power with an efficiency of 37 per cent HHV basis. The plant incorporated low NOx burners with SCR for NOx control, a limestone spray dryer for SO_2 control (LSD), an activated carbon injection system for mercury control (ACI), an ESP for particulate removal, and a subcritical pressure steam cycle for power generation. In the first approach at CO_2 removal an amine/MEA scrubbing system that removed 90 per cent of the CO_2 was installed downstream of the ESP; the plant net output and efficiency decreased to 388 MWe and 28.6 per cent respectively. In the second approach, the boiler was fired with a mixture of oxygen and recirculated flue gas to form an O_2/CO_2 combustion system. With air nitrogen eliminated there was a five fold reduction in flue gas volume which led to reduced flue gas treatment costs including elimination of the SCR The oxygen was supplied at a 99 per cent purity level by a cryogenic air separation unit and, even though the cryogenic system introduced a 100 MWe auxiliary power loss, a higher net plant output was obtained: 405 MWe if the recirculated flue gas was cooled to condense its moisture (Dry OC) versus 408 MWe if it wasn't dried (Wet OC).

Table 4.1.11 identifies the plant outputs and efficiencies, Figure 4.1.9 presents plant capital costs, and Figure 4.1.10 identifies the plant costs of electricity and CO_2 avoided costs. In addition to imposing a smaller efficiency penalty, O_2 combustion also imposes a smaller cost penalty on the plant. Compared to the baseline, the MEA absorption process increased the plant capital costs per KW of net power by 48 per cent whereas with O_2 combustion the increase was only 23 per cent. From a cost of electricity standpoint, the increase from the baseline was approximately 59 per cent for amine scrubbing (10 versus 6.3 cents/kWh) versus 27 per cent for the O_2 combustion plant (8 versus 6.3 cents/kWh) plus the latter's CO_2 avoided cost was less than half that of scrubbing ($20/ton versus $47/ton).

Despite its large requirement for oxygen, the greatly reduced flue gas flow rate associated with O_2 combustion allows for a more compact, less expensive boiler design and reduced flue gas cleanup costs; all of these make O_2 combustion a more cost effective technology for CO_2 removal and, should emerging technologies reduce oxygen production costs (see Section 4.1.4), its economics will become even more attractive, especially for retrofit applications.

Table 4.1.11 PRB Fueled PC Plant Performance With and Without CO_2 Capture

Boiler Oxidant	Air	Air	Oxygen	Oxygen
Flue Gas Recycle	No	No	Yes-Undried	Yes-Dried
CO2 Concentrated*	No	Yes	Yes	Yes
Technique Used	Not Applicable	MEA Scrubbing	O2 Combustion	O2 Combustion
Steam Turbine Power, MWe	533	434	533	533
Plant Auxiliary Power, MWe				
ASU			100	104
Other	31	47	24	24
Total	31	47	124	128
Plant Net Power, MWe	501	388	408	405
Plant Net Efficiency, % (HHV)	37.0	28.6	31.4	29.9

* Plant does not include CO2 processing or compression for pipeline transport

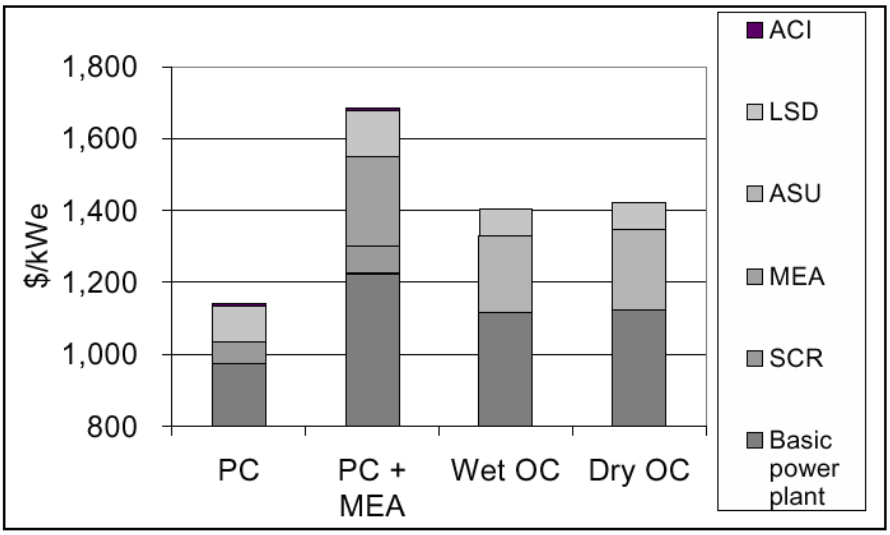

Figure 4.1.9 PRB Fired PC Plant Capital Costs With and Without CO_2 Capture

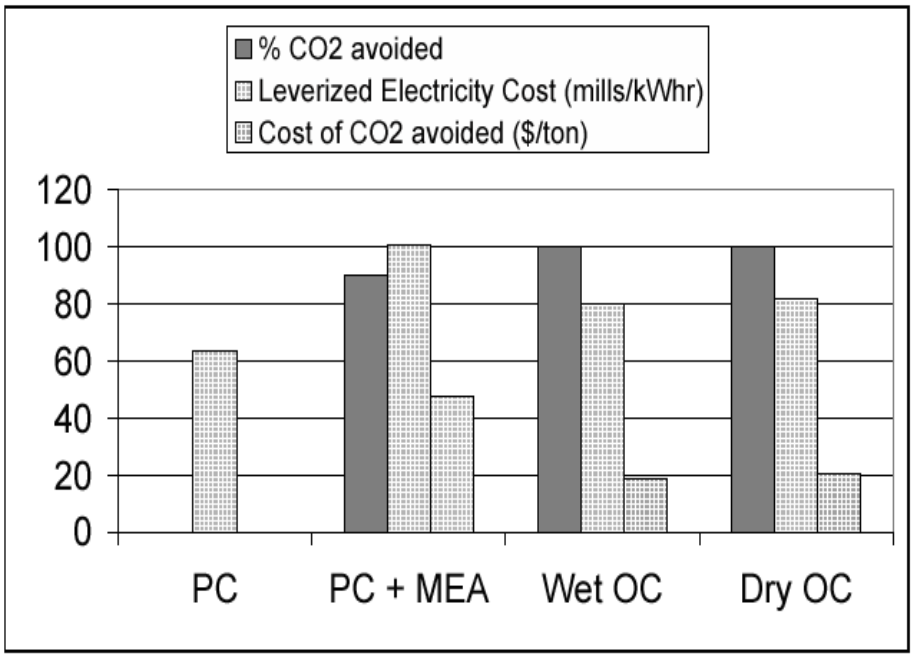

Figure 4.1.10 PRB Fired PC Plant COE and CO_2 Avoided Costs

4.1.3.4 Summary of New Plant Studies

The new plant studies described above were conducted with different coals, different steam cycles, different site conditions, different scopes of supply, different economic assumptions, etc, and some included CO_2 pipeline compression. In Table 4.1.12 the known key features of these studies have been summarized along with study results. Despite the differences between the studies, they indicate that O_2 combustion, when compared to MEA scrubbing, can provide a CO_2 rich stream for sequestration at a lower cost and at a lower efficiency penalty to the plant.

Table 4.1.12 Summary of Plant CO_2 Removal Studies

	New Plants						Repowering	
Study	IEA	Parsons	Parsons	Air Liquide	IEA	Air Liquide	Alstom	Alstom
Coal								
Type	Bit	Bit	Bit	SubBit	Bit	SubBit	Bit	Bit
Sulfur Content, %	0.86	2.5	2.5		0.86			
HHV, Btu/lb		11,666	11,666					
LHV, Btu/lb	11,114				11,114			
Cost, $/MMBtu	2.64	1.26	1.26		2.64			
Steam Cycle	SubC	SC	USC	SubC	SubC	SubC	SubC	SubC
Gas Clean Up								
Low NOx Burners	No	Yes	Yes	Yes	Yes	Yes	No	No
SCR	No	Yes	Yes	Yes	No	Yes	No	No
Sulfur Removal	FGD	FGD	FGD	LSD	No	LSD	FGD	FGD
Mercury Removal	No	No	No	ACI	No	ACI	No	No
Particulate Removal	ESP	ESP	ESP	ESP	ESP	ESP	ESP	ESP
Plant Without/With CO2 Capture								
Performance								
Plant Net Power, MWe	500/500*	462.1/329.3	506.2/367.4	501/388	500/500*	501/408	433.8/260.8	433.8/279.7
Plant Efficiency, %								
LHV	40/29				40/33			
HHV		40.5/28.9	42.7/31.0	37.0/28.6		37.0/31.4	35.0/21.0	35.0/23.1
Economics								
Year	1992	2000	2000	1999	1992	1999		
Specific Cost,$/KW	1058/1842				1058/2040			
Total Plant Cost, $/KW		1143/1981	1161/1943	1140/1690		1140/1400		
Plant Capacity Factor, %		80	80	70		70		
COE, mills/kWh	49.0/74.0	45.0/74.4	44.3/71.6	63/100	49.0/77.5	63/80		
Effects of CO2 Capture/Separation								
Technology Used	MEA	MEA	MEA	MEA	O2/CO2	O2/CO2	MEA	O2/CO2
CO2 Compression, psig	Not Inclu	1200	1200	Not Inclu	Not Inclu	Not Inclu	2000	2000
Decrease in Net Power, MWe		132.8	138.8	113		93	173	154.1
Points Lost in Efficiency	11	11.6	11.7	8.4	7	5.6	14	11.9
Increase in Plant Costs, %	74	73	67	48	93	23		
Increase in COE, %	51	65	62	59	58	27		

*Size increased to maintain output

4.1.4 Impact of CO_2 Removal On Existing Plants

In [16] Alstom Power Incorporated conducted a study to determine the impact of incorporating CO_2 removal into an existing pulverized coal-fired power plant via two different technologies/approaches. The plant selected was American Electric Power's bituminous coal fired Unit Number 2 at Conesville Ohio. It utilized a tangentially fired boiler together with a 2400 psig/1000°F/1000°F steam turbine, an ESP, and a wet FGD system; prior to CO_2 removal it produced 433.8 MWe of net power with an efficiency of 35 per cent and a CO_2 emission rate of 866.2 klb/h (1.997 lb/kWh).

The first case studied employed an MEA scrubber system to remove CO_2 from the unit's flue gas. The MEA system had a flue gas SO_2 limit of 10 ppm dry volume basis; to accommodate this limit, the sulfur removal efficiency of the FGD system was increased by the addition of a second absorber and the MEA system was installed at its outlet. Approximately 79 per cent of the intermediate pressure steam turbine exhaust was required to regenerate the MEA solvent and the released CO_2 was cooled, dried, and compressed to 2000 psig for delivery to a pipeline. The system removed 96 per cent of the plant CO_2 and in doing so the plant net power output and efficiency decreased by 173 MWe and 14 percentage points. It was also noted that a plot plan area of 5 acres was required to accommodate the MEA system.

In the second case O_2 combustion was used. Three trains of conventional cryogenic air separation units were used to supply 99 per cent pure oxygen to the boiler at a total rate of approximately 8924 tons per day. About 2/3rds of the flue gas was recirculated to the boiler to maintain its air-fired temperature and gas flow profiles and an air in-leakage rate of one per cent of the total oxygen requirement was assumed. Although the steam turbine power was maintained, the cryogenic system consumed approximately 96 MWe and the plant net output and efficiency decreased by 154 MWe and 12 percentage points. The O_2/CO_2 system was calculated to remove 94 per cent of the plant CO_2 and required half as much plot plan area (2 ½ acres) as the MEA system for its equipment.

Results of the two cases are summarized in Table 4.1.13. An O_2 combustion retrofit, based on conventional cryogenic air separation, yields an efficiency about 2 percentages points higher than an MEA retrofit, requires half the real estate, and its efficiency, according to the authors, might be increased by another 20 per cent if advanced oxygen separating ceramic membranes (see Section 4.1.5) were used instead of cryogenic air separation. The retrofit study results have been added to Table 4.1.12 and the referenced two percentage point efficiency advantage shown for O_2 combustion is similar to that predicted by American Air Liquide [9] for a new PRB coal-fired plant application. Although Table 4.1.13 does not present economic data, [9] also analyzed an MEA versus O_2 combustion retrofit and concluded that O_2 combustion involved significantly lower capital costs and significantly lower operating and maintenance costs.

Table 4.1.13 CO_2 Removal Incorporated Into An Existing PC Plant

Boiler Oxidant	Air	Air	Oxygen
Flue Gas Recycle	No	No	Yes-Dried
CO2 Concentrated*	No	Yes	Yes
Technique Used	Not Applicable	MEA Scrubbing	O2 Combustion
Steam Turbine Power, MWe	463.5	331.5	463.1
Plant Auxiliary Power, MWe			
ASU			95.9
Other	29.7	70.7	87.5
Total	29.7	70.7	183.4
Plant Net Power, MWe	433.8	260.8	279.7
Plant Net Efficiency, %			
HHV Basis	35.0	21.0	23.0
LHV Basis	36.7	22.0	24.1
Plant CO2 Emission			
Klb/h	866.2	31.0	51.7
lb/kWh	1.997	0.119	0.185
kg/h	0.906	0.054	0.084
Plant CO2 Removal, %		96.4	94.0

* Plant includes CO2 processing and compression to 2000 psig for pipeline transport

4.1.5 Oxygen Supply Systems

There are currently three major commercial methods for producing oxygen from air; they are cryogenic air separation, pressure swing adsorption, and membrane separation. When large quantities or very high purity levels of oxygen are required, cryogenic air separation is the most cost effective technology. In addition it is the only one that can produce liquid oxygen which is an attractive feature in that tank storage can be provided that allows the oxygen user to continue to operate even though the ASU may be down for short term repairs. As a result, cryogenic air separation has been used at numerous IGCC plants, i.e. Buggenum, Wabash, Polk County, Puertollano, etc. Unfortunately cryogenic units are both expensive and high power consumers; they represent 12 to 15 per cent of IGCC plant capital costs, consume upwards of 10 per cent of the plant gross power output, and provide oxygen at a cost of about $15/ton [15].

With cryogenic air separation being a mature technology, many people feel it offers very limited opportunities for significant reductions in cost or power consumption. As a result the DOE is funding research on emerging technologies that can hopefully provide “break through” advances to improve the economics of IGCC plants. The oxygen requirement of O_2 based plants, based on tons of O_2 per MWh of power generated, is estimated to be more than three times larger than that of IGCC plants [17] and, hence, it too will greatly benefit from such reductions.

Air Products and Chemicals Inc. (Air Products) and Praxair Inc. are working under separate DOE contracts to develop oxygen transport membranes that hopefully will achieve a significant reduction in both oxygen production costs as well as power requirements. The Air Products technology is based on a ceramic membrane which, when operated at high temperature (typically 1500 to 1650°F), will selectively transport oxygen ions. When subjected to an oxygen partial-pressure driving force at this temperature the membrane will produce high-purity oxygen at a high flux rate. Air Products has named their air separation technology Ion Transport Membrane (ITM) Oxygen. When applied to a single train IGCC plant incorporating a Texaco high-pressure quench gasifier and a Siemens Westinghouse 501G gas turbine, ITM Oxygen, when compared with cryogenic ASU, is projected to cost 35 per cent less. In addition it requires 37 per cent less power yielding a 7 per cent reduction in IGCC capital costs and a one percentage point increase in plant efficiency [18]. Air Products is pursuing a planar membrane system, has successfully manufactured and tested commercial scale wafers, and hopes to have a commercial scale unit with an oxygen capacity in the hundreds of tons per day in the year 2007-2008 time frame.

Praxair [19] reports similar success with the ceramic oxygen transport membrane (OTM) system it is developing. A ceramic material composed of synthetic inorganic compounds in an architecture suitable for a 10 year life appears feasible and a multi OTM element system, capable of delivering >99 per cent purity oxygen, has been successfully tested for 1000 hours at 1650°F and 275 psia; the multi element system is next undergoing cycle testing involving heating, oxygen production, and cool down to prove its integrity.

Although the ceramic membranes being pursued by both Air Products and Praxair are aimed at reducing the costs and increasing the efficiency of IGCC plants, they can also be applied to and will improve the performance and economics of O_2 combustion plants.

4.2 System Design and Analysis

4.2.1 Reference Site and Fuel Conditions

In December, 2000 Parsons published a study of the cost of electricity of several case studies in CO_2 sequestration from a PC boiler by post capture (Ref. 12). To provide a consistent comparison with the cases analyzed in the Parsons report, the same site conditions (59ºF, 14.7 psia, 60% RH) and the same fuel (Illinois #6) are used in the analysis presented herein. Site Conditions and fuel properties are presented in Table 4.2.1. Fuel HHV and LHV were estimated by a DuLong's method and the stoichiometric air ratio of 867 lb_{air}/lb_{coal} was calculated based on the fuel ultimate analysis.

The liquid CO_2 produced from the oxygen-based PC power plant is not chemically pure, but can readily sequestered in geologic formations (depleted oil and gas reservoirs, unmineable coal seams, saline formations, and shale formations). The liquid CO_2 exits the plant at 2000 psia (Parsons study used 1200 psia). The other gases in the delivered CO_2 are limited to H_2O < 50 ppm (to avoid acid corrosion), and $Ar+N_2$ < 3% (to avoid phase separation). The excess gases in CO_2 stream either have to be purged or recycled. However, since SO_2, as an acid gas, similar to CO_2, it can be sent to pipeline directly, and as mentioned in literature, it does not need to be separated out from CO_2 product. Furthermore, it is also not necessary to remove the small concentration of NOx in the CO_2 effluent since it can be sequestered along with the CO_2.

4.2.2 Air-Fired Reference Case

To study the effects of CO_2 removal on the performance of power plant, an air-fired PC boiler was been simulated in detail as a reference case. This model was used as the base, which was then extended to include the air separation unit (ASU) and CO_2 compression for O_2-fired PC cases.

The reference plant employs a subcritical pressure, natural circulation boiler firing high-volatile bituminous coal producing 2400 psig steam at 1000ºF and reheat steam at 1000ºF to generate 460 MWe (gross). A condenser pressure of 2.5" Hg was applied along with seven feedwater heaters, which raise the feedwater temperature to 494ºF.

Case 1 is the reference air-fired PC boiler case and the model and results are shown in Figure 4.2.1.

The Aspen Plus model includes coal mills, flue gas heater, pulverized coal-fired furnace, steam generator, superheater, reheater, economizer, ash-removal unit, nitrogen oxides (NOx) selective catalytic reactor (SCR), flue gas de-sulfurization reactor (FGD), air blower, induced draft (ID) fan, feed water pump, cooling water

pump, feed water heaters, and a single reheat steam turbine. A coal drying function has been modeled and added into mill module to result in the proper correct mill exit gas temperature. The furnace was simulated by a zero dimensional model. However, all key tube banks of the heat recovery area (HRA) were individually modeled. The furnace roof heat absorption is also simulated. The high pressure steam temperature is controlled by water spray for de-superheat. The simulation also included heat losses from boiler and HRA sides, as well as steam pipes. Some user-defined models are included to perform emission calculations. User built-in calculations were added to determine boiler efficiency, system net efficiency, and net power. The heat carried by exhaust streams was automatically calculated by program.

For a given steam turbine output and a fuel, ASPEN PLUS iterates to determine the feed rates of air, coal, etc., based on specified temperature approaches and the excess air requirement.

The system configuration, detailed setup parameters and summary of results for the case 1 reference case are shown in Figure 4.2.1 and Table 4.2.2. This system has a steam turbine cycle efficiency (generator power divided by heat transferred to the steam cycle) of 45.78%, a boiler efficiency (heat to steam cycle divided by heat input from fuel to boiler) of 88.2%, an unburned carbon loss (UBC) of 1.0%, and a net plant efficiency of 36.68% (net plant heat rate of 9302 Btu/kWh). It has a gross power as 460 MWe at generator, an auxiliary power of 42 MWe, and a net power of 418 MWe. Total heat input from fuel is 3890 MM Btu/hr.

The temperature of the flue gas exhausted to the stack is 292ºF. The flue gas exiting the boiler contains 3.0%, vol., wet O_2 (18% excess air) and contains 773 klb/hr (1.95 lb/kwh) of CO_2.This 3.0% O_2 level is kept constant for all of the O_2-fired cases. An SCR is applied to control NOx with NH_3/NOx=1.0, while an FGD is used to control SOx by lime solution with Ca/S=1.05, L/G=10, and 85% excess air for aeration (Table 4.2.2)

The breakdown of auxiliary power for case 1 is listed in Table 4.2.3. Most of these power consumptions were simulated directly by the ASPEN module. Some required user Fortran for those processes lacking ASPEN modules, such as solids handling. The power consumption was based on stream flows and design data. Fan power consumption was simulated based on the pressure drops from both air side and gas side. The total auxiliary power consumption, including FGD, for case 1 is approximately 9.2% of the gross power.

4.2.3 Oxygen-Based PC Plant

4.2.3.1 Boiler Plant Modifications

The oxygen-based (or oxygen-fired) plant model contains essentially all the components in the conventional plant model. In addition, it also includes an air separation unit (ASU) and a flue gas cooler. In the O_2-fired plant, the FGD is not needed because the SO_2 is acid gas similar to CO_2 and can thus be sent to pipeline together with the CO_2. A substantial portion of the SOx and H_2S will be removed as the flue gas is cooled down in the CO_2 cooling and compression equipment.

The steam side components remain very similar to the air-fired case with only some changes in heat bundle duties in the heat recover area (HRA).

In O_2-fired cases, flue gas is recycled is to control the flame temperature inside the PC-fired boiler to minimize NOx formation, minimize ash slagging in the furnace combustion zone, and avoid the application of exotic materials.

Before the flue gas is separated into a recycled and effluent stream (to the pipeline), it is cooled to 90ºF. Since this is below the acid/moisture dew point a heat exchanger containing acid-resistant materials must be used. The recycled gas is then reheated, before the forced draft (FD) fan, by mixing it with a bypassed hot gas to avoid reaching the dew point. After the O_2 from ASU plant is mixed with recycled flue gas, it is heated by the flue gas exiting the boiler in a gas-gas heat exchanger, which acts as a recuperator to improve cycle efficiency and reduce fan power requirements.

It is assumed in this study that there is no tramp air ingress through the sealed boiler.

4.2.3.2 Air Separation Unit

For an O_2-fired PC, O_2 purity is a key parameter for system performance and economics. A high purity O_2 will produce a high purity of product CO_2 gas that will reduce CO_2 purification and compression power. However, producing high purity O_2 requires high ASU plant operational and equipment costs. Furthermore, too high O_2 purity is not necessary because the fuel combustion itself will generate some gases, such as N_2 and some excess O_2 is required for complete combustion, in additional to CO_2 as flue gas. Therefore there is a balance point to give an optimum. After literature review and some trade studies, it was determined to use a complete ASU to separate air to O_2 and N_2/Ar, (Ar is separated out from the O_2 by additional column) to maintain an O_2 purity between 99.0 and 99.5%.

The method of air separation chosen for this study is the commercially available large-scale cryogenic air separation technique. A traditional cryogenic ASU plant, shown in Figure 4.2.2, was simplified in the simulation to include the power consumption, but without details of distillation columns and cold heat exchangers. The ASPEN simplified ASU model is shown in Figure 4.2.3. The ASPEN model does not include the air purifier, which removes moisture, hydrocarbons, CO_2, and NOx in an adsorber and is located between the cold box and air compressor. Although the separated N_2/Ar gases could potentially be sold as byproducts, no economic credit for this is taken in this study. No heat recovery from the ASU air compressor inter-stage coolers is included, because recovery of this low-grade heat recovery is very inefficient.

Power consumption is 23.6 kw/klb$_{air}$ [12] for 95% O_2 purity under 67 psia ASU pressure. From Ref. 20, the power increases by 4% when O_2 purity is increased from 95% to 99.5%. Thus, for the O_2 purity of 99.5% used in this study a power consumption of 24.5 kw/klb$_{air}$ was applied. For a 460 MW steam turbine generation, the ASU plant consumes about 70 MW, or 15% of generated power.

4.2.4 Parametric Cases

There were five O_2-fired parametric cases studied as follows:

1. Case 1: air fired reference case
2. Case 2: with ASU & gas recycle, the same mass flows of air and flue gas as case 1
3. Case 3: with ASU, reduced air, the same flue gas flow and O_2% as case 1
4. Case 4: reduced recycle gas flow, the same adiabatic temperature and O_2% as case 1
5. Case 5: reduced recycle gas flow, high adiabatic temperature and the same O_2% as case 1
6. Case 6: reduced recycle gas flow, higher adiabatic temperature and the same O_2% as case 1

Case 2 has the same system net excess air (exit plant O_2 flow rate divided by stoichiometric O_2 flow rate) as case 1, but because of gas recycle, more O_2 is carried by recycled gas back into boiler, which raised boiler excess air (boiler exit O_2 flow rate divided by stoichiometric O_2 flow rate) to a very high number of 69%, and a very high oxygen content of the flue gas of 15.3%. The cycle diagram for case 2 is shown in Figure 4.2.4.

In Case 3 the air flow rate was reduced to produce a 3%, vol. O_2 concentration at the boiler exit (similar to case 1). This corresponds to a boiler excess of 13.5% and a net excess of 3.1%. Compared to case 2 the air flow rate of case 3 was reduced by 13% from 3422 klb/hr to 2981 klb/hr. O_2 concentration in the boiler is 26.9%, compared to 20.4% for the air-fired case, and yields a higher combustion

efficiency. Flue gas flow to the sequestration plant is reduced from 927 klb/hr in case 2 to 820 klb/hr in case 3, which results in less CO_2 compression duty. Case 3 maintains the same flue gas flow rate as cases 1 and 2. The cycle diagram for case 3 is shown in Figure 4.2.5. In cases 4 to 6 the amount of flue gas recycled was reduced to increase the O_2 level in the boiler. This increase in boiler O_2 creates a higher adiabatic temperature, which reduces the size of the furnace and increases the overall cycle efficiency. The adiabatic temperature (used as the abscissa in Figure 4.2.10 to Figure 4.2.13) is the maximum theoretical temperature that can be reached by the products of combustion with no loss of heat and no dissociation. Actual flame temperature is lower than the adiabatic temperature especially at adiabatic temperatures greater than 3600ºF due to flue gas dissociation of CO_2 to CO and H_2O. The effect of adiabatic temperature on cycle efficiency is shown in Table 4.2.4 and Figure 4.2.10. Case 4 has the same adiabatic temperature as air-fired reference case, while cases 5 and 6 have higher adiabatic temperatures. Although there is little change in gas exhaust flow to the CO_2 compressor among cases 3-6 (listed as gas exit system in Table 4.2.4), the decreasing recycle gas flow results in reduced auxiliary power consumption for both the FD and ID fans. The reduction in FD and ID fan auxiliary power requirements is presented in Figure 4.2.11 (approximately 2.5 MW from case 3 to case 6) along with the reduction in ASU power requirements (approximately 1 MW from case 3 to case 6)

Figure 4.2.12 shows the relationship of flue gas flow to boiler adiabatic temperature. Figure 4.2.13 is a similar plot to Figure 4.2.12, but it uses volumetric flow rate as the ordinate instead of mass flow rate. Both figures show the air-fired data for comparison. It can be observed that the O_2-fired PC has a lower volume flow rate than does the air-fired PC due to the higher molecular weight of the flue gas (i.e. CO_2 versus N_2). From case 3 to case 6 the ratio of the O_2-fired PC volume flow rate to the air-fired PC volume flow rate drops from 75% to 57%, which means for a constant flue gas velocity, boiler size is reduced.

Another advantage from decreasing the quantity of recycle gas is to increase the O_2 content in the boiler (from 27% to 34% by vol. from case 3 to case 6), which improves the fuel combustion and reduces the required height of the furnace. This credit has not been simulated in this system study, but was modeled in the 3-D CFD boiler simulation study (Section 4.4.1).

4.2.5 Hot Recycle

A case with hot gas recycle (case 7, Figure 4.2.9) was run to evaluate its effect on the system performance. A hot gas recycle brings more energy back into boiler, reduces fuel and O_2 feed rates, and reduces ASU duty, but it requires more power to the fan because of the increased recycle gas volume flow.

Table 4.2.4 shows that increasing the recycle gas temperature from 95ºF to 148ºF increases the boiler efficiency from 89.60% to 90.94% and net efficiency

from 31.90% to 32.12%. The additional fan power increase of 0.3 MW was more than made up by a reduction in ASU power of 0.5 MW. The resultant fuel saving is approximately 0.7%. The size of the gas-gas heat exchanger increases due to the reduction in LMTD (fluid temperature difference is reduced from 213ºF to 176ºF for the hot end, and from 104ºF to 74ºF for the cold end).

There is a limit to increasing the recycle gas temperature without increasing the stack gas temperature, which will reduce efficiency and increase cooling duty. One option mentioned in literature is to raise both stack gas and recycle gas temperatures, and then recover heat from stack gas to replace part of the feedwater heaters. The merits of this approach are questionable because the efficiency improvement will be very small from replacing the low pressure feedwater heater.

Figure 4.2.14 shows the cooling curve for flue gas cooling before compressor. Part of the heat can be recovered to preheat the condensate. If 90 MMBtu/hr of heat is recovered (exit temperature = 142ºF), the steam saved from extraction will generate an additional 2.2 MW, or an efficiency increase of 0.2% point. If 150 MMBtu/hr of heat is recovered (exit temperature = 133ºF), the steam saved from extraction will generate an additional 3.4 MW, or an efficiency increase of 0.3% point. This potential energy savings will be further explored in Section 4.2.8.

4.2.6 CO_2 Compression

The flue gas effluent stream (mainly CO_2) has to be compressed to the high pipeline pressure of 1200 to 2000 psia. Using case 3 as a basis, case 8 is simulated in which the CO_2 sequestration equipment is added to the system and the effluent is conservatively compressed to 2000 psia. The dominant moisture in flue gas is condensed out first during flue gas cooling before the first stage compression. The condensed water contains acid gases and has to be treated before recycle or discharge.

The flue gas dry composition before the first stage CO_2 compressor from case 8 is:

CO_2	O_2	N_2+Ar	SOx	H_2O
90.9	2.9	1.3	1.3	3.6

In literature, a O_2 concentration as low as 1.3% was used. Reducing O_2 content, such as from 3.0% to 2.0% by reducing excess air, would be helpful in reducing CO_2 compression power, but it is judged that and oxygen content of approximately 3.0% is required for good combustion efficiency. Both CO_2 and SO_X are acid gases. They combine with moisture to form acid, which causes a corrosion problem along CO_2 pipeline. Therefore, after the 2nd stage, a chemical method of active dehydration with TEG (Triethyleneglycol), retarding hydrate formation and corrosion, has been applied to reduce the moisture to a very low

level of less than 50 ppm, where the TEG can be regenerated by heating. In the model, the TEG dehydration was simulated, but the TEG itself was not simulated.

A four-stage compression with inter-stage cooling was applied in case 8. To reduce power, an equal compression pressure ratio of approximately 3.4 was applied. The results are shown in Figure 4.2.15 and Table 4.2.5. The effects of the addition of the ASU and the CO_2 sequestration plant can be seen in Table 4.2.5 as follows:

Efficiency = 36.7% with air (case 1)
Efficiency = 31.2% with ASU (case 3)
Efficiency = 27.9% with ASU & CO_2 sequestration (case 8)

4.2.7 Vent Gas Recycle

Because of limitation of the other gases in CO_2 pipeline (i.e., H_2O < 50 ppm and $Ar+N_2$ < 3%), the excess gases have to be purged. A novel idea applied in this study is to recycle this O_2-rich purge gas back to system and to reduce ASU duty and to recover power. The vent gas recycle has been simulated in case 9 (Figure 4.2.16). To effectively separate out the non-CO_2 gases, the compressed CO_2 stream from the 3rd stage is cooled down to its dew point (Figure 4.2.20) and condensed out by phase separation by a stripper tower (not simulated in this study). Instead of using a compressor for the 4th stage CO_2 of compression as in case 8, a CO_2 liquid pump is used in case 9 to save power and cost.

The composition of the purge gas is as follows:

	O_2	N_2+Ar	others
Case 9	71.6	28.1	0.3

Although the flue gas flow discharged to CO_2 plant is nearly identical for both cases 8 and 9 as shown in Table 4.2.5, the net excess O_2 reduces to near zero when vent gas recycle is applied, and consequently the air flow rate to system is reduced from 2981 to 2905 klb/hr. However since the boiler is still operated at 27.5% O_2 inlet, and a 3% O_2 outlet, the boiler combustion performance will not be affected.

The addition of vent gas recycle (compare case 8 to case 9 in Table 4.2.5) increases the net efficiency from 27.9% to 28.3%, increases the net power from 317.3 to 321.8 MW, and decreases the auxiliary power from 143.1 to 138.6 MW (a net 4.5 MW saving). Gas recycle will also reduce NOx in the effluent since the majority of the NOx will be separated out with the purge gas and removed by the gas adsorber in ASU plant.

Since the vent gas from the CO_2 compression plant is at 920 psia and the ASU is at 67 psia, the vent gas can be sent to an expander to generate power and

reduce its pressure and temperature. This power generation is not included in case 9, but is added in a subsequent case (see Section 4.2.8). Furthermore, the low temperature expanded recycled gas could be used as extra coolant for the ASU distillation column. However, this energy savings has not been accounted at present time because the model does not include the details for ASU plant.

In cases 10 and 11 the amount of flue gas recycled was reduced to increase the O_2 level in the boiler (similar to cases 4 to 6). This increase in boiler O_2 creates a higher adiabatic temperature, which reduces the size of the furnace and increases the overall cycle efficiency. The effect of adiabatic temperature on cycle efficiency is shown in Table 4.2.5, which demonstrates that raising the adiabatic temperature from 3575ºF to 4343ºF increases the net efficiency from 28.3% to 29.5% (boiler efficiency is also increased from 88.3% to 90.8%). Figure 4.2.17 presents the net cycle efficiency versus the recycle flow rate. Cycle diagrams for cases 10 and 11 are shown in Figure 4.2.18 and Figure 4.2.19, respectively.

4.2.8 Case 12

Based on the results of the parametric cases, cases 12 is modeled

Since all processes that capture CO_2 must include some kind of wet gas cooler, due to the low temperature to which the flue gas is cooled, case 12 utilizes a wet-end economizer to recover as much of this heat as practical. In case 12 a heat exchanger is added to recover the flue gas sensible energy prior to separation into recycle and outlet streams. The heat exchanger cools the flue gas to 142ºF and removes 90 MM Btu/hr. This significantly increases the boiler efficiency by reducing the energy content of the flue gas effluent. The LMTD of the heat exchanger is 34ºF and it is judged that reducing the flue gas temperature further (below 142ºF) could be uneconomical since the required heat exchanger would be too large. Figure 4.2.24 shows that reducing the flue gas temperature from 142ºF to 139ºF (increasing the heat exchanger absorption from 90 MM Btu/hr to 100 MM Btu/hr) reduces the LMTD from 34ºF to 26ºF.

Although the flue gas outlet temperature of this additional heat exchanger is nominally at the moisture condensation temperature, the presence of SOx in the flue gas raises the dew point of gas such that sulfuric acid solutions will condense below 300ºF. Consequently the heat exchanger must be constructed from acid-resistant materials.

There are two possible applications for this wet-end economizer: 1) replace the first stage FWH1 or 2) heat up a split stream from the condensate pump. The second option results in a higher thermal efficiency since it reduces the higher pressure steam extractions. This is demonstrated in Figure 4.2.26, which shows that the efficiency (work/steam thermal energy) of the steam, if it is not extracted,

increases with increasing pressure (stage). Therefore the split stream method yields higher efficiency and is applied in the design case (Figure 4.2.23).

Case 12 also incorporates a turbine expander to recover power from the recycled purge gas pressure reduction. The turbine generates 0.41 MW of power as the pressure is reduced from 925 psia to 67 psia. The expanded gas is quite cold (-183ºF) and could potentially be used as a coolant for distillation operation. However, since the ASU was not modeled in detail in this study no credit for this cooling effect is taken.

Due to the possible danger of pre-combustion in the mill and primary gas stream, a modification is made to the cycle to use the vitiated air (3.0% O_2) as the coal-carrying primary gas stream. The recycled flue gas is mixed with the secondary gas stream after the primary gas take-off.

Figure 4.2.23 shows the cycle diagram for case 12. The boiler efficiency is 93.2% and the overall cycle efficiency is 29.8% (Table 4.2.5). The 4.7% losses in the boiler efficiency is comprised of 17% sensible heat, 66% latent heat (H_2O), 14% unburned carbon, 3% radiation. Since it is likely that with O_2-fired combustion and a high flame temperature, the unburned carbon loss will be nearly zero (confirmed in Section 4.4.1.5), the boiler efficiency would be 94.1% and the overall cycle efficiency would be 30.1%.

4.2.9 Design Case: Case 13

To further reduce the required furnace surface area while increasing the net cycle efficiency, the flue gas recycle flow rate was reduced from 65% (case 12) to 56% (case 13). All features of case 12 are incorporated in case 13. In addition part of the CO_2 compressor inter-stage cooling is used to replace part of the economizer duty in the feed water heating train.

Figure 4.2.25 shows the cycle diagram for case 13. The boiler efficiency is 93.5% and the overall cycle efficiency is 30.3% (Table 4.2.5). The 4.7% losses in the boiler efficiency is comprised of 15% sensible heat, 67% latent heat (H_2O), 14% unburned carbon, 3% radiation. Since it is likely that with O_2-fired combustion and a high flame temperature, the unburned carbon loss will be nearly zero (confirmed in Section 4.4.1.5), the boiler efficiency would be 94.5% and the overall cycle efficiency would be 30.6%.

4.2.10 Furnace Waterwall Temperature

The level of radiation in the O_2-fired boiler is significantly higher than an air-fired boiler due to greater concentrations of radiating gas species (CO_2 and H_2O) and higher flame temperature. Consequently, it is important to select the proper

amount of recycled flue gas to limit the water wall temperature such that a reasonable waterwall material can be used.

The maximum waterwall temperature and furnace heat flux was calculated from the ASPEN results using the Foster Wheeler computer program, EMISS. The EMISS computer program calculates radiative heat flux of CO_2 and H_2O gases as follows:

$$Q/A = \left(\frac{\varepsilon_{wall}+1}{2}\right)\sigma(\varepsilon_g T_g^4 - \alpha_g T_w^4)$$

$$Q/A = U_O(T_W - T_f)$$

where,

ε = $\varepsilon_{CO2} + \varepsilon_{H2O} - \Delta\varepsilon$
$\Delta\varepsilon$ = Correction factor due to spectral overlap
ε_{CO2} = Emissivity of CO_2 (function of temperature, mean beam length, and partial pressure of CO_2)
ε_{H2O} = Emissivity of H_2O (function of temperature, mean beam length, and partial pressure of H_2O)
ε_g = Emissivity of gas at gas temperature
α_g = Absorptivity of gas at wall temperature (equal to emissivity)
ε_{wall} = Tube wall emissivity (assumed to be 0.7)
σ = Stefan-Boltzmann constant = 1.714×10^{-9} Btu/hr-ft^2-R^4
Q/A = Heat Flux (Btu/hr-ft^2)
T_f = Water/Steam fluid temperature (ºR)
T_g = Gas temperature (ºR)
T_w = Wall temperature (ºR)
U_o = Heat transfer coefficient from outside of wall to steam/water (Btu/hr-ft^2-F)

Table 4.2.6 presents the calculated furnace heat flux for cases 1 to 13. Both the maximum heat flux (based on the maximum furnace gas temperature) and the average heat flux (based on the average furnace gas temperature) are presented. Based on the maximum heat flux, the maximum water wall temperature is computed. From this maximum wall temperature and the selected material, the minimum tube wall thickness is computed using stress allowables from the ASME Boiler and Pressure Vessel Code.

Due to CO_2 dissociation into CO and O_2, the equilibrium flame temperature is lower than the adiabatic temperature. Figure 4.2.21 presents the equilibrium values of CO_2 and CO concentration versus flue gas recycle flow. The effect of CO_2 dissociation is shown in Figure 4.2.22, which presents the adiabatic temperature (without CO_2 dissociation) and equilibrium temperature (with CO_2 dissociation) versus flue gas recycle flow. The maximum flame temperature applied for furnace wall temperature calculations is based on a temperature

slightly lower than the equilibrium temperature to account for heat loss by the flame.

Table 4.2.6 shows that for the air-fired reference case (case 1), the waterwalls are carbon steel with a 0.30" wall thickness. Even though the O_2-fired cases 2 and 3 have similar furnace gas temperatures than case 1, the substantially greater concentrations of CO_2 and H_2O results in a radiative heat flux of approximately 50% higher. Thus, to maintain the same wall thickness requires an upgrade in the material to the T2 alloy. As the flame temperature is increased in cases 4 to 6 and cases 9 to 11, the heat flux and wall temperature increases requiring further material upgrades. For case, the maximum wall temperature is 960ºF for which 0.24" thick T91 material is required.

The ratio of the average furnace heat flux of the O_2-fired furnace to the average furnace heat flux of the air-fired furnace is also presented in Table 4.2.6. For case 13 this ratio is 0.53, which means that case 13 requires only approximately 53% of the case 1 heating surface area. This can be used as a preliminary estimate of the O_2-fired furnace size. Table 4.2.6 shows that the air-fired furnace dimensions of 36' x 51' x 207' (D x W x H) are substantially reduced to 30' x 43' x 142' (D x W x H) in case 12 and 27' x 38' x 134' (D x W x H) in case 13. Section 4.4.1.5 conducted a detailed design of the O_2-fired boiler in detail by performing a three-dimensional CFD simulation.

4.2.11 Comparison With Post CO_2 Capture

CO_2 cannot be free captured and sequestrated without reducing both the plant power and efficiency because of a potential energy stored in the pressurized liquid CO_2. A minimum of 40 kw/klb$_{CO2}$ additional auxiliary power is required for CO_2 compression. The difference between technologies lies in the difference in power requirements of the different CO_2 or O_2 separation techniques.

Parsons [12] performed some studies on CO_2 removal by a post capture method for a conventional PC boiler. The plant efficiency drops from 40.5% to 28.9% for a supercritical (3500 psia/1050ºF/1050ºF/1050ºF/2.0"Hg) boiler, and from 42.7% to 31.0% for an ultra supercritical (5000 psia/1200ºF/1200ºF/1200ºF/2.0"Hg) boiler. In the study presented herein, the CO_2 removal using an O_2-fired PC is used, which relies on an ASU. The efficiency drops from 36.7% (case 1) to 30.6% (case 13 with minimal UBC loss) for a subcritical (2415 psia/1000ºF/1000ºF/2.5"Hg) boiler. Since the Parsons study compressed the effluent CO_2 to 1200 psia, whereas this study herein compressed the CO_2 to 2000 psia, the 1200 psia pressure is used as comparison basis, which increases the case 13 efficiency to 30.8%. The net efficiency drops for these cases are

11.7% points for supercritical, post combustion CO_2 removal
11.7% points for ultra supercritical, post combustion CO_2 removal
5.9% point for subcritical, O_2 fired

Based on the Parson's study it appears that the efficiency reduction is independent of steam cycle. However, there is a big difference between the efficiency reductions for post capture and O_2-fired. Furthermore, the O_2-fired method gives near 100% CO_2 removal, while the post capture is practically limited to about 90% (limited by a vapor-liquid equilibrium from absorption-regeneration cycle).

Another comparison basis is the kw/lb_{CO2} removal, where the kw is power generation difference between cases with and without CO_2 removal. Comparing the post CO_2 capture to the O_2-fired case:

187 kwh/lb_{CO2} for supercritical, 90% post combustion CO_2 removal
188 kwh/lb_{CO2} for ultra supercritical, 90% post combustion CO_2 removal
80 kwh/lb_{CO2} for subcritical, O_2 fired 100% removal

Again, the change in power penalty for CO_2 removal appears independent of steam cycle. From above data, it is very clear that the O_2-PC has advantages over the post CO_2 capture.

The efficiency of carbon sequestration in oxygen-firing boilers even can rival competing gasification plants**.** Figure 4.2.27 compares the power consumption of adding CO_2 removal equipment to various competing technologies. Figure 4.2.27 shows that the power consumption of CO_2 removal for O_2-fired PC plants is less than one-third of natural gas combined cycles (NGCC), less than one-half of post CO_2 removal PCs and 80% of integrated gasification combined cycles (IGCC). Figure 4.2.28 compares the reduction in power plant efficiency of adding CO_2 removal equipment to various competing technologies. Figure 4.2.28 shows that the reduction in power plant efficiency of CO_2 removal for O_2-fired PC plants is nearly half of either natural gas combined cycles (NGCC) or post CO_2 removal PCs and slightly less than integrated gasification combined cycles (IGCC). And once again note that the O_2-firing PC is the only technology that removes 100% of the CO_2.

Table 4.2.1 – Site Conditions and Coal Properties

Elevation	ft	0	
Ambient pressure	psia	14.70	
Ambient Temperature	F	59.0	
Ambient Temperature, wet	F	51.5	
Relative Humidity	%	60.0	
P-H2O	psia	0.247	
Y-H2O	%, vol	1.010	
Condenser Pressure	" Hg	2.50	
Air Composition		Dry	Wet
N2	%, vol	78.085	77.297
O2	%, vol	20.947	20.735
Ar	%, vol	0.935	0.926
CO2	%, vol	0.033	0.033
H2O	%, vol	0.000	1.010
Total	%, vol	100.000	100.000

Illinois No. 6 Coal		
C	%	63.75%
H	%	4.50%
O	%	6.88%
N	%	1.25%
Cl	%	0.29%
S	%	2.51%
Ash	%	9.70%
H2O	%	11.12%
Total	%	100.00%
LHV	Btu/lb	11,283
HHV	Btu/lb	11,631

Figure 4.2.1 – Cycle Analysis of Case 1 (Air-Fired Reference Case)

Case: O2-PC-01, 05/30/2003

ST=2415/1000/1000/2.5"Hg=460 MW

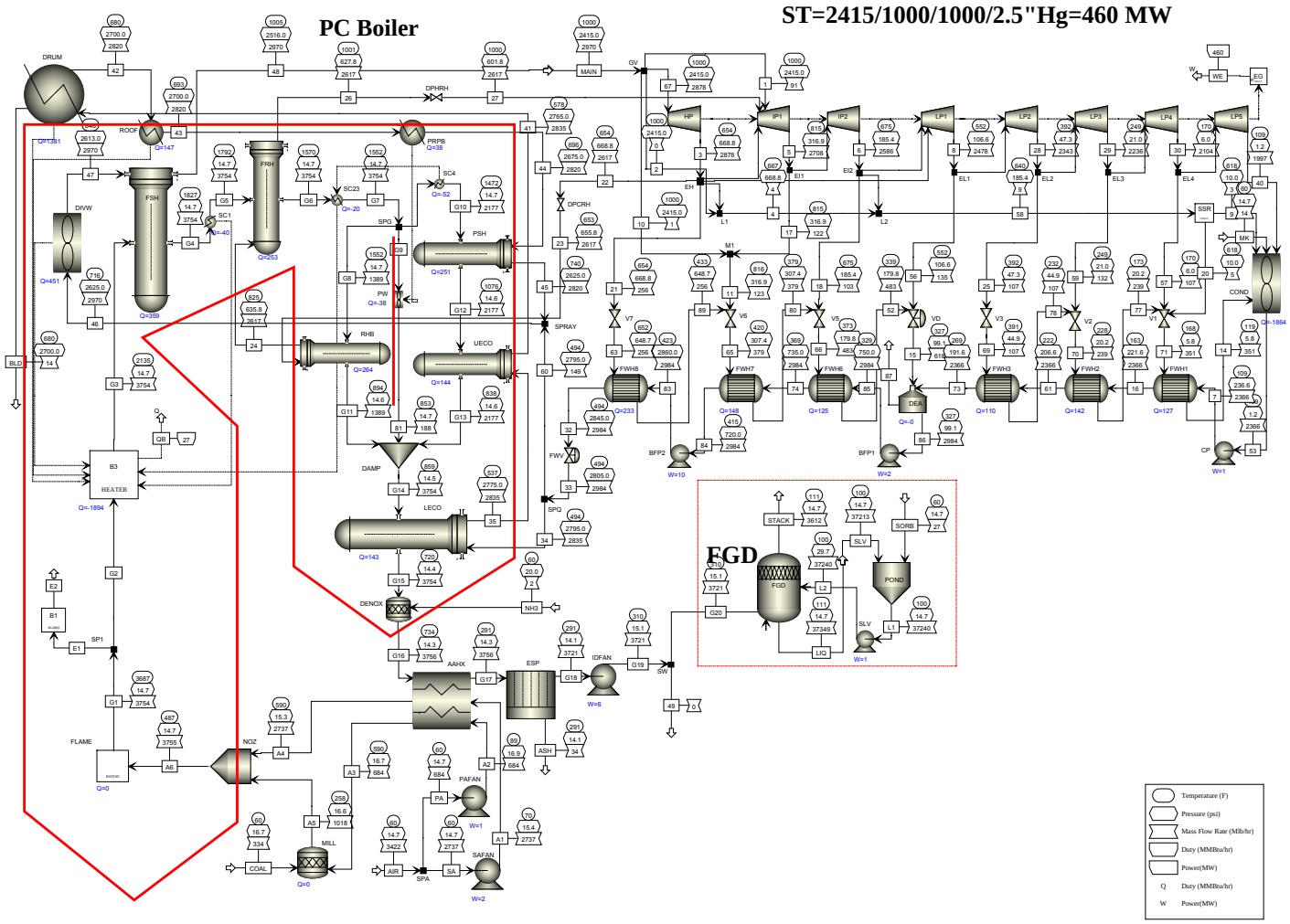

Table 4.2.2 – Case 1 (Air-Fired Reference) Boundary Conditions and Results

SETUPS & RESULTS									
amb			**dP-air**	"H2O		**ST**			**result**	
elevation, ft	0		AAHX	4.0		main P, psia	2415		net power, MWe	418
amb T, F	60		duct	6.0		main T, F	1000		net eff, %	36.68
amb P, psia	14.7		nozzle	10.0		RH P, psia	602		gross @ST, MW	460
RH, %	60		sum	20.0		RH T, F	1000		aux power, MW	42.1
						FWHs	7		as %	9.2
air	%v		**dp-gas**	"H2O		end wet, %	9.9			
O2	20.74		FSH	0.5		end P, "Hg	2.5		HHV in, mmbtu	3890
N2	77.3		FRH	0.5					Q to ST, mmbtu	3431
Ar	0.93		RH	1.0		**FWH**	F		Q, cond, mmbtu	1864
CO2	0.03		PSH	0.7		TD	5		boiler eff, %	88.2
H2O	1.01		UECO	0.3		DC	10		ST cycle eff, %	45.78
sum	100.0		ECO	2.0		FW T	494		Generator eff, %	98.3
			AAHX	1.6						
coal	%w		Damper	4.3		**DeSuperheat**			air, klb	3422
C	63.75		BHG	5.5		SH, %	5		coal, klb	334
H	4.5		FGD	12.0		water T, F	494		sorb, klb	26
O	6.88		sum	28.4					flue gas, klb	3721
N	1.25					**Boiler**			O2, %	3.0
S	2.51		**dP**	"H2O		UBC, %	1.0		H2O, %	8.5
A	9.99		PAFan	60		margin, %	0.5		CO, ppmv	71
M	11.12		IDFan	28		radiation, %	0.22		NOx, ppmv	733
V	34.99		SAFan	20		Exa, %	18		SOx, ppmv	2082
F	44.19					flame T, F	3839		after FGD	42
sum	100.0		**eff**	%		stack T, F	292		Ash, klb	34
			FDFan	75		blowdown, %	0.5		C, %	6.0
fuel HHV	btu/lb		IDFan	70		miller exit T, F	258			
given	11666		CWPump	80					main st flow, klb	2970
aspen	11631		BFPump	80		**FGD & SCR**			RH st flow, klb	2878
			Motor/mechanic	95		L/G	10		end st flow, klb	1997
sorb	%w					Ca/S	1.05			
CaCO3	100		**air**	%		Excess air, %	85		DeSOx, %	98
			PA	20		NH3/NOx	1.0		DeNOx, %	90

Table 4.2.3 – Auxiliary Power Requirements for Case 1

Aux power		MWe
condensed water pump		0.6
LP feed water pump		2.5
HP feed water pump		9.8
circulating water pump		3.9
FGD pump		0.7
PA Fan		1.5
SA Fan		2.0
ID Fan		5.6
FGD Fan		4.1
cooling tower Fan		2.1
coal handling		2.1
sorb handling		0.8
ash handling + ESP		1.8
others (=1%)		4.6
total		42.1

Figure 4.2.2 – Air Separation Unit

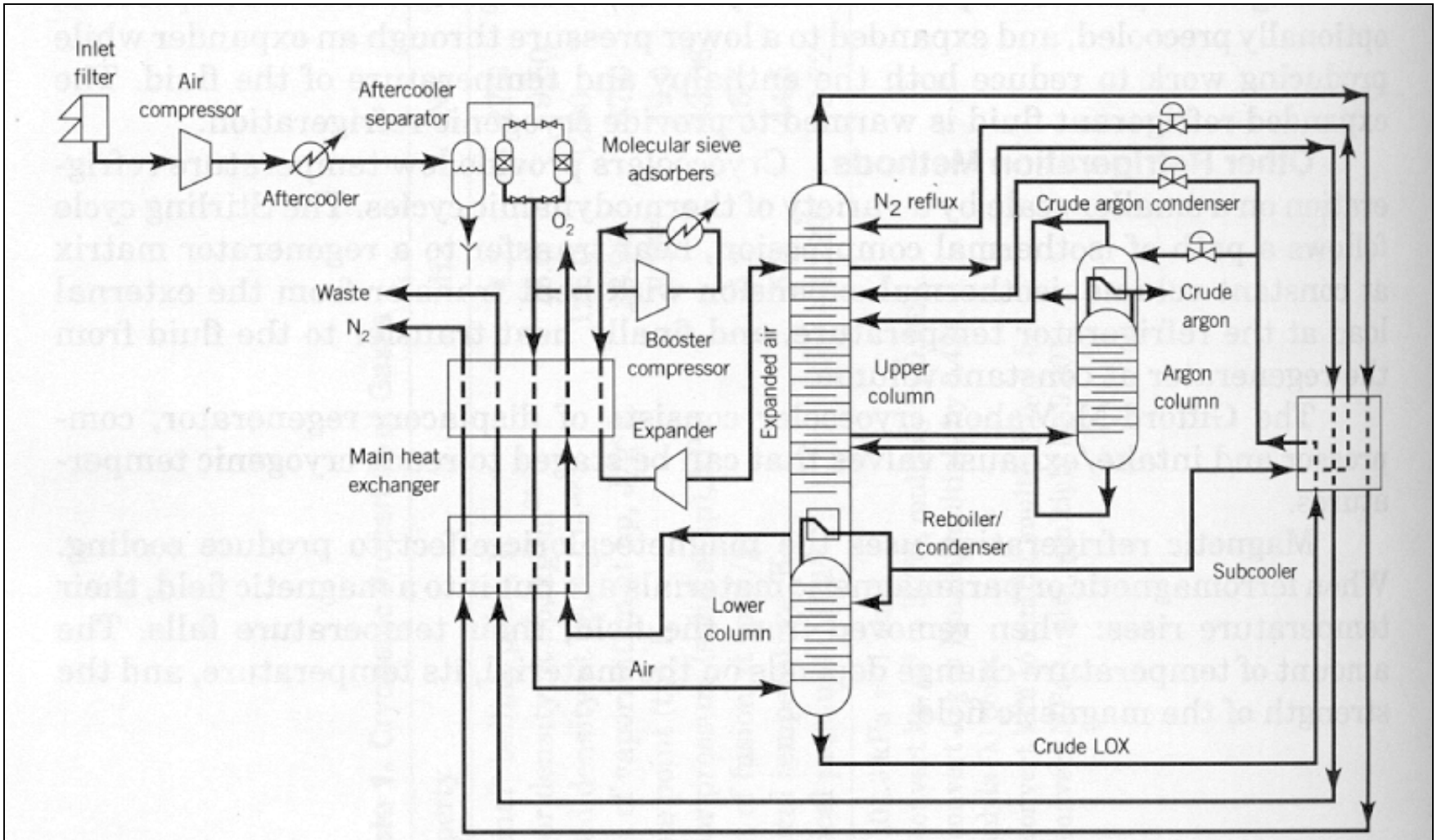

Fig. 1. Cryogenic air separation process. LOX = liquid oxygen.

Figure 4.2.3 – ASPEN ASU Model

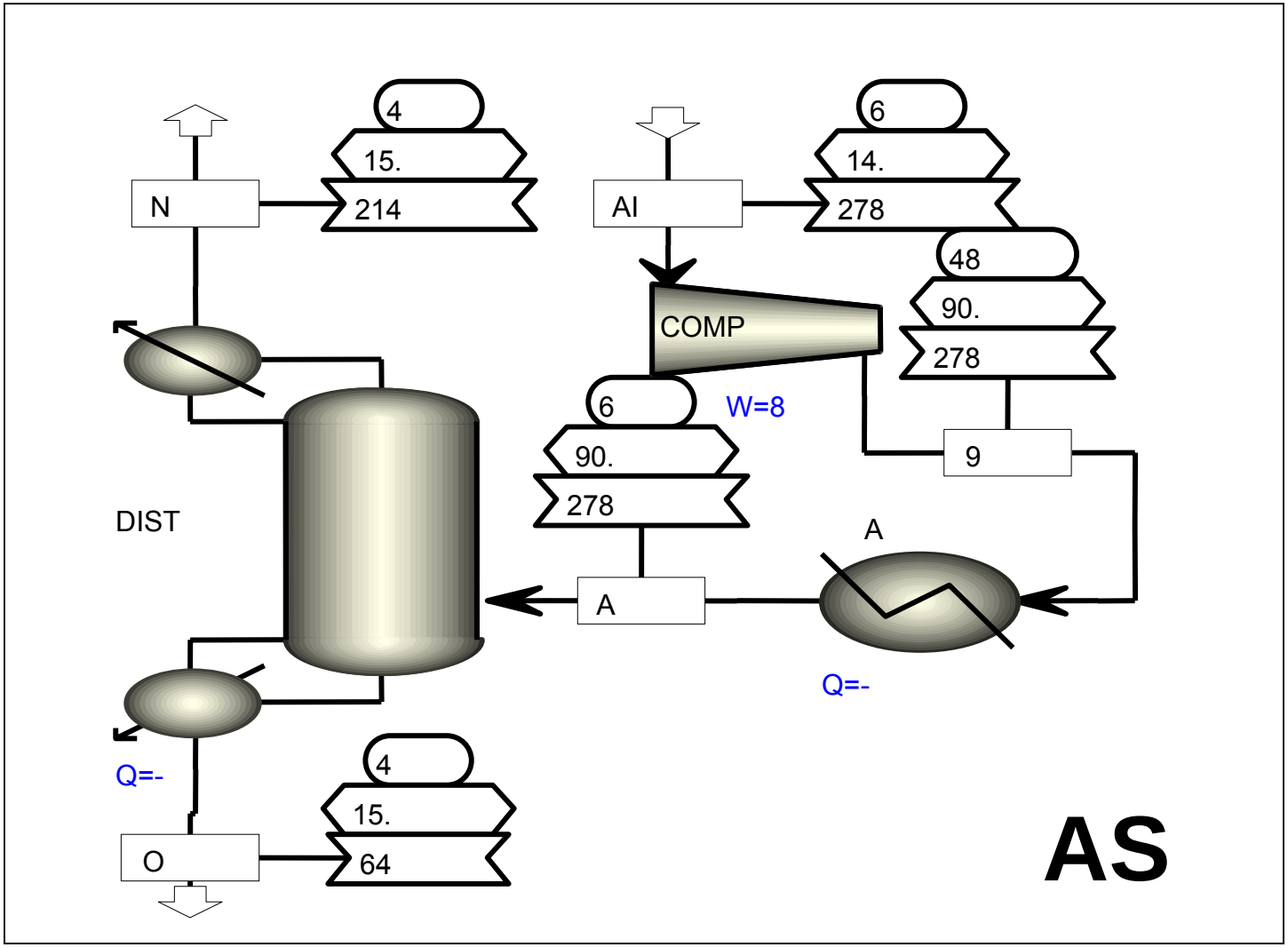

Figure 4.2.4 – Case 2 Cycle Diagram

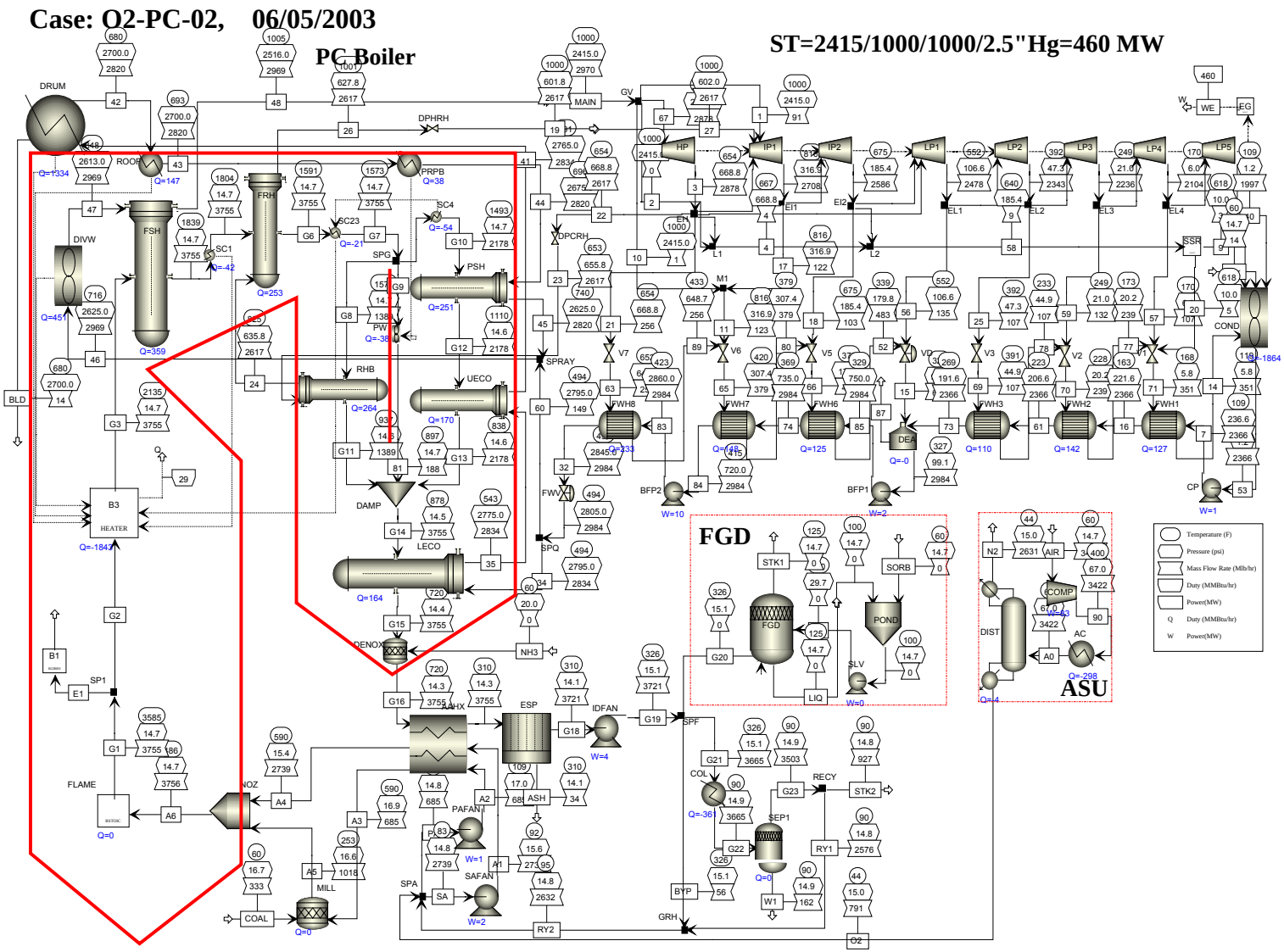

Figure 4.2.5 – Case 3 Cycle Diagram

Case: O2-PC-03, 06/05/2003

ST=2415/1000/1000/2.5"Hg=460 MW

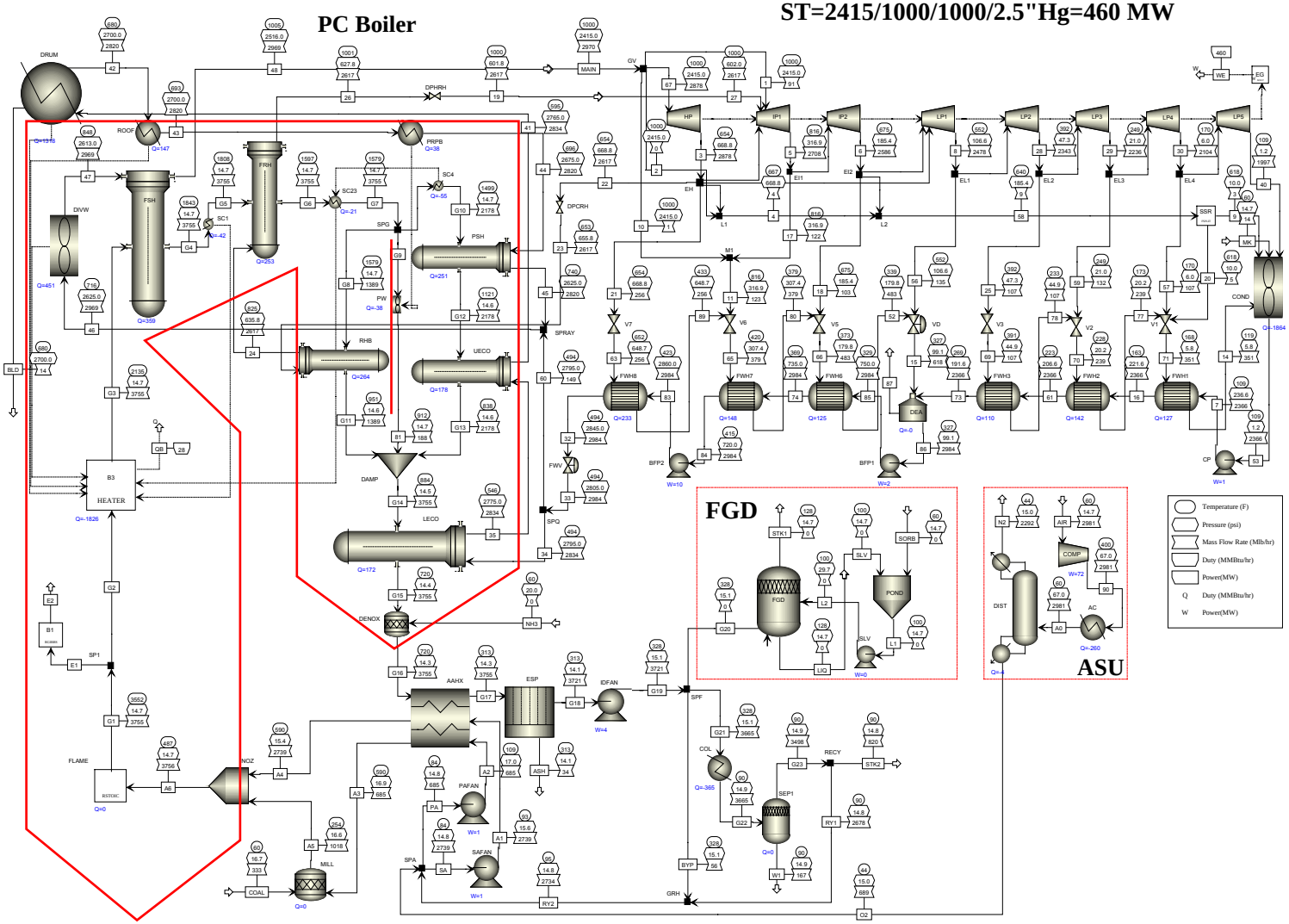

Figure 4.2.6 – Case 4 Cycle Diagram

Case: O2-PC-04, 06/05/2003

ST=2415/1000/1000/2.5"Hg=460 MW

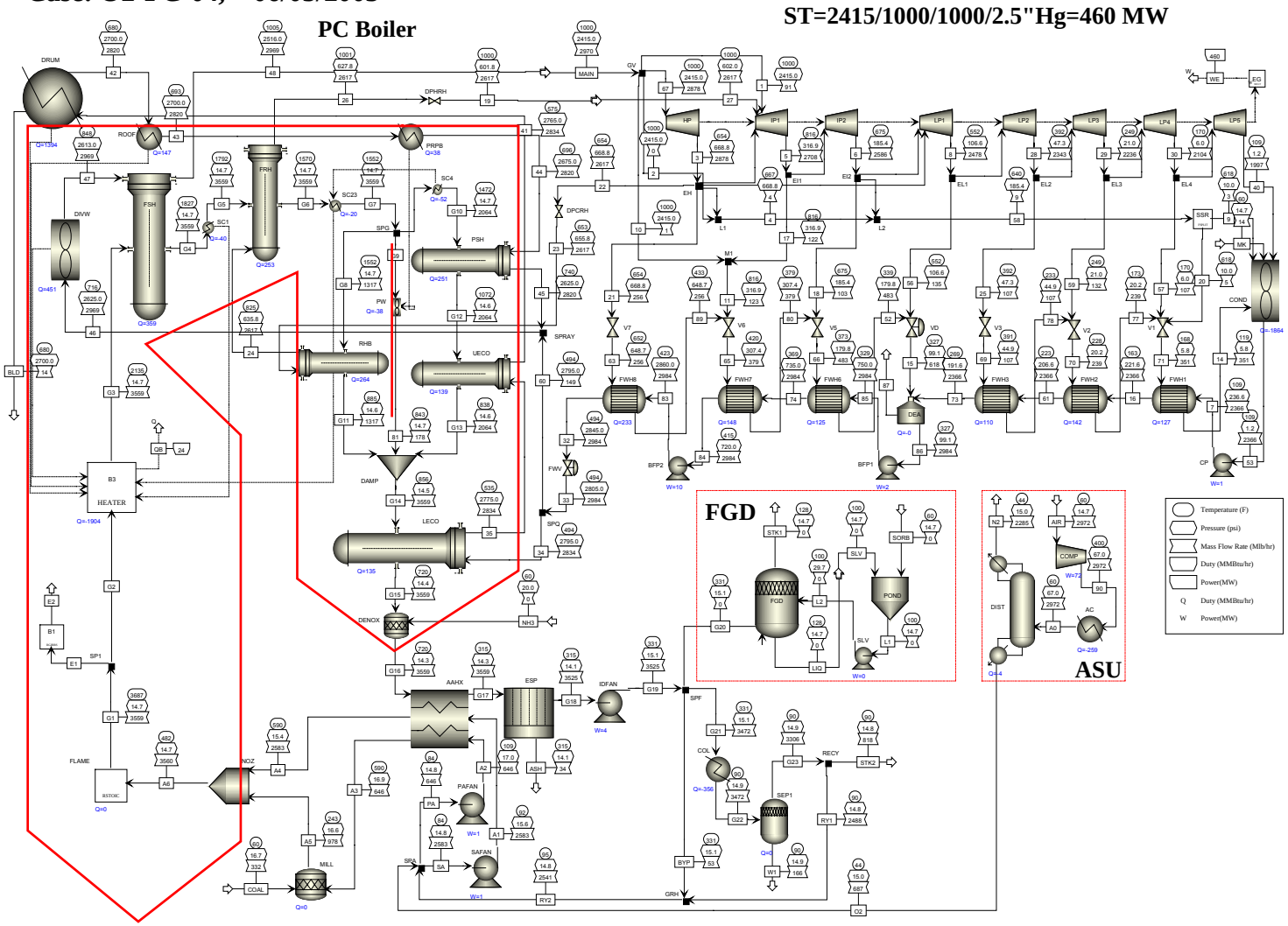

Figure 4.2.7 – Case 5 Cycle Diagram

Case: O2-PC-05, 06/05/2003

ST=2415/1000/1000/2.5"Hg=460 MW

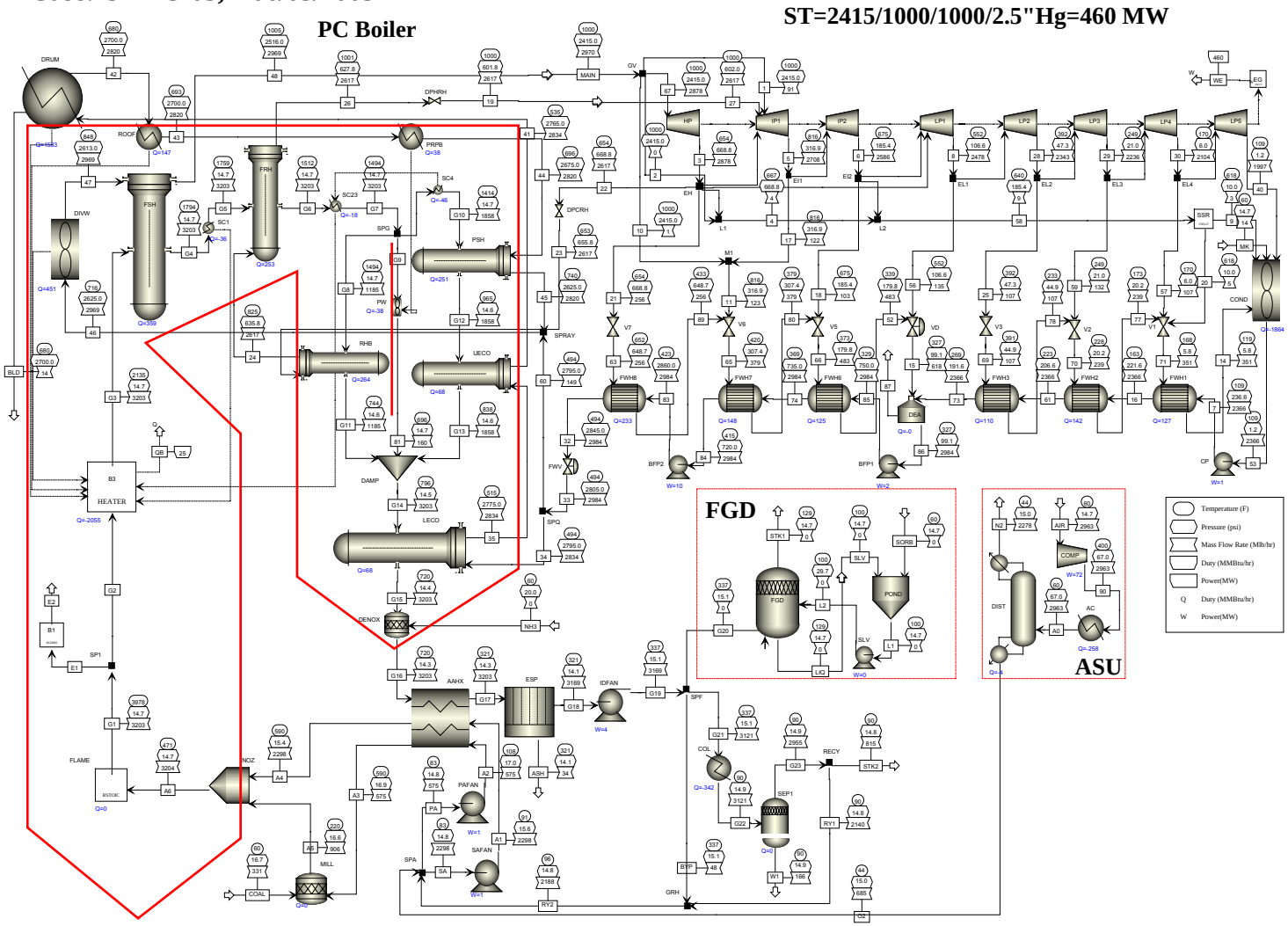

Figure 4.2.8 – Case 6 Cycle Diagram

Case: O2-PC-06, 06/05/2003

ST=2415/1000/1000/2.5"Hg=460 MW

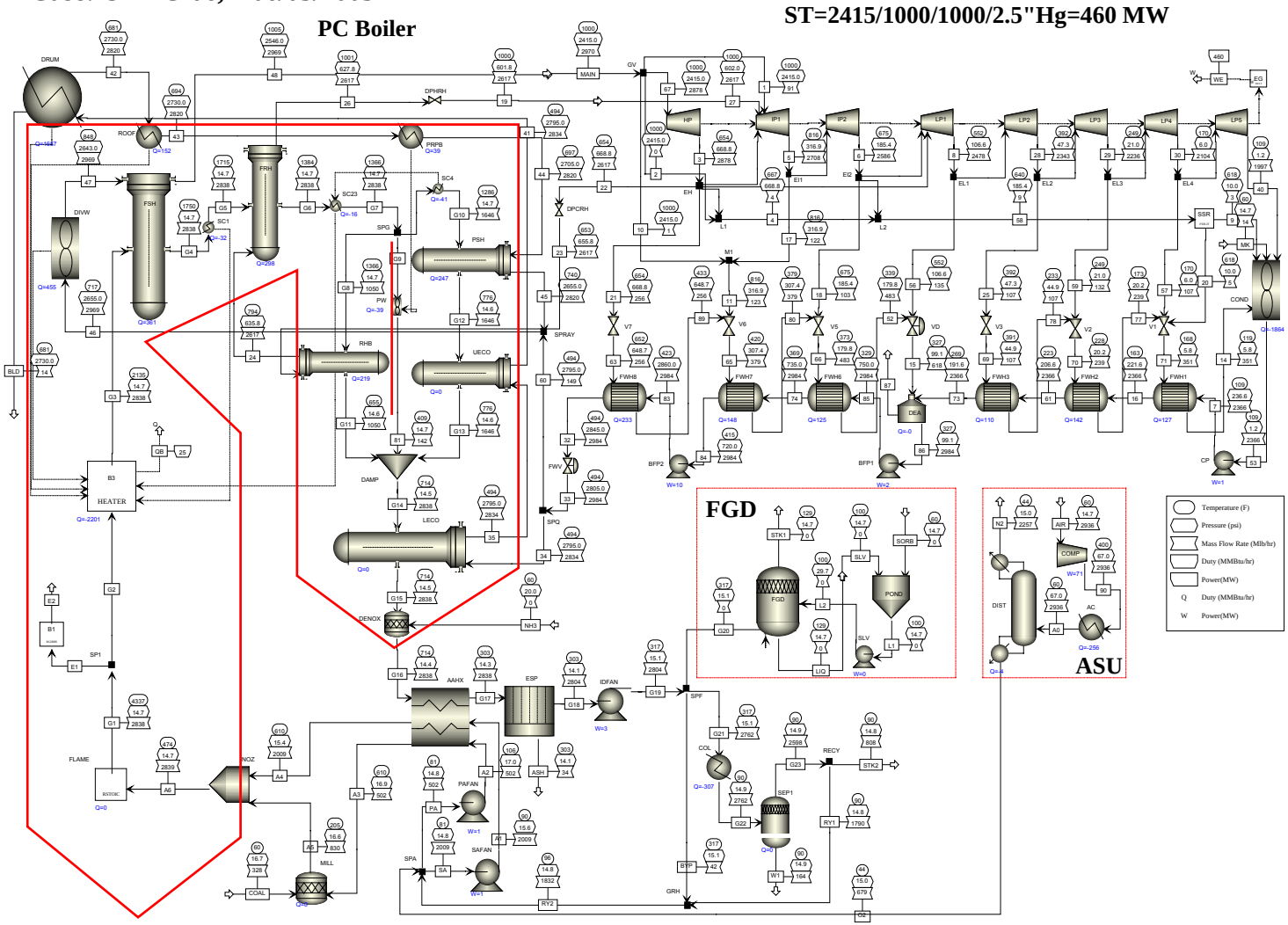

Figure 4.2.9 – Case 7 Cycle Diagram

Case: O2-PC-07, 06/05/2003

ST=2415/1000/1000/2.5"Hg=460 MW

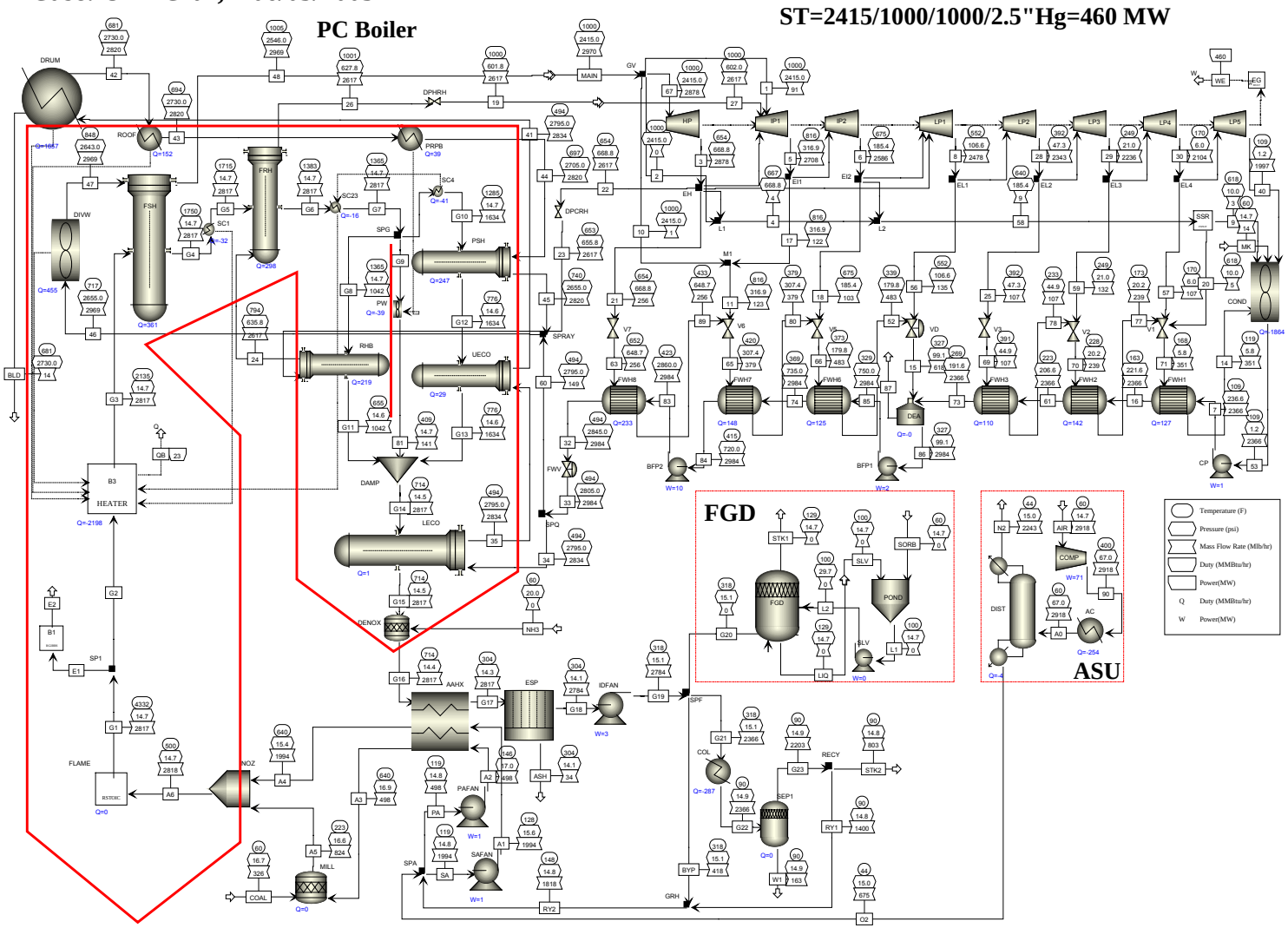

Table 4.2.4 – Parametric Cases Summary (Without CO_2 Compression)

case	1	2	3	4	5	6	7
ASU	no	yes	yes	yes	yes	yes	yes
coal to boiler, klb/h	334	333	333	332	331	328	326
air to plant, klb/h	3422	3422	2981	2972	2963	2936	2918
O2 purity, %	20.7	99.6	99.6	99.6	99.6	99.6	99.6
O2 level to boiler, %	20.4	39.7	26.9	28.1	30.9	34.1	33.7
O2 level exit boiler, %	3.0	15.3	3.0	3.0	3.0	3.0	3.0
Net EXA, %	18.0	18.0	3.1	3.1	3.0	3.2	3.2
Boiler EXA, %	18.0	69.1	13.6	12.5	11.2	10.4	10.4
adiabatic temperature, F	3687	3608	3574	3687	3978	4337	4332
gas to boiler exit, klb/h	3721	3721	3721	3525	3169	2804	2784
gas to boiler exit, mmcft/h	237	181	175	167	151	134	135
gas recycle to boiler, klb/h	0	2632	2734	2541	2188	1832	1818
gas T before IDFan, F	291	307	309	315	321	303	304
Recycled gas T, F	-	95	95	95	95	96	148
gas exit system, klb/h	3721	927	820	818	815	808	803
CO2, %v	14.0	76.4	89.6	89.6	89.6	89.6	89.6
ASU plant power, MW	0	83.0	72.3	72.1	71.8	71.2	70.7
Aux power, MW	42.1	116.7	105.8	105.3	104.4	102.7	102.5
Boiler eff, %	88.2	88.3	88.3	88.6	88.9	89.60	90.94
Net eff (w/o CO2), %	36.68	30.19	31.15	31.29	31.46	31.90	32.12

Figure 4.2.10 – Net Efficiency (without CO_2 compression) Versus Adiabatic Temperature

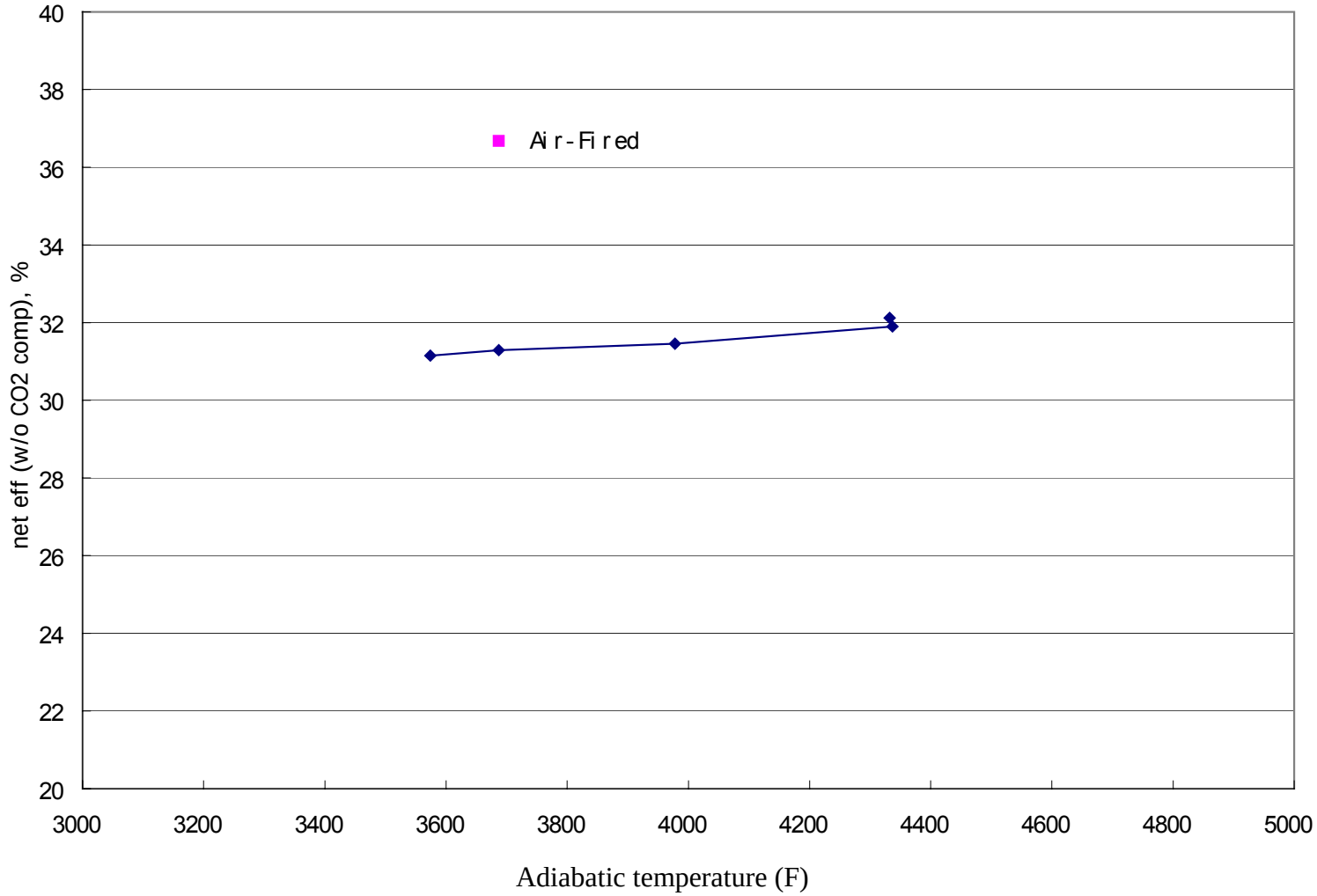

Figure 4.2.11 - ASU and Auxiliary Power Requirements Versus Adiabatic Temperature

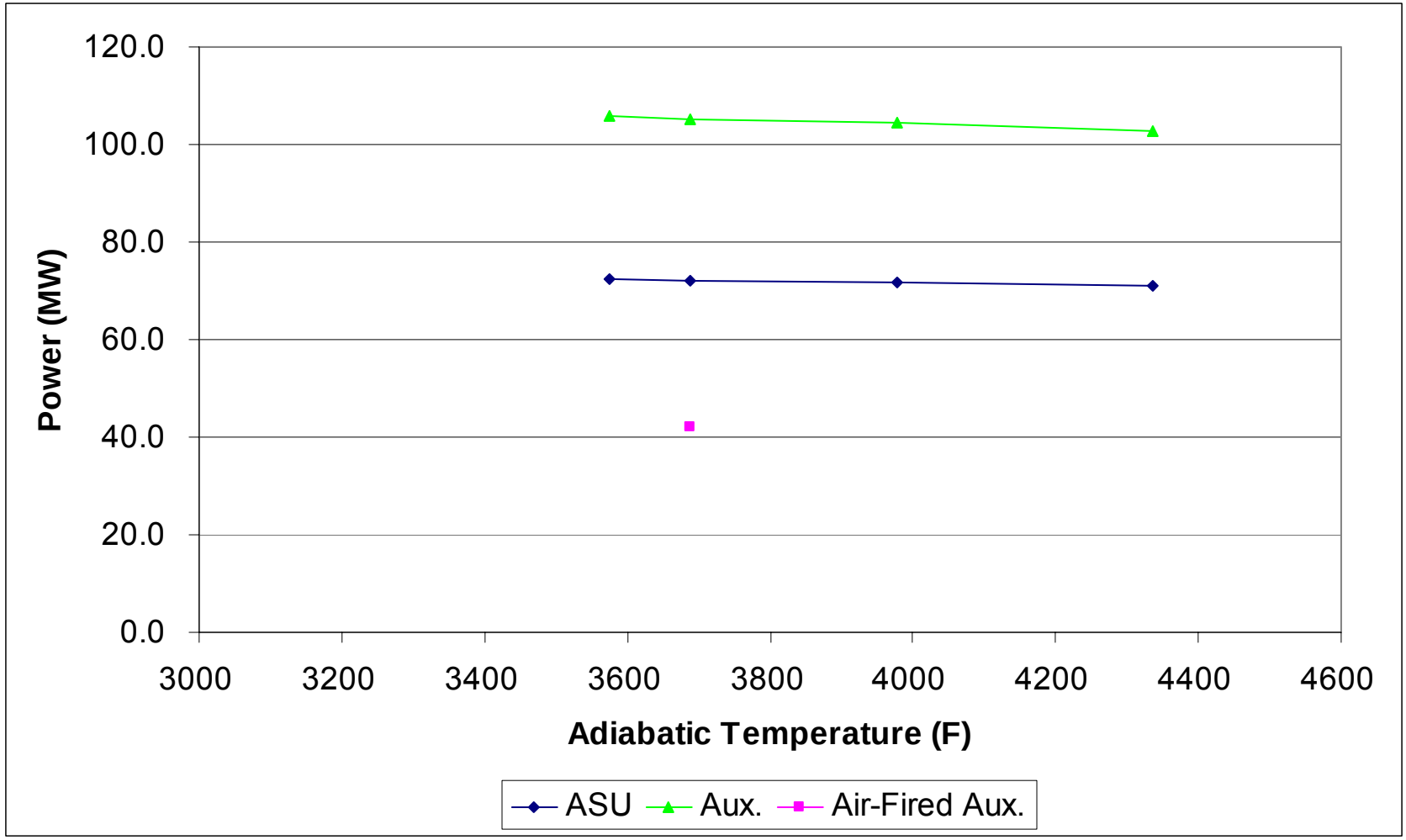

Figure 4.2.12 – Recycled Gas Mass Flow Rate Versus Adiabatic Temperature

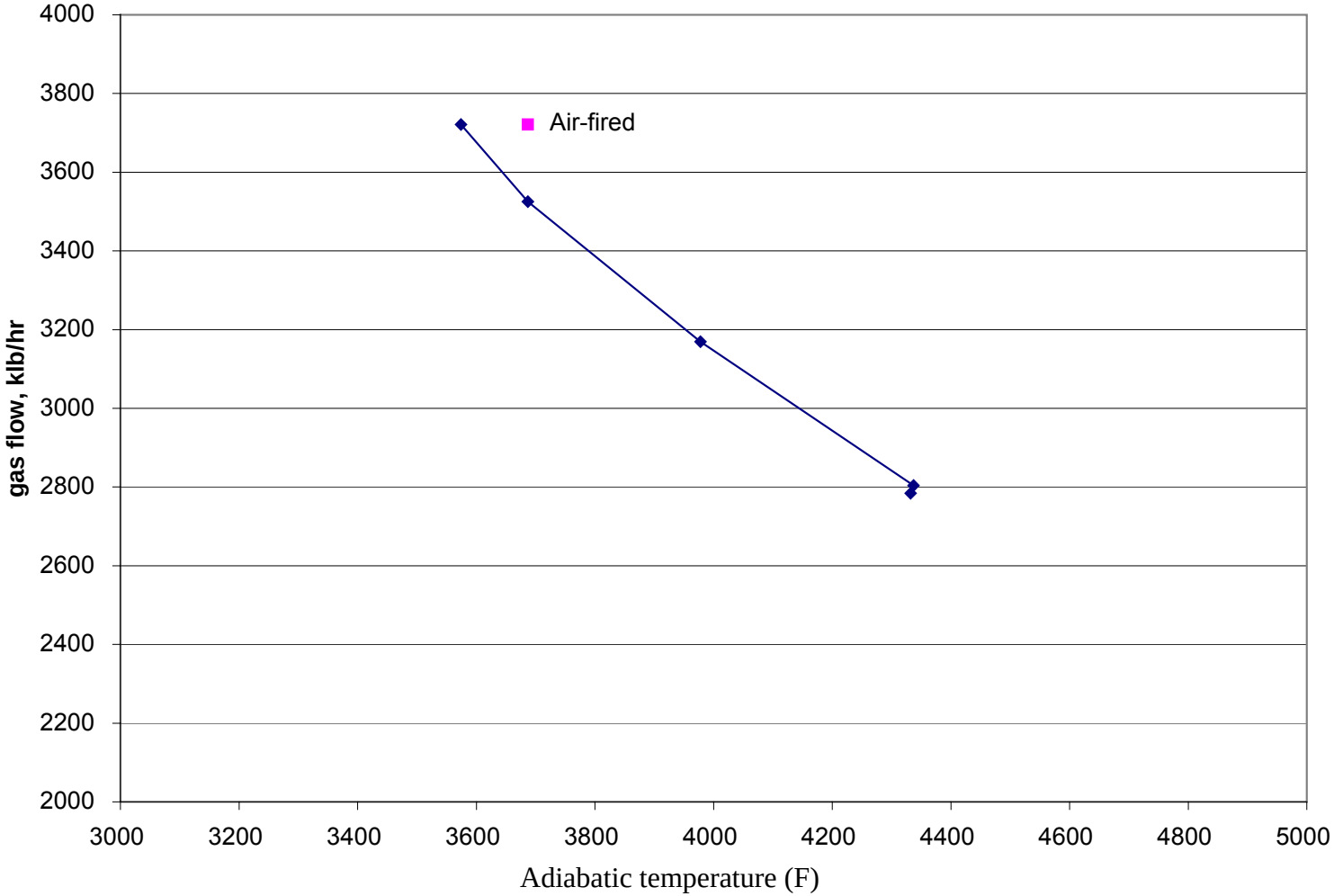

Figure 4.2.13 – Recycled Gas Volumetric Flow Rate Versus Adiabatic Temperature

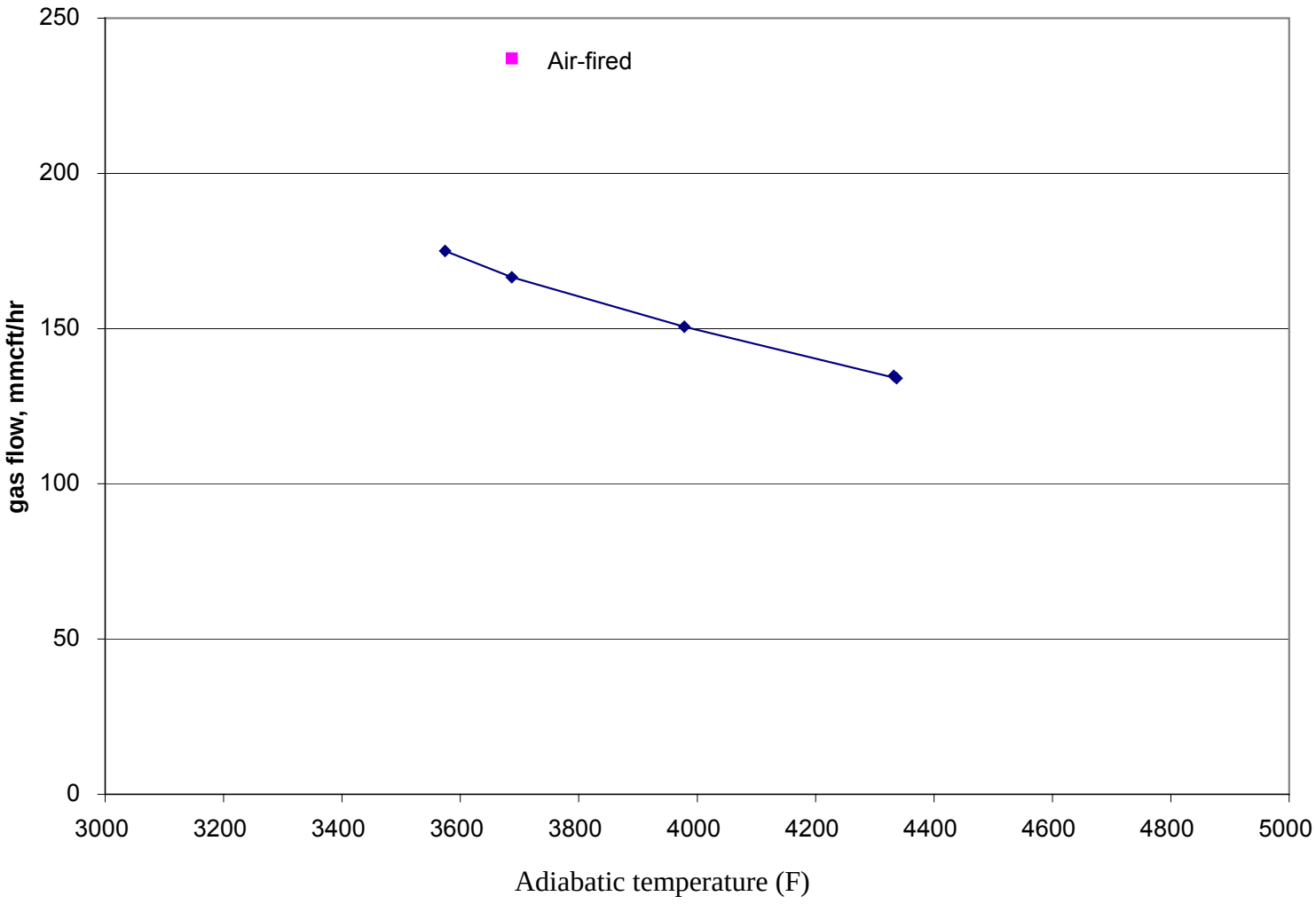

Figure 4.2.14 – Flue Gas Cooling Curve

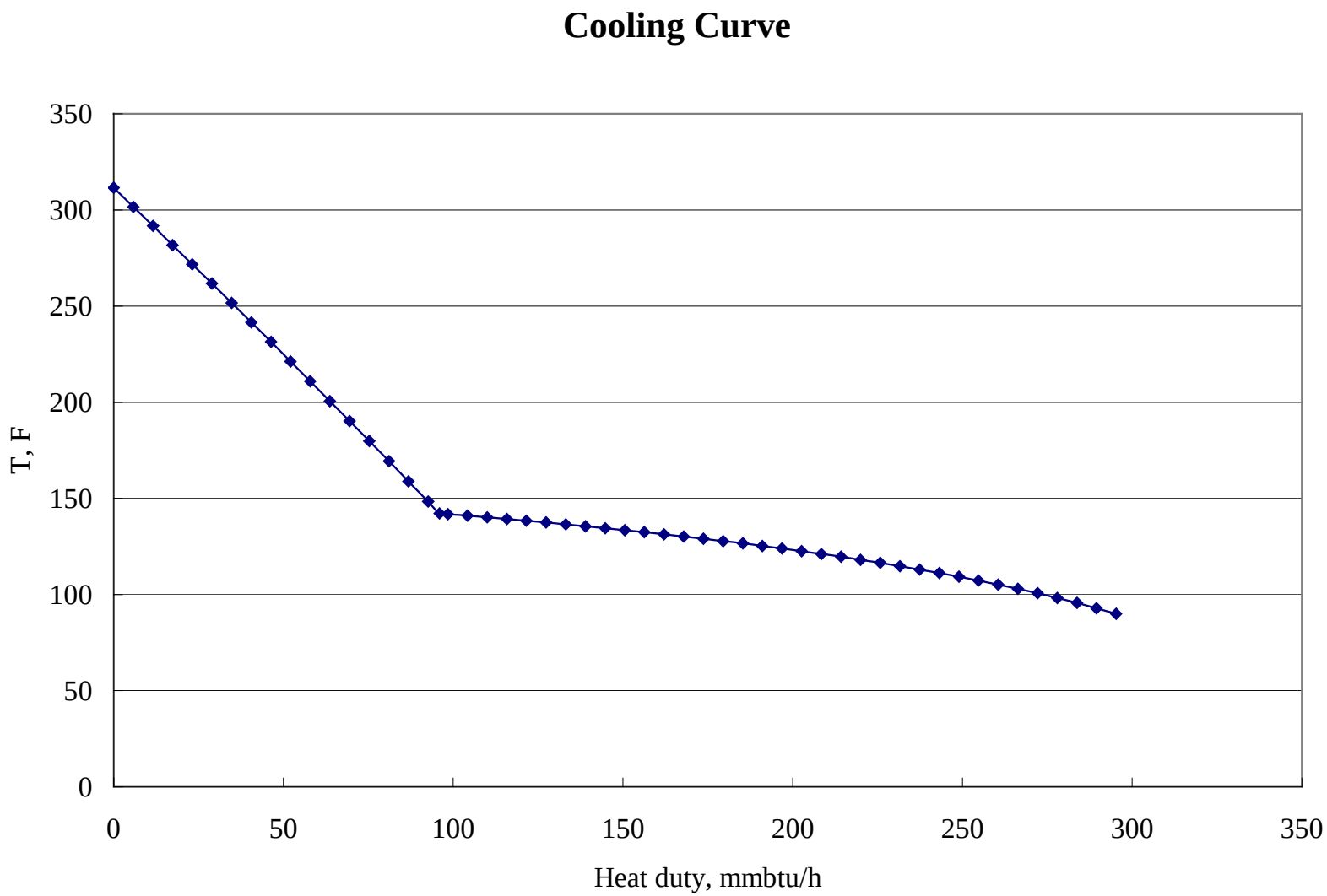

Figure 4.2.15 – Case 8 Cycle Diagram

Case: O2-PC-11, 08/04/2003

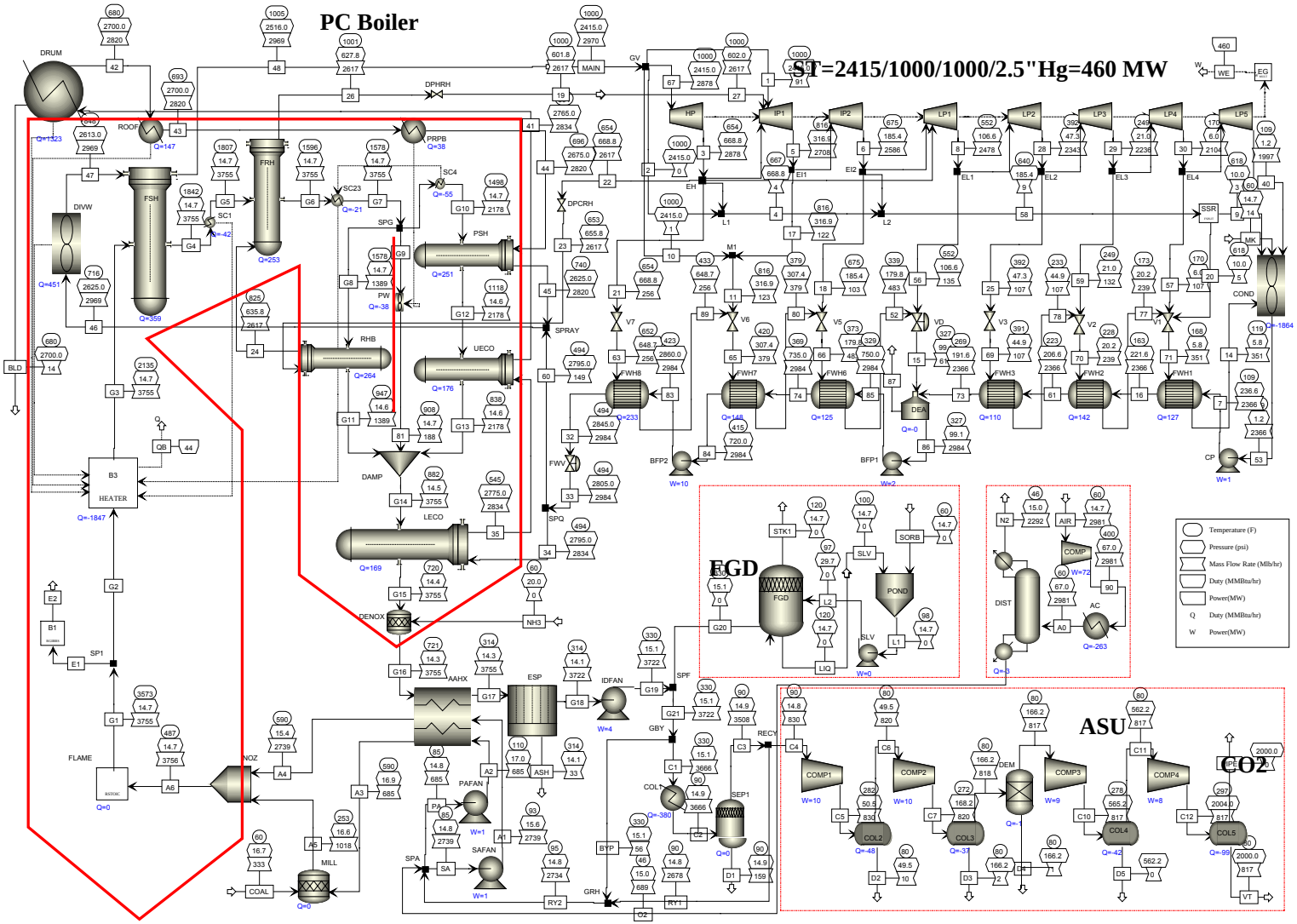

Figure 4.2.16 – Case 9 Cycle Diagram

Case: O2-PC-12, 08/07/2003

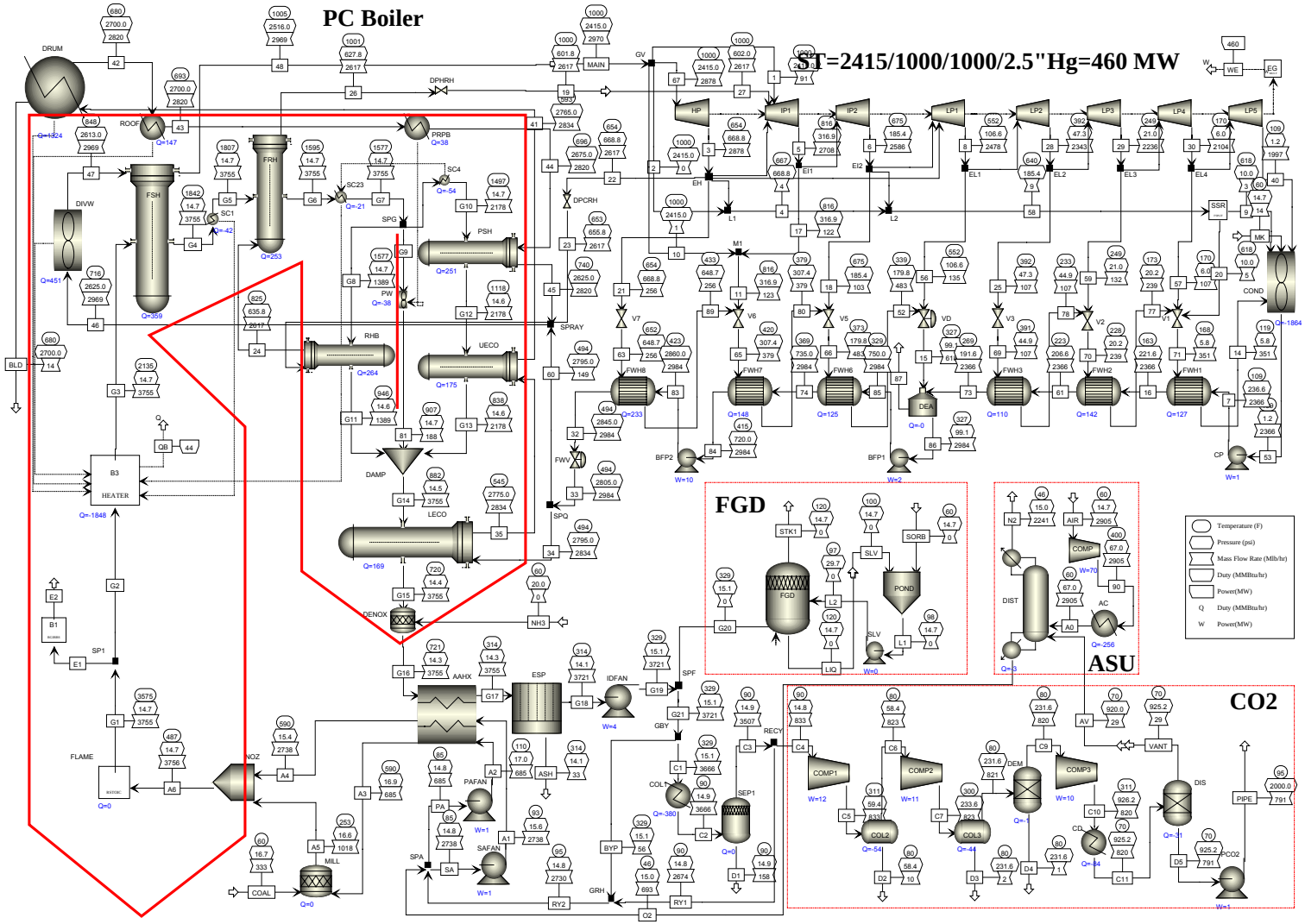

Figure 4.2.17 – Net Cycle Efficiency Vs. Flue Gas Recycle Flow

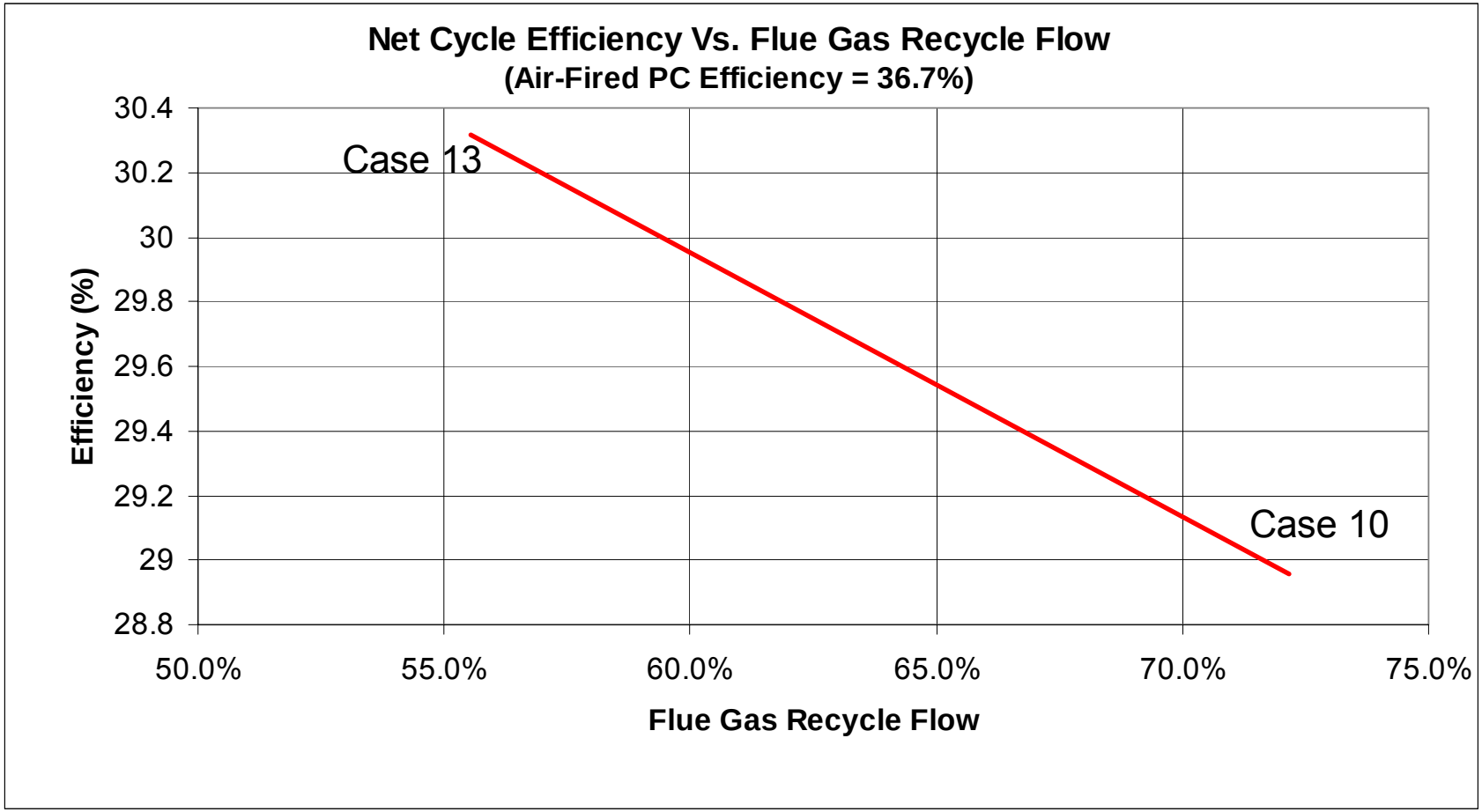

Figure 4.2.18 – Case 10 Cycle Diagram

Case: O2-PC-13, 09/08/2003

ST=2415/1000/1000/2.5"Hg=460 MW

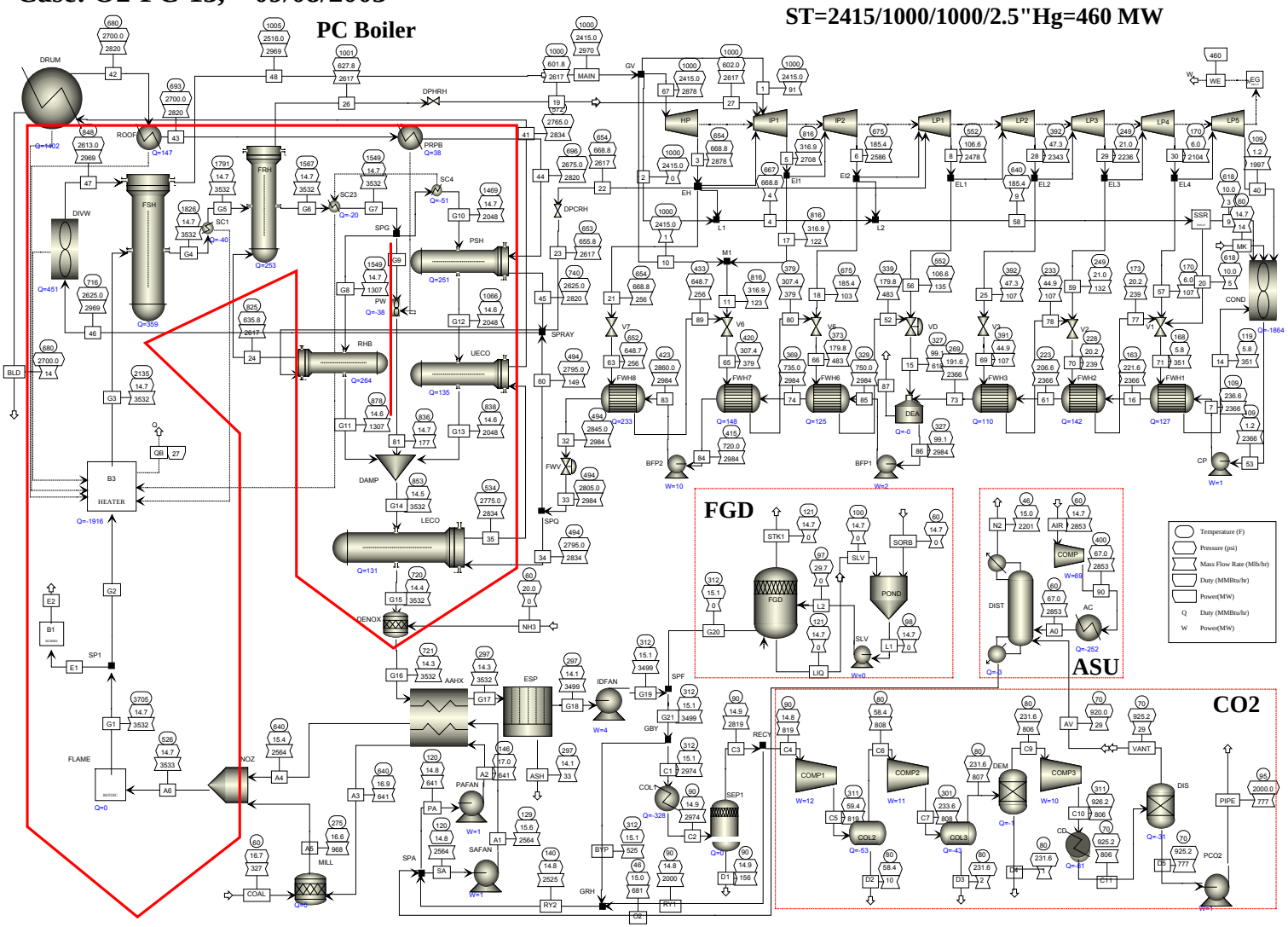

Figure 4.2.19 – Case 11 Cycle Diagram

Case: O2-PC-14, 10/22/2003

ST=2415/1000/1000/2.5"Hg=460 MW

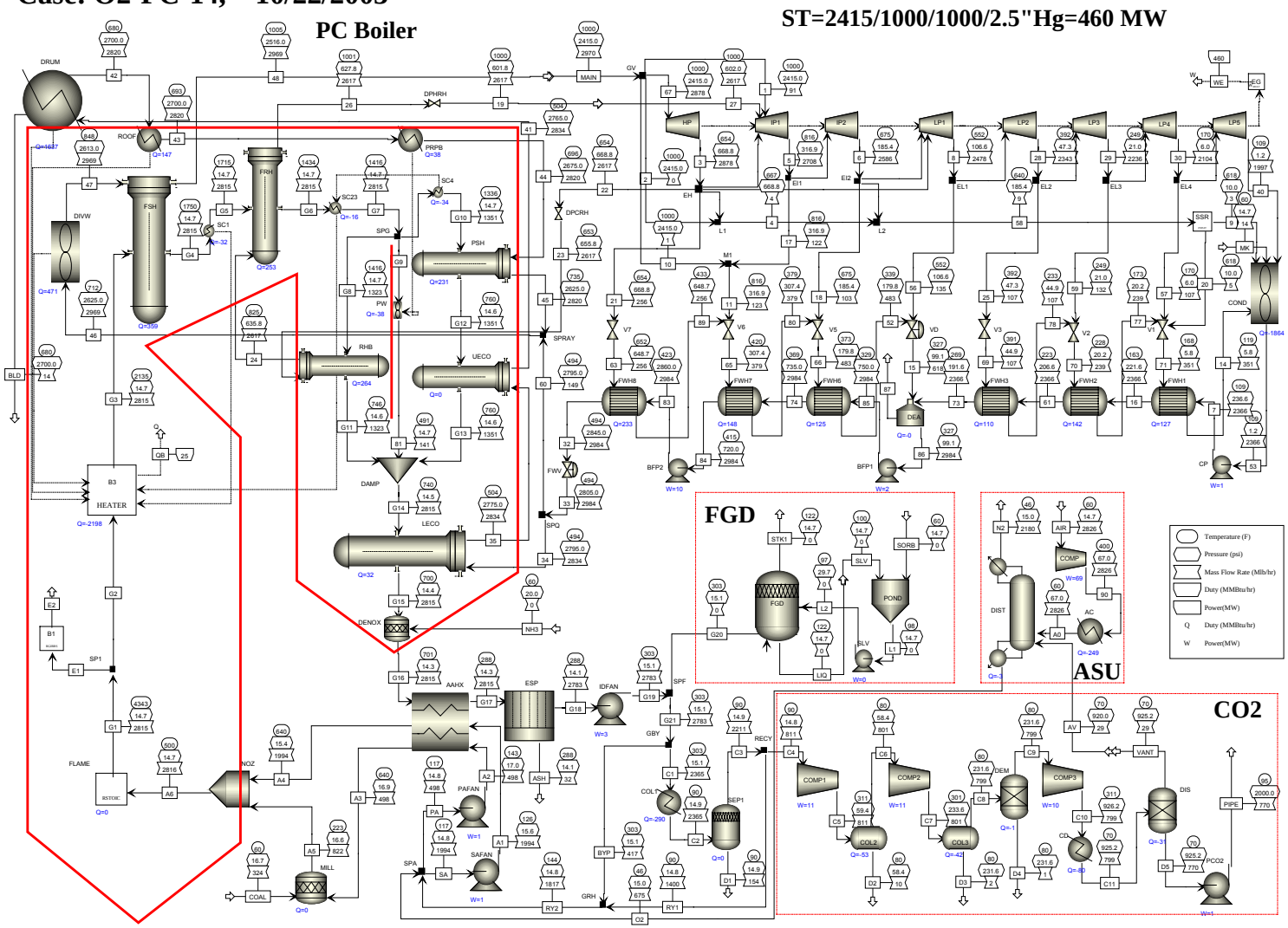

Table 4.2.5 – Parametric Cases Summary (With CO_2 Compression)

case	1	3	8	9	10	11	12	13
ASU	no	yes	yes	yes	yes	yes	yes	yes
CO2 Sequestration	no	no	yes	yes	yes	yes	yes	yes
Vent gas recover	no	no	no	yes	yes	yes	yes	yes
Wet-end economizer	no	no	no	no	no	no	yes	yes
coal to boiler, klb/h	334	333	333	333	327	324	324	324
air to plant, klb/h	3422	2981	2981	2905	2853	2826	2826	2817
O2 purity, %	20.7	99.6	99.6	99.5	99.5	99.5	99.5	99.5
O2 level to boiler, %	20.4	26.9	26.7	27.1	28.0	33.9	33.9	42.4
O2 level exit boiler, %	3.0	3.0	3.0	3.0	3.0	3.0	3.0	3.0
Excess Air, %	18.0	3.1	3.1	0.3	0.3	0.3	0.3	0.3
adiabatic temperature, F	3687	3574	3573	3575	3705	4343	4343	5164
gas to boiler exit, klb/h	3721	3721	3722	3721	3499	2783	2783	2169
gas to boiler exit, mmcft/h	237	175	175	174	166	134	134	104
gas recycle to boiler, klb/h	0	2734	2734	2730	2525	1817	1817	1205
gas exit system, klb/h	3721	820	820	833	819	811	811	810
ASU plant power, MW	0	72.3	72.3	70.5	69.2	68.6	68.6	68.6
CO2 compression power, MW	0	0	37.2	34.6	34.0	33.7	33.7	32.0
Gross power, MW	460	460	460.0	460.0	460.0	460.0	464	468
Aux power, MW	42.1	105.8	143.1	138.6	136.4	133.9	134.6	132
Net Power, MW	417.9	354.2	317.3	321.8	324.0	326.5	329.6	336.0
Boiler efficiency, %	88.2	88.3	88.3	88.3	89.9	90.8	93.2	93.4
Net efficiency, %	36.68	31.15	27.87	28.27	28.98	29.48	29.75	30.33

Figure 4.2.20 – Vapor Pressure of CO_2

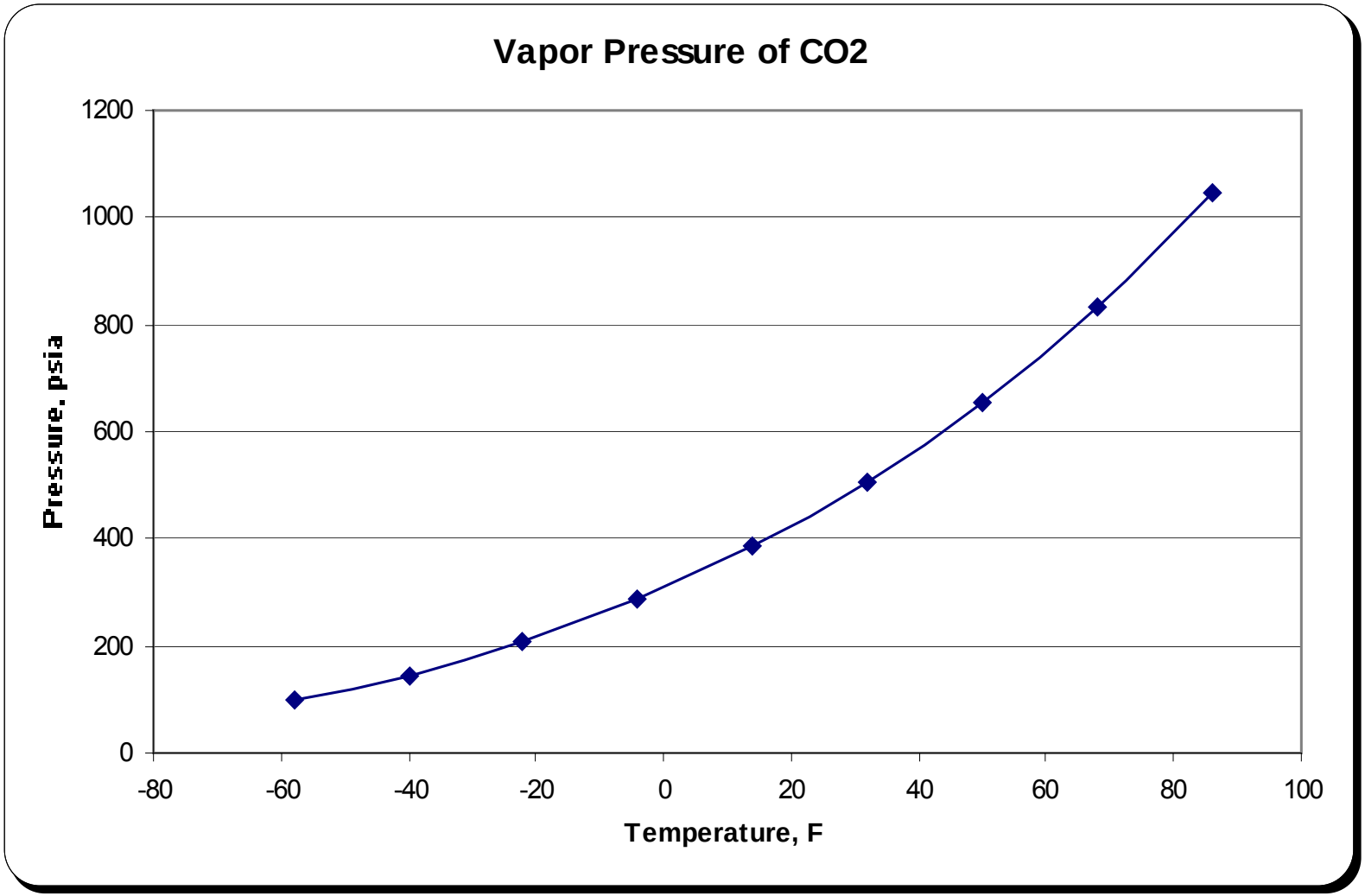

Figure 4.2.21 – Equilibrium CO and CO2 Versus Flue Gas Recycle Flow

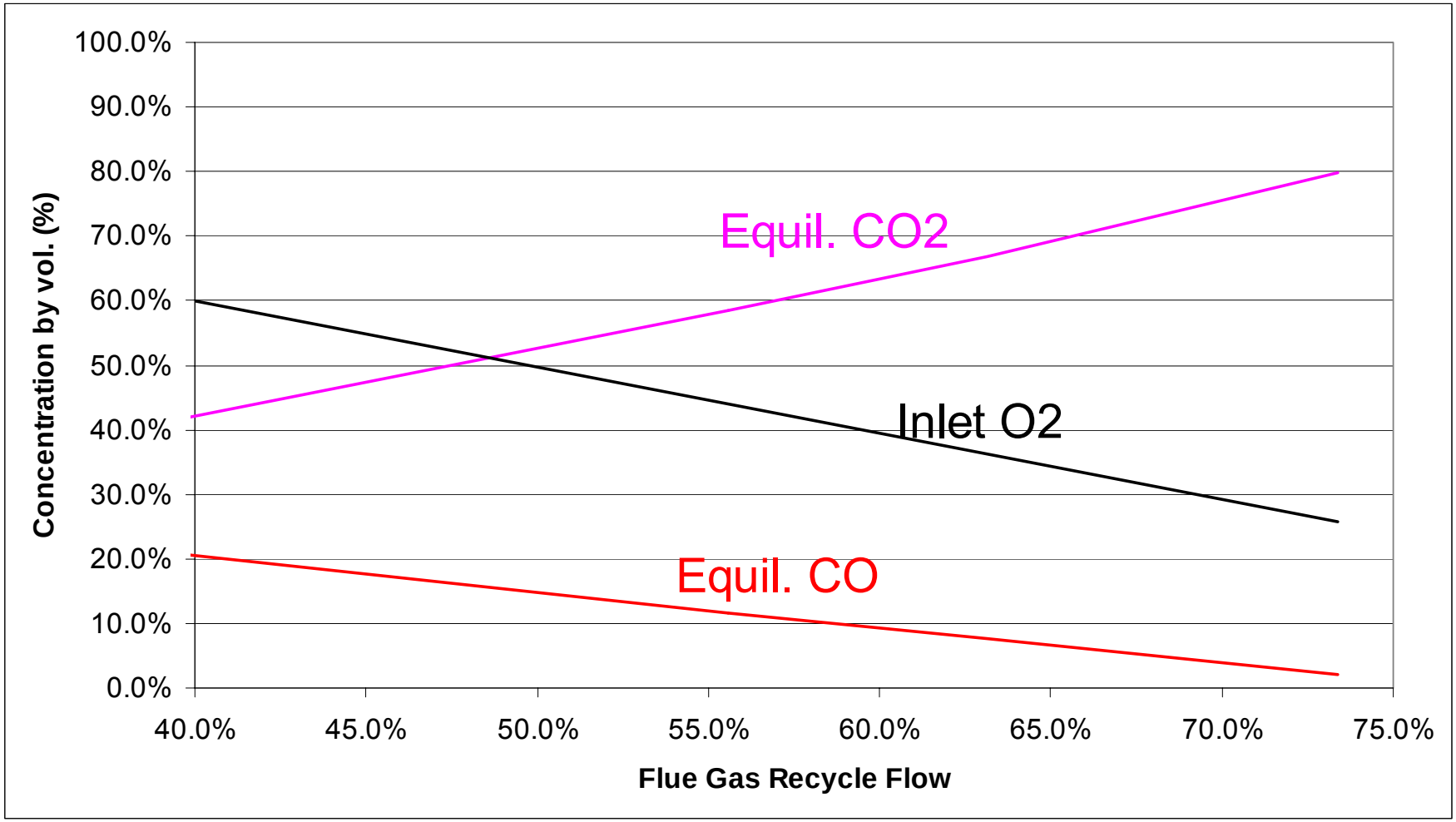

Figure 4.2.22 – Adiabatic and Equilibrium Temperatures Versus Flue Gas Recycle Flow

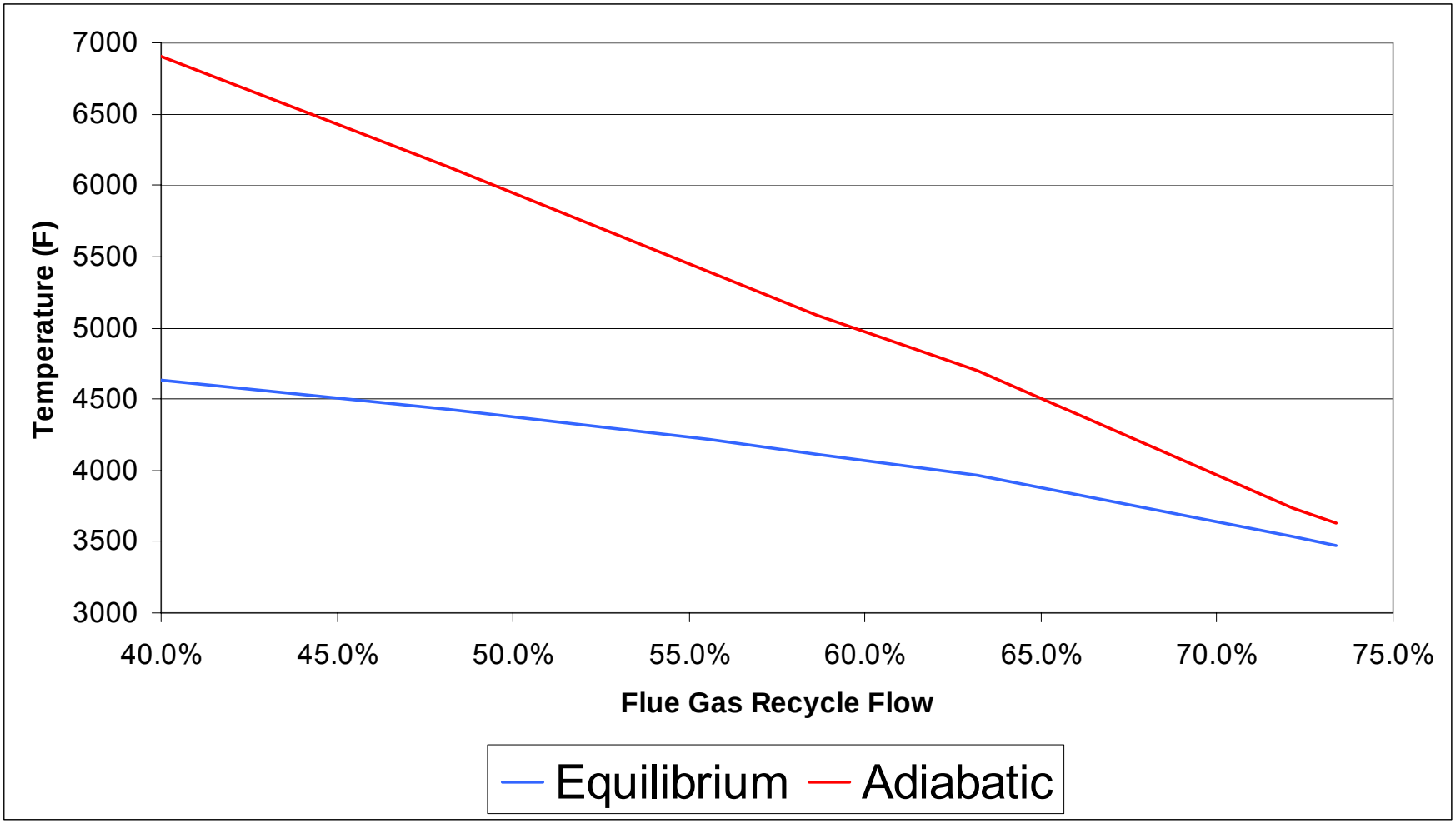

Table 4.2.6 – Radiation Heat Flux and Water Wall Temperature

		1	2	3	4	5	6	7	8	9	10	11, 12	13
Gas Flow Rate	MM ft3/hr	320.8	223.1	222.7	212.1	193.3	174.3	173.0	219.9	219.9	208.7	173.7	173.7
Furnace Heat Duty	MM Btu/hr	1894	1848	1826	1904	2055	2201	2198	1847	1848	1916	2198	2198
Furnace H2O	%	5.0	11.1	11.6	11.9	12.8	13.8	15.2	11.1	11.0	12.6	14.7	17.6
Furnace CO2	%	7.0	59.2	68.9	68.6	67.8	66.9	65.5	69.8	69.4	67.8	65.9	63.0
Depth	ft	39.6	33.0	33.0	32.2	30.7	29.2	29.1	32.8	32.8	31.9	30.2	27.0
Width	ft	56.3	46.9	46.9	45.8	43.7	41.5	41.3	46.6	46.6	45.4	42.9	38.0
Height	ft	176.5	150.3	144.2	152.7	166.0	174.9	172.6	155.2	155.4	158.5	141.9	133.7
Mean Beam Length	ft	32.9	27.2	27.0	26.7	26.0	25.0	24.9	27.2	27.2	26.7	24.9	22.2
Tube wall Properties													
Outside Diameter	in	2.75	2.75	2.75	2.75	2.75	2.75	2.75	2.75	2.75	2.75	2.75	2.75
Wall Thickness	in	0.3	0.285	0.285	0.285	0.285	0.23	0.23	0.285	0.285	0.285	0.23	0.24
Inside Diameter	in	2.15	2.18	2.18	2.18	2.18	2.29	2.29	2.18	2.18	2.18	2.29	2.27
inside H.T.C.	Btu/hr-ft2-F	2500	2500	2500	2500	2500	2500	2500	2500	2500	2500	2500	2500
Material		SA-210C	SA-213-T2	SA-213-T2	SA-213-T2	SA-213-T22	SA-213-T91	SA-213-T91	SA-213-T2	SA-213-T2	SA-213-T2	SA-213-T91	SA-213-T91
Wall Therm. Cond.	Btu/hr-ft-F	22.0	21.8	22.2	22.2	20.0	16.1	16.1	22.2	22.2	22.2	16.1	16.1
Overall U	Btu/hr-ft2-F	557.5	579.6	587.0	587.0	544.9	560.8	560.8	587.0	587.0	587.0	560.8	540.6
Stress Allowable	psi	12,362	14,502	14,482	14,439	14,753	19,435	19,292	14,492	14,492	14,404	19,129	17,463
Min. Wall	in	0.30	0.26	0.26	0.26	0.26	0.20	0.20	0.26	0.26	0.26	0.21	0.22
Max. Furnace Temp.	F	3492	3467	3456	3492	3584	3710	3710	3372	3372	3433	3640	4013
Max. Heat Flux	Btu/hr-ft2	63,300	98,408	100,700	102,800	109,400	115,550	118,900	100,210	100,210	104,500	122,700	152,040
Max. Wall Temp.	F	794	850	852	855	881	886	892	851	851	858	899	961
Ave. Furnace Temp.	F	3128	2989	2981	3008	3076	3171	3171	2920	2920	2964	3118	3404
Ave. Wall Flux	Btu/hr-ft2	49,460	68,140	69,900	71,150	75,028	81,100	82,320	66,684	66,684	69,900	78,410	93,901
flux/flux(case1)		1.00	0.73	0.71	0.70	0.66	0.61	0.60	0.74	0.74	0.71	0.63	0.53

Figure 4.2.23 – Case 12 Cycle Diagram

Case: O2-PC-16, 01/20/2004

ST=2415/1000/1000/2.5"Hg=460 MW

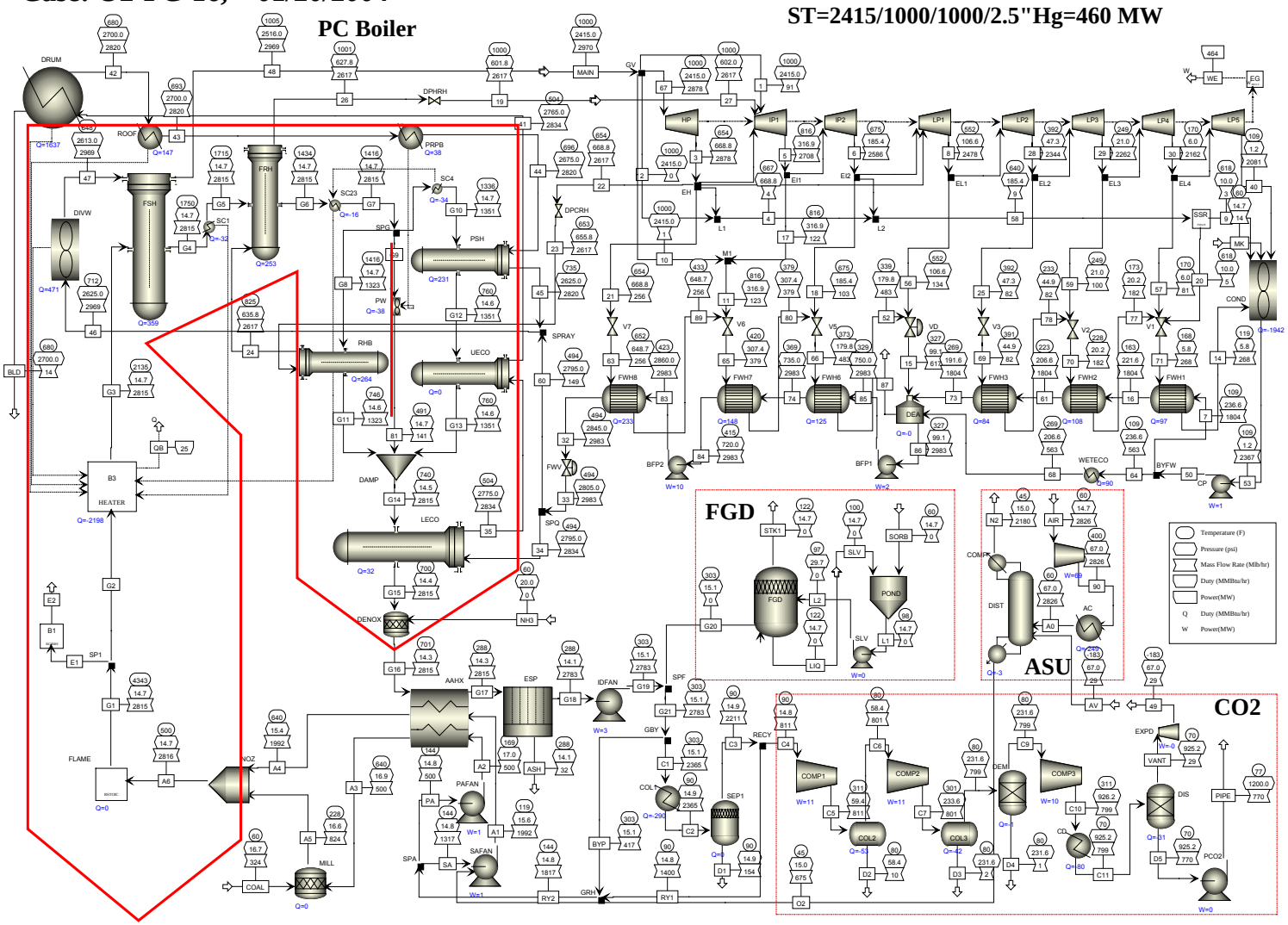

Figure 4.2.24 – Wet End Economizer Temperature Vs. Heat Duty

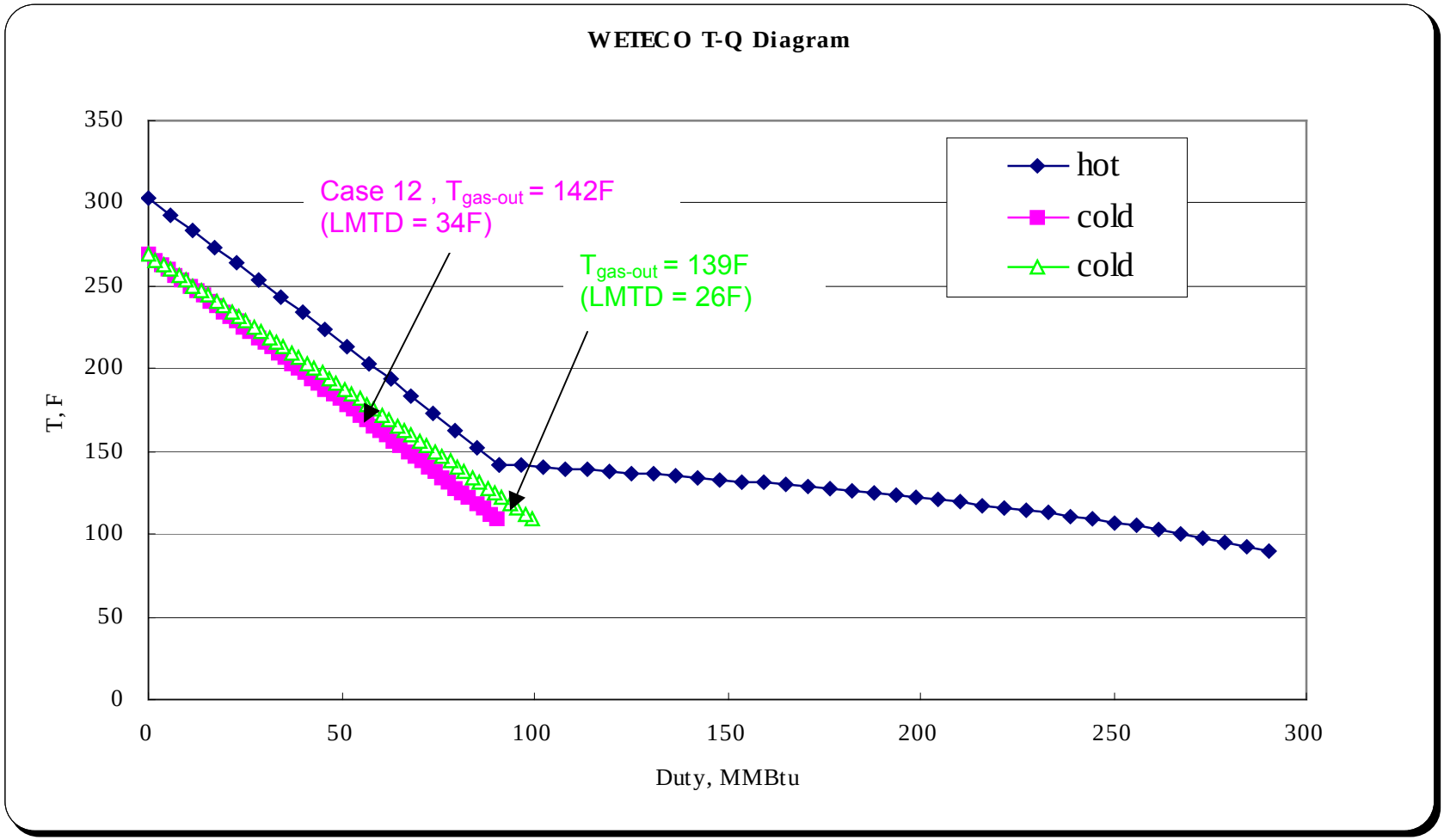

Figure 4.2.25 – Case 13 Cycle Diagram

Case: O2-PC-18, 09/07/2004

ST=2415/1000/1000/2.5"Hg=460 MW

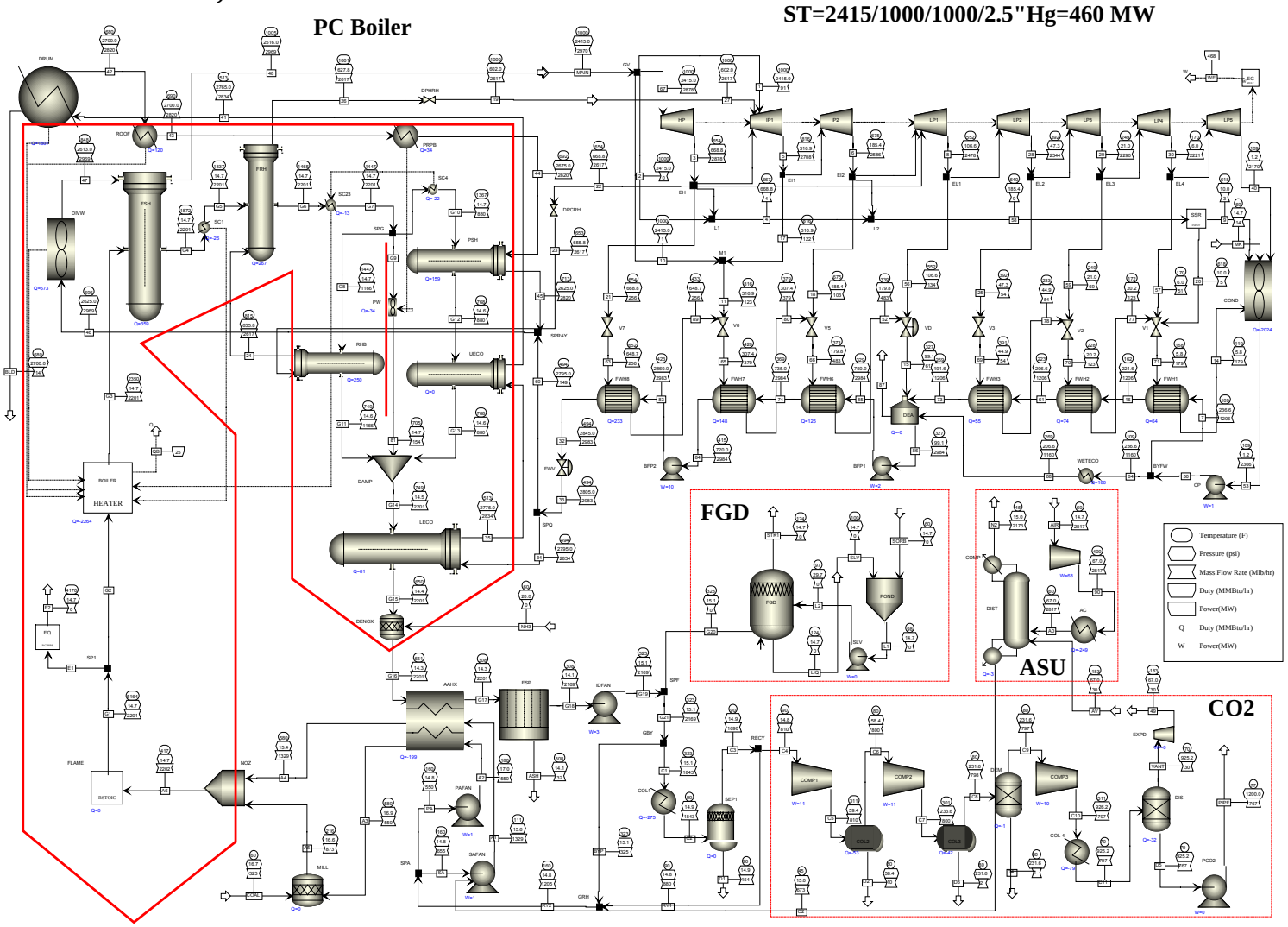

Figure 4.2.26 – Efficiency of Saved Extraction Steam Versus Stage

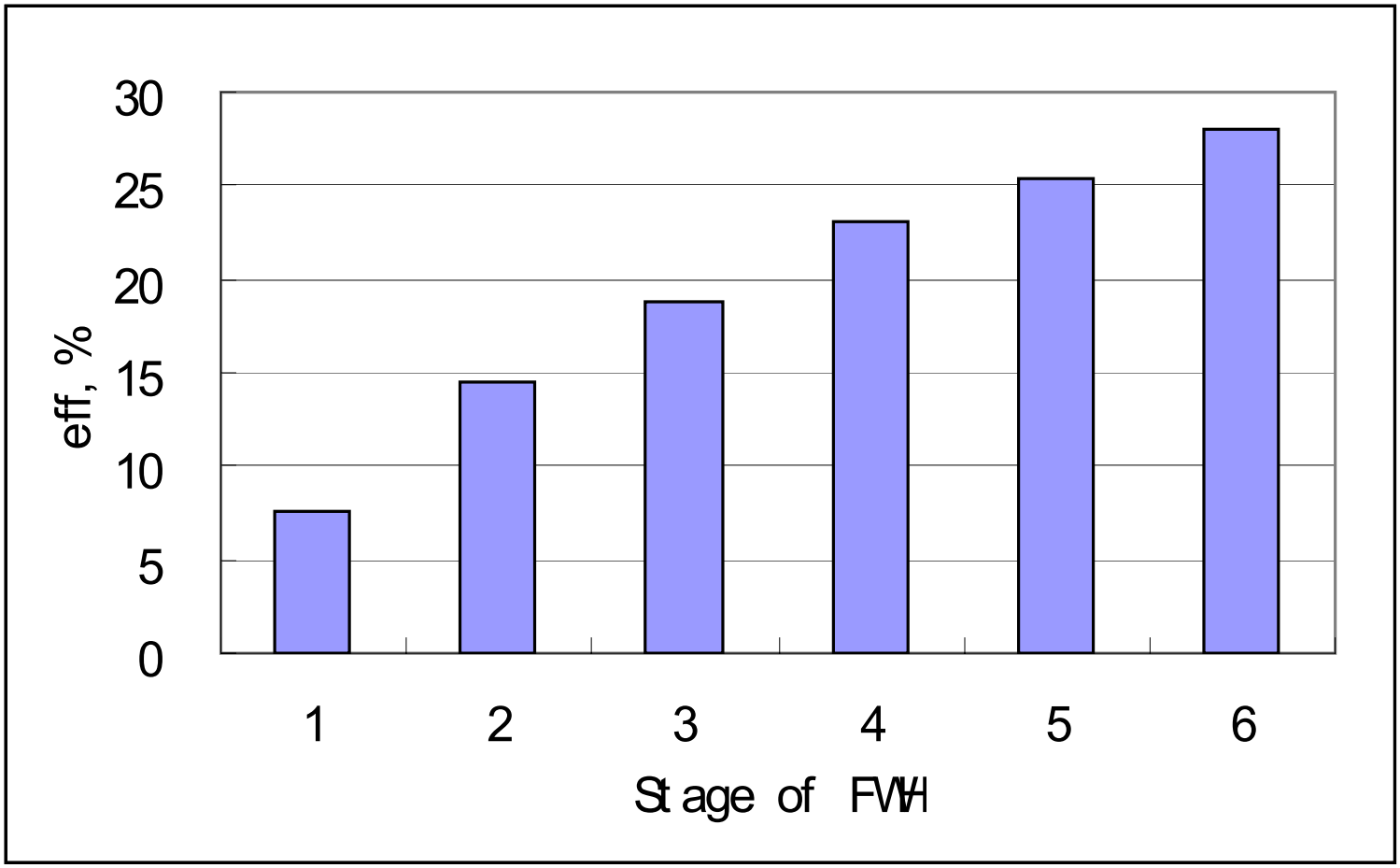

Figure 4.2.27 – Comparison of Power Consumption of CO_2 Removal of Different Technologies

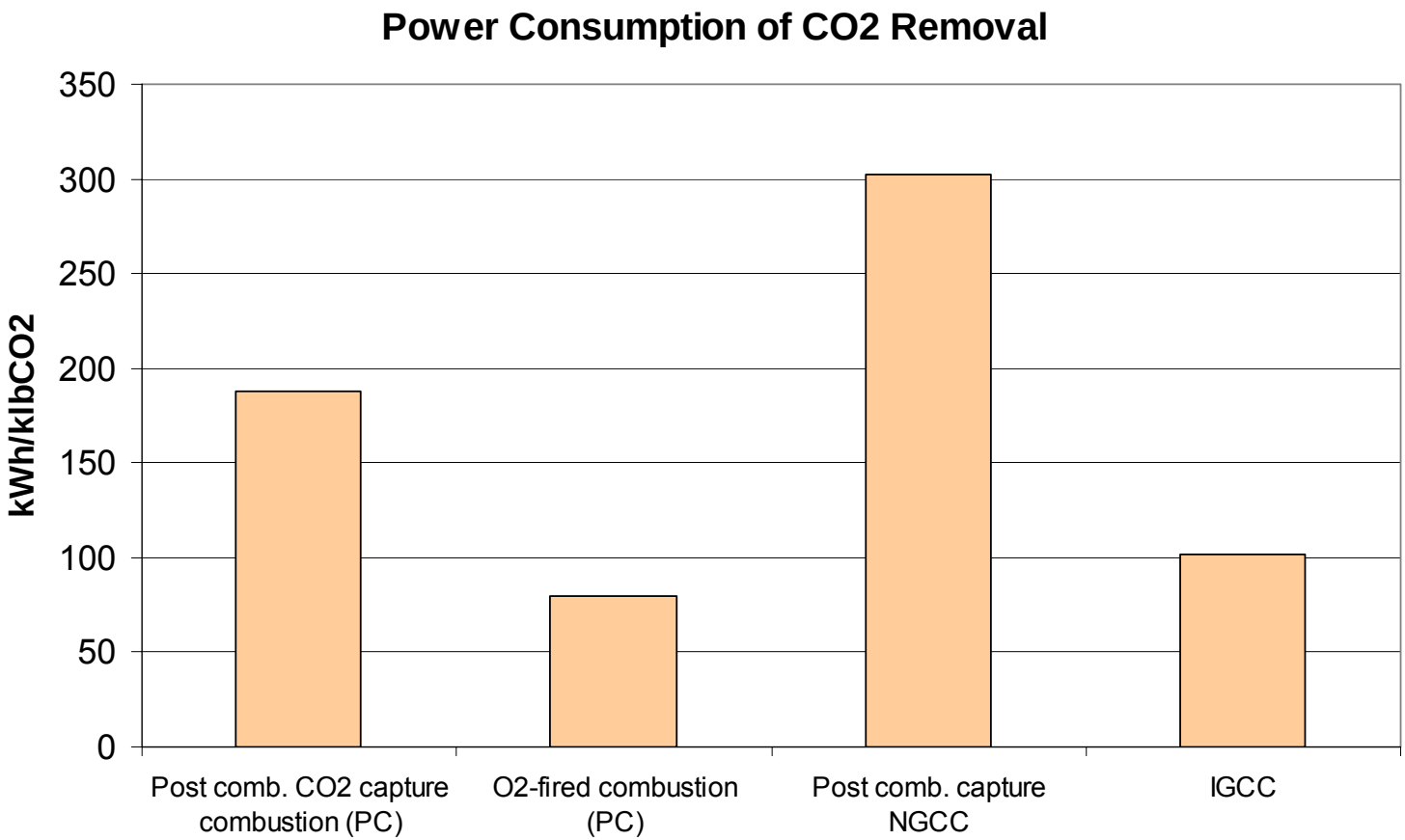

Figure 4.2.28 – Comparison of Overall Cycle Efficiency Point of CO_2 Removal of Different Technologies

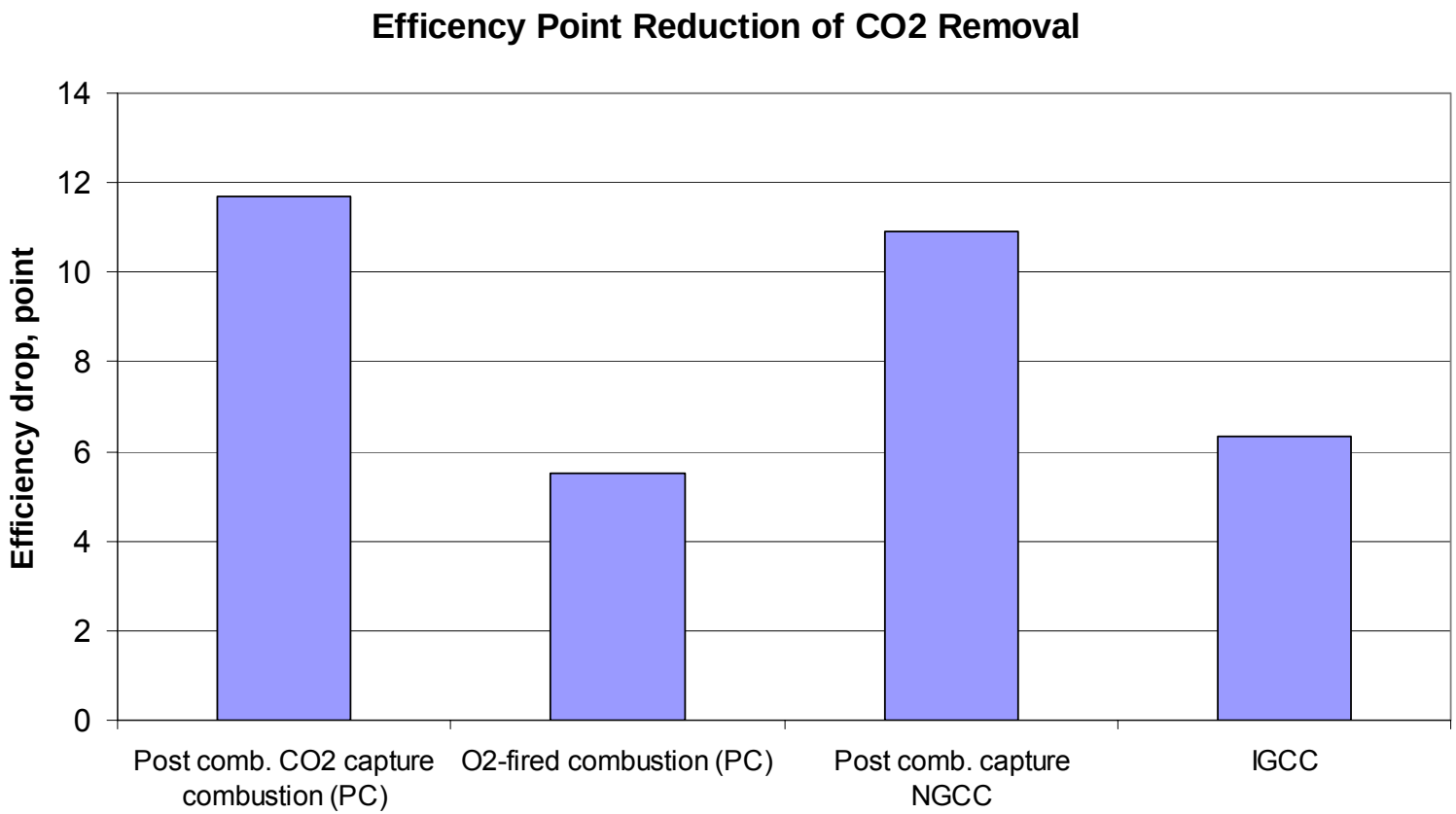

4.3 Low NOx Burner Design and Analysis

4.3.1 Model Geometry

A 3-D simulation was made of a single wall-fired burner and horizontal portion of the furnace from the wall to the center. Burner geometry is based upon FW low NOx burner experience adapted for O_2 firing. Figure 4.3.1 presents the burner geometry and dimensions for the four models. Figure 4.3.2 presents a 3-D view of the CFD model near the burner outlet. The CFD model contains 60,254 cells and is shown in Figure 4.3.1.

4.3.2 Sub Models

The following fluent sub-models were utilized:

Turbulence:	standard two-equation k-ε model.
Radiation:	discrete ordinate
Species Transport:	Non-premixed combustion (pdf)
Gaseous radiation emissivity:	domain based
Solver:	Segregated with SIMPLE pressure-velocity coupling and PRESTO! pressure discretation
Char devolatilization:	two competing rates
Char oxidation:	kinetics/diffusion limited

4.3.3 Boundary Conditions

Boundary conditions are based on ASPEN simulations of the power plant (Section 4.2). The oxygen-fired ASPEN reference cycle diagrams are presented in Figure 4.2.23 (case 12) and Figure 4.2.25 (case 13), respectively The input data required by Fluent include fuel analysis, coal particle size distribution (mass percentage for each size bin), and the velocities, flow rates and temperatures of primary and secondary gas streams. Coal properties are presented in Table 4.3.1 and boundary conditions are detailed in Table 4.3.2.

For the front wall (waterwall) of the furnace an emissivity of 0.7 and temperature of 980°F were applied. For the tunnel, emissivity of 0.7 and a temperature of approximately 2700 ^{o}F corresponding to the average burner heat absorption were applied.

For coal devolatilization kinetic properties, Ubhayakar rate parameters were employed for bituminous coal. For bituminous char oxidation, high volatile bituminous first order reaction coefficients were applied.

4.3.4 65% Recycle Case With No OFG

The boundary conditions were applied to the computational model (Figure 4.3.1) and Fluent was run until steady state conditions were achieved. The modeling results are summarized in Table 4.3.3. The coal burnout shown in the table is the percentage of dry ash-free based coal burned.

4.3.4.1 No Primary Gas Swirl

Figure 4.3.4 presents the velocity distribution and Figure 4.3.5 presents the temperature distribution. The O_2 mole fraction is shown in Figure 4.3.6. The trajectories and burnout of the 69 micron and 169 micron coal particles are shown in Figure 4.3.7 and Figure 4.3.8. Due to the low oxygen content of the primary gas (3.0%, by vol.), coal burnout is relatively small, especially for the larger particles as can be seen in Figure 4.3.8. Consequently, it is necessary to add swirl to the primary gas to bring the coal particles (especially the larger sizes) in contact with the secondary gas. However, as the primary gas swirl is increased the NOx generally increases since the combustion staging is reduced. Figure 4.3.3 shows the effect of primary gas swirl ratio on burnout and NOx. Note that the NOx at the burner outlet can be significantly lower than the NOx at the furnace outlet, which is predicted in Section 4.4.1.5. Based on Figure 4.3.3 a primary gas swirl ratio of 0.5 was chosen as optimal.

4.3.4.2 Primary Gas Swirl Ratio = 0.5

Figure 4.3.9 presents the velocity distribution and Figure 4.3.10 presents the temperature distribution. Comparing Figure 4.3.5 with Figure 4.3.10 demonstrates that the addition of the 0.5 PG swirl increases the maximum flame temperature by 450°F and also increases the flame core temperature. Increasing the core temperature creates a more stable flame since the secondary gas swirl recirculates the hot flue gas back to the flame ignition point as shown in Figure 4.3.12. The O_2 mole fraction is shown in Figure 4.3.11. The trajectories and burnout of the 69 micron and 169 micron coal particles are shown in Figure 4.3.13 and Figure 4.3.14. Note that with the 0.5 PG swirl ratio approximately 55% of the larger coal particles are burned (Figure 4.3.14) as compared to only about 25% for a zero PG swirl ratio (Figure 4.3.8).

4.3.5 65% Recycle Case With 20% OFG

The boundary conditions were applied to the computational model (Figure 4.3.1) and Fluent was run until steady state conditions were achieved. The modeling results are summarized in Table 4.3.3.

4.3.5.1 No Primary Gas Swirl

Figure 4.3.15 presents the velocity distribution and Figure 4.3.16 presents the temperature distribution. The O_2 mole fraction is shown in Figure 4.3.17. The trajectories and burnout of the 69 micron and 169 micron coal particles are shown in Figure 4.3.18 and Figure 4.3.19. Due to the low oxygen content of the primary gas (3.0%, by vol.), coal burnout is relatively small, especially for the larger particles as can be seen in Figure 4.3.19. Consequently, it is necessary to add swirl to the primary gas to bring the coal particles (especially the larger sizes) in contact with the secondary gas.

4.3.5.2 Primary Gas Swirl Ratio = 0.5

Figure 4.3.20 presents the velocity distribution and Figure 4.3.21 presents the temperature distribution. Comparing Figure 4.3.16 with Figure 4.3.21 demonstrates that the addition of the 0.5 PG swirl increases the maximum flame temperature by 160°F and also increases the flame core temperature. Increasing the core temperature creates a more stable flame since the secondary gas swirl recirculates the hot flue gas back to the flame ignition point. The O_2 mole fraction is shown in Figure 4.3.22. The trajectories and burnout of the 69 micron and 169 micron coal particles are shown in Figure 4.3.23 and Figure 4.3.24. Note that with the 0.5 PG swirl ratio approximately 45% of the larger coal particles are burned (Figure 4.3.24) as compared to only about 33% for a zero PG swirl ratio (Figure 4.3.19).

4.3.6 56% Recycle Case With No OFG

The boundary conditions were applied to the computational model (Figure 4.3.1) and Fluent was run until steady state conditions were achieved. The modeling results are summarized in Table 4.3.3.

4.3.6.1 No Primary Gas Swirl

Figure 4.3.25 presents the velocity distribution Figure 4.3.26 presents the temperature distribution. The O_2 mole fraction is shown in Figure 4.3.27. The trajectories and burnout of the 69 micron and 169 micron coal particles are shown in Figure 4.3.28 and Figure 4.3.29. Due to the low oxygen content of the primary gas (3.0%, by vol.), coal burnout is relatively small, especially for the larger particles as can be seen in Figure 4.3.29. Consequently, it is necessary to add swirl to the primary gas to bring the coal particles (especially the larger sizes) in contact with the secondary gas.

4.3.6.2 Primary Gas Swirl Ratio = 0.5

Figure 4.3.30 presents the velocity distribution and Figure 4.3.31presents the temperature distribution. Comparing with Figure 4.3.26 with Figure 4.3.31

demonstrates that the addition of the 0.5 PG swirl increases the maximum flame temperature by 100°F and also increases the flame core temperature. Increasing the core temperature creates a more stable flame since the secondary gas swirl recirculates the hot flue gas back to the flame ignition point. The O_2 mole fraction is shown in Figure 4.3.32. The trajectories and burnout of the 69 micron and 169 micron coal particles are shown in Figure 4.3.33 and Figure 4.3.34. Note that with the 0.5 PG swirl ratio approximately 47% of the 169μ coal particles are burned (Figure 4.3.34) as compared to only about 44% for a zero PG swirl ratio (Figure 4.3.29) and 85% of the 69μ coal particles are burned (Figure 4.3.33) as compared to only about 52% for a zero PG swirl ratio (Figure 4.3.28)

4.3.7 56% Recycle Case With 20% OFG

The boundary conditions were applied to the computational model (Figure 4.3.1) and Fluent was run until steady state conditions were achieved. The modeling results are summarized in Table 4.3.3.

4.3.7.1 No Primary Gas Swirl

Figure 4.3.35 presents the velocity distribution and Figure 4.3.36 presents the temperature distribution. The O_2 mole fraction is shown in Figure 4.3.37. The trajectories and burnout of the 69 micron and 169 micron coal particles are shown in Figure 4.3.38 and Figure 4.3.39. Due to the low oxygen content of the primary gas (3.0%, by vol.), coal burnout is relatively small, especially for the larger particles as can be seen in Figure 4.3.39. Consequently, it is necessary to add swirl to the primary gas to bring the coal particles (especially the larger sizes) in contact with the secondary gas.

4.3.7.2 Primary Gas Swirl Ratio = 0.5

Figure 4.3.40 presents the velocity distribution and Figure 4.3.41 presents the temperature distribution. Comparing Figure 4.3.36 with Figure 4.3.41 demonstrates that the addition of the 0.5 PG swirl increases the maximum flame temperature by 220°F and also increases the flame core temperature. Increasing the core temperature creates a more stable flame since the secondary gas swirl recirculates the hot flue gas back to the flame ignition point. The O_2 mole fraction is shown in Figure 4.3.42. The trajectories and burnout of the 69 micron and 169 micron coal particles are shown in Figure 4.3.43 and Figure 4.3.44. Note that with the 0.5 PG swirl ratio approximately 49% of the larger coal particles are burned (Figure 4.3.44) as compared to only about 18% for a zero PG swirl ratio (Figure 4.3.39).

Figure 4.3.1 – Oxygen-Fired Burner Geometry

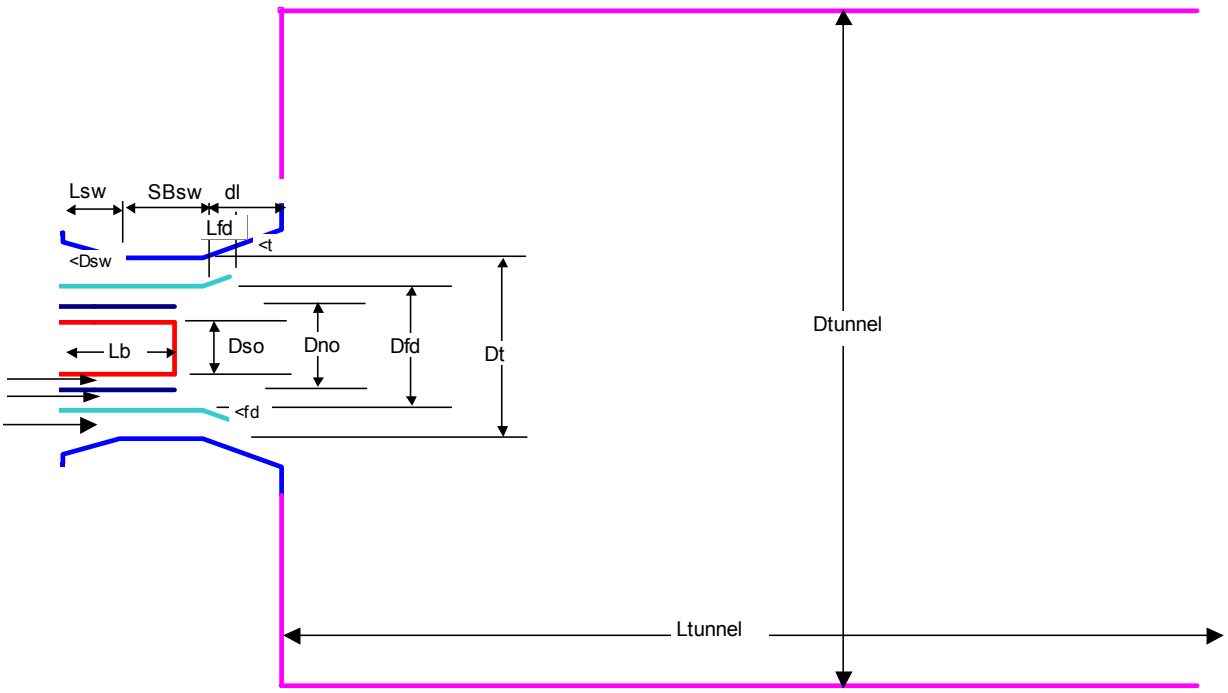

		65 % Flue Gas Recycle		56 % Flue Gas Recycle	
		No OFG	20% OFG	No OFG	20% OFG
Dt	in.	32	29	29	25
Dfd	in.	22.25	21	21	19
SBsw	in.	13	12	11.875	11.875
Lsw	in.	9	8.375	8.375	8.375
<Dsw	deg.	18	18	18	18
Lfd	in.	4	4	4	4
<fd	deg.	22.5	22.5	22.5	22.5
dl	in.	12	11	11.25	11.25
<t	deg.	22.5	22.5	22.5	22.5
Dno	in.	15.5	15.5	15.5	15.5
Dso	in.	10	10	10	10
Lb	in.	20	20	20	20
Dtunnel	in.	120	120	120	120
Ltunnel	in.	144	144	144	144

Figure 4.3.2 – Computational Model of Oxygen-Fired Burner

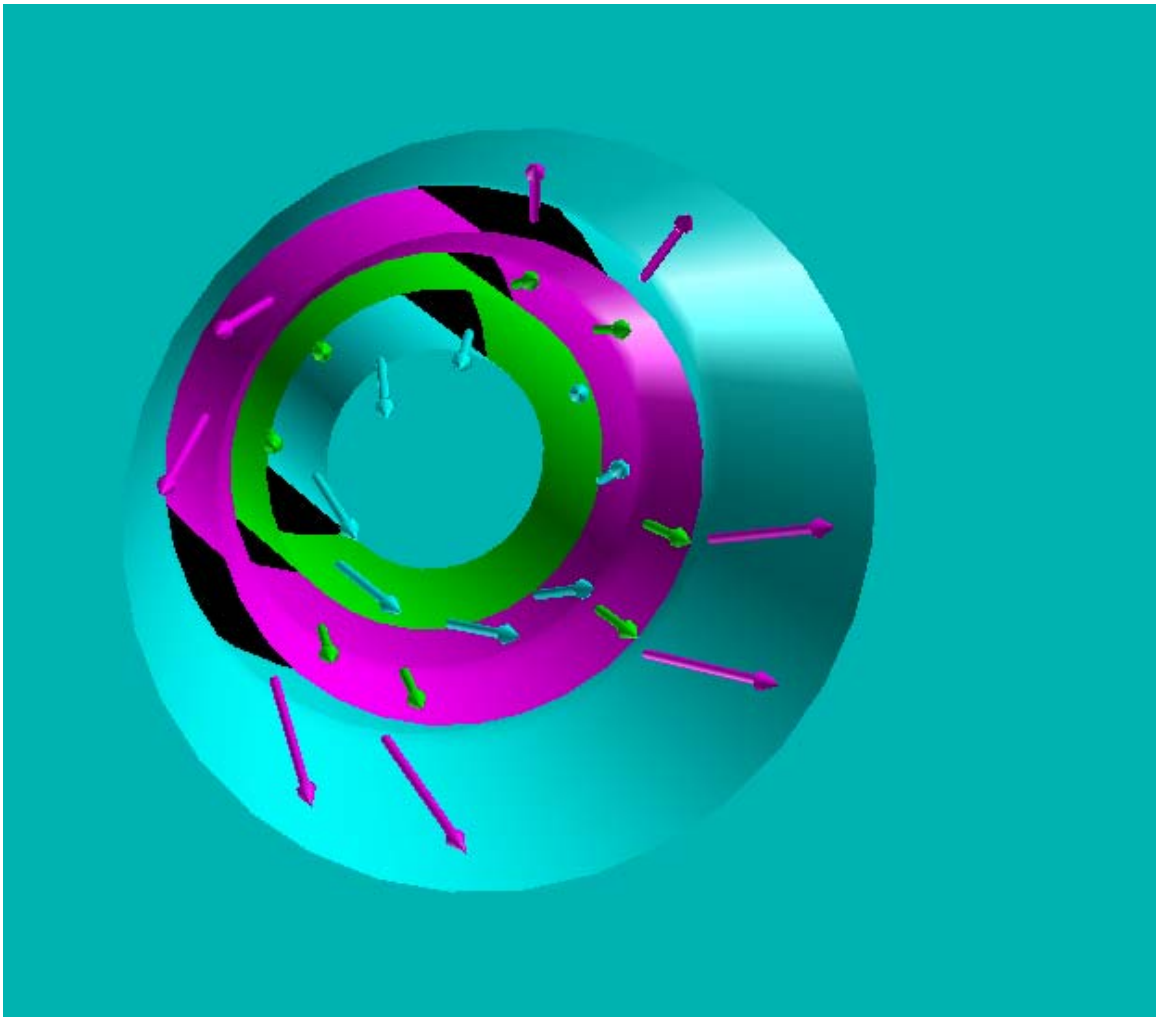

Vector Key

- Outer Secondary Gas
- Inner Secondary Gas
- Primary Gas

Table 4.3.1 – Coal Properties

Coal Size Distribution		
< 75 micron	%	85
< 150 micron	%	99
Size (micron)		
10.7	lb/hr	3,540
33.7	lb/hr	4,580
69.3	lb/hr	3,106
118.2	lb/hr	654
169.2	lb/hr	120
Total	lb/hr	12,000
Coal Ultimate Analysis		
Ash	%	9.99%
S	%	2.51%
H	%	4.50%
C	%	63.75%
H2O	%	11.12%
N	%	1.25%
O	%	6.88%
Total	%	100.00%
Volatile Matter (daf)	%	44.35%
Density	lb/ft3	80.0
HHV, as received	Btu/lb	11,666

Table 4.3.2 –Model Boundary Conditions

65% Recycle

			No OFG		20% OFG	
		Primary	Inner Sec.	Outer Sec.	Inner Sec.	Outer Sec.
Flow Area						
Inlet	in2	110.2	157.7	585.3	94.8	444.3
Outlet	in2	110.2	157.7	314.2	94.8	207.3
Total Mass Flow Rate	lb/hr	530,000	276,433	1,105,732	201,383	805,533
No. of Burners		24	24	24	24	24
OFG			0.0%	0.0%	20.0%	20.0%
Mass Flow Rate	lb/hr	22,083	11,518	46,072	8,391	33,564
Temperature	F	216	580	580	580	580
Molecular weight	lb/lb-mol	38.82	36.08	36.08	36.08	36.08
Density	lb/ft3	0.080	0.049	0.049	0.049	0.049
Velocity						
Inlet	ft/sec	99.8	60.2	64.9	72.9	62.3
Outlet	ft/sec	99.8	60.2	120.9	72.9	133.5
Swirl Ratio		0.0, 0.5	0.0	1.00	0.0	1.00
Composition, by Vol.						
H2O	%	18.80%	3.70%	3.70%	3.70%	3.70%
O2	%	3.10%	58.30%	58.30%	58.30%	58.30%
N2	%	0.70%	0.30%	0.30%	0.30%	0.30%
AR	%	0.40%	0.50%	0.50%	0.50%	0.50%
CO2	%	75.90%	36.60%	36.60%	36.60%	36.60%
SO2	%	1.00%	0.50%	0.50%	0.50%	0.50%
SO3	%	0.10%	0.10%	0.10%	0.10%	0.10%
Total	%	100.00%	100.00%	100.00%	100.00%	100.00%
Coal Flow Rate	lb/hr	12,000	0	0	0	0

56% Recycle

			No OFG		20% OFG	
		Primary	Inner Sec.	Outer Sec.	Inner Sec.	Outer Sec.
Flow Area						
Inlet	in2	110.2	200.1	736.3	157.7	585.3
Outlet	in2	110.2	200.1	415.4	157.7	314.2
Mass Flow Rate	lb/hr	22,083	16,600	66,400	12,458	49,833
Temperature	F	228	640	640	640	640
Molecular weight	lb/lb-mol	39.05	37.97	37.97	37.97	37.97
Density	lb/ft3	0.078	0.047	0.047	0.047	0.047
Velocity						
Inlet	ft/sec	103.1	70.1	76.3	66.8	72.0
Outlet	ft/sec	103.1	70.1	135.1	66.8	134.1
Swirl Ratio		0.0, 0.5	0.0	1.00	0.0	1.00
Composition, by Mass						
H2O	%	8.48%	1.99%	1.99%	1.99%	1.99%
O2	%	2.38%	35.31%	35.31%	35.31%	35.31%
N2	%	0.50%	0.29%	0.29%	0.29%	0.29%
AR	%	0.82%	0.84%	0.84%	0.84%	0.84%
CO2	%	86.08%	60.49%	60.49%	60.49%	60.49%
SO2	%	1.64%	1.18%	1.18%	1.18%	1.18%
SO3	%	0.13%	0.13%	0.13%	0.13%	0.13%
Total	%	100.03%	100.24%	100.24%	100.24%	100.24%
Coal Flow Rate	lb/hr	12,000	0	0	0	0

Table 4.3.3 – Summary of Fluent Burner Modeling Results

`

Results at Outlet		65% Flue Gas Recycle				56% Flue Gas Recycle			
		O% OFG		2O% OFG		O% OFG		2O% OFG	
		0.0 PG Swirl	0.5 PG Swirl	0.0 PG Swirl	0.5 PG Swirl	0.0 PG Swirl	0.5 PG Swirl	0.0 PG Swirl	0.5 PG Swirl
Burnout	%	0.61	0.85	0.61	0.71	0.67	0.79	0.59	0.73
O2	%	20.4	11.2	15.0	11.4	23.4	19.3	18.8	14.2
NOx	ppmvw	230	459	320	360	666	754	427	820
NOx/Burnout	ppmvw	376	541	526	507	1000	960	726	1123
Temperature	F	2140	3300	2590	2920	2918	3093	2943	3148

Figure 4.3.3 – Burnout and NOx/burnout vs. Primary gas Swirl for 65% Recycle, No OFG

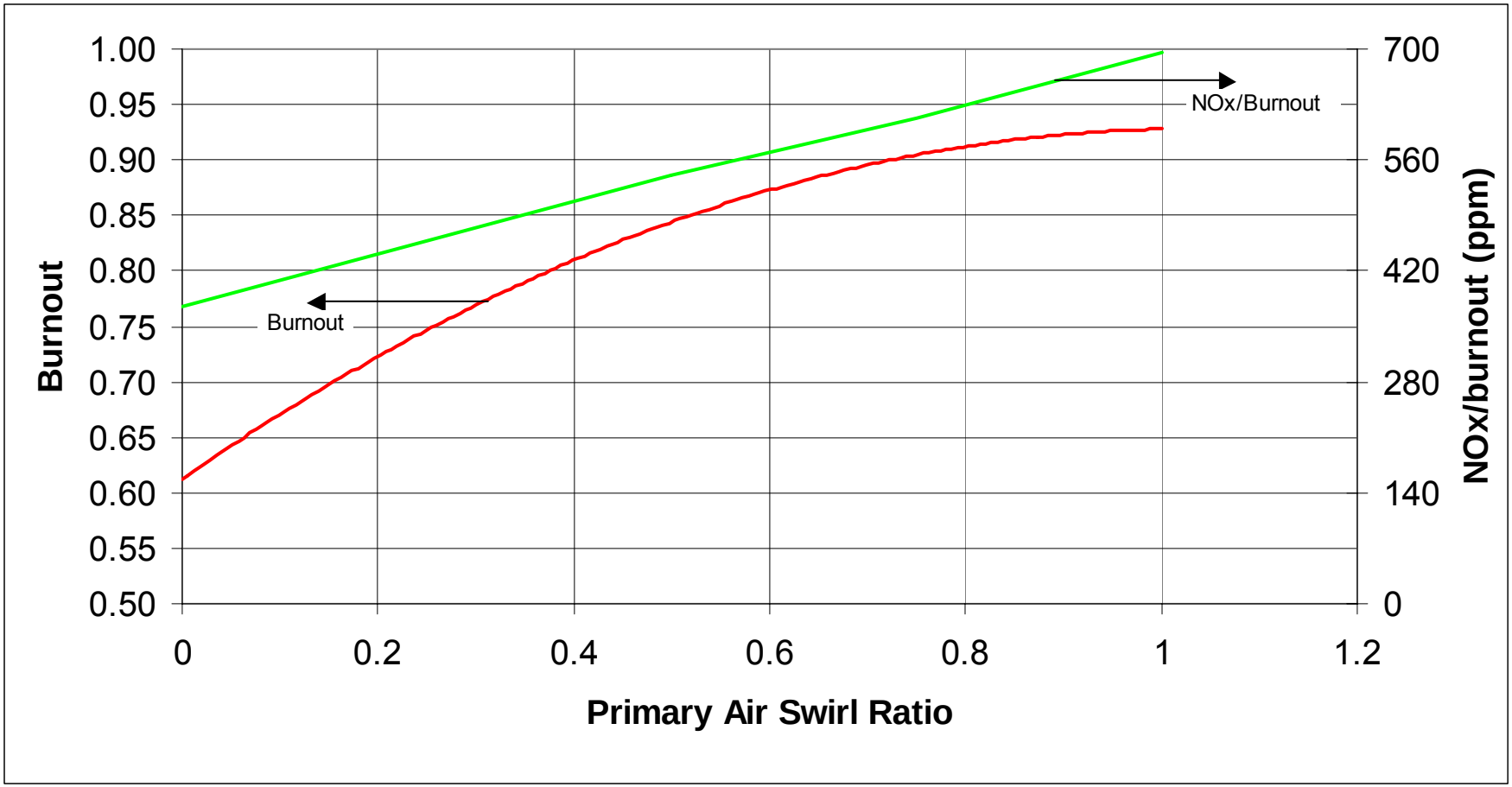

Figure 4.3.4 – Gas Velocity for 65% Recycle, No OFG, 0.0 PG Swirl

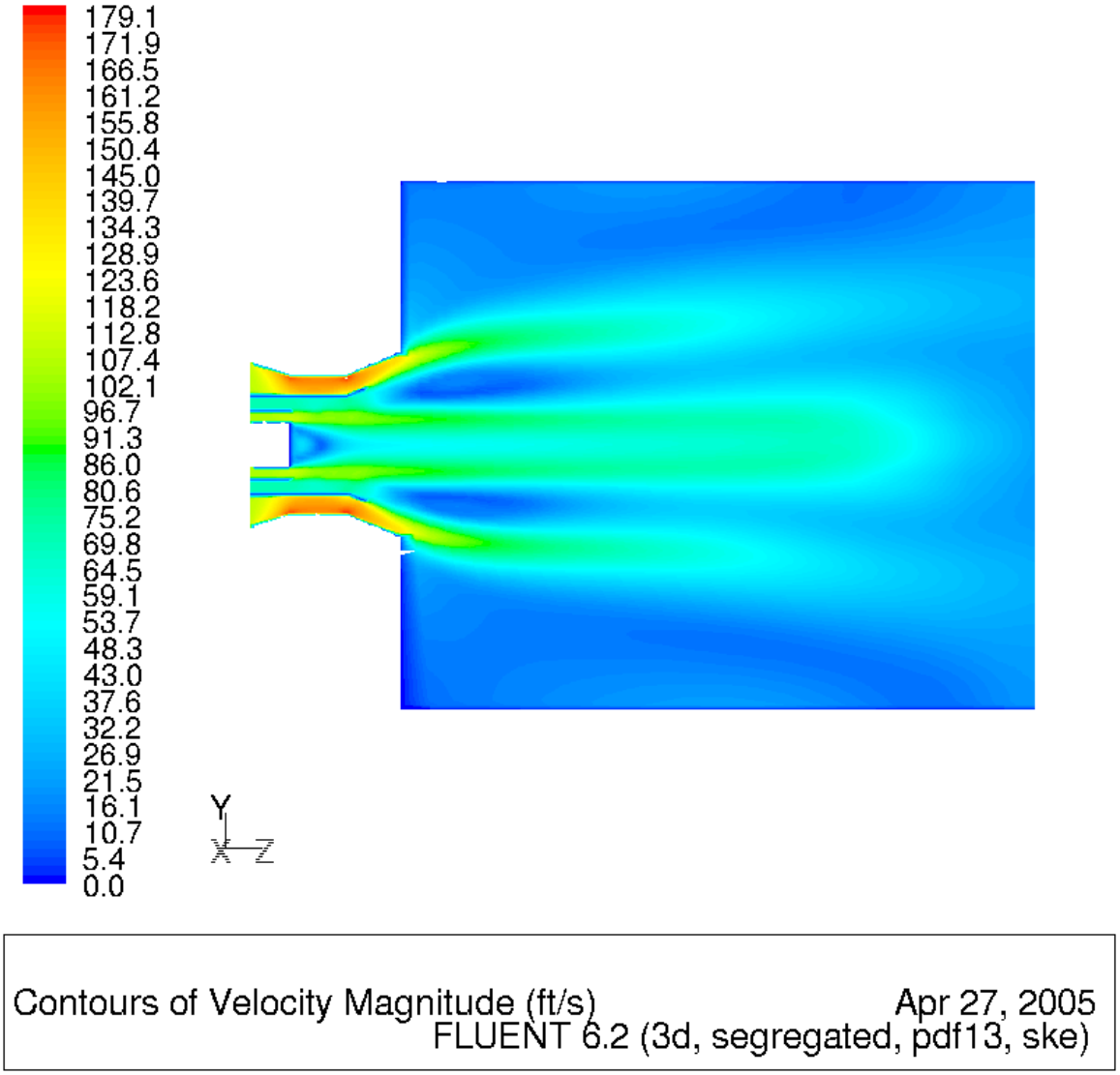

Figure 4.3.5 – Gas Temperature for 65% Recycle, No OFG, 0.0 PG Swirl

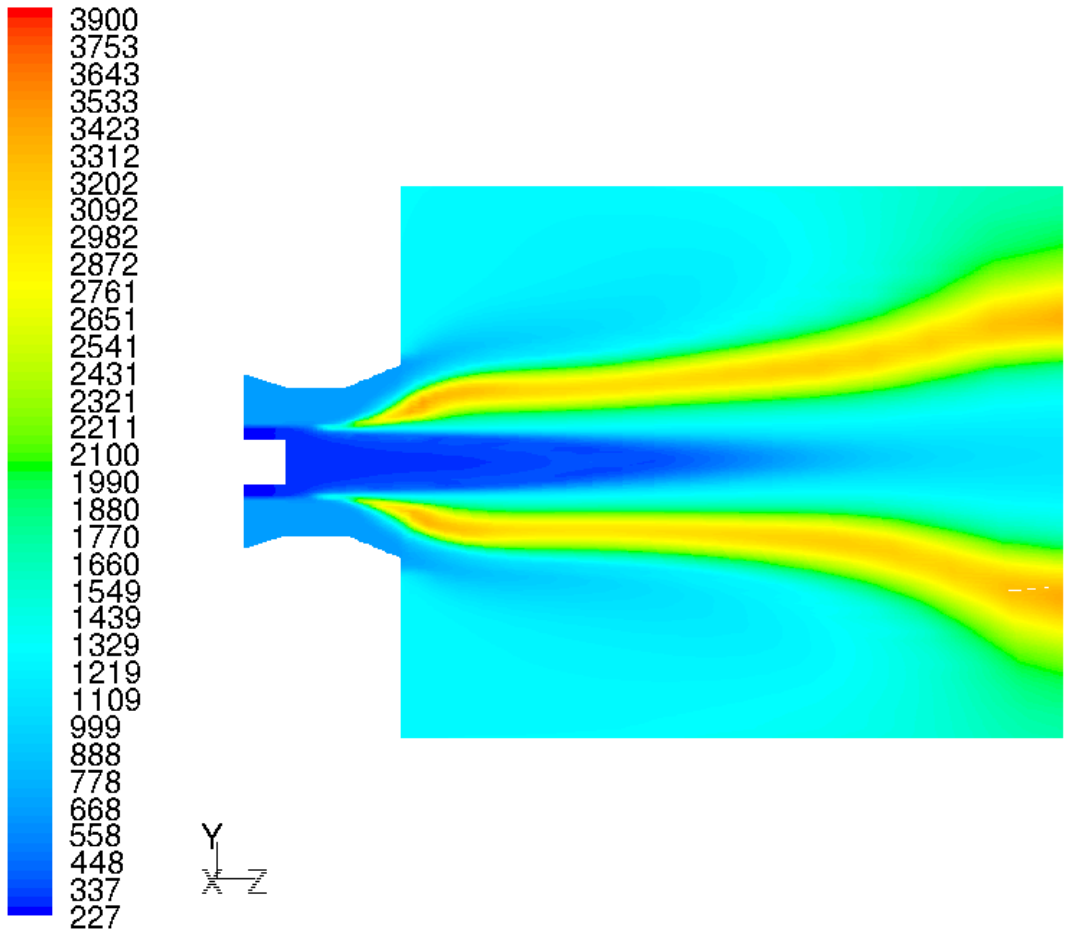

Contours of Static Temperature (f) May 10, 2005
FLUENT 6.2 (3d, segregated, pdf13, ske)

Figure 4.3.6 – O_2 Mole Fraction for 65% Recycle, No OFG, 0.0 PG Swirl

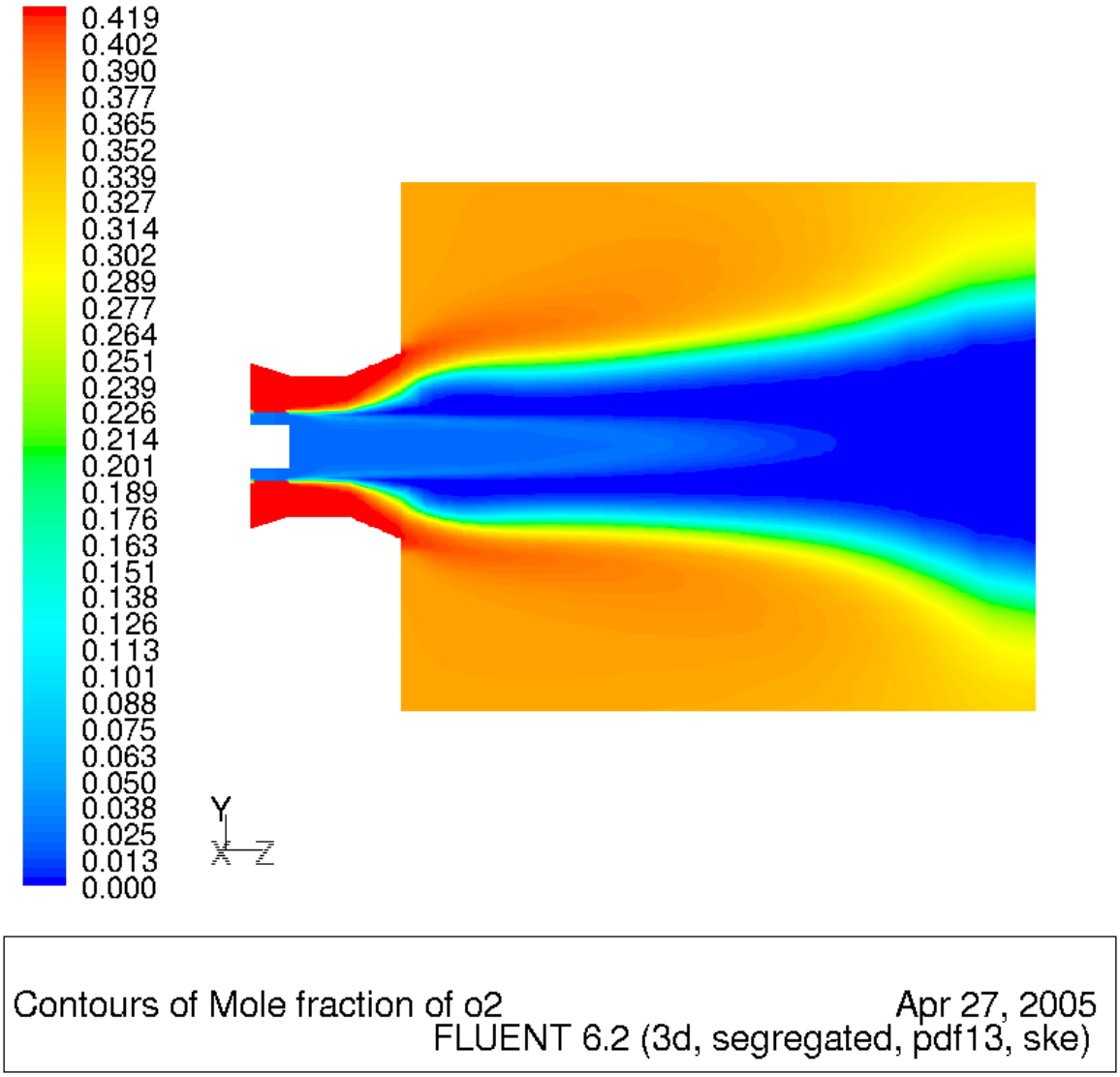

Figure 4.3.7 – Burnout of 69μ Particles for 65% Recycle, No OFG, 0.0 PG Swirl

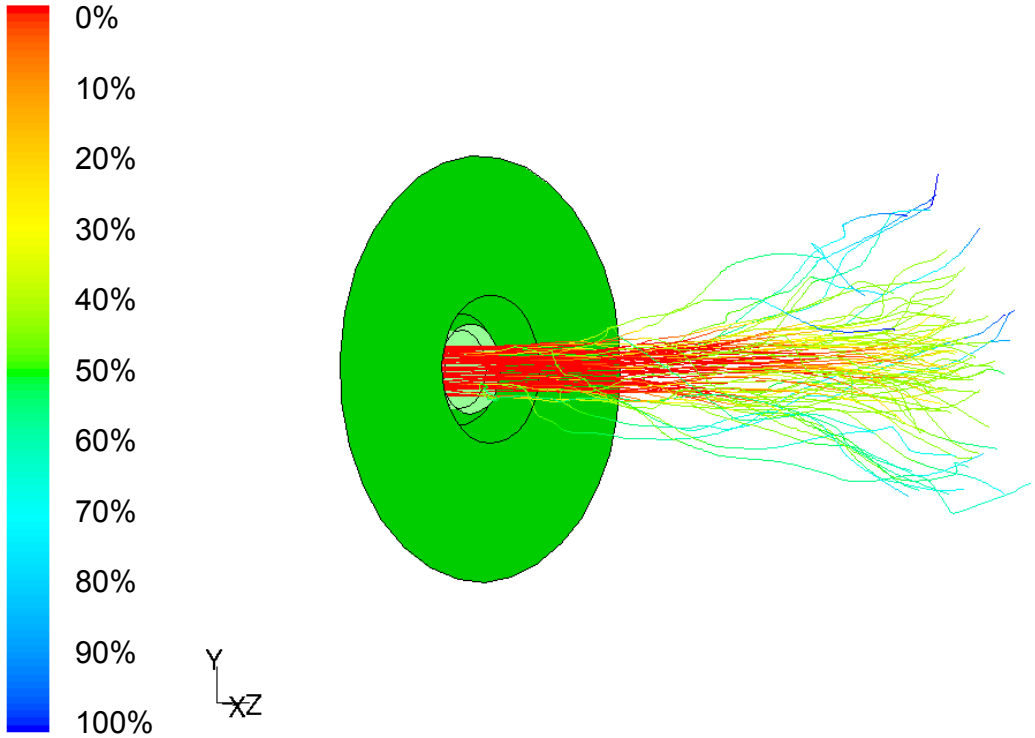

Particle Traces Colored by Particle Mass

Apr 28, 2005
FLUENT 6.2 (3d, segregated, pdf13, ske)

Figure 4.3.8 – Burnout of 169µ Particles for 65% Recycle, No OFG, 0 PG Swirl

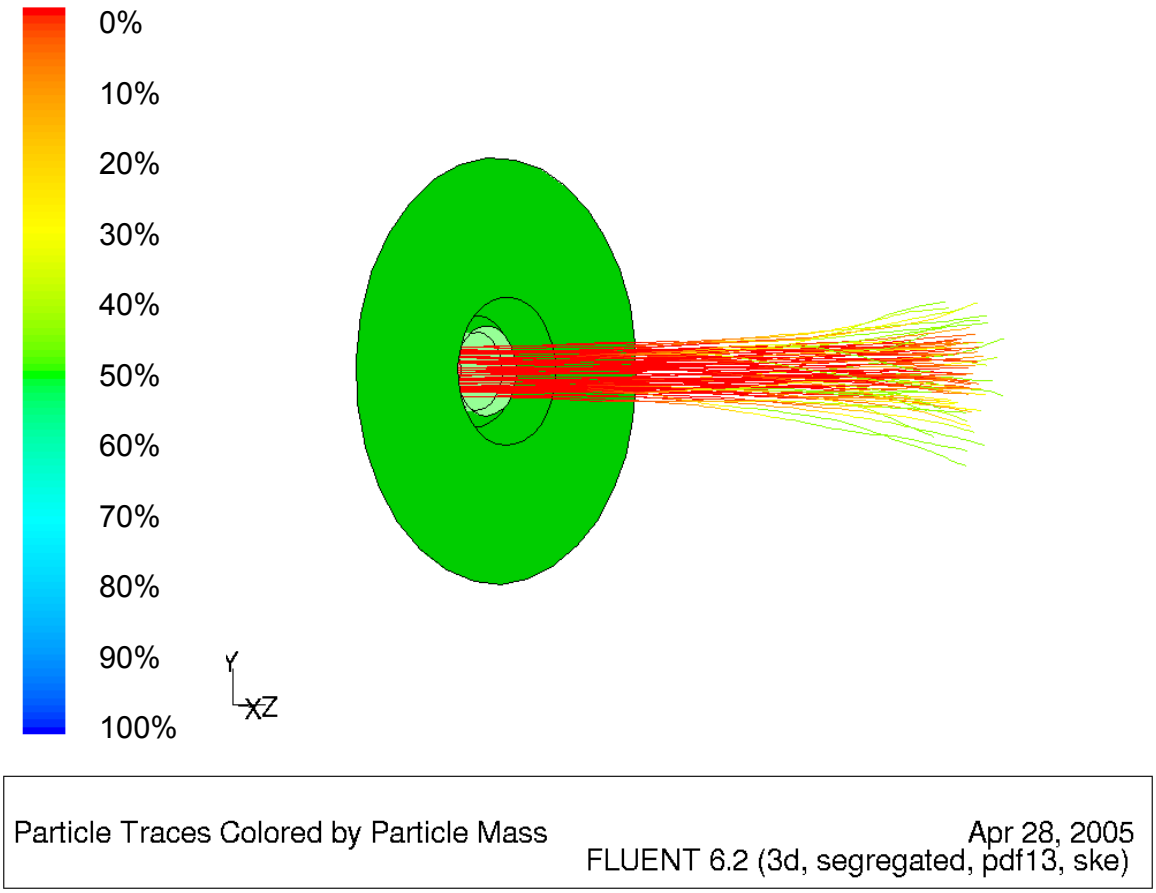

Figure 4.3.9 – Gas Velocity for 65% Recycle, No OFG, 0.5 PG Swirl

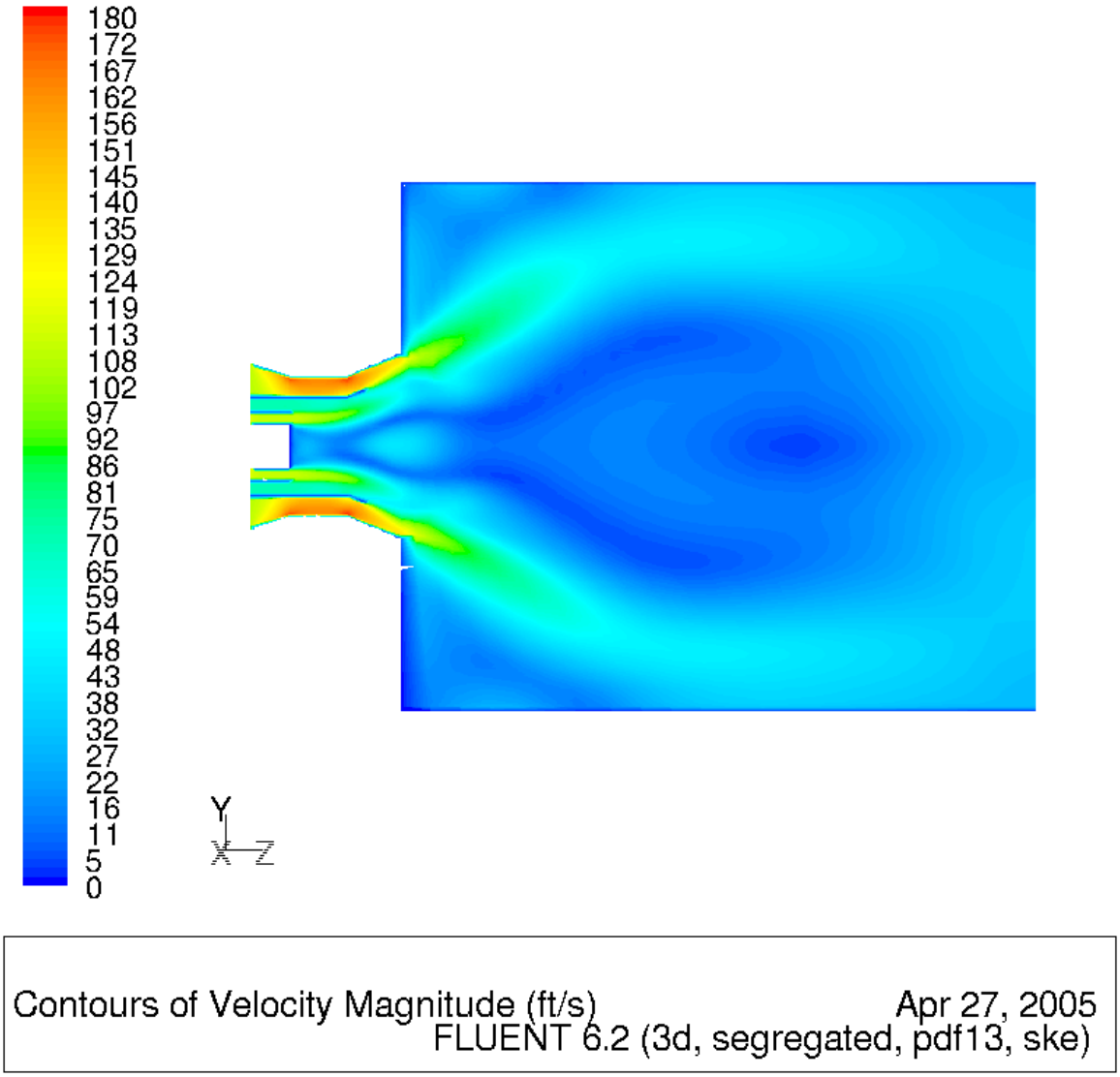

Figure 4.3.10 – Gas Temperature for 65% Recycle, No OFG, 0.5 PG Swirl

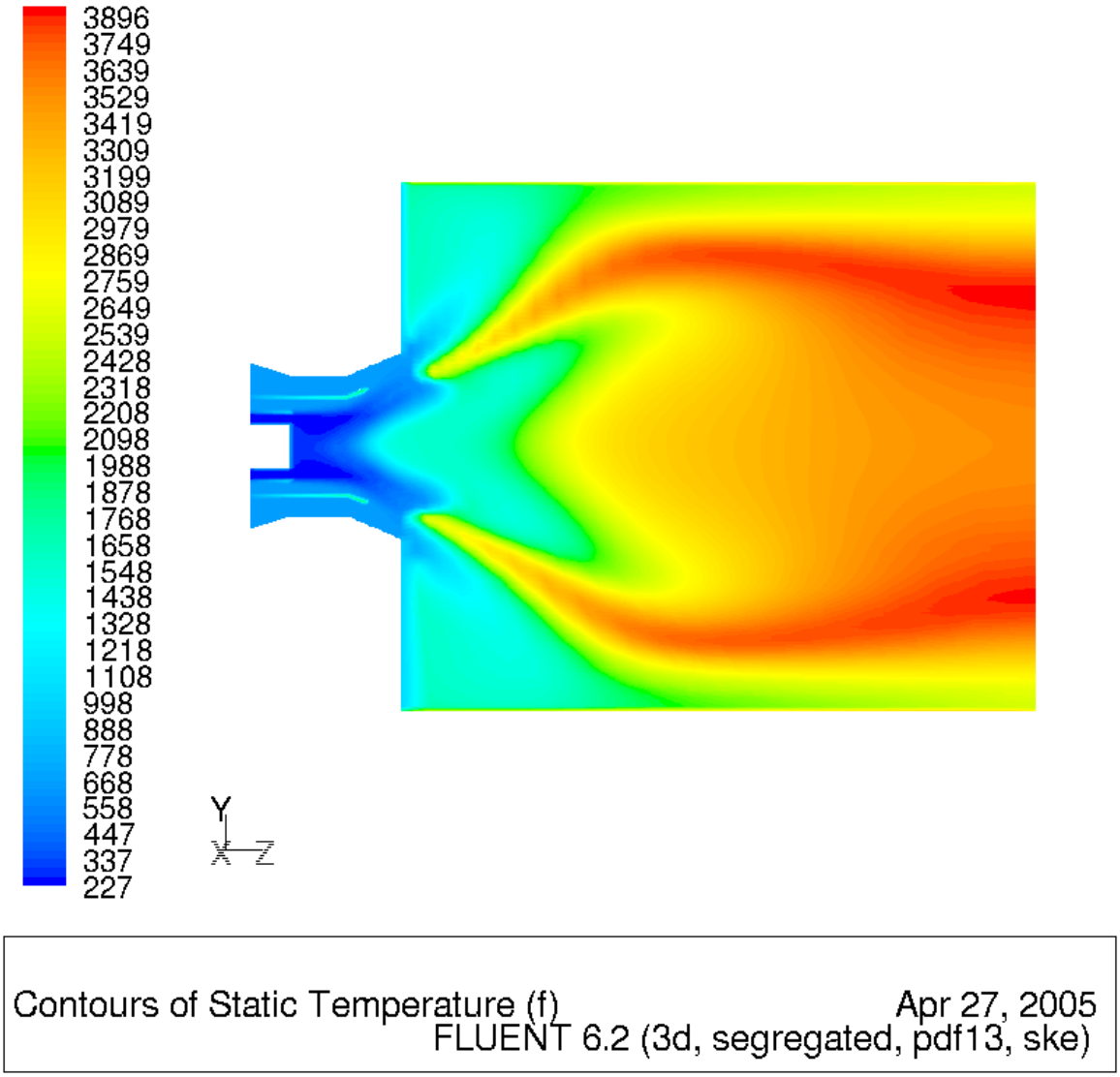

Figure 4.3.11 – O_2 Mole Fraction for 65% Recycle, No OFG, 0.5 PG Swirl

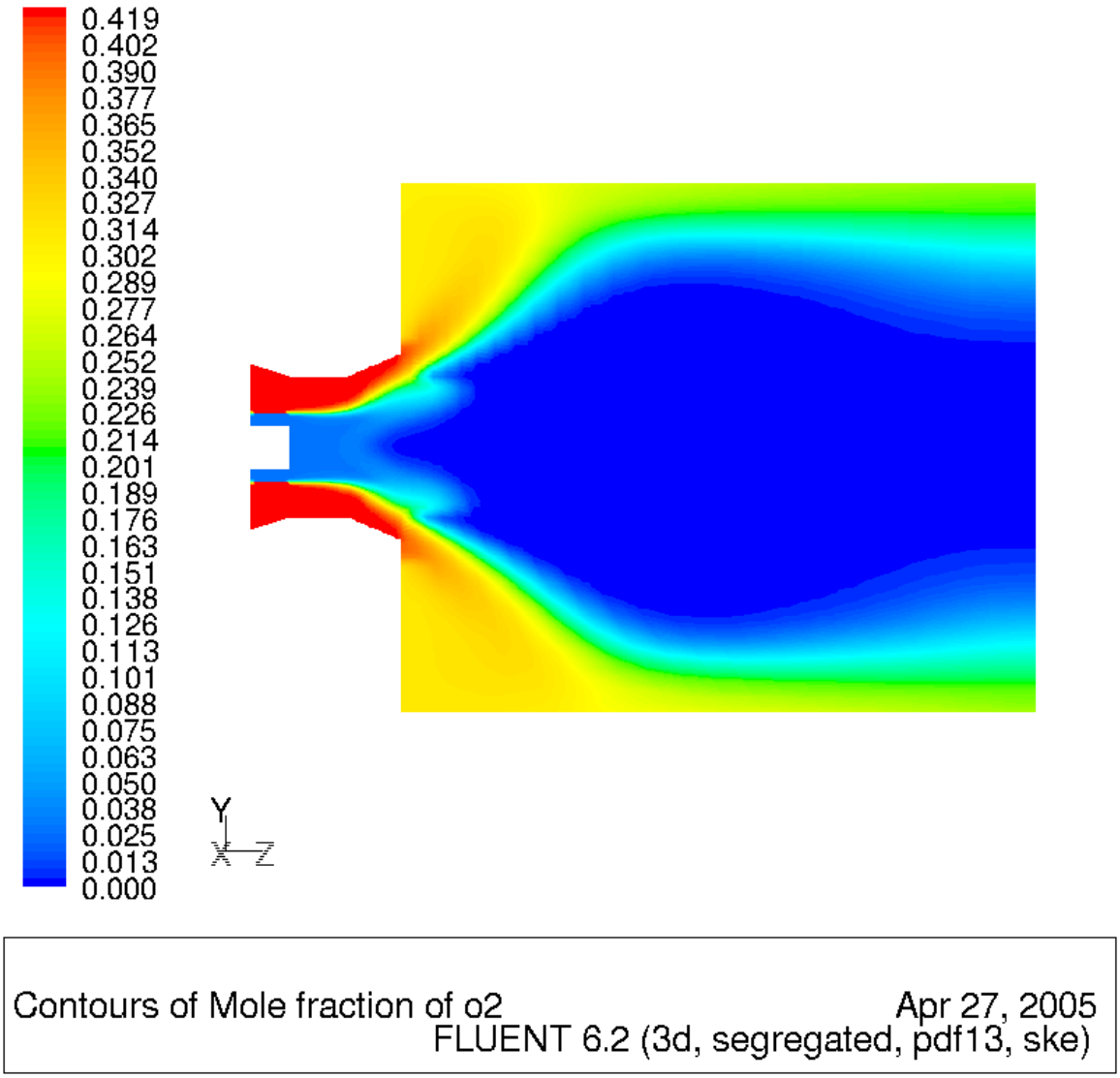

Figure 4.3.12 – Velocity Vectors Colored by Axial Velocity (ft/sec) for 65% Recycle, No OFG, 0.5 PG Swirl

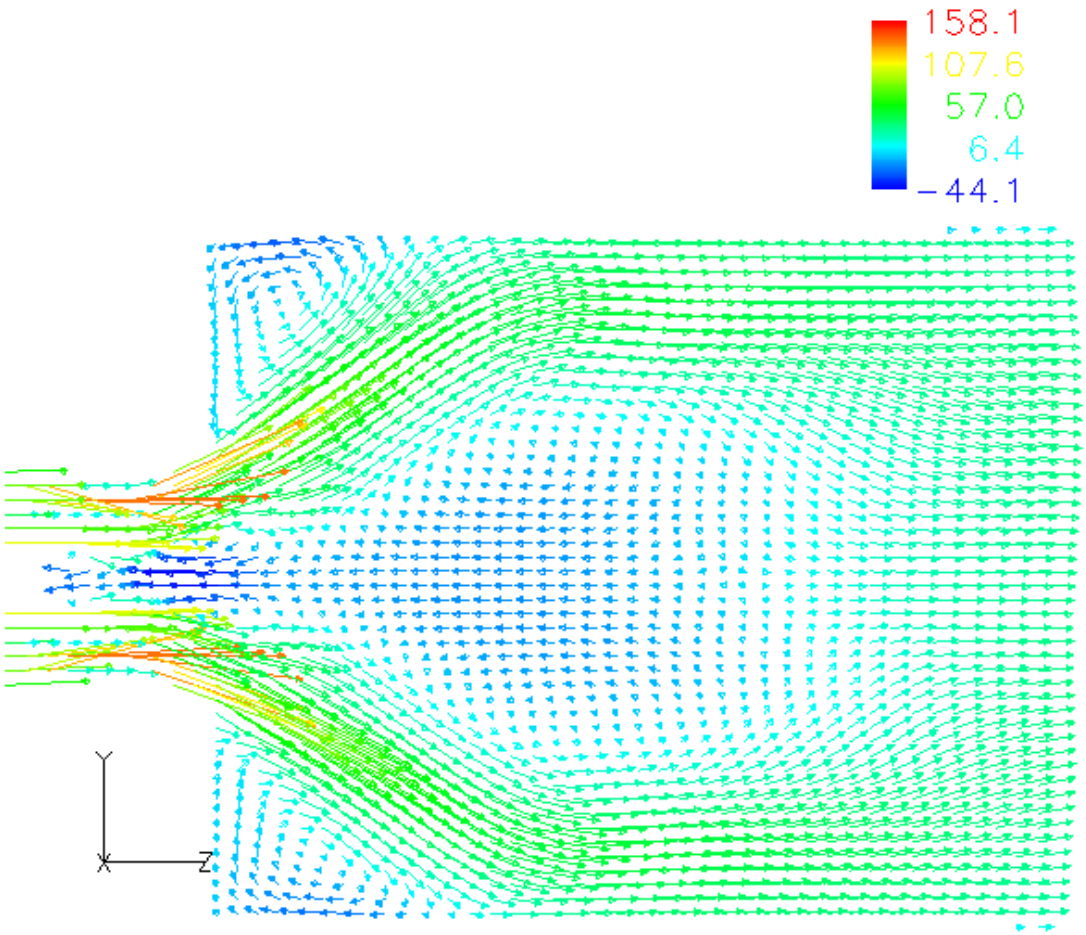

Figure 4.3.13 – Burnout of 69µ Particles for 65% Recycle, No OFG, 0.0 PG Swirl

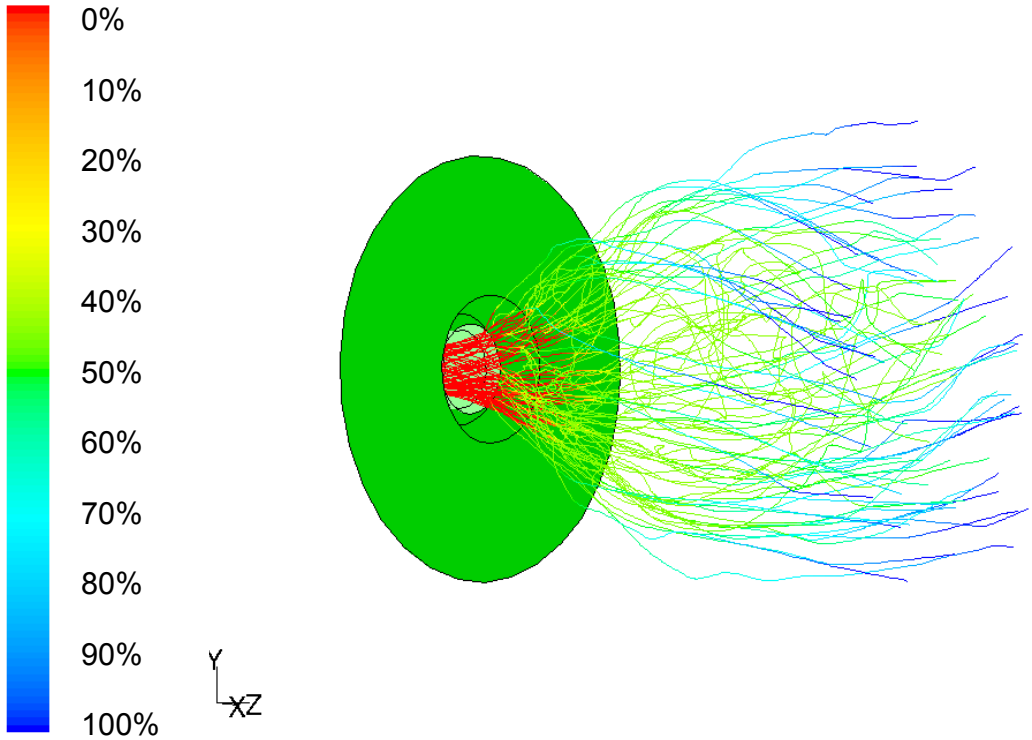

Particle Traces Colored by Particle Mass

Apr 28, 2005
FLUENT 6.2 (3d, segregated, pdf13, ske)

Figure 4.3.14 – Burnout of 169μ Particles for 65% Recycle, No OFG, 0 PG Swirl

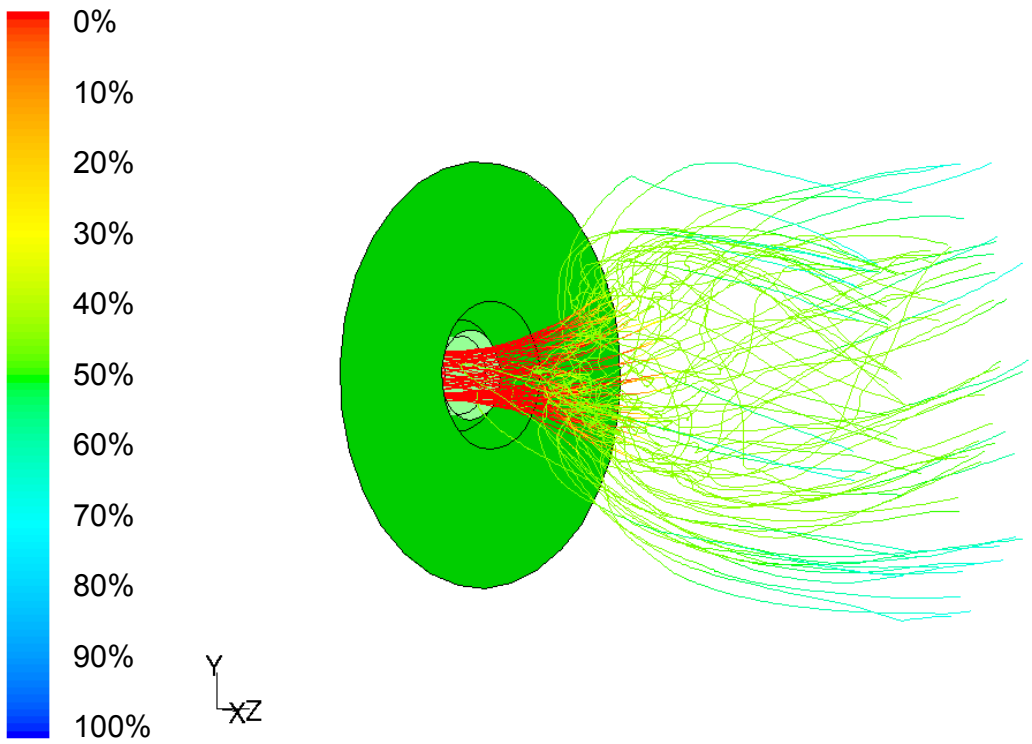

Particle Traces Colored by Particle Mass

Apr 28, 2005
FLUENT 6.2 (3d, segregated, pdf13, ske)

Figure 4.3.15 – Gas Velocity for 65% Recycle, 20% OFG, 0.0 PG Swirl

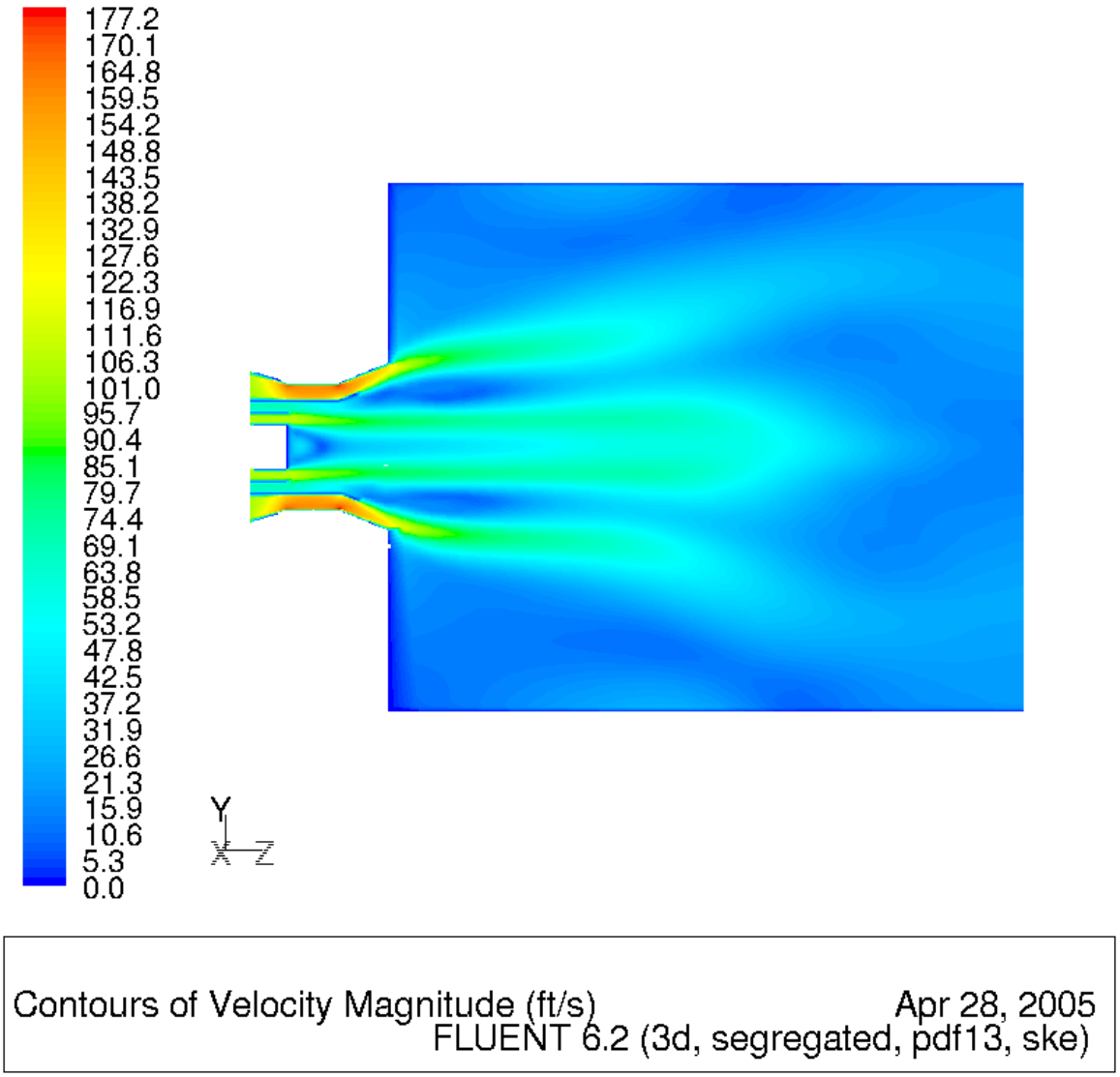

Figure 4.3.16 – Gas Temperature for 65% Recycle, 20% OFG, 0.0 PG Swirl

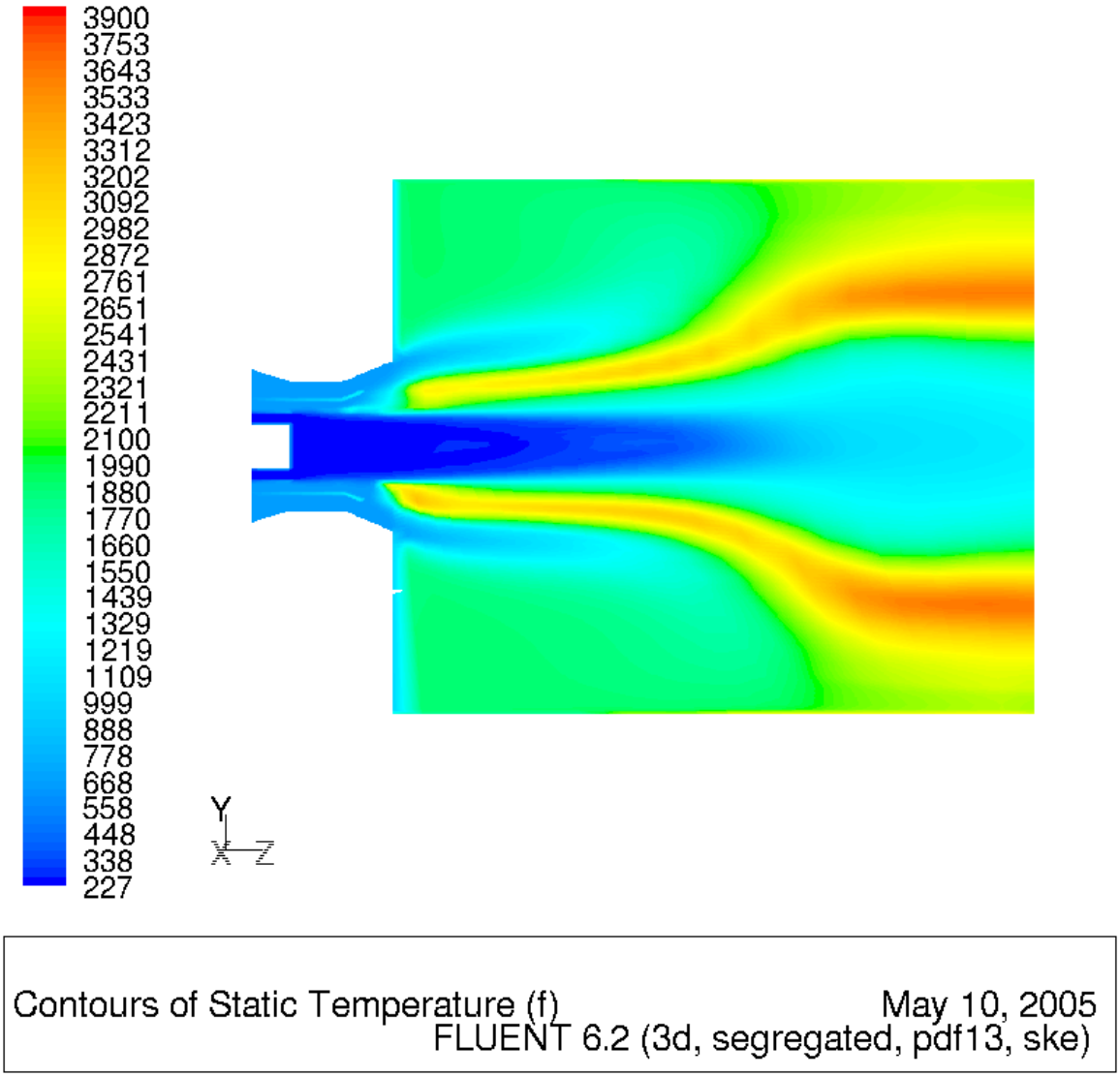

Figure 4.3.17 – O2 Mole Fraction for 65% Recycle, 20% OFG, 0.0PG Swirl

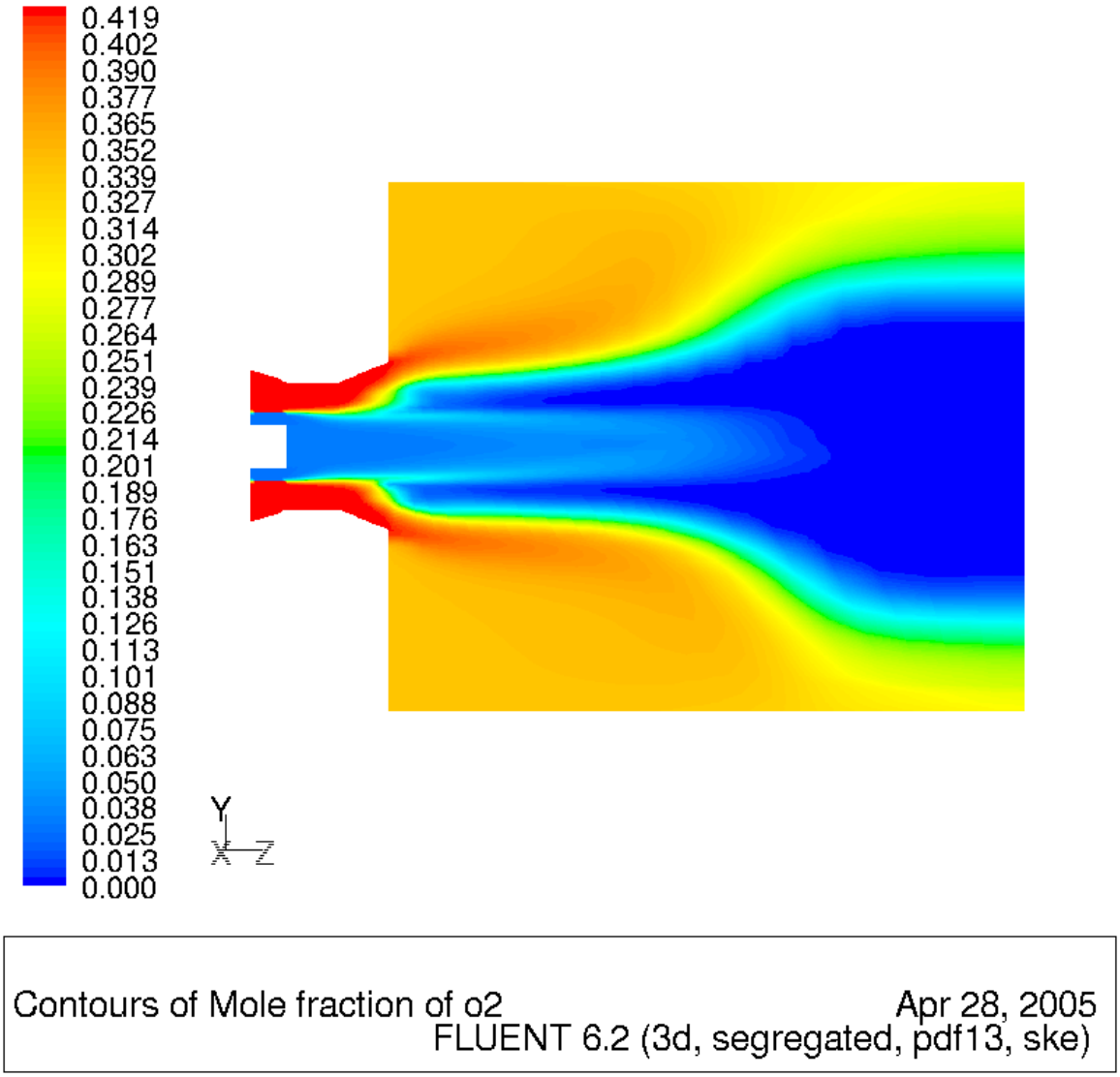

Figure 4.3.18 – Burnout of 69µ Particles for 65% Recycle, 20% OFG, 0 PG Swirl

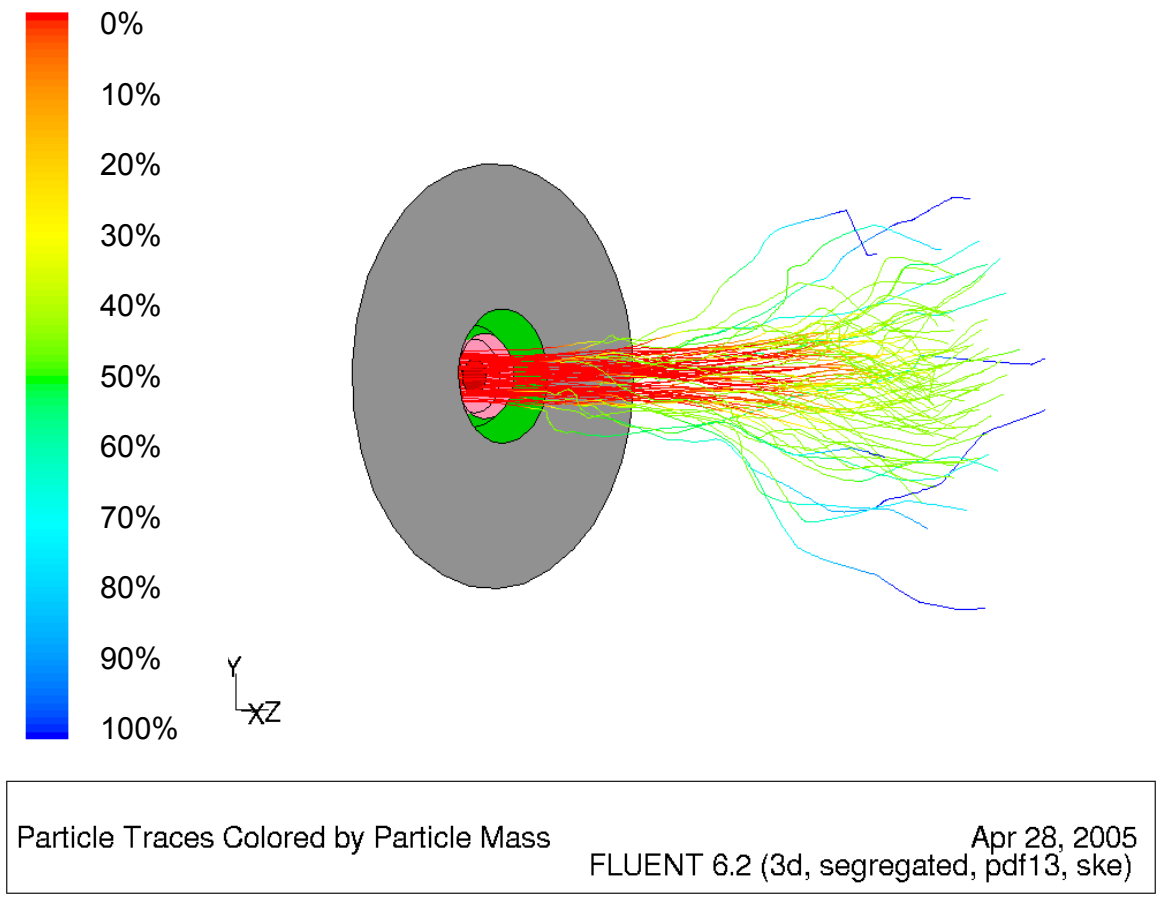

Figure 4.3.19 – Burnout of 169µ Particles for 65% Recycle, 20% OFG, 0 PG Swirl

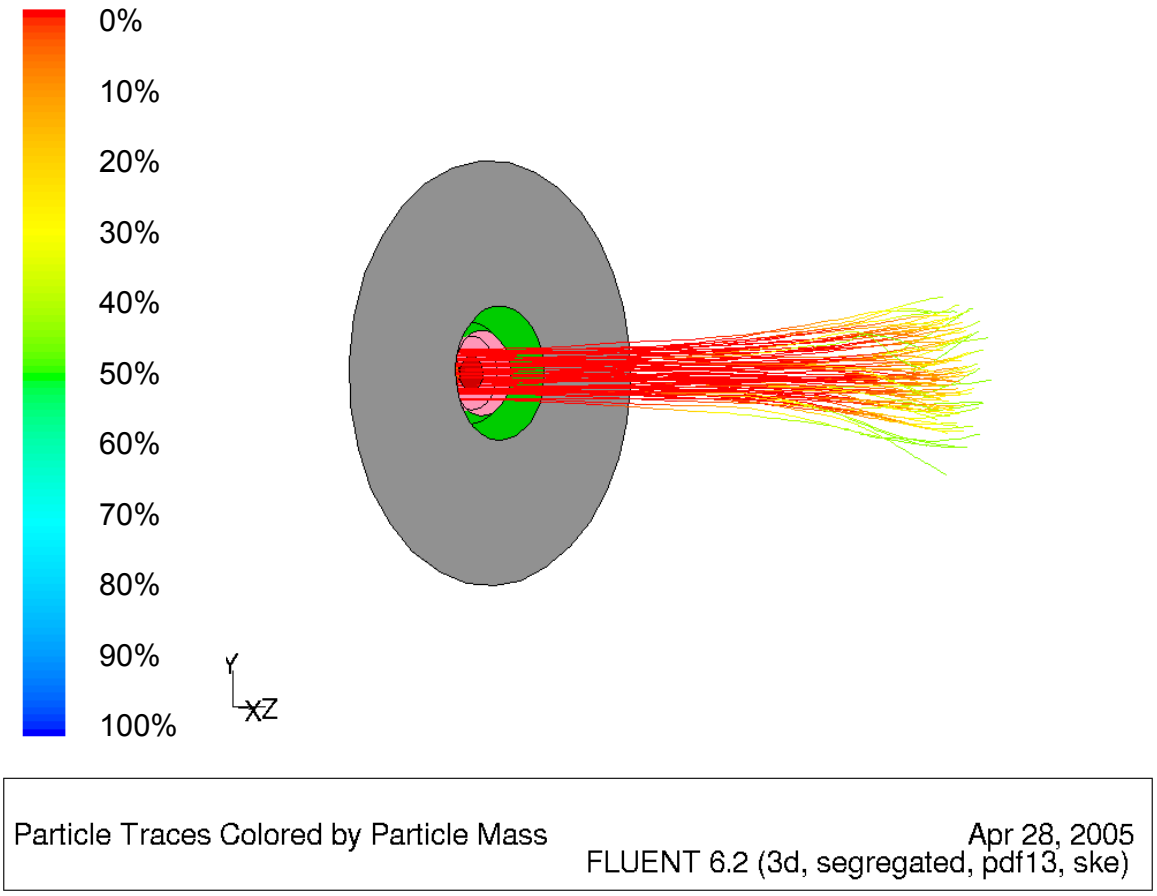

Figure 4.3.20 – Gas Velocity for 65% Recycle, 20% OFG, 0.5 PG Swirl

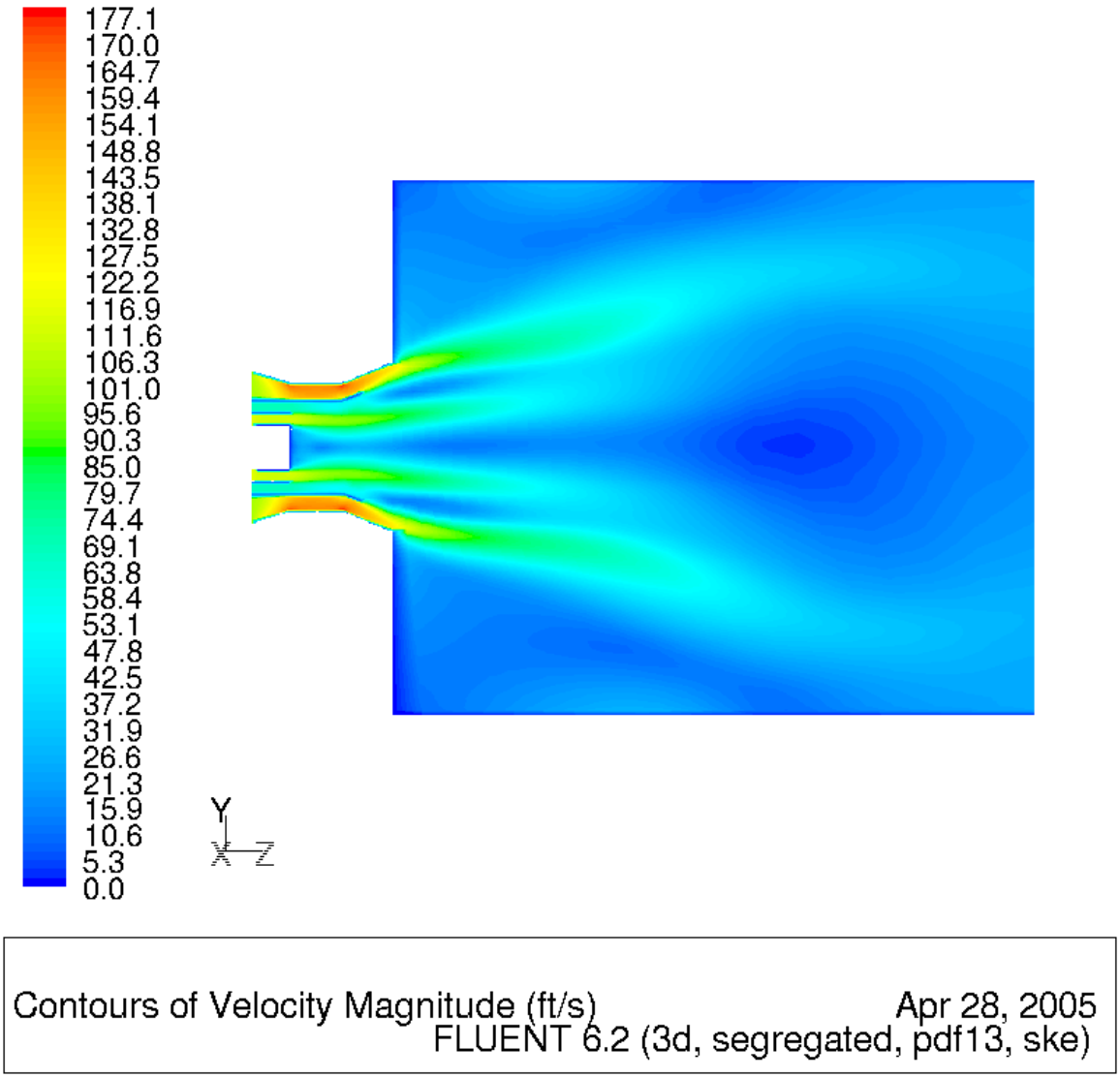

Figure 4.3.21 – Gas Temperature for 65% Recycle, 20% OFG, 0.5 PG Swirl

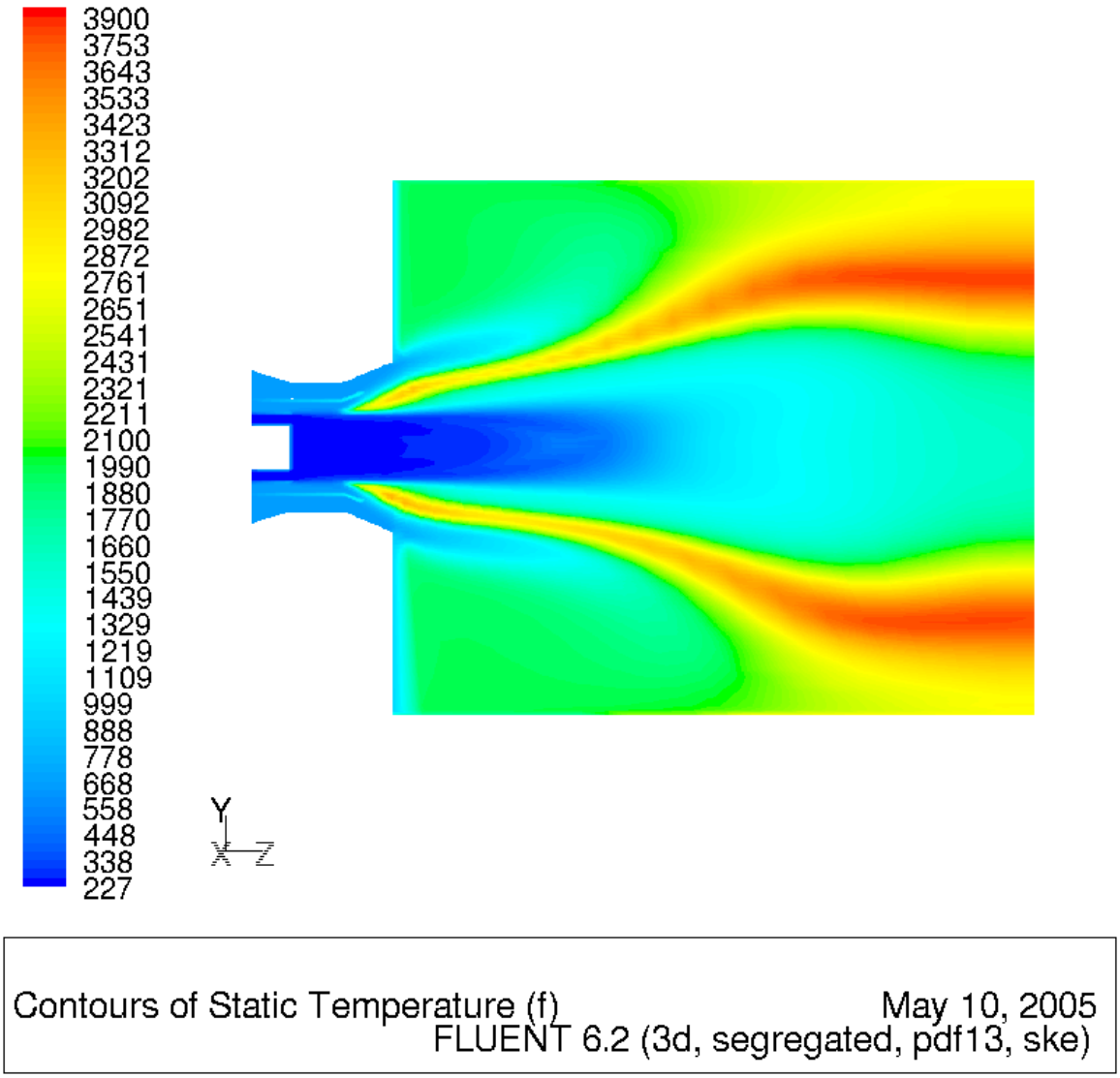

Figure 4.3.22 – O2 Mole Fraction for 65% Recycle, 20% OFG, 0.5 PG Swirl

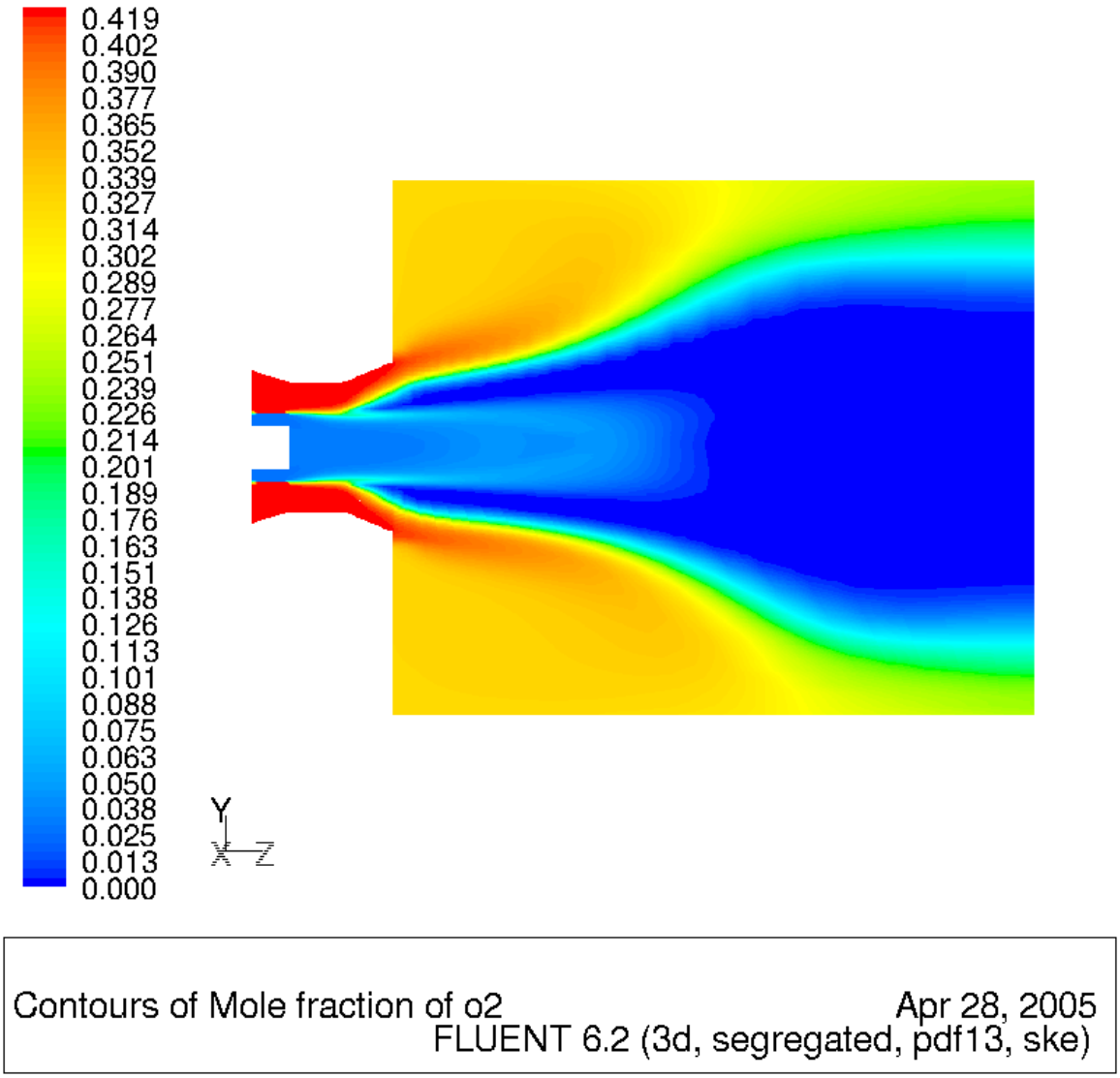

Figure 4.3.23 – Burnout of 69μ Particles for 65% Recycle, 20% OFG, 0.5 PG Swirl

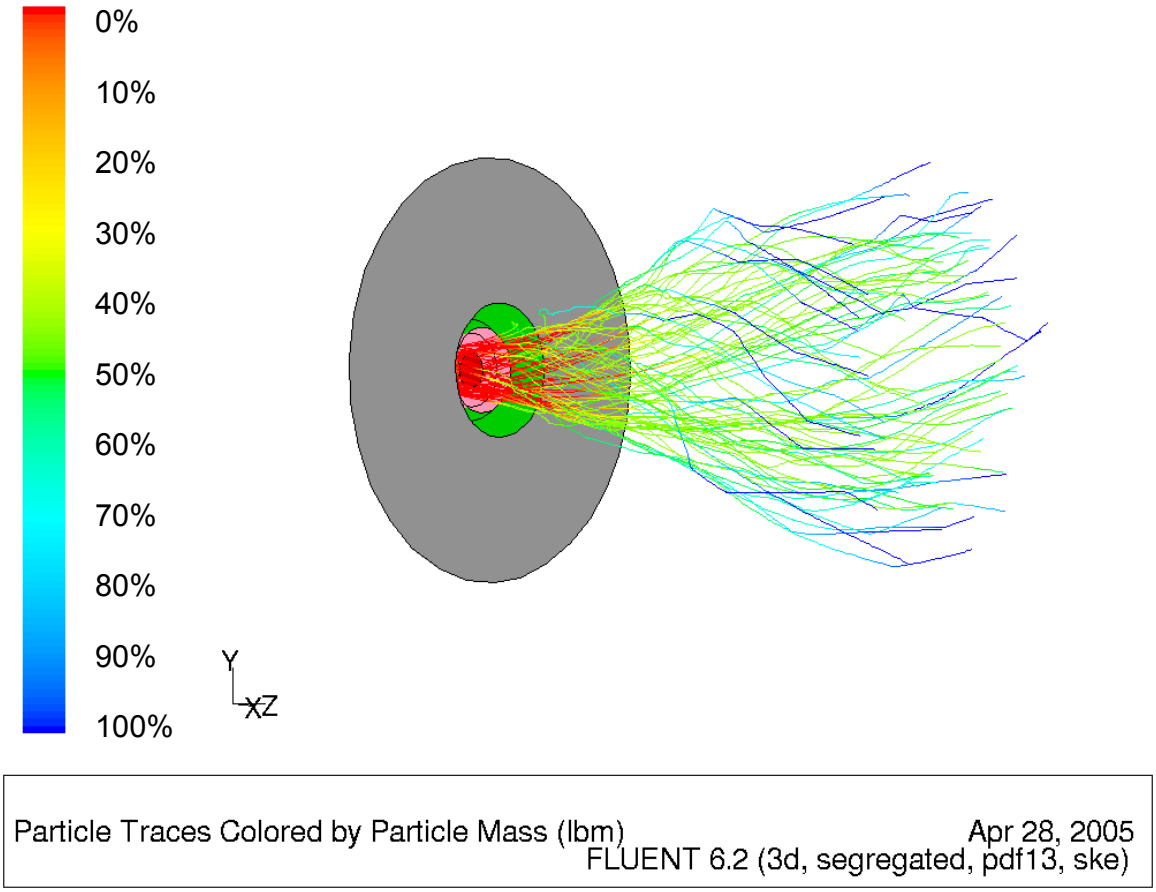

Figure 4.3.24 – Burnout of 169μ Particles for 65% Recycle, 20% OFG, 0.5 PG Swirl

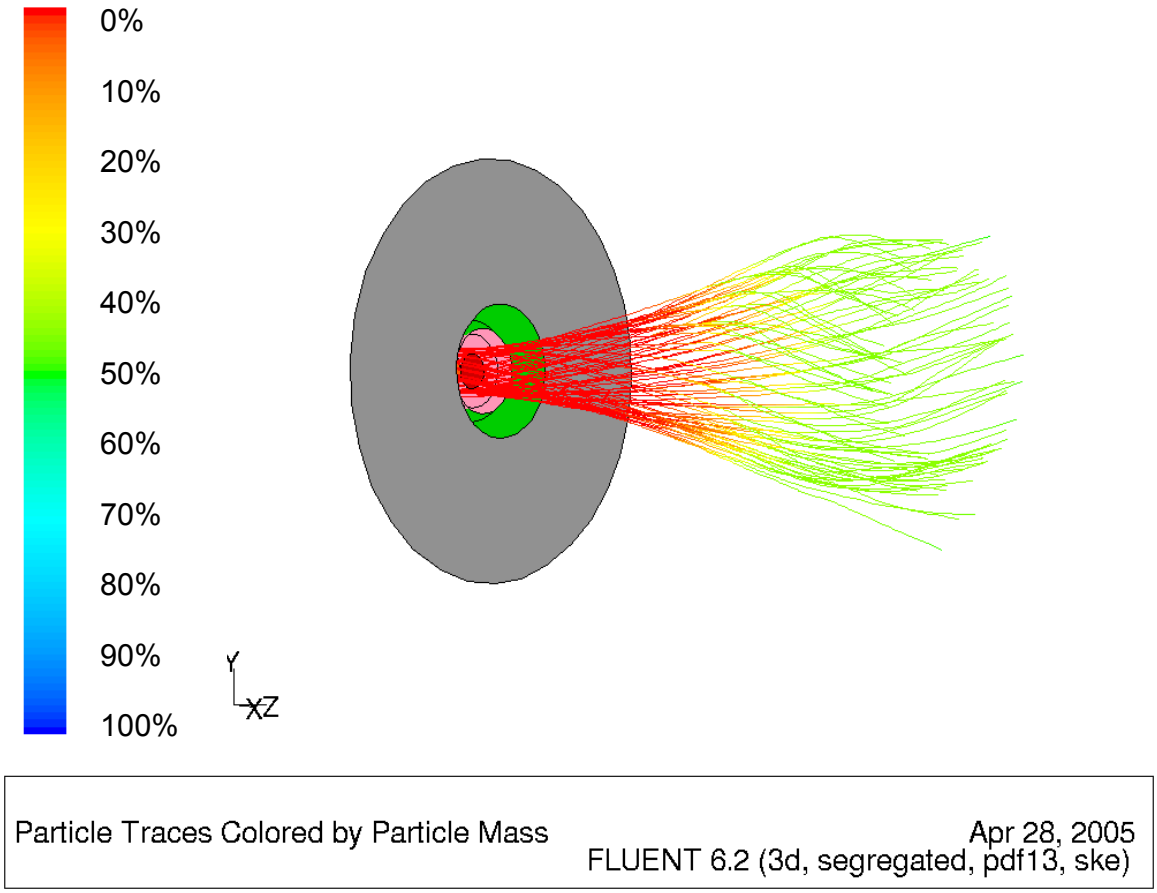

Figure 4.3.25 – Gas Velocity for 56% Recycle, 0% OFG, 0.0 PG Swirl

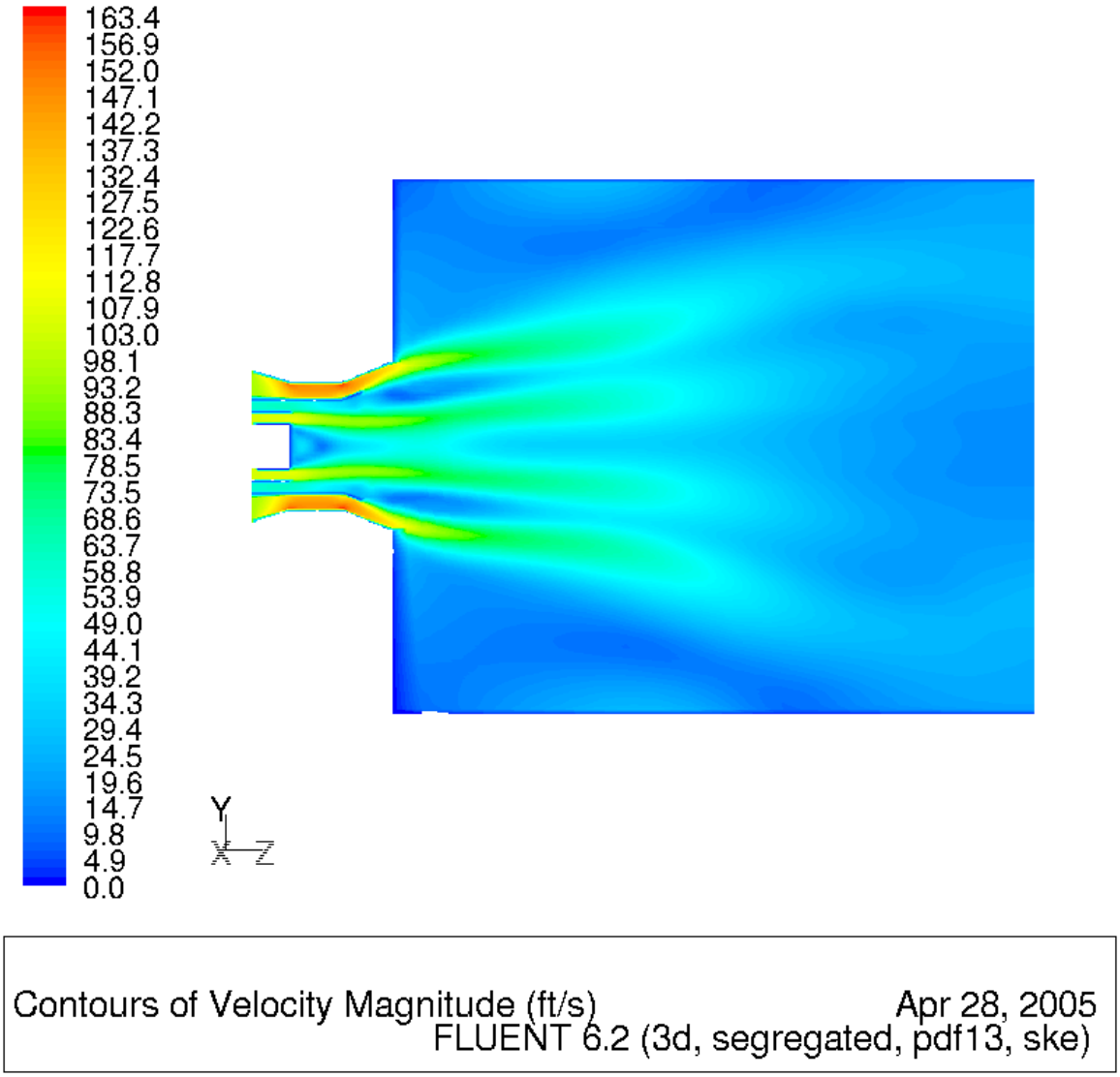

Figure 4.3.26 – Gas Temperature for 56% Recycle, 0% OFG, 0.0 PG Swirl

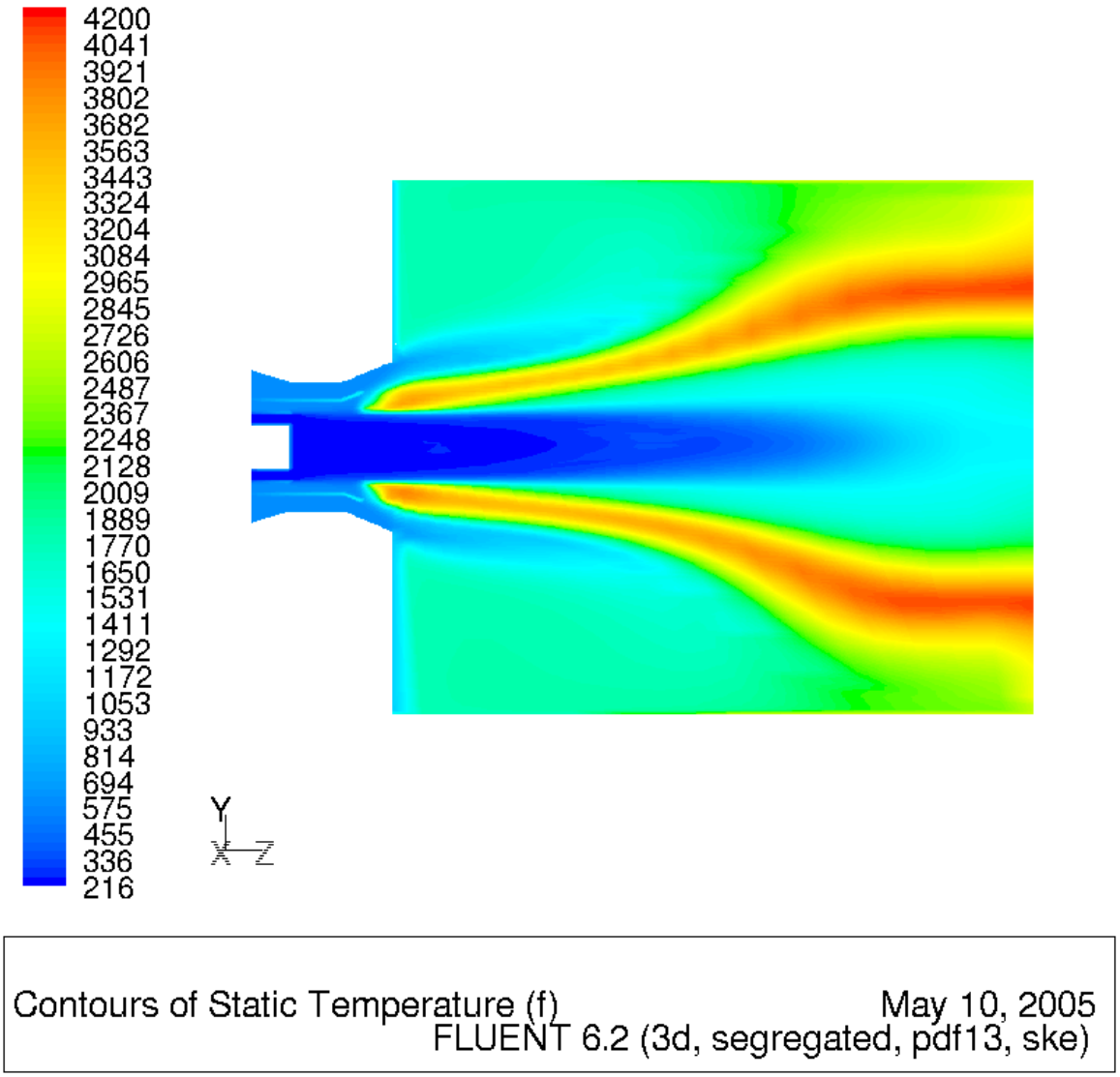

Figure 4.3.27 – O2 Mole Fraction for 56% Recycle, 0% OFG, 0.0 PG Swirl

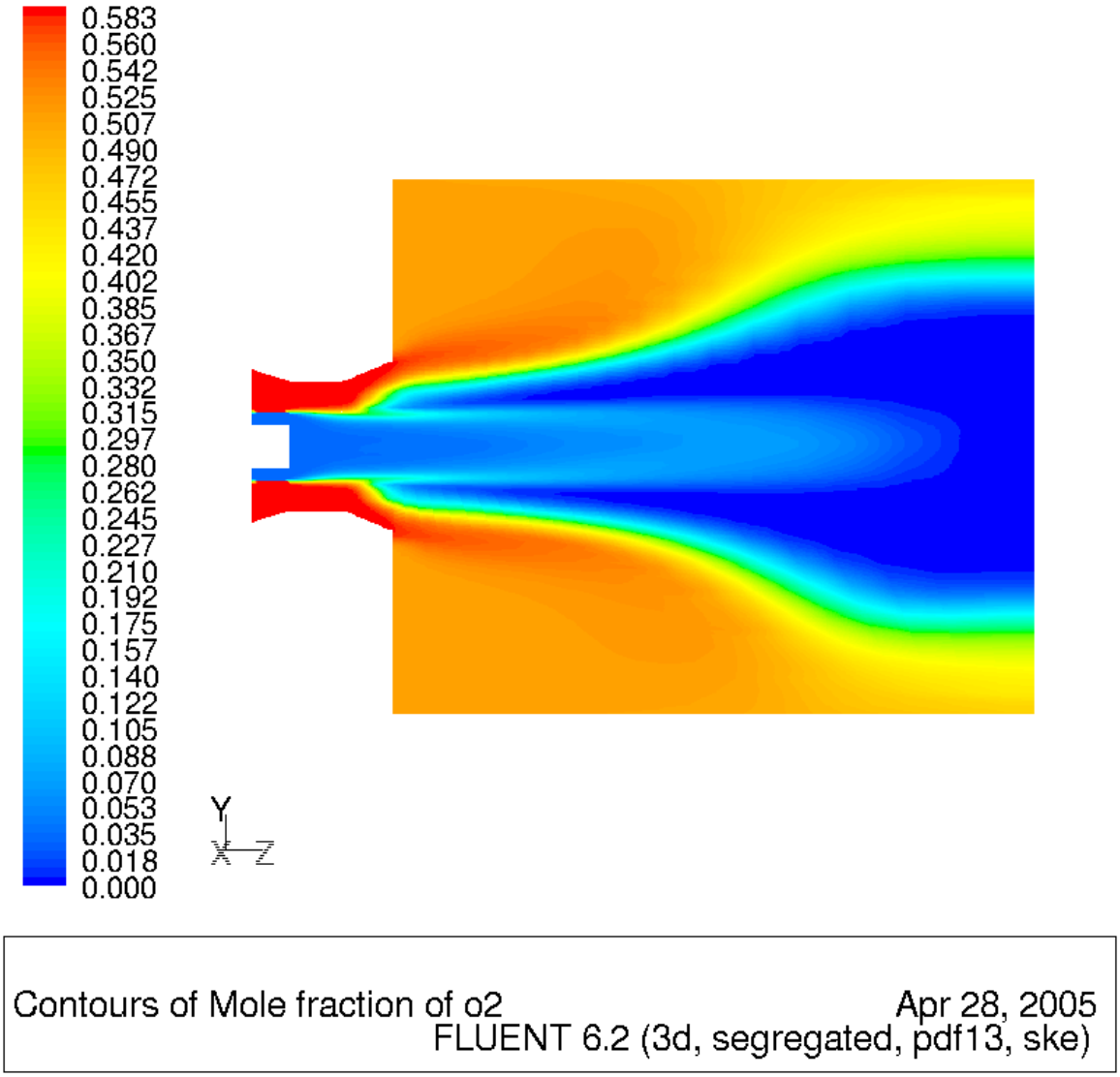

Figure 4.3.28 – Burnout of 69µ Particles for 56% Recycle, 0% OFG, 0 PG Swirl

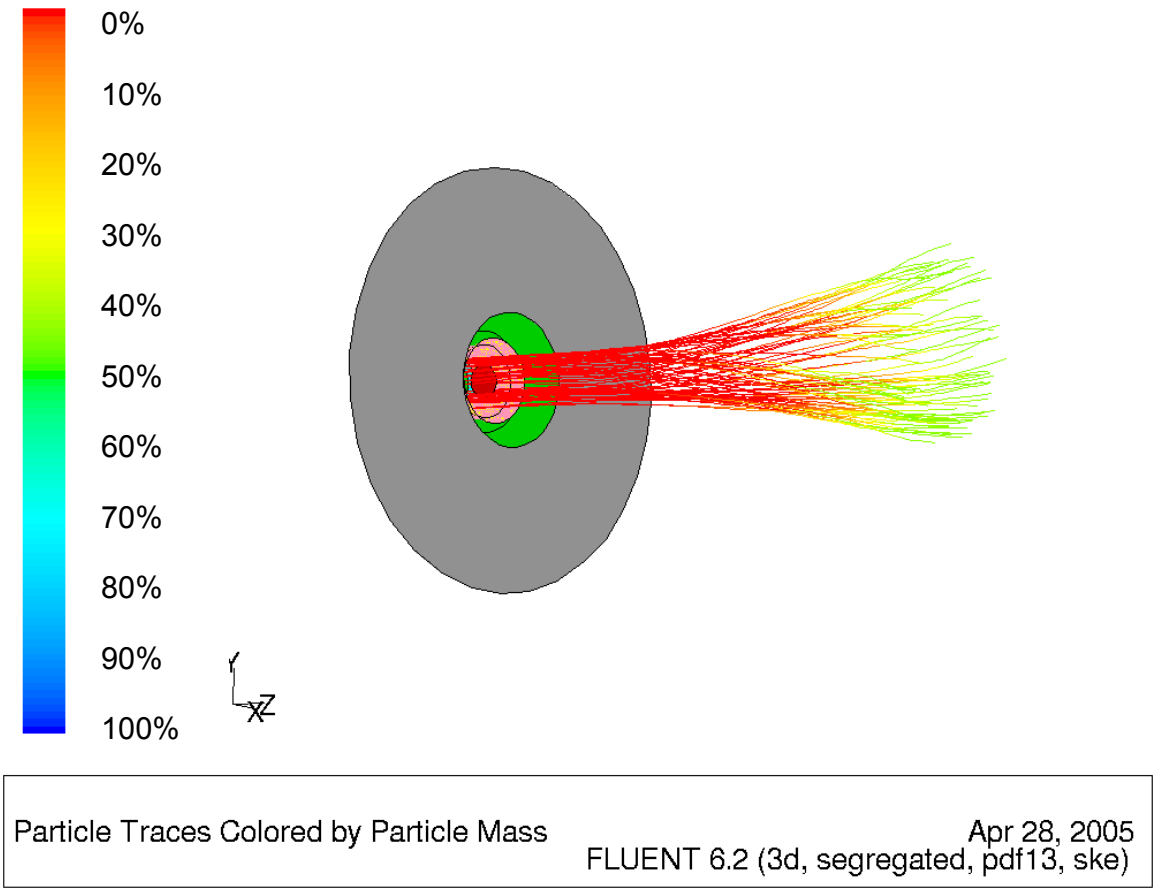

Figure 4.3.29 – Burnout of 169μ Particles for 56% Recycle, 0% OFG, 0 PG Swirl

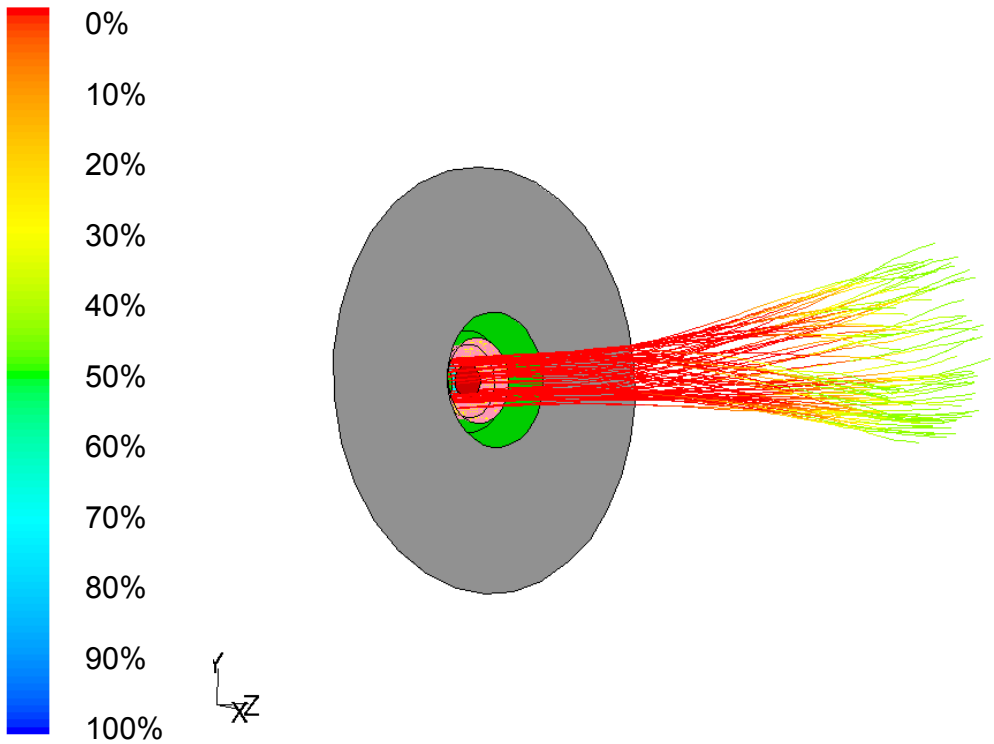

Particle Traces Colored by Particle Mass

Apr 28, 2005
FLUENT 6.2 (3d, segregated, pdf13, ske)

Figure 4.3.30 – Gas Velocity for 56% Recycle, 0% OFG, 0.5 PG Swirl

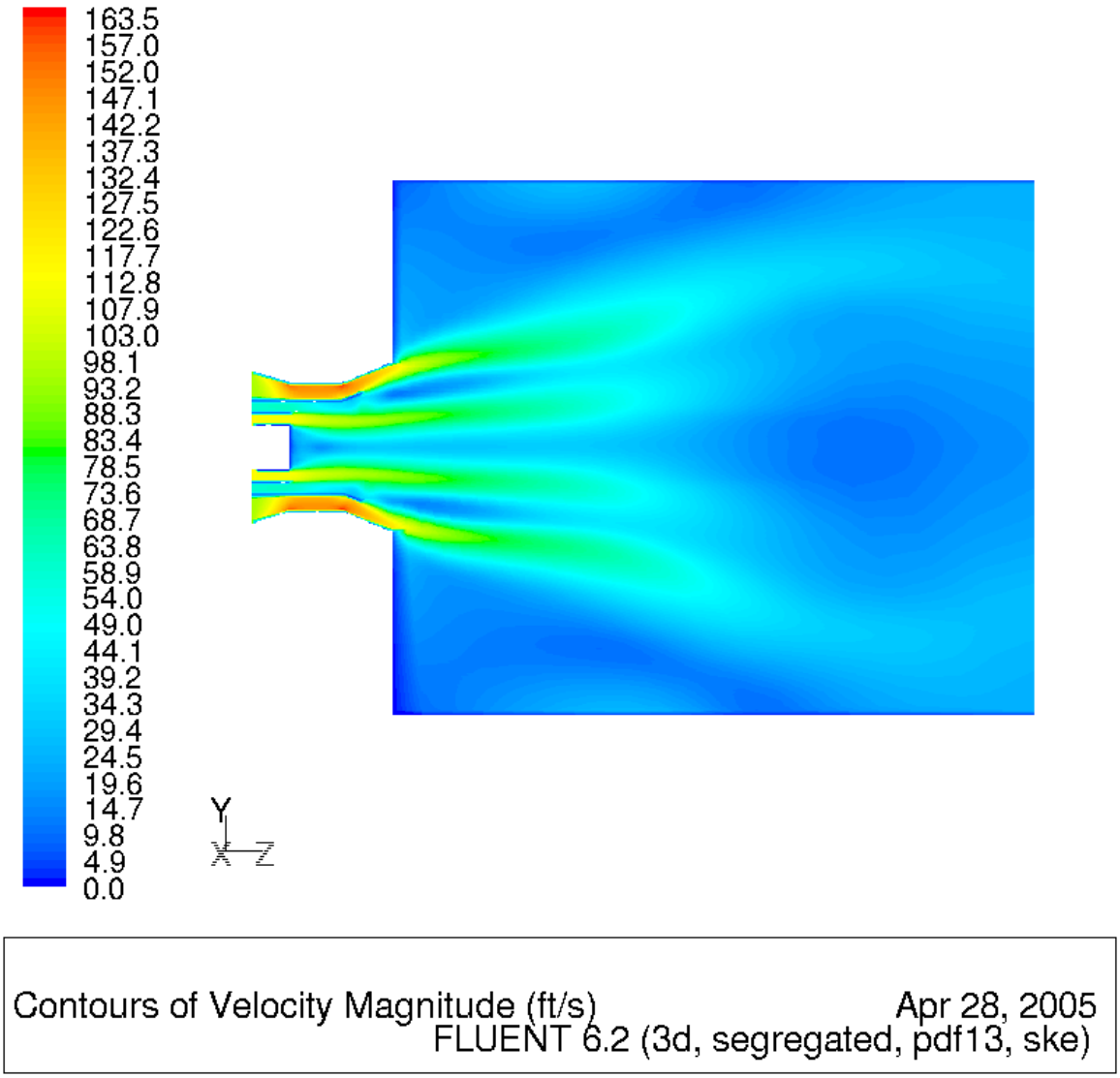

Figure 4.3.31 – Gas Temperature for 56% Recycle, 0% OFG, 0.5 PG Swirl

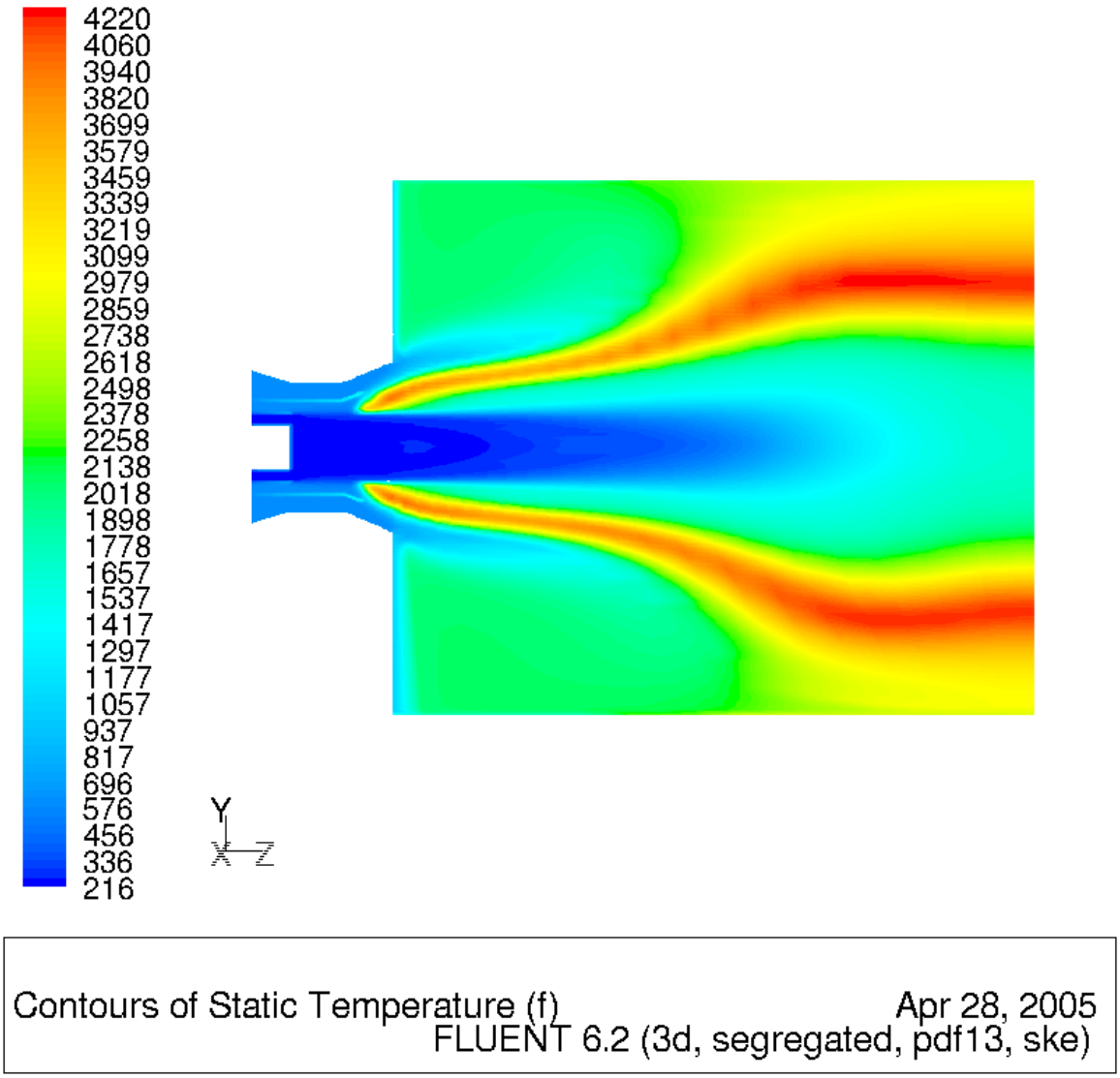

Figure 4.3.32 – O2 Mole Fraction for 56% Recycle, 0% OFG, 0.5 PG Swirl

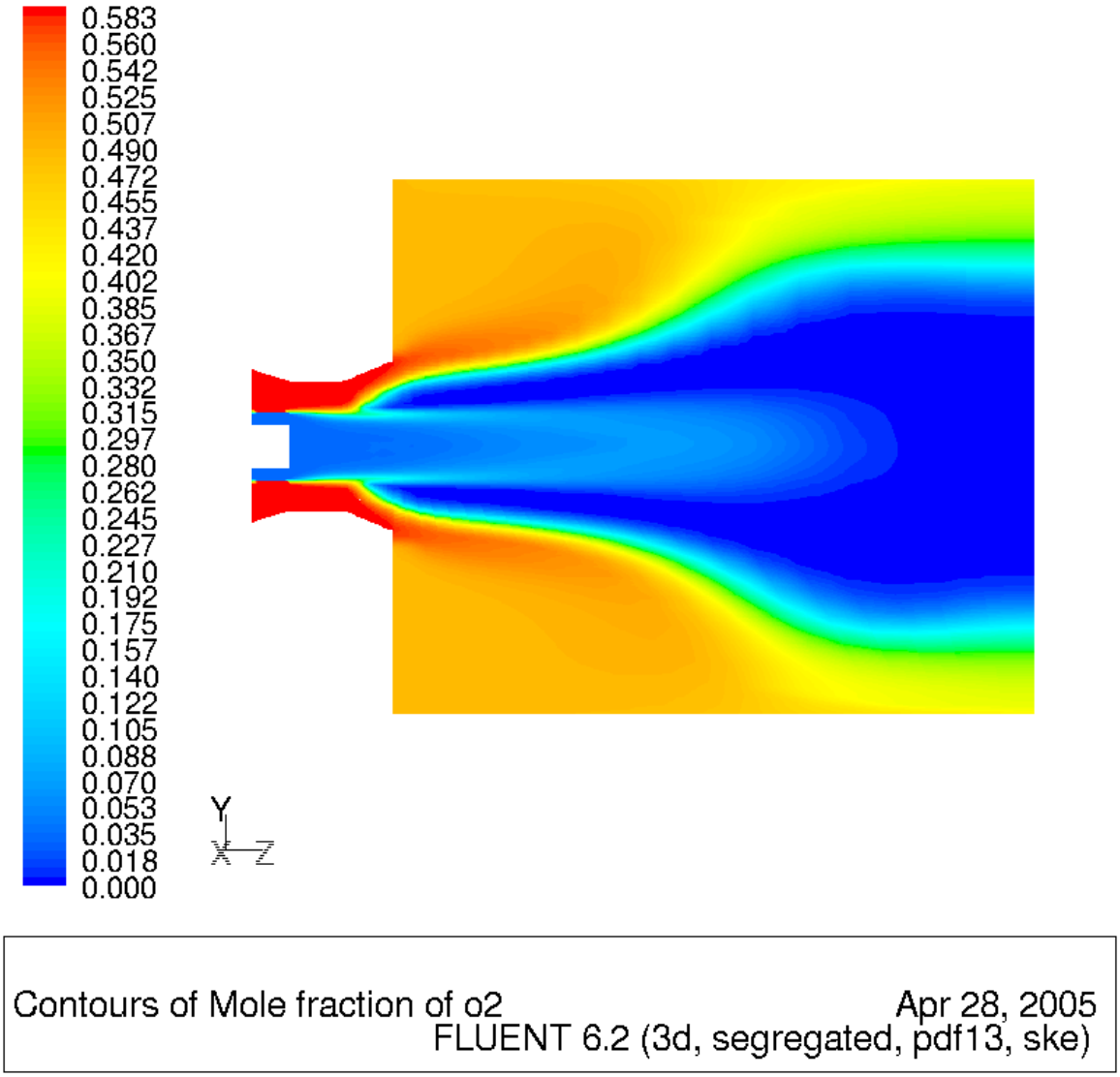

Figure 4.3.33 – Burnout of 69µ Particles for 56% Recycle, 0% OFG, 0.5 PG Swirl

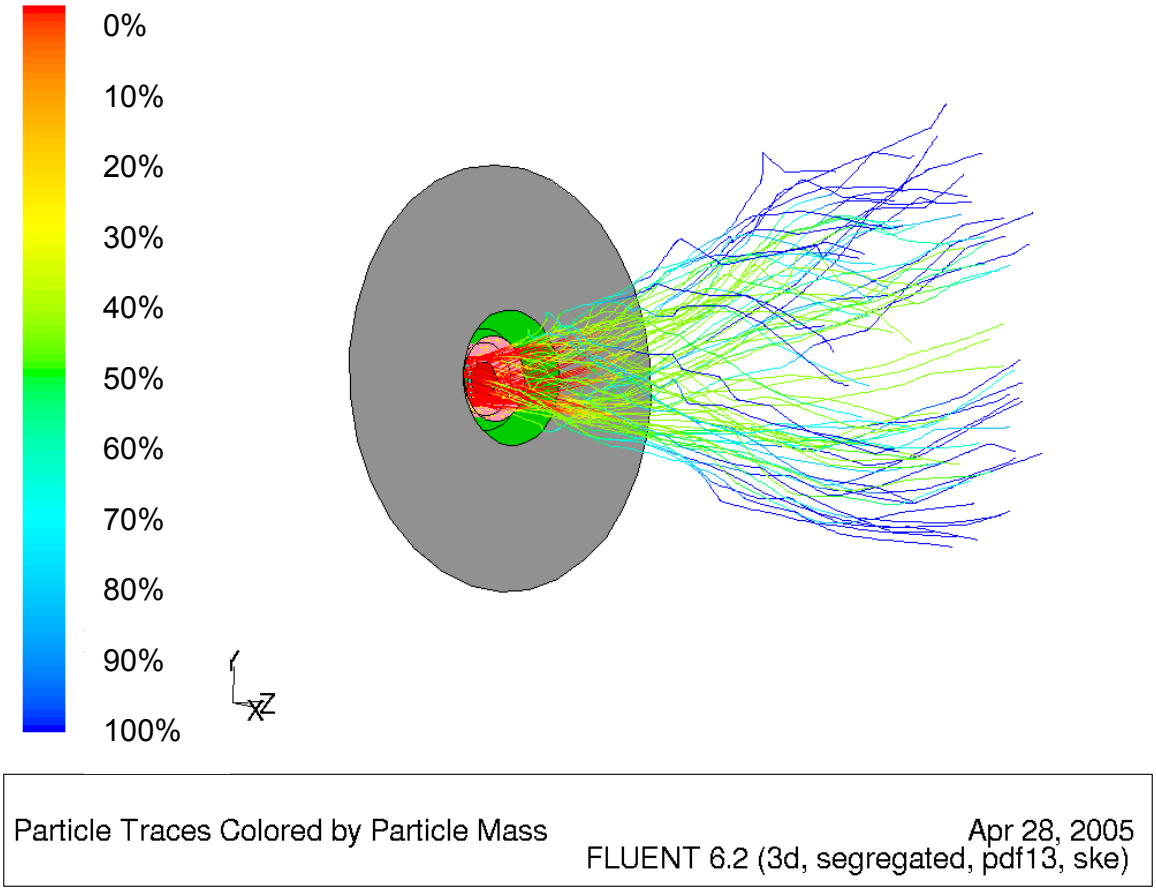

Figure 4.3.34 – Burnout of 169μ Particles for 56% Recycle, 0% OFG, 0.5 PG Swirl

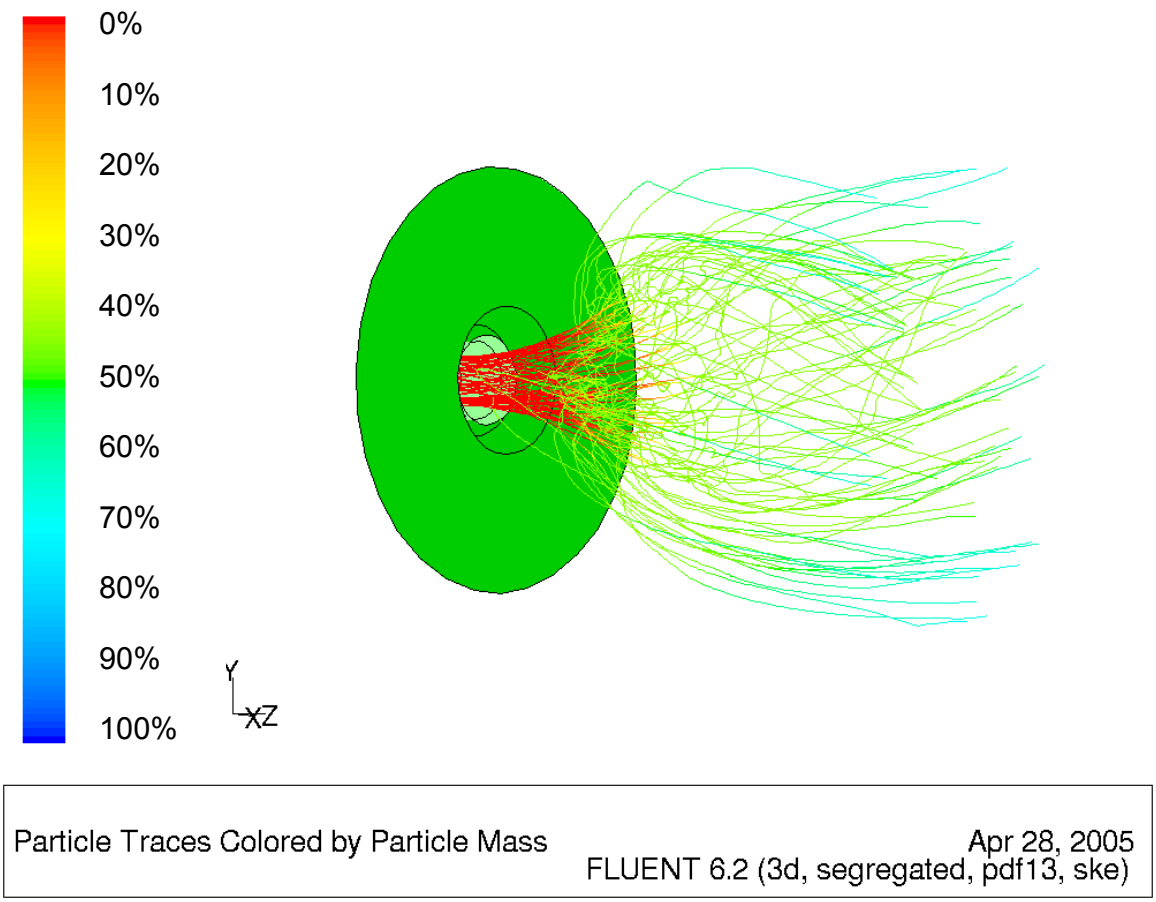

Figure 4.3.35 – Gas Velocity for 56% Recycle, 20% OFG, 0. PG Swirl

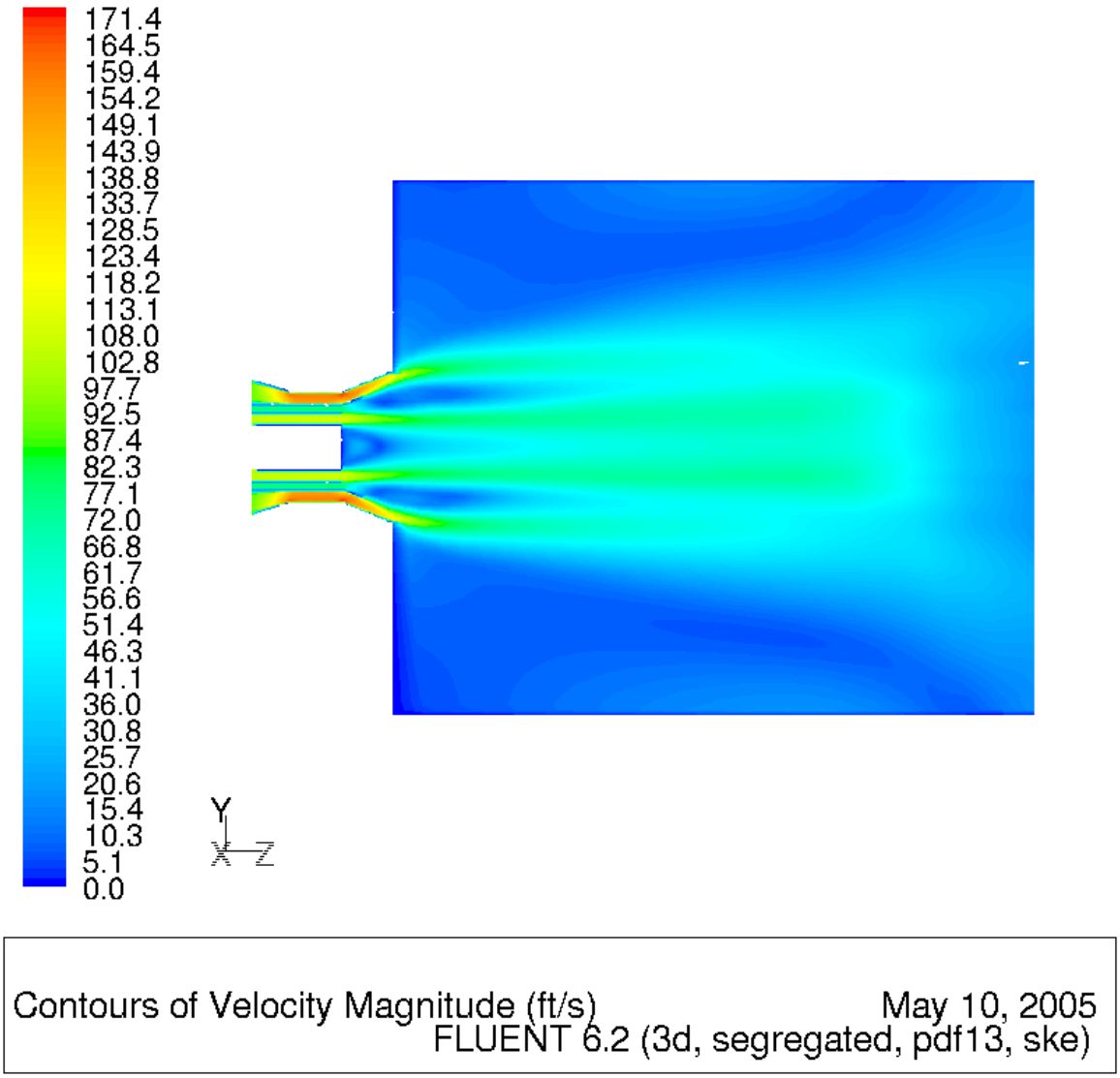

Figure 4.3.36 – Gas Temperature for 56% Recycle, 20% OFG, 0. PG Swirl

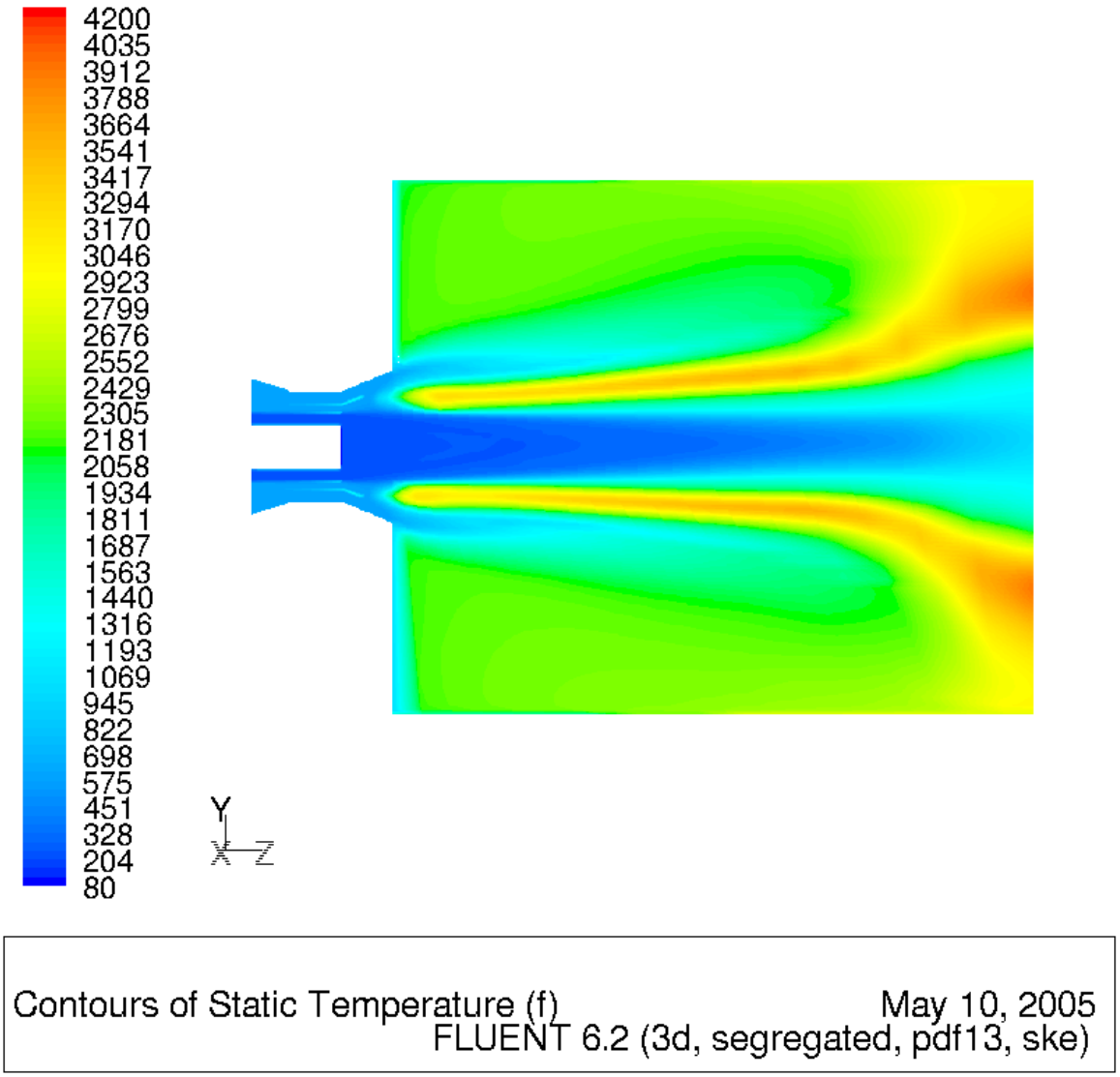

Figure 4.3.37 – O2 Mole Fraction for 56% Recycle, 20% OFG, 0. PG Swirl

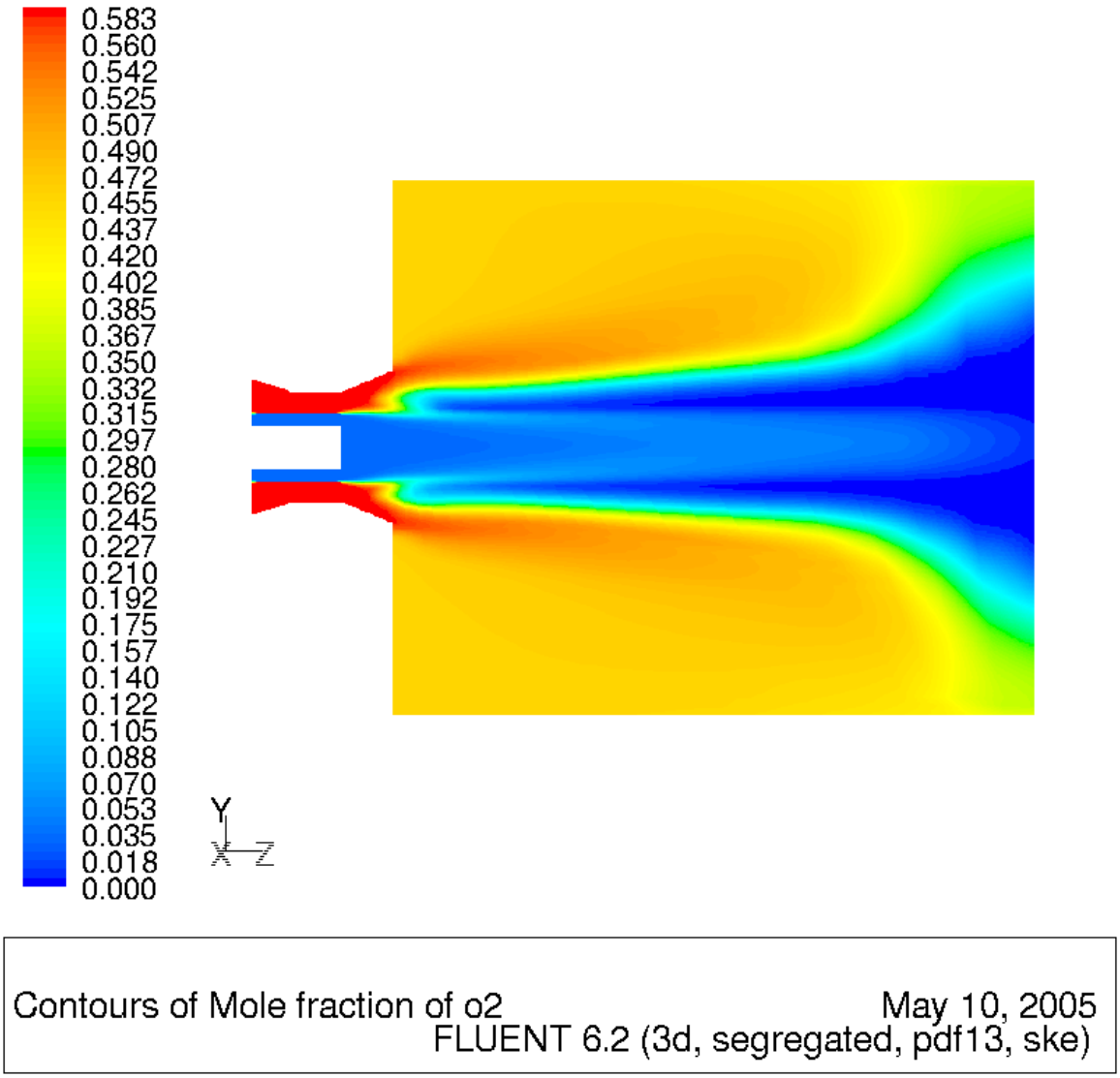

Figure 4.3.38 – Burnout of 69μ Particles for 56% Recycle, 20% OFG, 0. PG Swirl

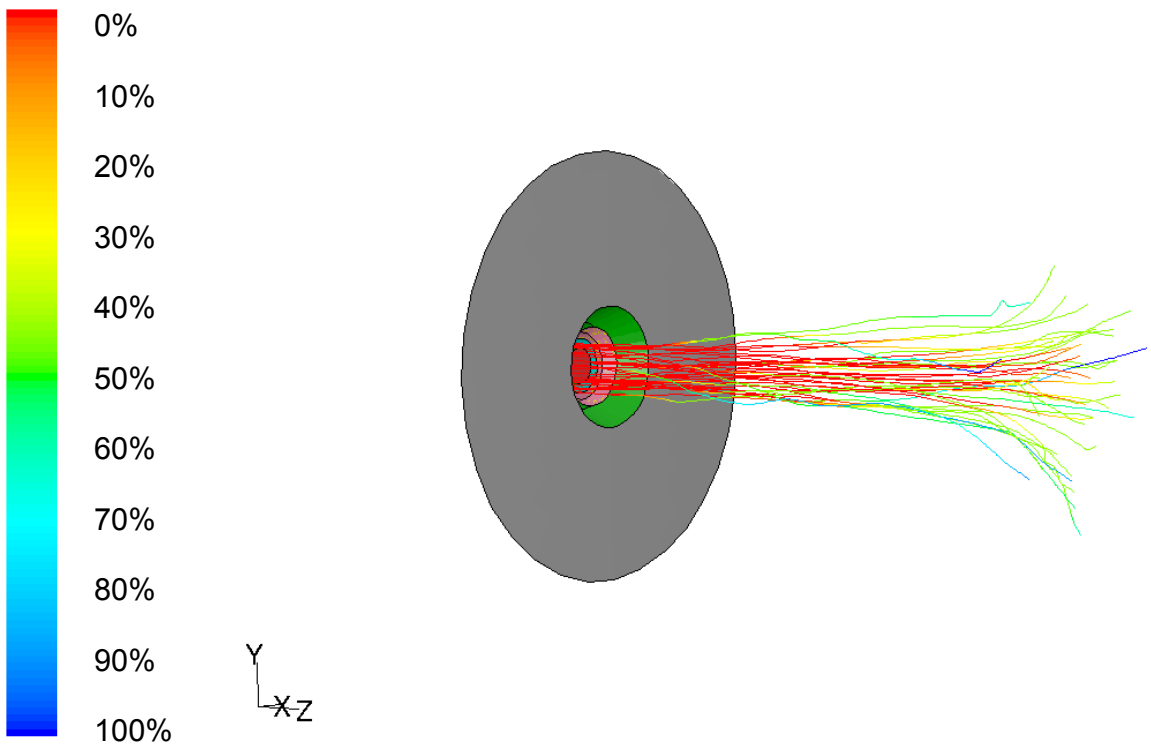

Particle Traces Colored by Particle Mass (kg)

May 06, 2005
FLUENT 6.2 (3d, segregated, pdf13, ske)

Figure 4.3.39 – Burnout of 169μ Particles for 56% Recycle, 20% OFG, 0. PG Swirl

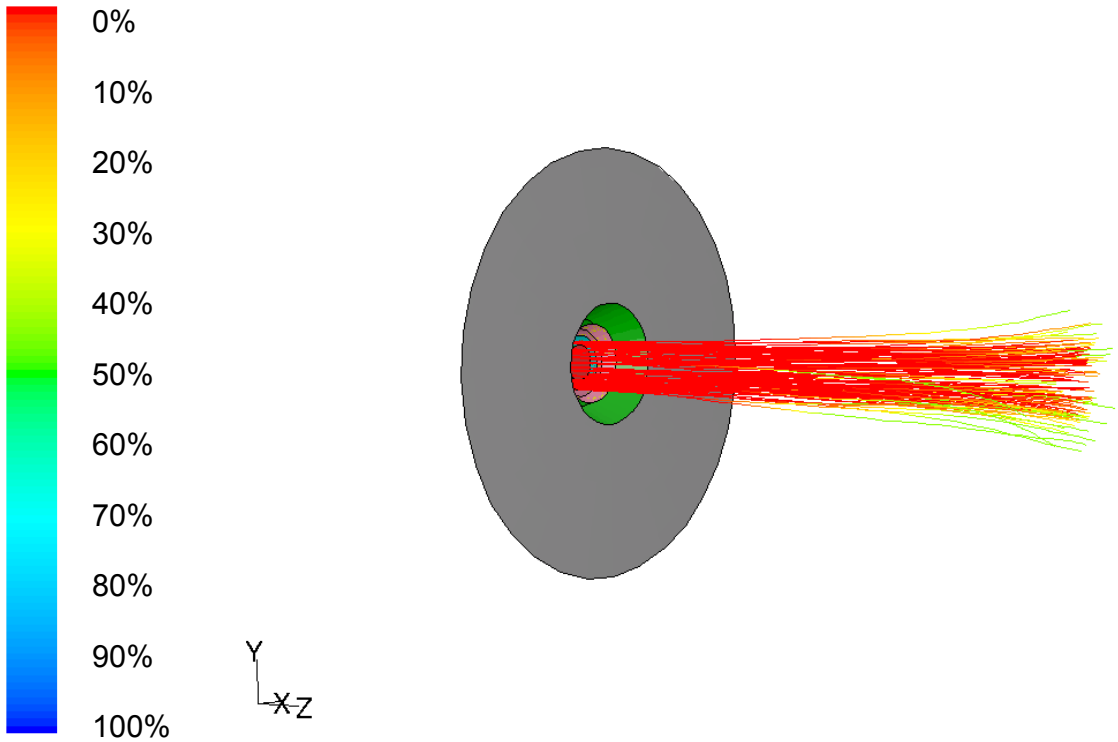

Particle Traces Colored by Particle Mass

May 06, 2005
FLUENT 6.2 (3d, segregated, pdf13, ske)

Figure 4.3.40 – Gas Velocity for 56% Recycle, 20% OFG, 0.5 PG Swirl

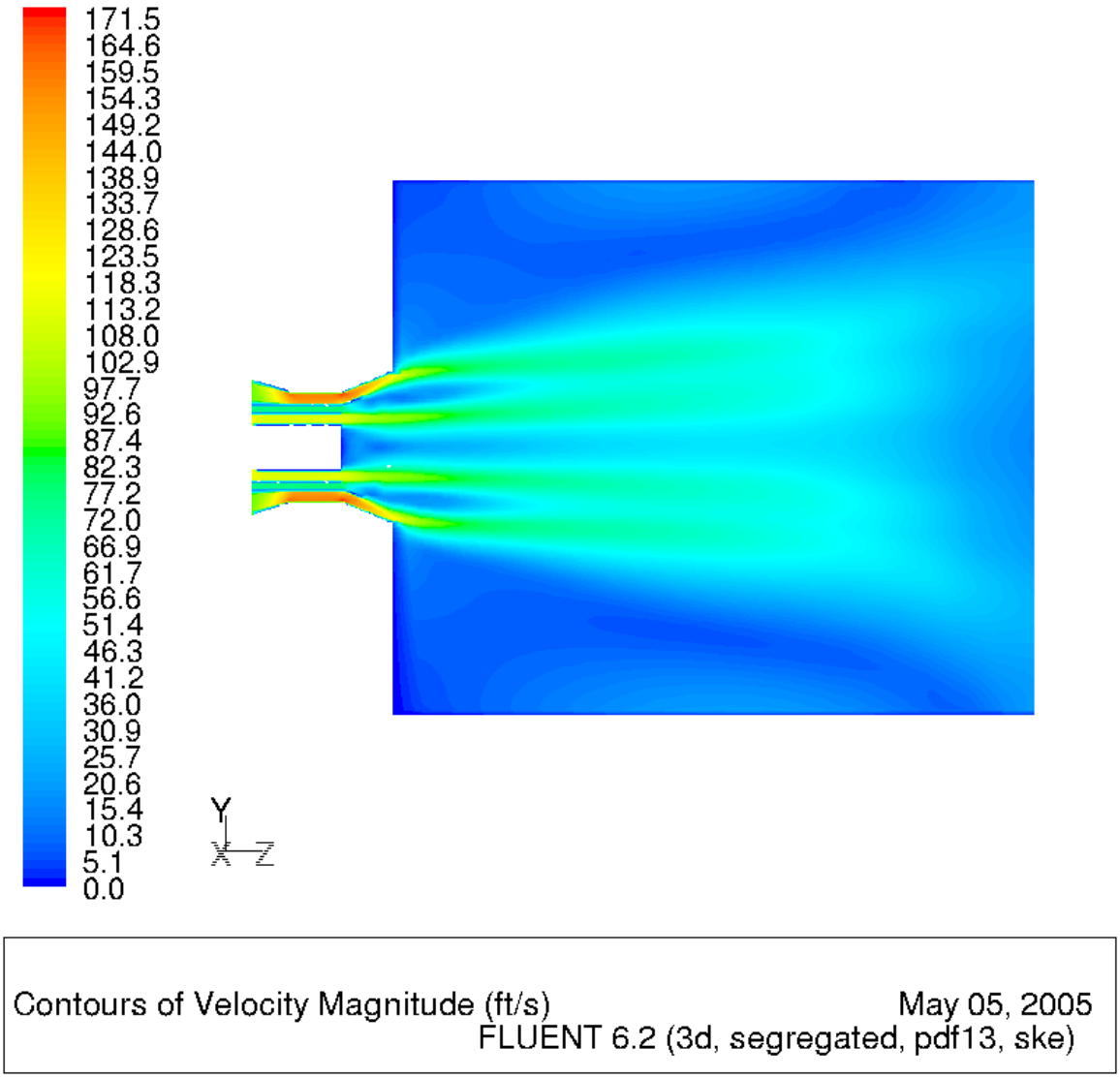

Figure 4.3.41 – Gas Temperature for 56% Recycle, 20% OFG, 0.5 PG Swirl

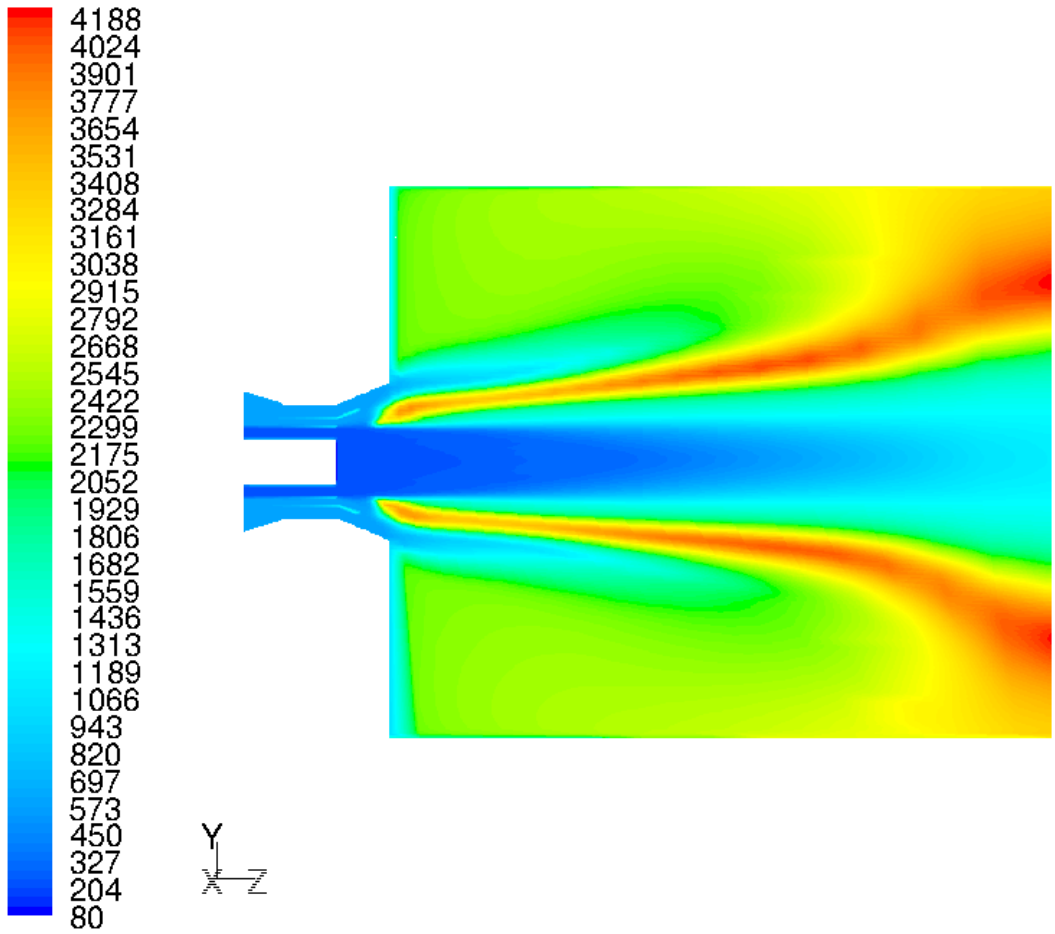

Contours of Static Temperature (f) May 06, 2005
FLUENT 6.2 (3d, segregated, pdf13, ske)

Figure 4.3.42 – O2 Mole Fraction for 56% Recycle, 20% OFG, 0.5 PG Swirl

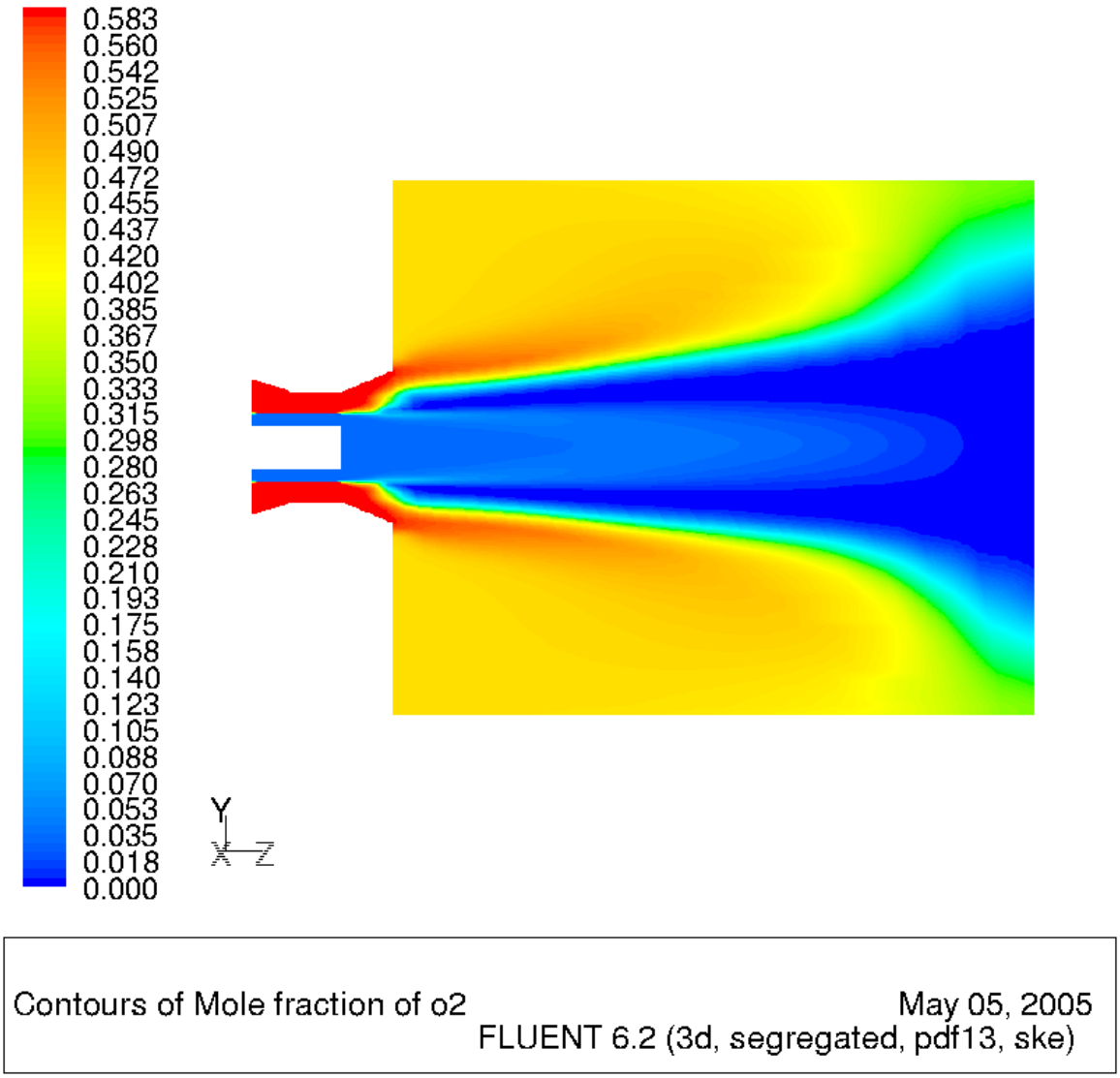

Figure 4.3.43 – Burnout of 69µ Particles for 56% Recycle, 20% OFG, 0.5 PG Swirl

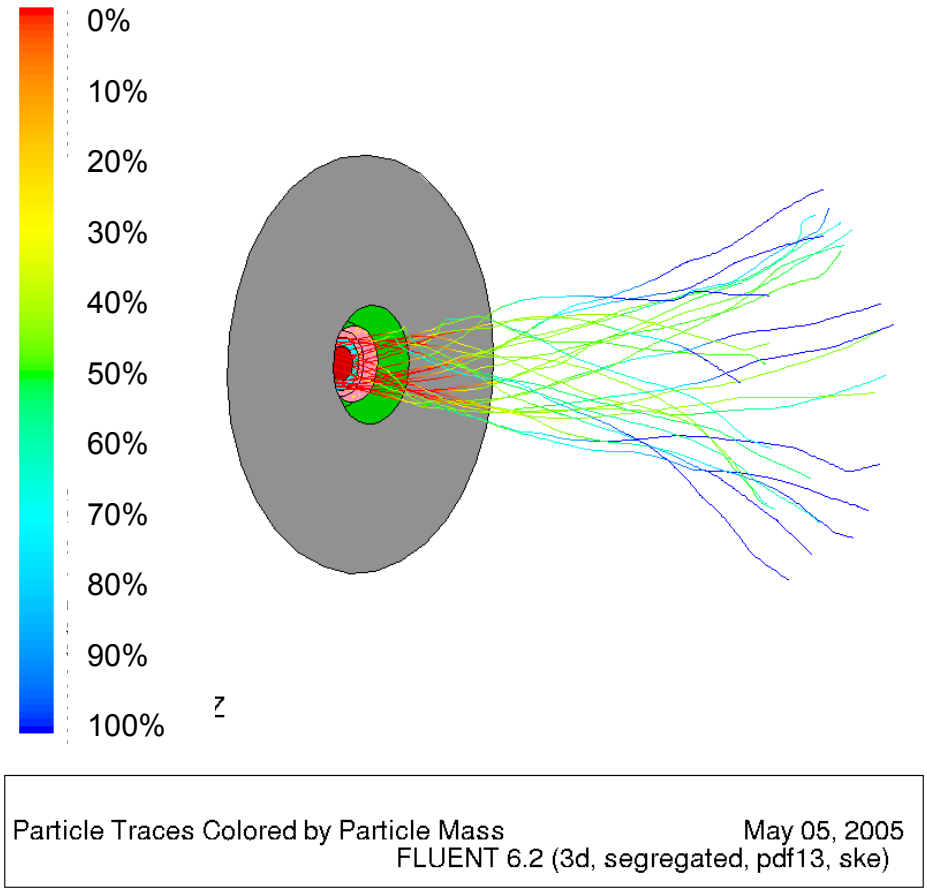

Figure 4.3.44 – Burnout of 169µ Particles for 56% Recycle, 20% OFG, 0.5 PG Swirl

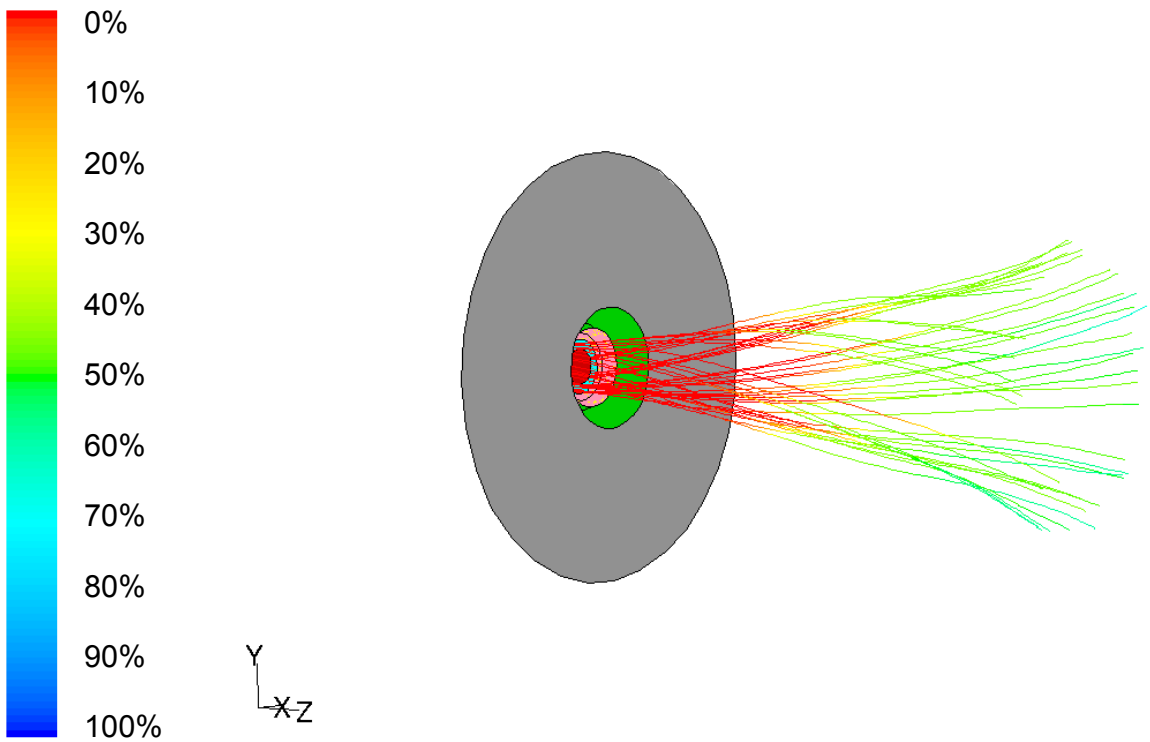

Particle Traces Colored by Particle Mass

May 05, 2005
FLUENT 6.2 (3d, segregated, pdf13, ske)

4.4 Furnace and HRA Design and Analysis

4.4.1 Furnace Design and Analysis

4.4.1.1 FW-FIRE Computer Program Description

FW-FIRE (Fossil fuel, Water-walled Furnace Integrated Reaction and Emission Simulation) simulates furnace combustion, heat transfer and pollutant formation based on fundamental principles of mass, momentum, and energy conservation [21]. FW-FIRE is an extended and enhanced version of PCGC-3, which was developed over a period of ten years by the Advanced Combustion Engineering Research Center (ACERC), operated jointly by Brigham Young University and the University of Utah. The FW-FIRE computer program incorporates the latest state-of-art coal combustion/gasification, pollutant formation, and physical analysis techniques based on extensive empirical research.

The FW-FIRE code performs general three dimensional multiphase gas combustion steady state analysis of reactive fluid flows. The program is fully capable of analyzing gas-fired and coal-fired boilers although FW-FIRE was initially tailored for pulverized coal combustion and gasification.

The FW-FIRE program models the gas flow field as a three dimensional (Cartesian or cylindrical) turbulent reacting continuum that is described locally by the Newtonian form of the Navier-Stokes equations coupled with the energy equation and other appropriate constitutive equations. These equations are solved in Eulerian framework to predict gas properties such as pressure, temperature, velocity, and pollutants and other species concentrations.

The Reynolds stress terms, which result from Favre-averaging of the conservation equations, are approximated using the Boussinesq assumption and effective eddy viscosity. The value of the eddy viscosity and subsequent closure of the turbulence equations is made using either a linear or non-linear k-ε two-equation model. The effects of turbulence of the flow field on the combustion reactions are included.

The turbulent flow field is also coupled with the combustion chemistry. Since gaseous reactions are limited by mixing rates and not reaction kinetics, the process chemistry is calculated using locally instantaneous equilibrium based on the degree of mixing of the species. Rate constants for processes such as devolatilization (two step process) and char oxidation are built-in to the program based on empirical testing.

A Lagrangian model of the particle conservation equations is used to predict particle transport by characterizing the particle field as a series of discrete particle trajectories through the gas continuum. Particles interact with the gas

field via mass, momentum, and energy exchange. Particle properties such as burnout, velocities, temperatures, and particle component compositions are obtained by integrating the governing equations along the trajectory paths. The program possesses the capability to input a particle size distribution and chemical composition.

In a pulverized coal flame, the radiation field is a multi-component, non-uniform, emitting, absorbing, gas-particle system. The coal particles cause anisotropic and multiple scattering, and the flame is surrounded by non-uniform, emitting, reflecting, absorbing surfaces. The radiation field calculations are based on an energy balance on a beam of radiation passing through a volume element containing the absorbing-reflecting-emitting medium. An Eulerian framework using a discrete-ordinates approach is used to model this process. Heat transfer via radiation and convection to waterwall and tube banks is determined by specifying a local wall temperature and emissivity.

The set of non-linear differential equations is discretized and combined by a upwind and weighted central-differencing scheme. The resulting gas flow field finite difference equations are solved using variations of the SIMPLE/SIMPER algorithm.

FW-FIRE contains a sub-model for the prediction of nitrogen pollutant emissions. This sub-model has the capability of predicting both fuel and thermal NOx formation. Fuel NO formation can proceed directly to N_2 and NO (such as in the case of char) or through HCN and NH_3 which are oxidized to form NO and reduced to N_2 (such as in the case of volatiles). Global reaction rates are based on work by de Soete and Bose. Thermal NO formation is governed by the extended Zel dovich mechanism.

4.4.1.2 Model Geometry

A simulation was made for both the reference air-fired case and for the oxygen-fired case. The FW-FIRE model simulates the furnace, in height from the bottom of the hopper to the roof, in depth from the front wall to the rear wall, and in width from the left side wall to the right side wall. Furnace partial division walls are also included in the model. Finer meshes are used to model the burners and over-fire air (OFA) ports. The air-fired model contains 528,840 (117x113x40) nodes and is shown in Figure 4.4.1. Two oxygen-fired models were constructed: one with no OFG ports and the second with OFG ports. The oxygen-fired model without OFG ports contains 364,320 (132x69x40) and is shown in Figure 4.4.2. The oxygen-fired model with OFG ports contains 484,160 (136x89x40) nodes and is shown in Figure 4.4.3.

4.4.1.3 Boundary Conditions

Boundary conditions are based on ASPEN simulations of the power plant (Section 4.2). The air-fired and oxygen-fired ASPEN reference cycle diagrams are presented in Figure 4.2.1 and Figure 4.2.25, respectively The input data required by FW-FIRE include fuel analysis, coal particle size distribution (mass percentage for each size bin), waterwall fluid temperatures, and the velocities, flow rates and temperatures of primary and secondary gas streams. Boundary conditions are detailed in Table 4.4.1 and Table 4.4.2.

The waterwalls of the furnace are assumed to be gray and diffusive. The wall temperature at each location is calculated based on the fluid temperature and the heat flux at the wall cell. For the waterwalls, a fluid saturation temperature of 680°F corresponding to a pressure of 2700 psia is applied. For the partial division walls, a steam inlet temperature of 712°F and a steam outlet temperature of 848°F are applied.

For coal devolatilization kinetic properties, Ubhayakar rate parameters were employed for bituminous coal. For bituminous char oxidation, Sandia kinetic and burning mode parameters were applied for Illinois #6 coal.

4.4.1.4 Air-Fired Reference Case

The general layout drawing of the air-fired reference case is shown in Figure 4.4.4. The furnace has a total 24 opposed wall-fired burners (3 vertical x 4 horizontal x 2 walls) and 10 overfire air ports. 30% of the total combustion air is injected through the over-fire air ports located at one burner pitch above the top burner row. The radiant heat transfer surface consists of 2.75” OD tube waterwalls and five 2.0” OD tube partial divisional wall panels. Water is circulated in the furnace by natural circulation.

The boundary conditions were applied to the computational model and FW-FIRE was run until steady state conditions were achieved. The modeling results are summarized in Table 4.4.3. The coal burnout shown in the table is the percentage of dry ash-free based coal burned. The furnace exit gas temperature (FEGT) shown in the table is the average temperature of flue gas before the platen superheaters (vertical plane above the nose). The energy absorption listed is the total energy absorbed by water walls and partial division walls prior to the vertical plane above the nose. Total furnace absorption and FEGT predicted by FW-FIRE and ASPEN match closely.

Figure 4.4.5 is a plot of the flue gas velocity magnitude in a vertical plane through the second burner column. It can be seen that the gas velocity near the burners accelerates to greater than 150 ft/s due to the reduced gas density after particle ignition. Figure 4.4.6 presents a plot of gas temperature in a vertical plane through the second burner column. The maximum flue gas temperature is

approximately 3300°F. The mole fraction of O_2 through the second burner column is presented in Figure 4.4.7.

The heat flux at the furnace water wall is shown in Figure 4.4.8. The maximum heat flux is approximately 70,000 Btu/hr-ft^2 and is located on the side wall at the top of the burner zone. The total heat absorbed by the furnace walls before the furnace exit is 1840 MM Btu/hr. Figure 4.4.9 displays temperatures of the furnace walls and roof. The maximum temperature of the waterwalls is approximately 800°F and of the division walls is approximately 875°F. Figure 4.4.10 presents the CO concentration at the wall, peaks at approximately 10% due to the sub-stoichiometric conditions of the lower furnace (without overfire air the wall CO would be below 2%).

The trajectories of the 72-micron particles are plotted in Figure 4.4.11 with colors in each trajectory representing the mass fraction of char in the particle. Char is formed from devolatilization and consumed by oxidation. The maximum char mass fraction is usually less than the mass fraction of fixed carbon in a proximate analysis. Figure 4.4.11 shows that all of the 72-micron particles are completely burned before the furnace exit. The trajectories of 176-micron particles are plotted in Figure 4.4.12. It can be observed from Figure 4.4.12 that some particles are not completely burned at the exit of the furnace, causing unburned carbon in the fly ash. Total burnout of all particle sizes is 99.66% (2.61% LOI).

Average NOx concentration at the furnace outlet is 227 ppmvw (0.34 lb/MMBtu). A series of runs were made to determine the furnace average outlet NOx as a function of over-fire air flow. Figure 4.4.13 presents the NOx concentration at the furnace outlet as a function of OFA flow. Increasing OFA can have a negative effect on fuel burnout. Figure 4.4.14 presents the fuel burnout versus OFA flow.

4.4.1.5 Oxygen-Fired Design Case

The preliminary size of the furnace heat transfer area was based on a calculation of average wall heat flux using the Foster Wheeler computer program, EMISS [23]. The EMISS computer program calculates radiative heat flux of CO_2 and H_2O gases. A three dimensional CFD run was then made using FW-FIRE to more accurately determine the total heat absorption. Based on the CFD results, the height of the furnace model was adjusted until the total heat absorption approximately matched that required in the ASPEN oxygen-fired design case. Figure 4.4.15 shows a comparison between the sizes of the resultant oxygen-fired furnace and the air-fired reference furnace. Compared to the air-fired furnace, the oxygen furnace has only approximately 65% of the surface area and approximately 45% of the volume. Figure 4.4.16 presents the oxygen-fired design general layout drawing.

The oxygen-fired furnace has a total 24 opposed wall-fired burners (4 vertical x 3 horizontal x 2 walls) and 8 overfire gas ports. The burner designs (including 0.5

primary gas swirl) are based on the Low NOx Burner Design Task (see Section 4.3). The radiant heat transfer surface consists of 2.75" OD tube waterwalls and ten 2.0" OD tube partial divisional wall panels. Water is circulated in the furnace by natural circulation.

Two designs were simulated: 1) without over-fire air and 2) with over-fire air. Since it is somewhat unknown how much NOx will be tolerated in the liquid CO_2 effluent stream, a case with no OFG and a case with 20% OFG were run.

The modeling results are summarized in Table 4.4.3. The coal burnout for the oxygen-fired case is 100% due to the high furnace temperature and high concentration of O_2. Total furnace absorption and FEGT predicted by FW-FIRE and ASPEN match well. NOx is 333 ppmvw for the no OFG case and 257 ppmvw for the 20% OFG case. Thus, the injection of 20% OFG results in a NOx reduction of 23%. Although the average NOx concentration at the furnace outlet is similar on a volume basis for both air-fired and O_2-fired PC, it is substantially less on a mass basis for the O_2-fired PC due to the substantially lower volumetric flue gas flow rate of the O_2-fired PC.

4.4.1.5.1 No OFG Case

Figure 4.4.17 is a plot of the flue gas velocity magnitude in a vertical plane through the middle burner column. It can be seen that the gas velocity near the burners accelerates to nearly 150 ft/s due to the reduced gas density after particle ignition. Figure 4.4.18 presents a plot of gas temperature in a vertical plane through the middle burner column. The maximum flue gas temperature is approximately 3900°F. The mole fraction of O_2 through the middle burner column is presented in Figure 4.4.19. The mixed primary/secondary gas O_2 content (before combustion) is 42%.

The heat flux at the furnace water wall is shown in Figure 4.4.20. The maximum heat flux is approximately 175,000 Btu/hr-ft^2 and is located on the side wall at the top of the burner zone. This maximum heat flux is approximately 2.5 times the air-fired case due to the higher flame temperature and higher H_2O and CO_2 concentrations. The total heat absorbed by the furnace walls before the furnace exit is 2287 MM Btu/hr. Figure 4.4.21 displays temperatures of the furnace walls and roof. The maximum temperature of the waterwalls is approximately 935°F and of the division walls is approximately 945°F. Because of the higher temperature of the oxygen-fired case compared to the air-fired case, furnace water wall material was upgraded from 0.285" thick carbon steel (SA-210C) to 0.240" thick SA-213-T91. Figure 4.4.22 presents the CO concentration at the wall, which is significantly greater than for the air-fired case (Figure 4.4.10) and its effects on corrosion will need to be studied in future work.

The trajectories of the 69-micron particles are plotted in Figure 4.4.23 with colors in each trajectory representing the mass fraction of char in the particle. Figure 4.4.23 shows that all of the 69-micron particles are completely burned before the

furnace exit. The trajectories of 169-micron particles are plotted in Figure 4.4.24. Note that due to the higher temperature and O_2 concentration all the 169-micron particles are completely burned as compared to the air-fired case (Figure 4.4.12) where there is some residual unburned char at the outlet. Figure 4.4.25 shows the trajectories of 169-micron particles without primary gas swirl (this case was run prior to the finalization of the burner design analysis). Comparing Figure 4.4.24 with Figure 4.4.25 demonstrates that primary gas swirl achieves an earlier burnout of the large coal particles.

4.4.1.5.2 20% OFG Case

Figure 4.4.26 is a plot of the flue gas velocity magnitude in a vertical plane through the middle burner column. It can be seen that the gas velocity near the burners accelerates to nearly 150 ft/s due to the reduced gas density after particle ignition. Figure 4.4.27 presents a plot of gas temperature in a vertical plane through the middle burner column. The maximum flue gas temperature is approximately 3750°F. The mole fraction of O_2 through the middle burner column is presented in Figure 4.4.28. The mixed primary/secondary gas O_2 content (before combustion) is 42%.

The heat flux at the furnace water wall is shown in Figure 4.4.29. The maximum heat flux is approximately 165,000 Btu/hr-ft^2 and is located on the side wall at the above the over-fire ports. This maximum heat flux is approximately 2.4 times the air-fired case due to the higher flame temperature and higher H_2O and CO_2 concentrations. The total heat absorbed by the furnace walls before the furnace exit is 2186 MM Btu/hr. Figure 4.4.30 displays temperatures of the furnace walls and roof. The maximum temperature of the waterwalls is approximately 930°F and of the division walls is approximately 945°F. Because of the higher temperature of the oxygen-fired case compared to the air-fired case, furnace water wall material was upgraded from 0.285” thick carbon steel (SA-210C) to 0.240” thick SA-213-T91. Figure 4.4.31 presents the CO concentration at the wall, which is significantly greater than for the air-fired case (Figure 4.4.10) and its effects on corrosion will need to be studied in future work.

The trajectories of the 69-micron particles are plotted in Figure 4.4.32 with colors in each trajectory representing the mass fraction of char in the particle. Figure 4.4.32 shows that all of the 69-micron particles are completely burned before the furnace exit. The trajectories of 169-micron particles are plotted in Figure 4.4.33. Note that due to the higher temperature and O_2 concentration all the 169-micron particles are completely burned as compared to the air-fired case (Figure 4.4.12) where there is some residual unburned char at the outlet. Figure 4.4.34 shows the trajectories of 169-micron particles without primary gas swirl (this case was run prior to the finalization of the burner design analysis). Comparing Figure 4.4.33 with Figure 4.4.34 demonstrates that primary gas swirl achieves an earlier burnout of the large coal particles.

4.4.2 Heat Recovery Area Design and Analysis

4.4.2.1 HEATEX Program Description

HEATEX [22] is a Foster Wheeler general-purpose program for thermal/hydraulic analysis of tube banks. The program performs heat transfer calculations on a local basis by dividing the tube bundle into a number of small heat transfer elements.

4.4.2.2 Air-Fired Reference Case

HEATEX was used to determine the heat recovery area (HRA) design of the convective tube banks between the furnace exit and the SCR/air heater. These tube banks include the finishing superheater, finishing reheater, primary superheater, primary reheater, upper economizer, and lower economizer. Flue gas exits the furnace at 2135ºF and flows over the finishing superheater and finishing reheater tube bundles where it heats the main steam and reheat steam to 1000ºF and 1005ºF, respectively. The gas flow is then split into two parallel flows: one passing over the primary reheater and the other passing over the primary superheater and upper economizer. The gas split is controlled by dampers to achieve the proper reheater outlet temperature. Attemperating spray is used to control superheat temperature. The flue gas is combined downstream of the dampers and flows over the lower economizer, which receives water from the last feedwater heater stage. Flue gas exits the lower economizer at 720ºF and is sent to the SCR and then to the air heater. Figure 4.2.1 presents the heat transfer requirements of the HRA banks. Table 4.4.4 presents the corresponding design of the HRA banks. Total surface area of all convective banks is 294,111 ft^2. The performance of HRA tube banks is shown Table 4.4.5. The total heat transferred to the water/steam is 1354 MM Btu/hr as 3.88 MM lb/hr of flue gas is cooled from 2135ºF to 720ºF.

4.4.2.3 Oxygen-Fired Case

Due to the 40% lower flue gas flow rate of the oxygen-fired case versus the air-fired case, the cross sectional area of the HRA is reduced to maintain the same gas side velocity (and pressure drop). HEATEX was used to determine the heat recovery area design of the convective tube banks between the furnace exit and the gas recuperator. These tube banks include the finishing superheater, finishing reheater, primary superheater, primary reheater, and lower economizer. Flue gas exits the furnace at 2350ºF and flows over the finishing superheater and finishing reheater tube bundles where it heats the main steam and reheat steam to 1000ºF and 1005ºF, respectively. The gas flow is then split into two parallel flows: one passing over the primary reheater and the other passing over the primary superheater. The gas split is controlled by dampers to achieve the proper reheater outlet temperature. Attemperating spray is used to control superheat

temperature. The flue gas is combined downstream of the dampers and flows over the lower economizer, which receives water from the last feedwater heater stage. Flue gas exits the lower economizer at 650ºF and is sent to the gas recuperator.

Figure 4.2.25 presents the heat transfer requirements of the HRA banks. Table 4.4.4 presents the corresponding design of the HRA banks. Total surface area of all convective banks is 215,700 ft^2. The performance of HRA tube banks is shown in Table 4.4.5.The total heat transferred to the water/steam is 1096 MM Btu/hr as 2.20 MM lb/hr of flue gas is cooled from 2350ºF to 650ºF. The total heat transfer surface required in the oxygen-fired HRA is 25% less than the air-fired HRA due to the following main reasons:

1. More heat is absorbed in the oxygen-fired furnace (2264 MM Btu/hr) than the air-fired furnace (1894 MM Btu/hr) due to the higher adiabatic temperature and greater the specific heat of the oxygen-fired furnace flue gas. This requires less heat transfer duty in the HRA (as a consequence the upper economizer is not needed)

2. A higher heat transfer coefficient can be achieved in the oxygen-fired HRA than the air-fired HRA for the same flue gas pressure loss due to greater molecular weight (38 mol/lb-mol vs. 29 mol/lb-mol) of the oxygen-fired flue gas.

The HRA tube materials and wall thickness are practically the same for the air-fired and oxygen-fired design since the flue gas and water/steam temperature profiles encountered by the heat transfer banks are very similar.

Figure 4.4.1– Computational Model of Air-Fired Furnace (with right side wall removed)

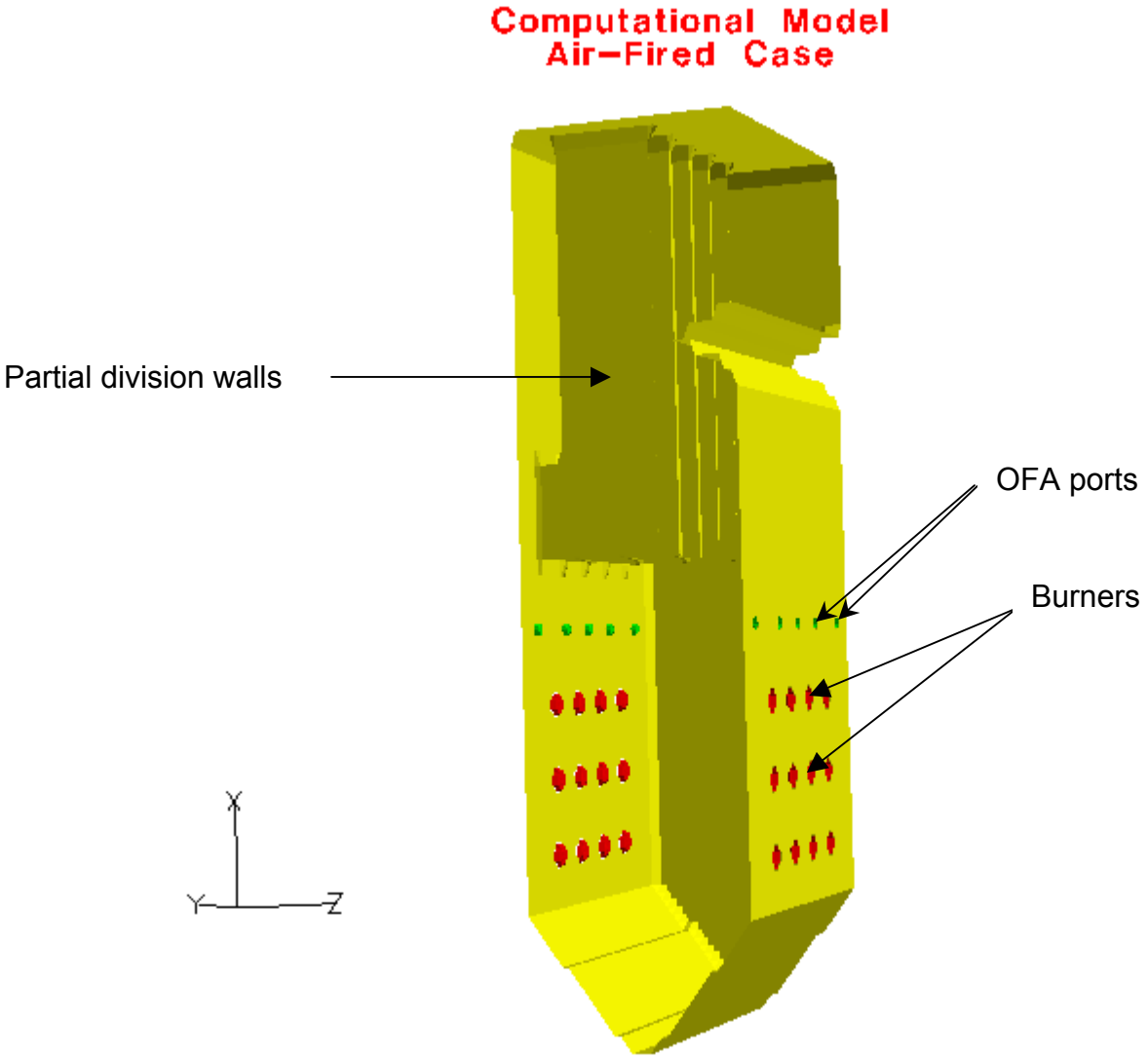

Figure 4.4.2 – Computational Model of Oxygen-Fired Furnace Without OFG

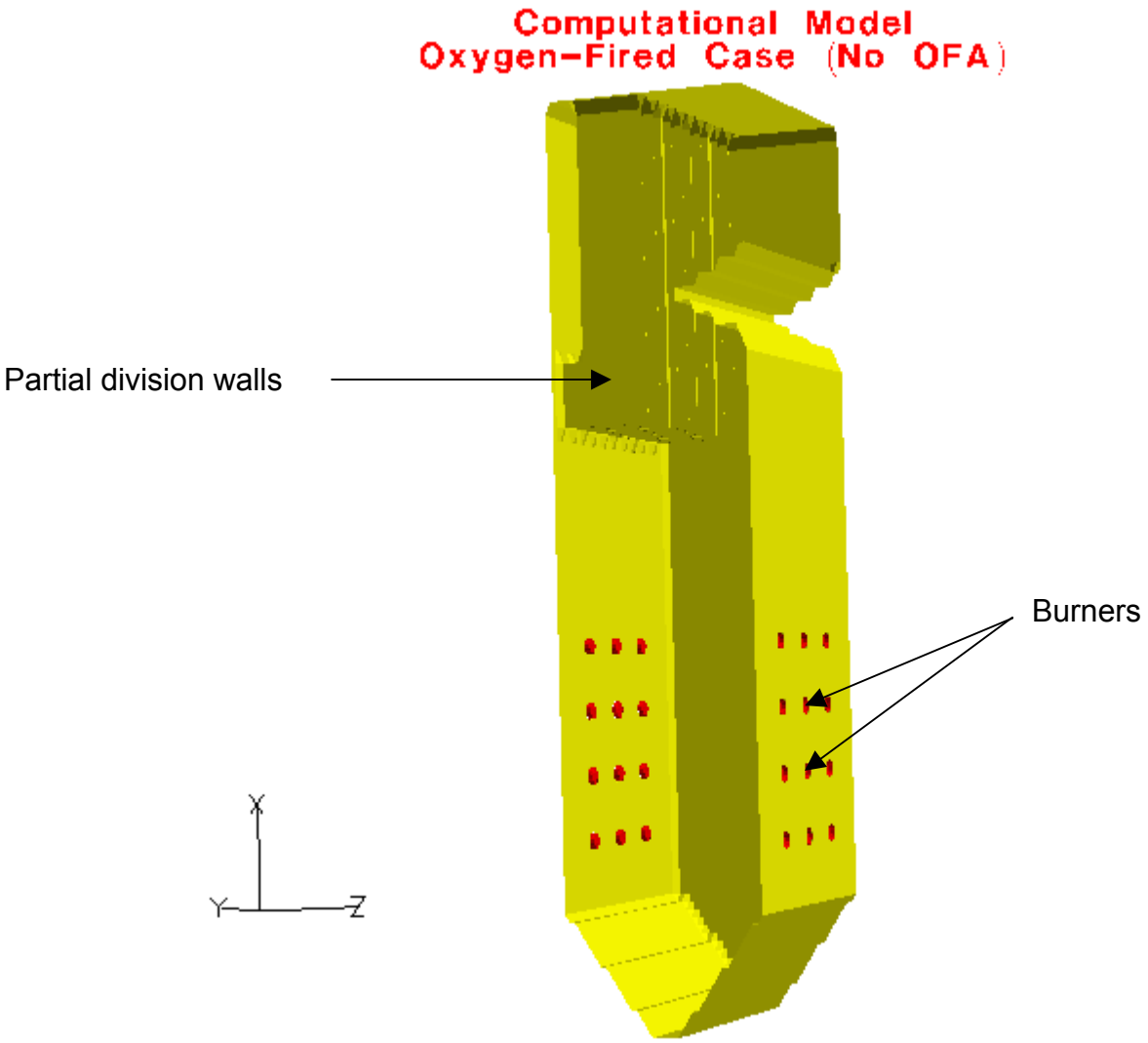

Figure 4.4.3 – Computational Model of Oxygen-Fired Furnace With OFG

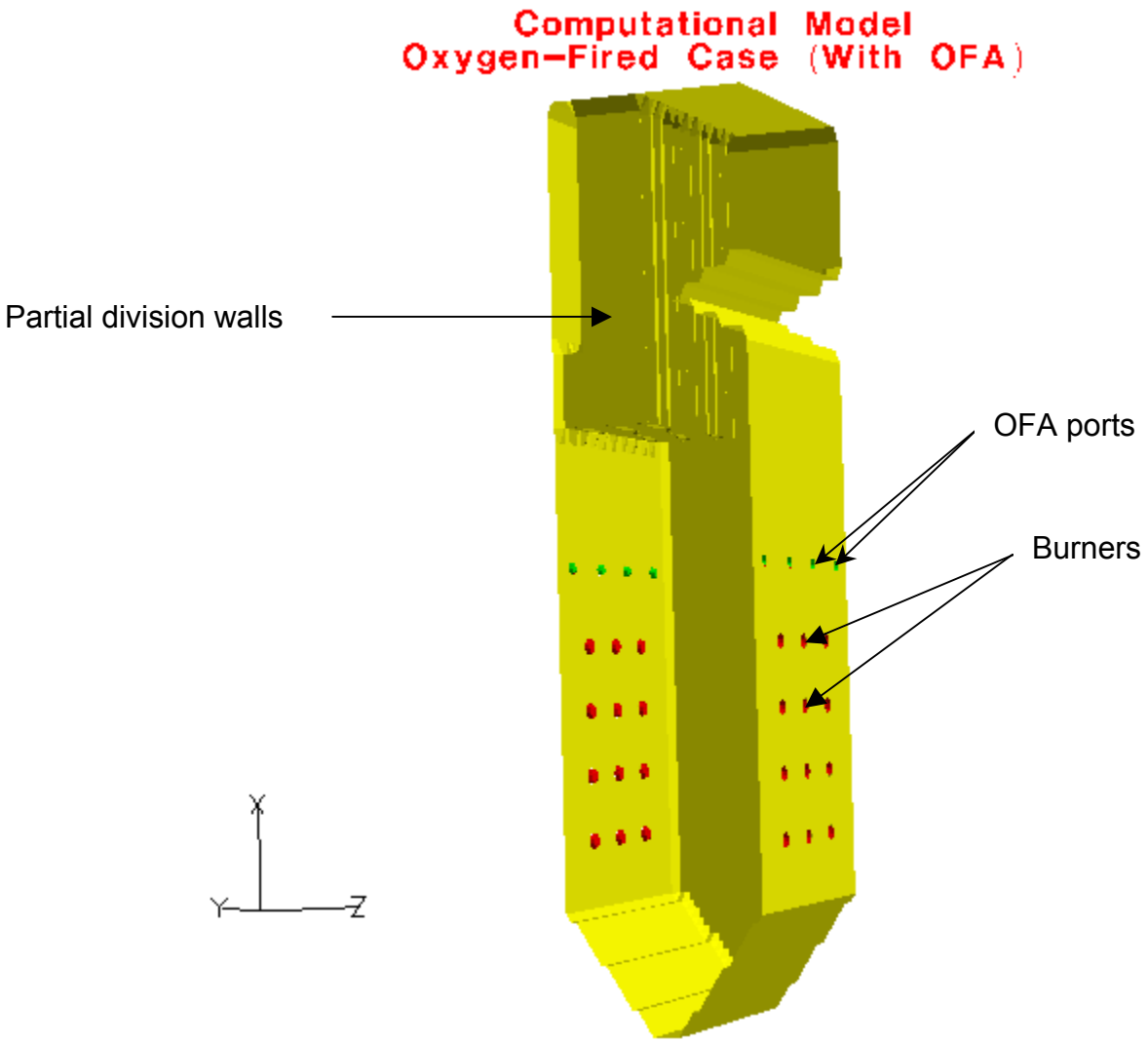

Table 4.4.1 – Air-Fired Boundary Conditions

Coal			Size (micron)		
Ultimate Analysis			Distribution		Mass Percent
Ash	%	9.99%	9.3	%	28.9
S	%	2.51%	33.7	%	27.3
H	%	4.50%	71.7	%	23.9
C	%	63.75%	121.8	%	10.7
H2O	%	11.12%	175.5	%	9.2
N	%	1.25%	Total	%	100.0
O	%	6.88%			
Total	%	100.00%	< 75 micron	%	70
			< 150 micron	%	99
Volatile Matter (daf)	%	44.35%			
Density	lb/ft3	80.0			
HHV, as received	Btu/lb	11,666			

Coal Flow	333,500
Moisture in Coal	37,085

Heat Input	3890.61	MM Btu/hr

TCA	lb/hr	3,428,000
Excess O2	%	11.0
Drum Pressure	psia	2700
OFA	%	30.0%

Divwall	Temp (F)	Temp (K)
Inlet	712	651
Outlet	848	726
Average	780	689

	Flow Rate		Temperature	Density	Inner Diam.	Outer Diam.	Area per Port	No. of Ports	Axial Velocity	Tan./Axial	Rad./Axial	Coal Flow
	lb/hr	%	F	lb/ft3	in	in	ft2		ft/sec	Velocity	Velocity	lb/hr
Primary	685,600	19.8	258	0.056	13.100	22.750	1.887	24	75.2	0.00	0.00	296,415
Inner Sec. Air	350,217	10.1	590	0.038	23.750	33.375	2.999	24	35.4	0.00	0.21	
Outer Sec. Air	1,400,868	40.4	590	0.038	33.875	49.000	6.837	24	62.0	0.41	0.41	
Tertiary Air	0	0.0	590	0.038	0.000	12.100	0.799	24	0.0	0.00	0.00	
Overfire Air - Inner	523,075	15.1	590	0.038	0.000	19.000	1.969	10	193.1	0.00	0.00	
Overfire Air - Outer	505,325	14.6	590	0.038	19.500	27.000	1.902	10	193.1	0.00	0.21	
	3,465,085	100.0										

Table 4.4.2 – Oxygen-Fired Boundary Conditions

Coal			Size (micron)		
Ultimate Analysis			Distribution		Mass Percent
Ash	%	9.99%	10.7	%	29.5
S	%	2.51%	33.7	%	38.2
H	%	4.50%	69.3	%	25.9
C	%	63.75%	118.2	%	5.5
H2O	%	11.12%	169.2	%	1.0
N	%	1.25%	Total	%	100.0
O	%	6.88%			
Total	%	100.00%	< 75 micron	%	85
			< 150 micron	%	99
Volatile Matter (daf)	%	44.35%			
Density	lb/ft3	80.0			
HHV, as received	Btu/lb	11,666			

Coal Flow	323,000
Moisture in Coal	35,918

Heat Input	3768.12 MM Btu/hr

TCA	lb/hr	1,876,248
Excess O2	%	11.0
Drum Pressure	psia	2700

Divwall	Temp (F)	Temp (K)
Inlet	712	651
Outlet	848	726
Average	780	689

No OFG

	Flow Rate		Temperature	Density	Inner Diam.	Outer Diam.	Area per Port	No. of Ports	Axial Velocity	Tan./Axial	Rad./Axial	Coal Flow
	lb/hr	%	F	lb/ft3	in	in	ft2		ft/sec	Velocity	Velocity	lb/hr
Primary	530,000	27.7	216	0.079	9.500	15.000	0.735	24	106.2	0.50	0.00	287,082
Inner Sec. Air	276,433	14.5	580	0.049	16.000	22.000	1.244	24	52.9	0.00	0.21	
Outer Sec. Air	1,105,732	57.8	580	0.049	22.500	32.000	2.824	24	93.1	0.41	0.41	
Tertiary Air	0	0.0	580	0.049	0.000	8.500	0.394	24	0.0	0.00	0.00	
Overfire Air - Inner	0	0.0	580	0.049	0.000	23.500	3.012	12	0.0	0.00	0.00	
Overfire Air - Outer	0	0.0	580	0.049	24.000	35.000	3.540	12	0.0	0.00	0.21	
	1,912,166	100.0										

20% OFG

	Flow Rate		Temperature	Density	Inner Diam.	Outer Diam.	Area per Port	No. of Ports	Axial Velocity	Tan./Axial	Rad./Axial	Coal Flow
	lb/hr	%	F	lb/ft3	in	in	ft2		ft/sec	Velocity	Velocity	lb/hr
Primary	530,000	27.7	216	0.079	9.500	15.000	0.735	24	106.2	0.50	0.00	287,082
Inner Sec. Air	201,383	10.5	580	0.049	16.000	20.750	0.952	24	50.3	0.00	0.21	
Outer Sec. Air	805,533	42.1	580	0.049	21.750	29.000	2.007	24	95.4	0.41	0.41	
Tertiary Air	0	0.0	580	0.049	0.000	8.500	0.394	24	0.0	0.00	0.00	
Overfire Air - Inner	177,060	9.3	580	0.049	0.000	13.500	0.994	8	127.1	0.00	0.00	
Overfire Air - Outer	198,190	10.4	580	0.049	14.000	20.000	1.113	8	127.1	0.00	0.21	
	1,912,166	100.0										

Figure 4.4.4 – Air-Fired Boiler Design

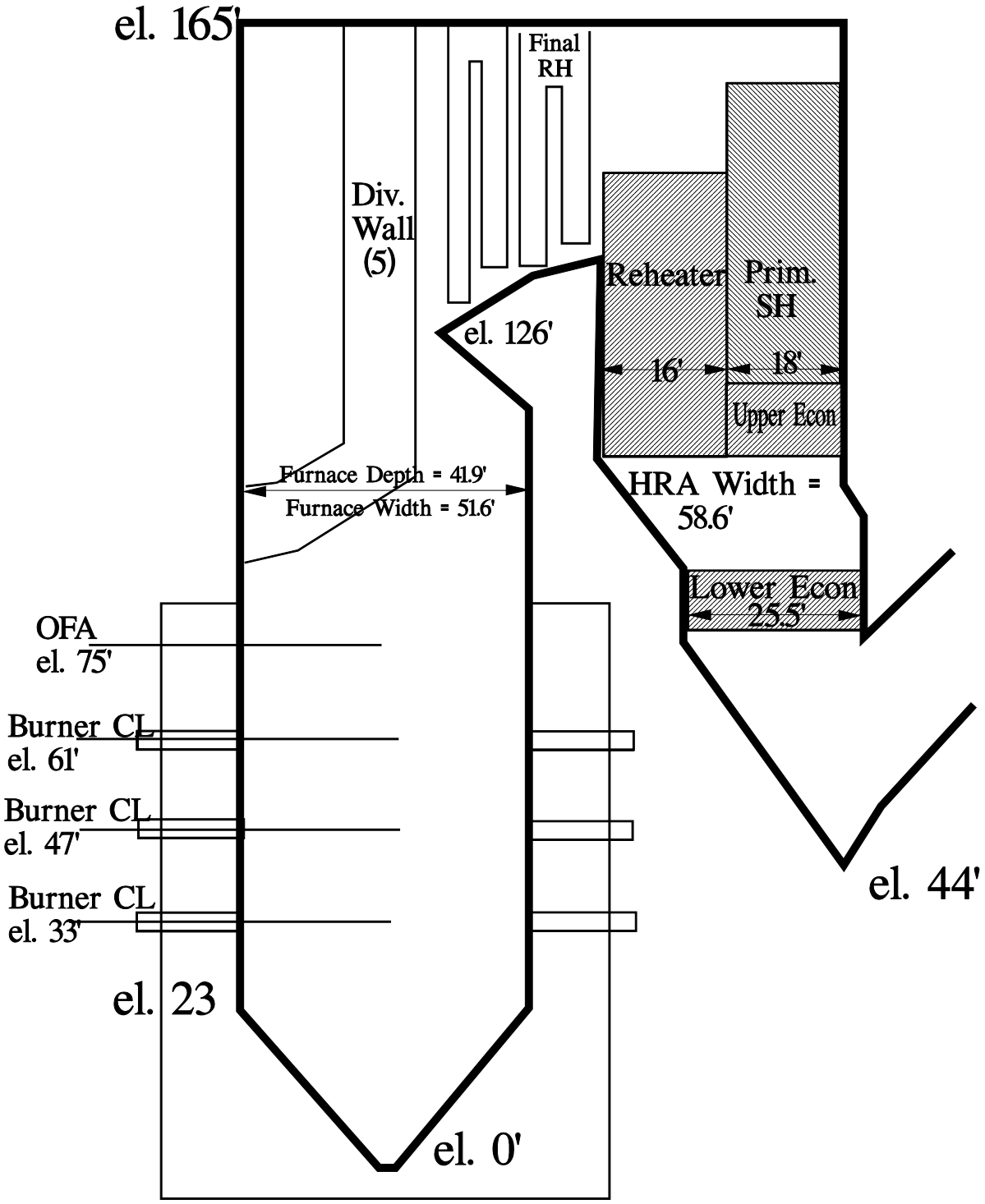

Table 4.4.3 – Summary of FW-FIRE Furnace Modeling Results

Air-Fired

		FW-FIRE	ASPEN
Burnout	%	99.66	99.0
LOI	%	2.61	7.32
Total Furnace Absorption	M Btu/hr	1840	1838
Division Wall Absorption	0.0	494	451
FEGT	F	2101	2135
NOx	ppmvw	227	
	lb/MMBtu	0.34	

Oxygen-Fired (No OFG)

		FW-FIRE	ASPEN
Burnout	%	100.0	99.5
LOI	%	0.00	3.80
Total Furnace Absorption	M Btu/hr	2287	2264
Division Wall Absorption	M Btu/hr	499	573
FEGT	F	2190	2350
NOx	ppmvw	333	
	lb/MMBtu	0.23	

Oxygen-Fired (20% OFG)

		FW-FIRE	ASPEN
Burnout	%	100.0	99.5
LOI	%	0.00	3.80
Total Furnace Absorption	M Btu/hr	2186	2264
Division Wall Absorption	M Btu/hr	550	573
FEGT	F	2262	2350
NOx	ppmvw	257	
	lb/MMBtu	0.18	

Figure 4.4.5 – Gas Velocity for Air-Fired Case

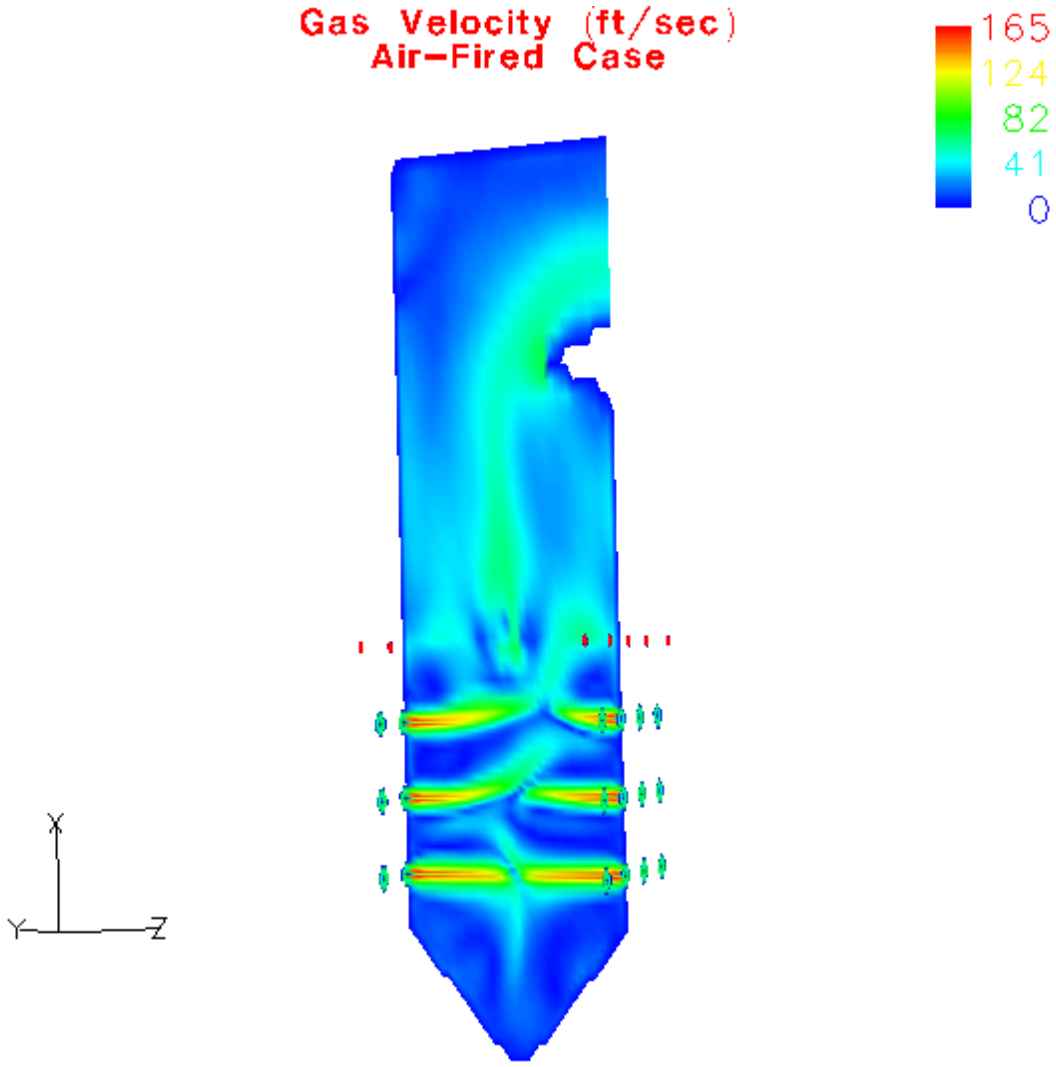

Figure 4.4.6 – Gas Temperature for Air-Fired Case

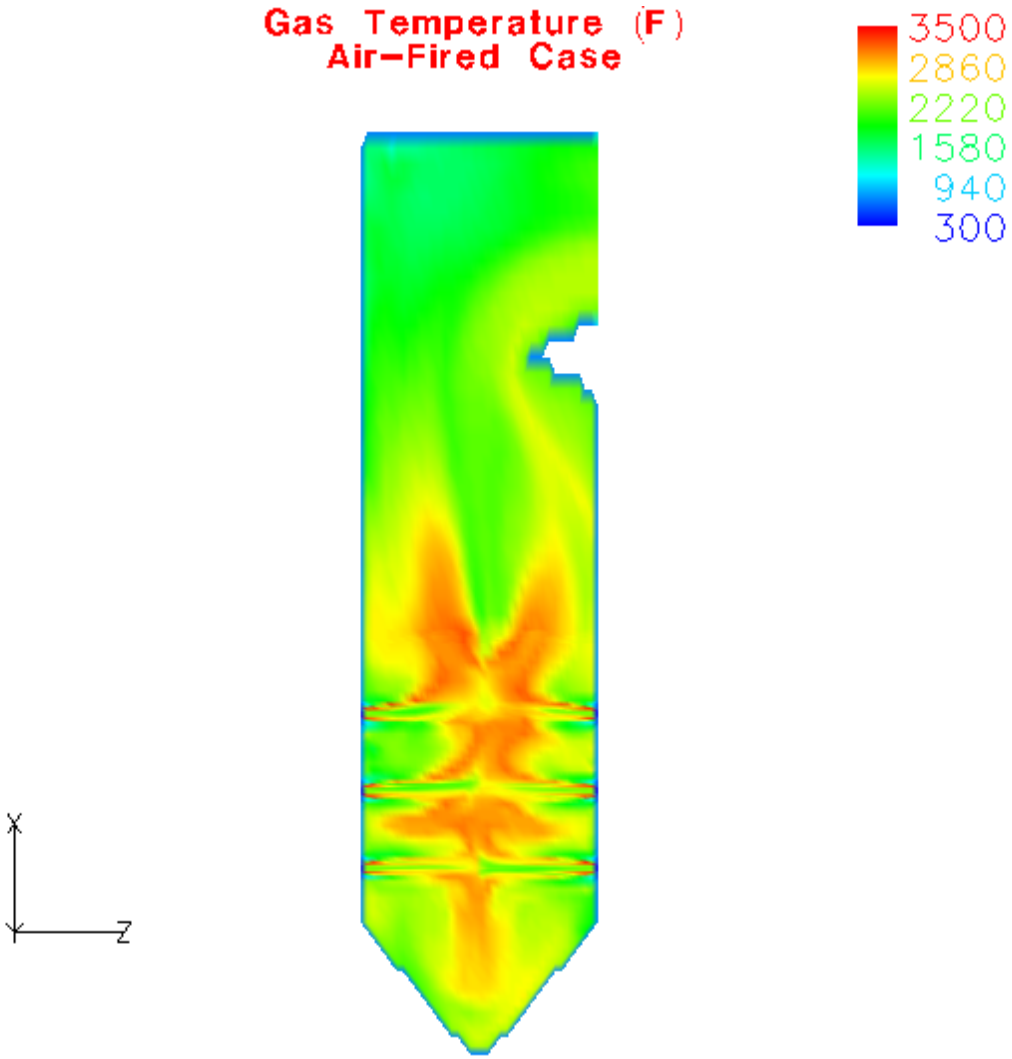

Figure 4.4.7 – O_2 Mole Fraction for Air-Fired Case

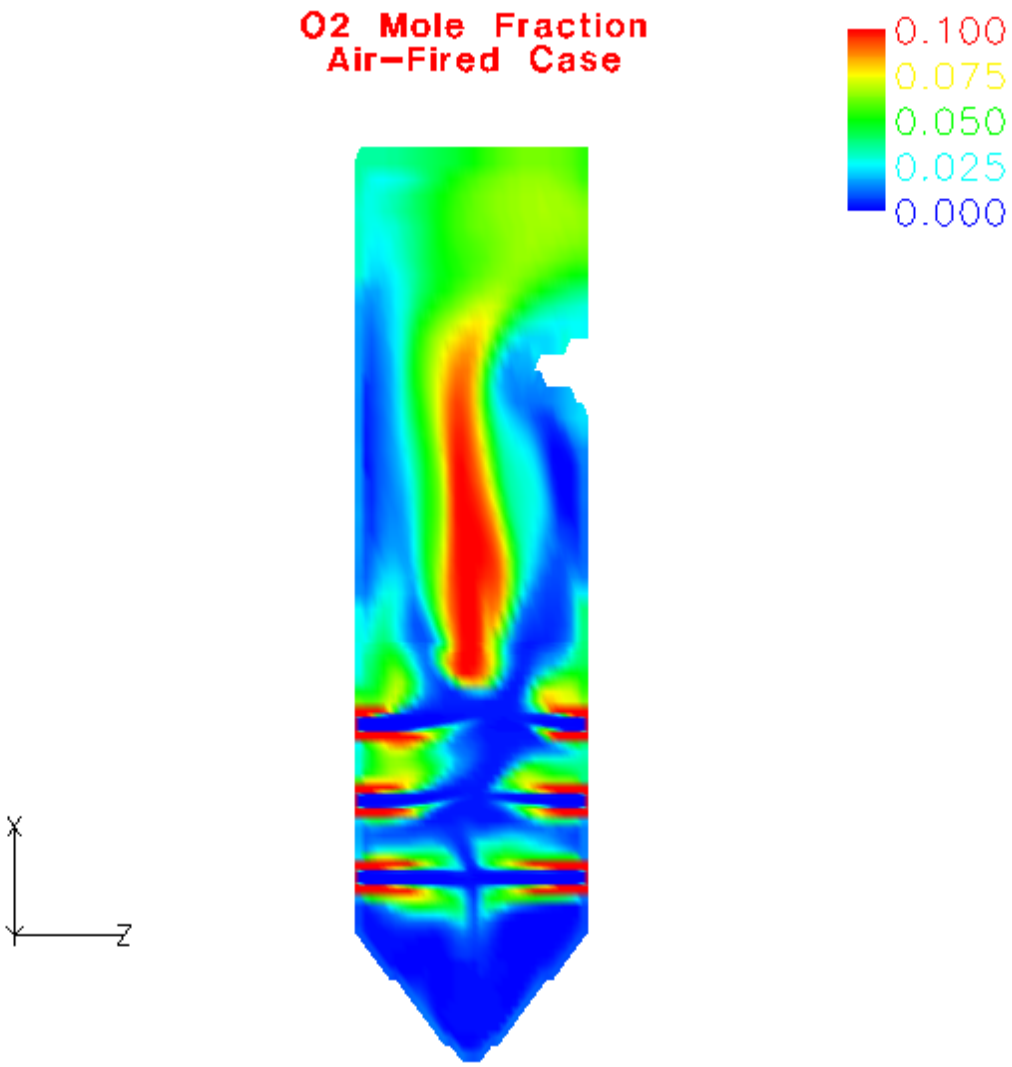

Figure 4.4.8 – Wall Heat Flux for Air-Fired Case

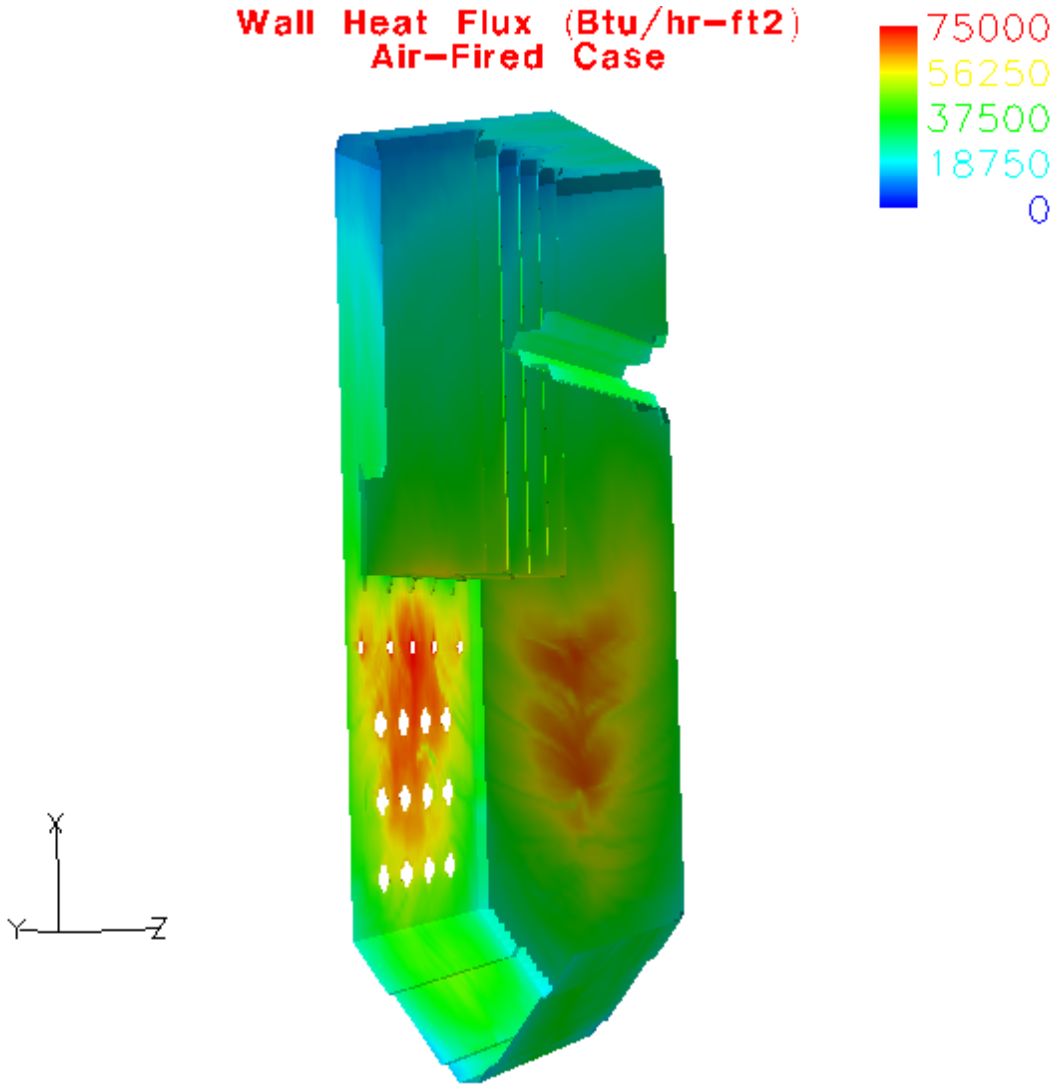

Figure 4.4.9 – Wall Temperature for Air-Fired Case

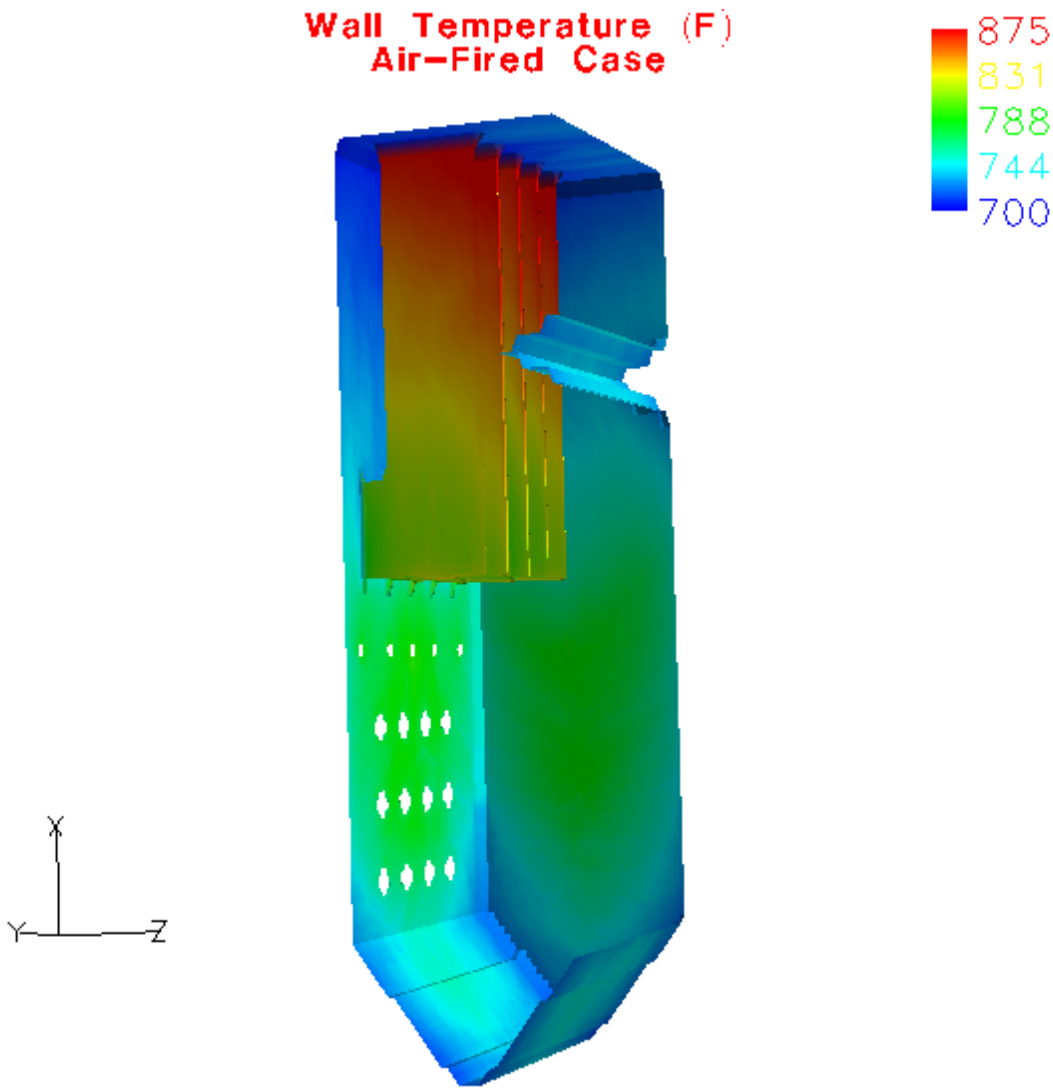

Figure 4.4.10 – Wall CO for Air-Fired Case

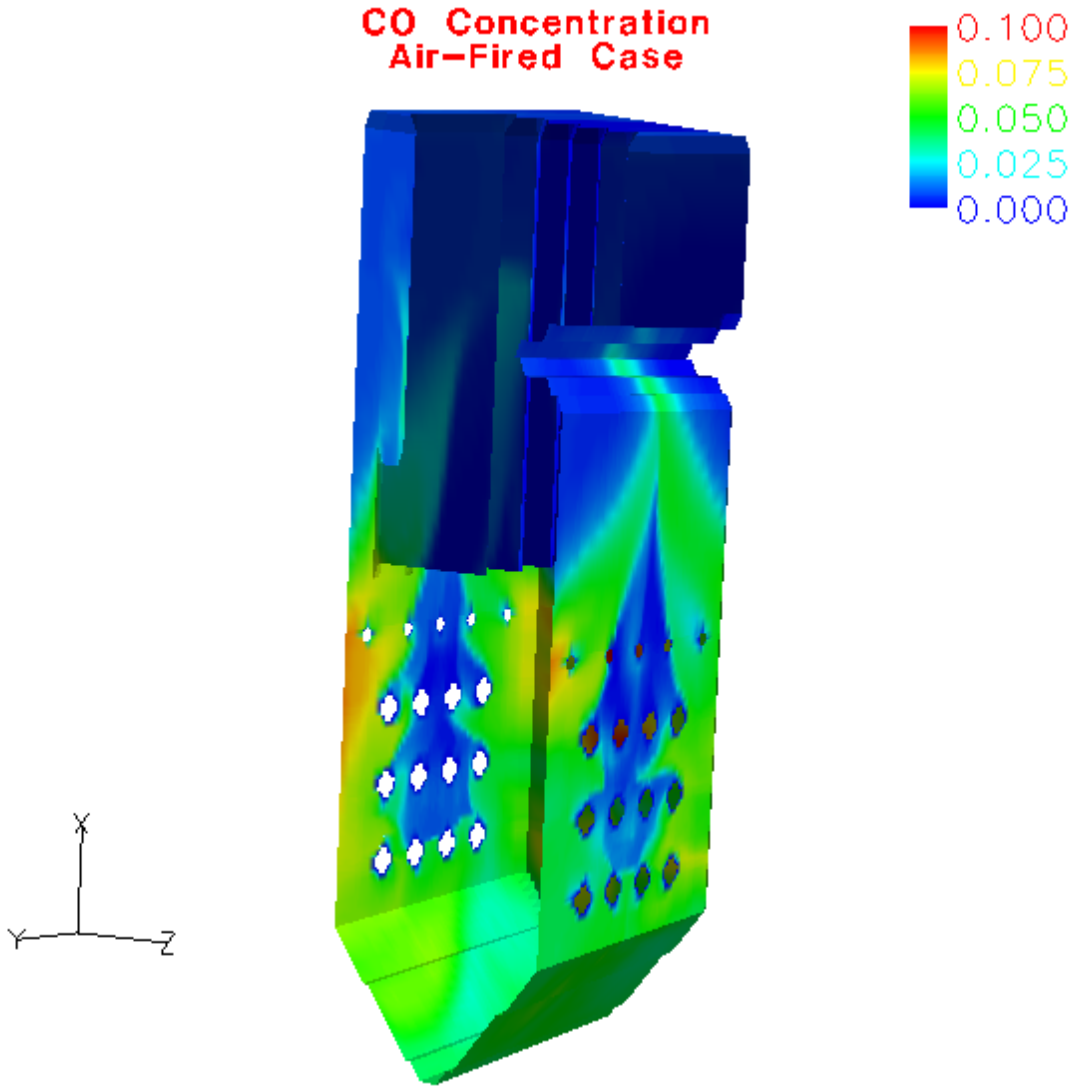

Figure 4.4.11 – Char Mass Fraction (72 microns) for Air-Fired Case

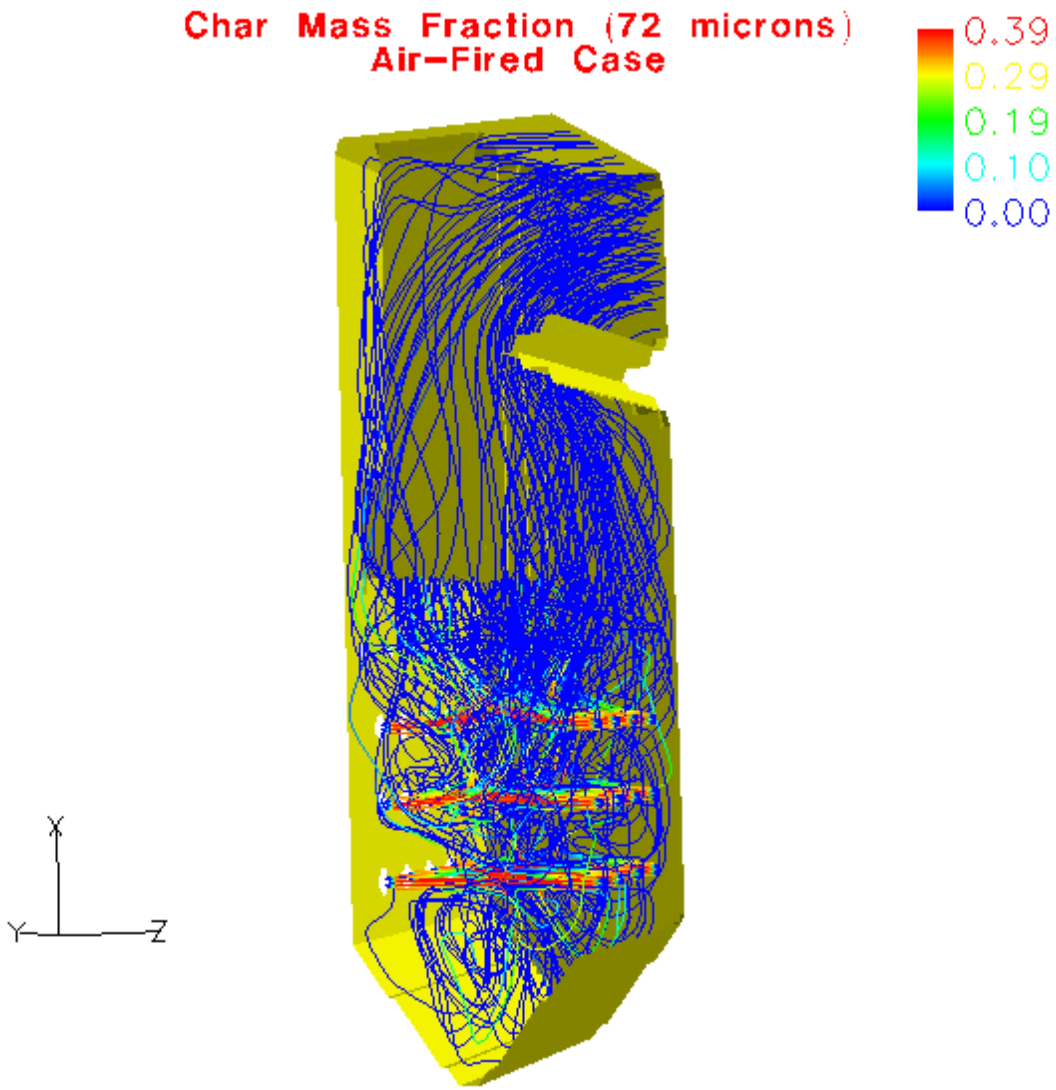

Figure 4.4.12 – Char Mass Fraction (176 microns) for Air-Fired Case

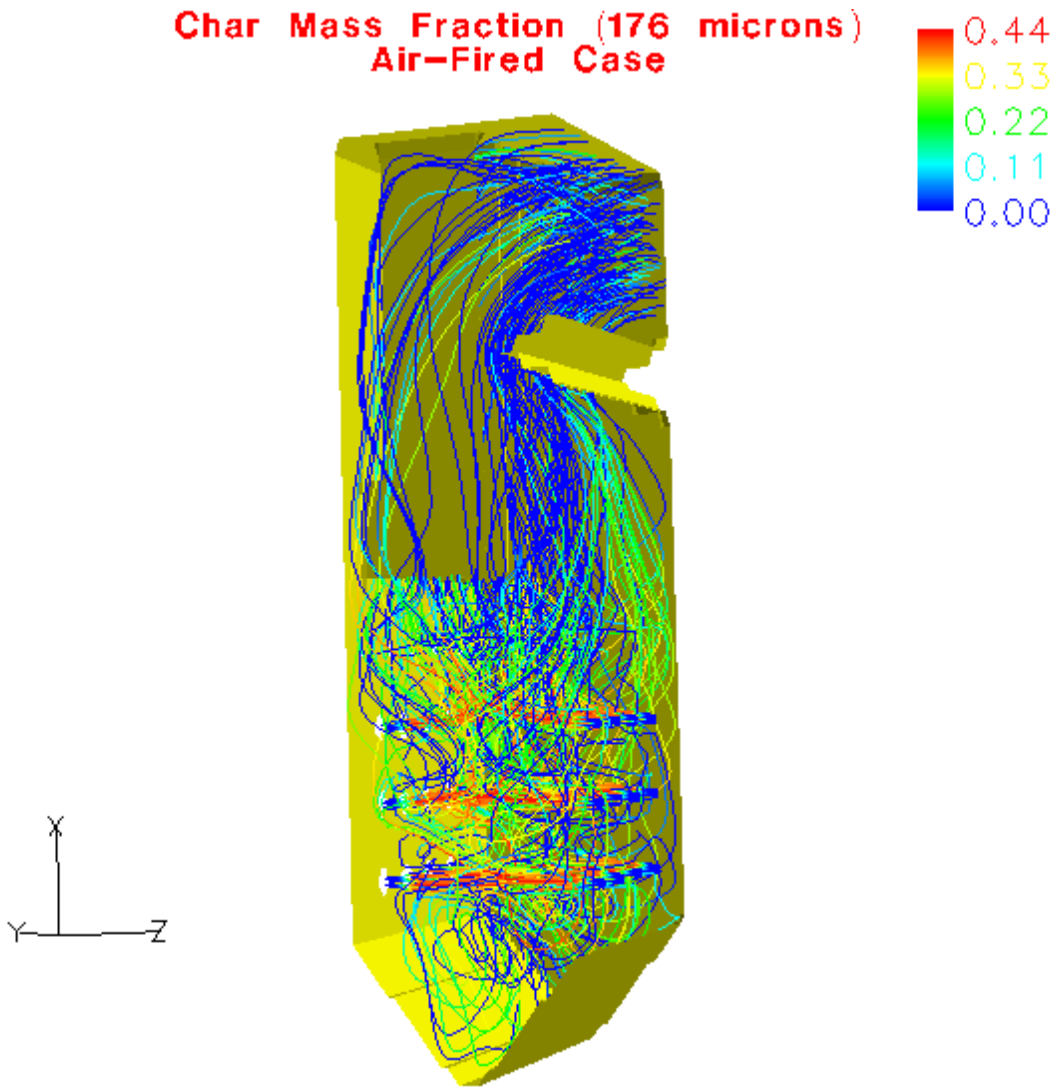

Figure 4.4.13 – Outlet NOx Versus OFA Flow Rate for Air-Fired Furnace

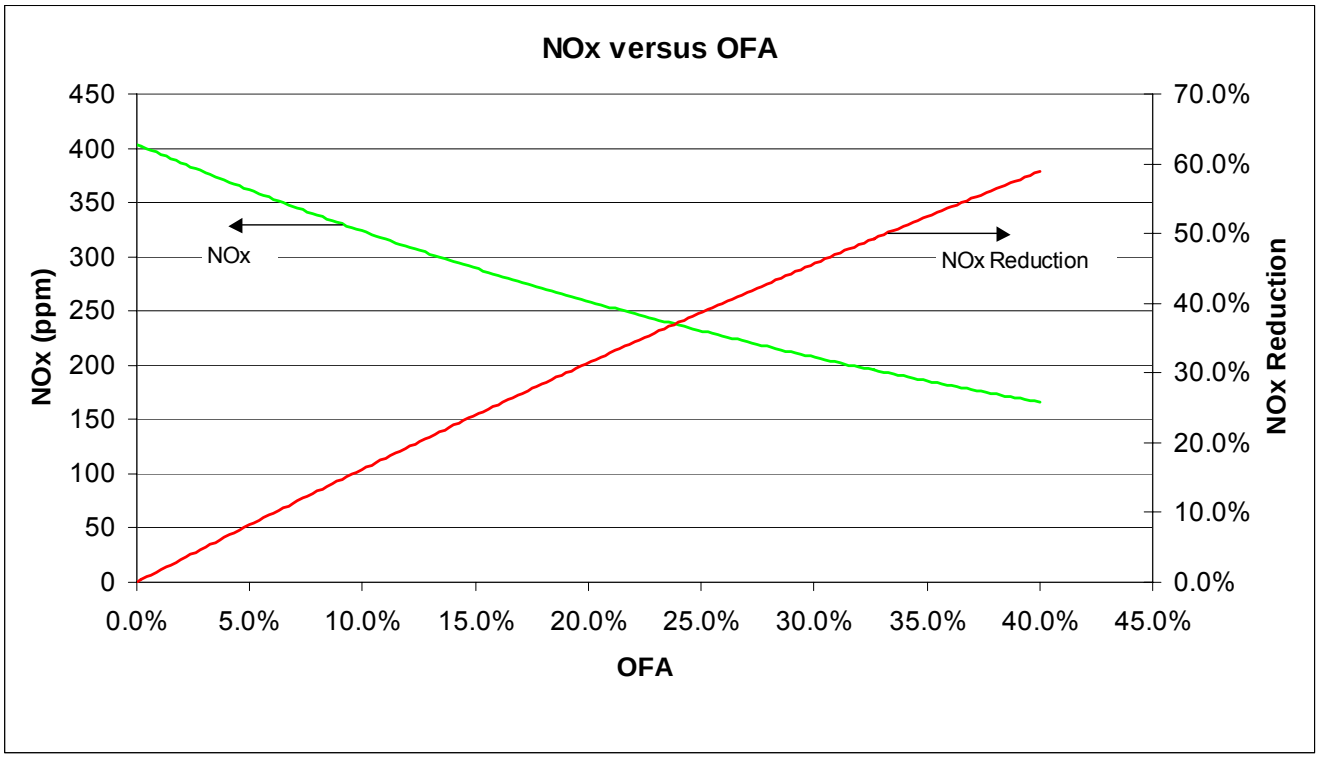

Figure 4.4.14 – Coal Burnout Versus OFA Flow Rate for Air-Fired Furnace

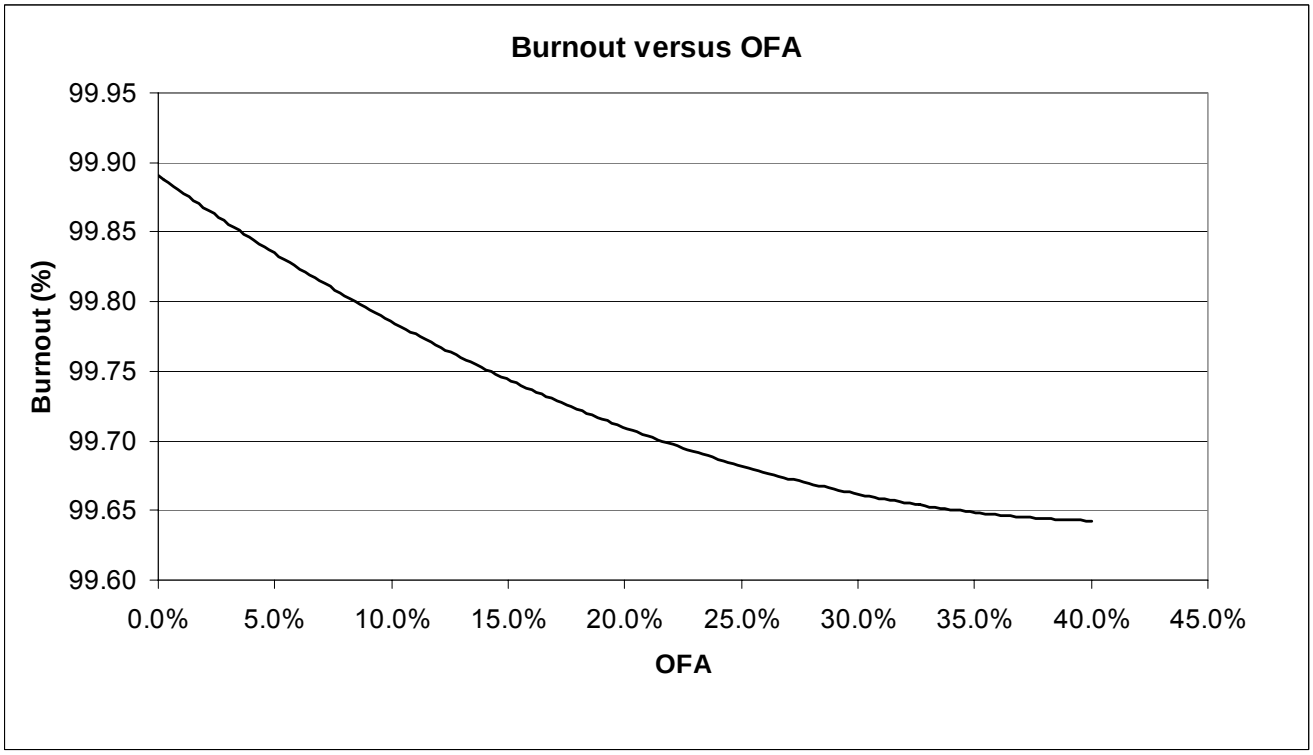

Figure 4.4.15 – Air-Fired and Oxygen-Fired Boiler Outlines

(Black = Air-Fired, Red = Oxygen Fired)

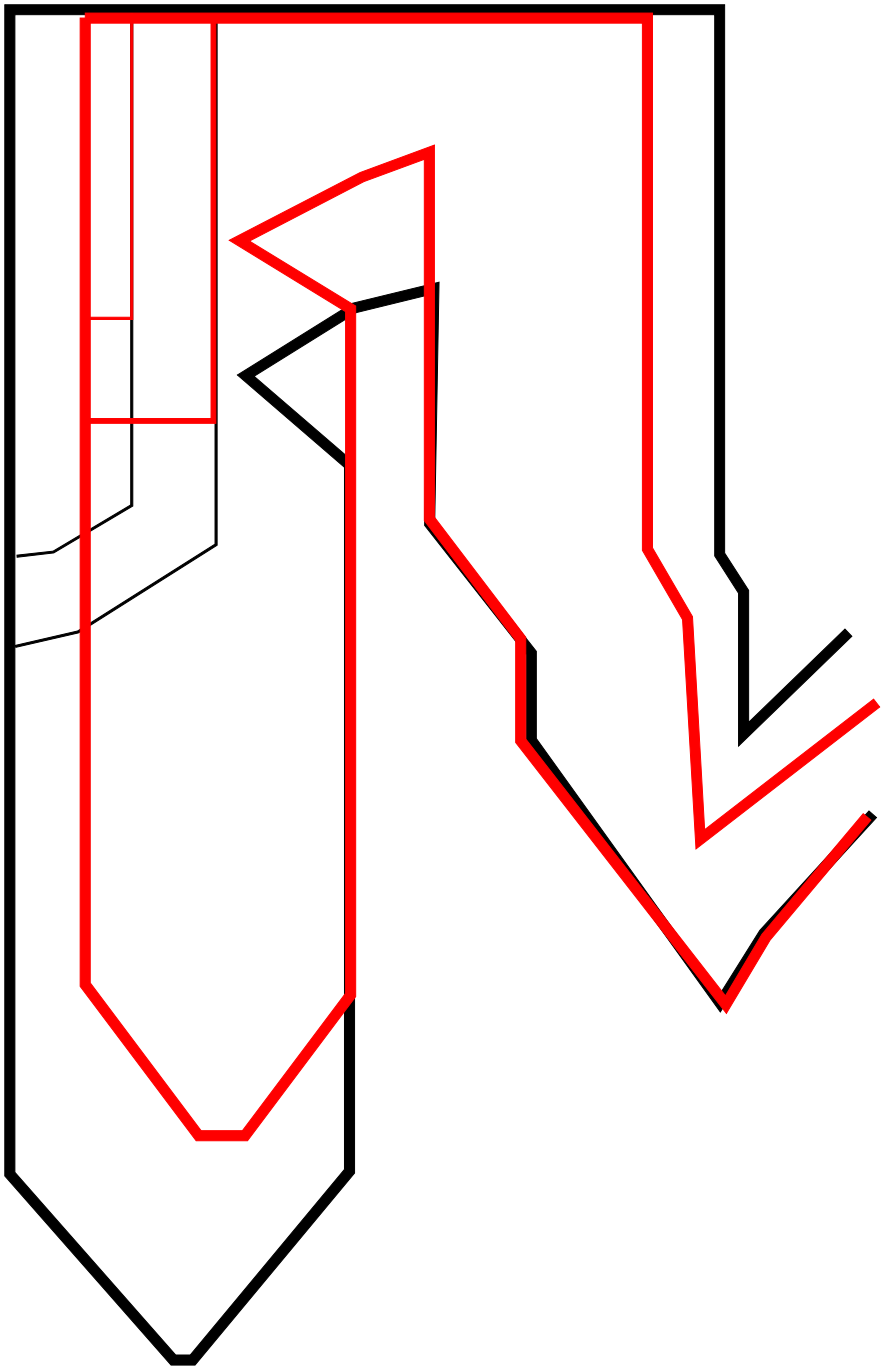

Figure 4.4.16 – Oxygen-Fired Boiler Design

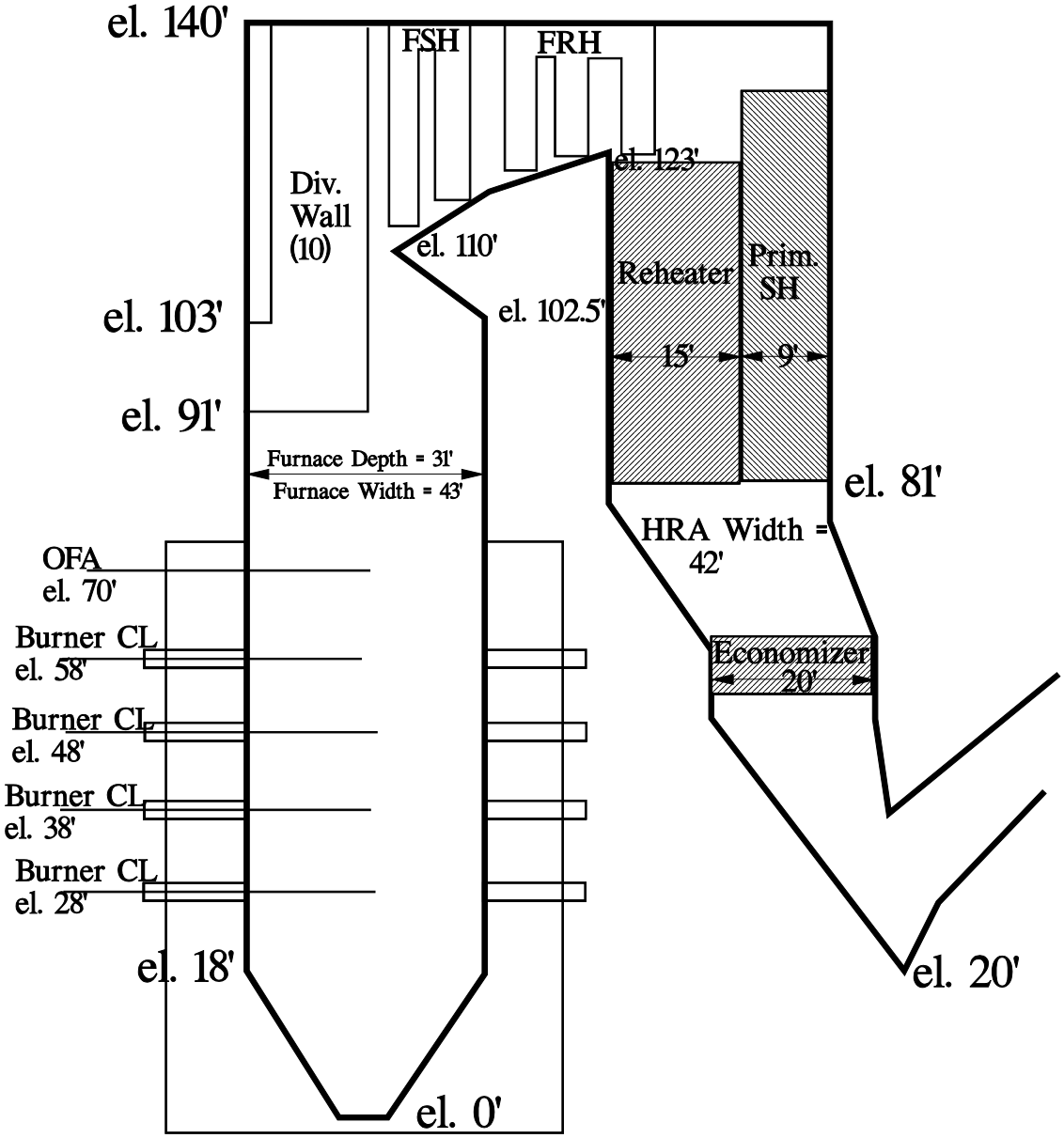

Figure 4.4.17 – Gas Velocity for O_2-Fired Case Without OFG

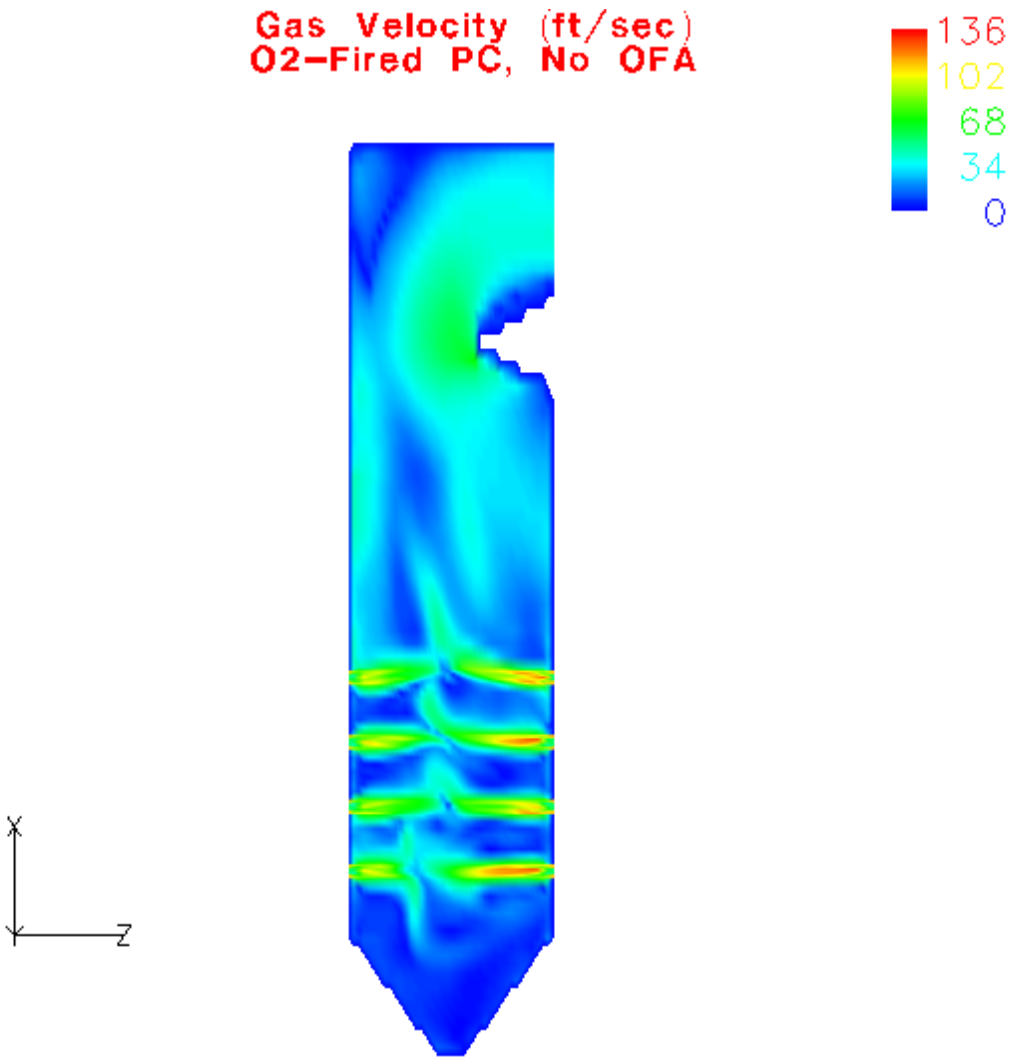

Figure 4.4.18 – Gas Temperature for O_2-Fired Case Without OFG

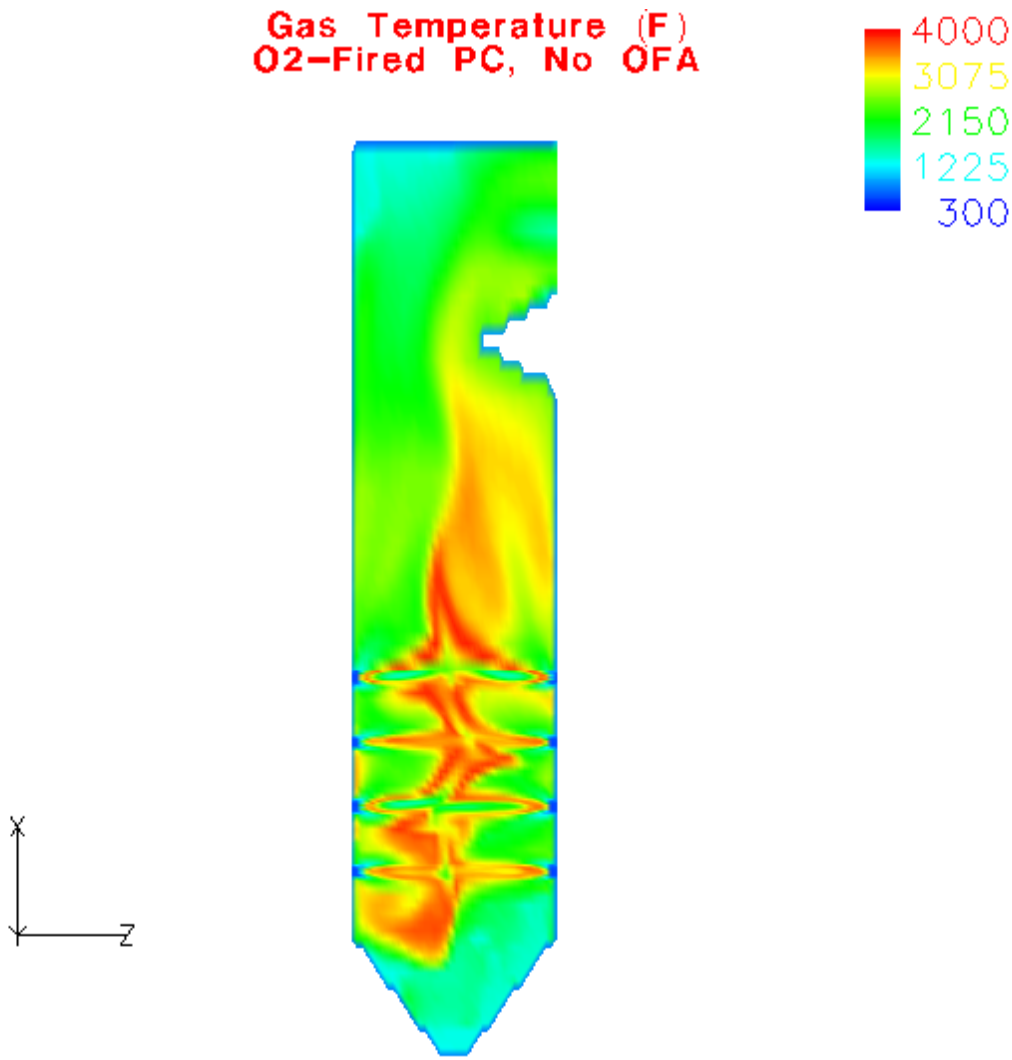

Figure 4.4.19 – O_2 Mole Fraction for O_2-Fired Case Without OFG

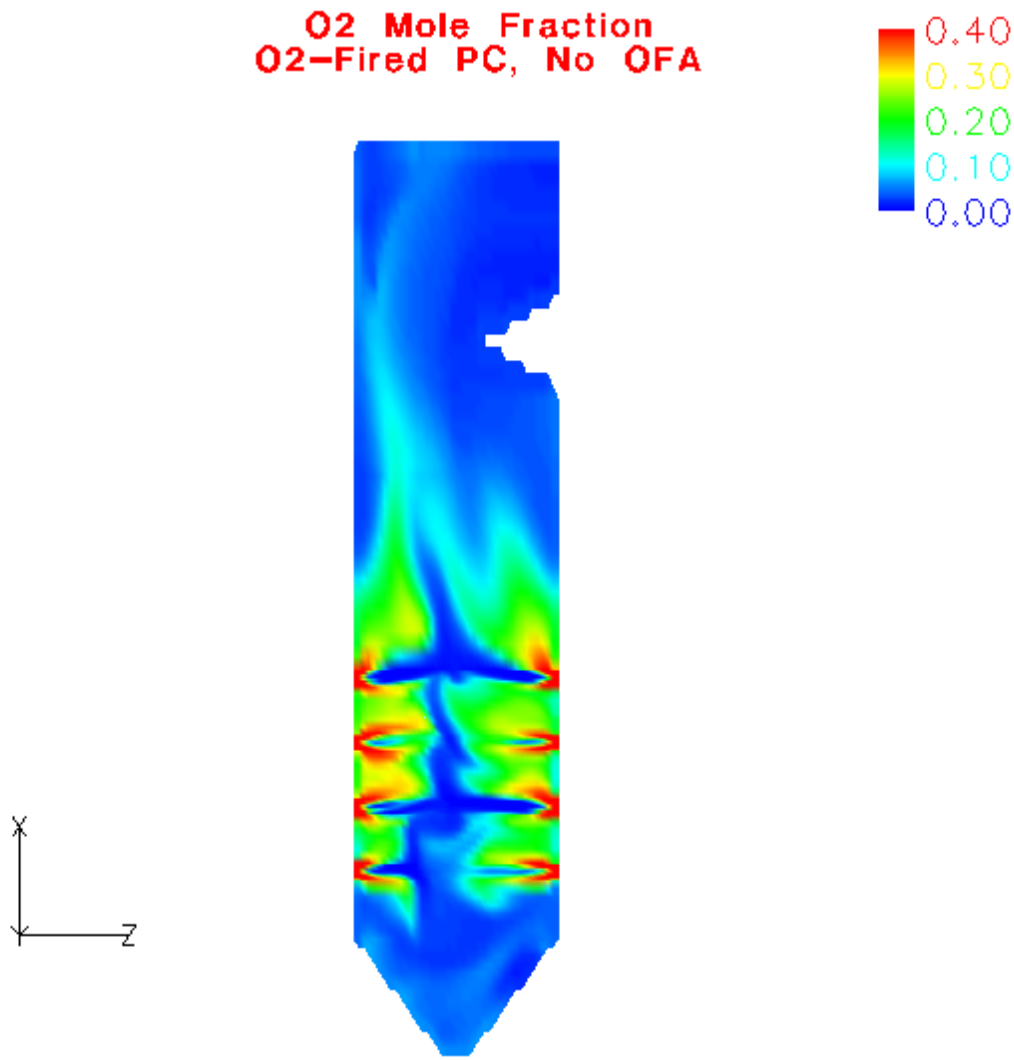

Figure 4.4.20 – Wall Heat Flux for O_2-Fired Case Without OFG

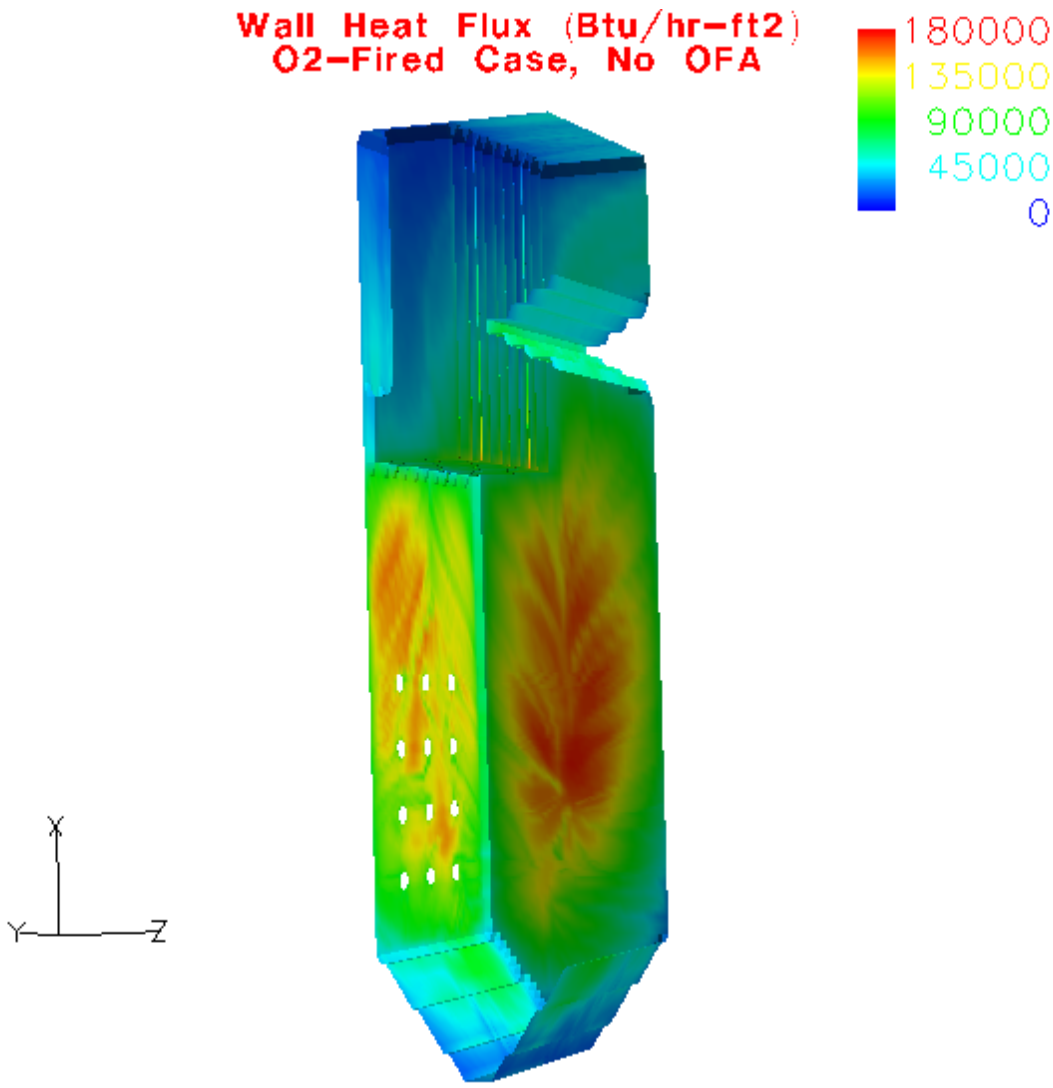

Figure 4.4.21 – Wall Temperature for O_2-Fired Case Without OFG

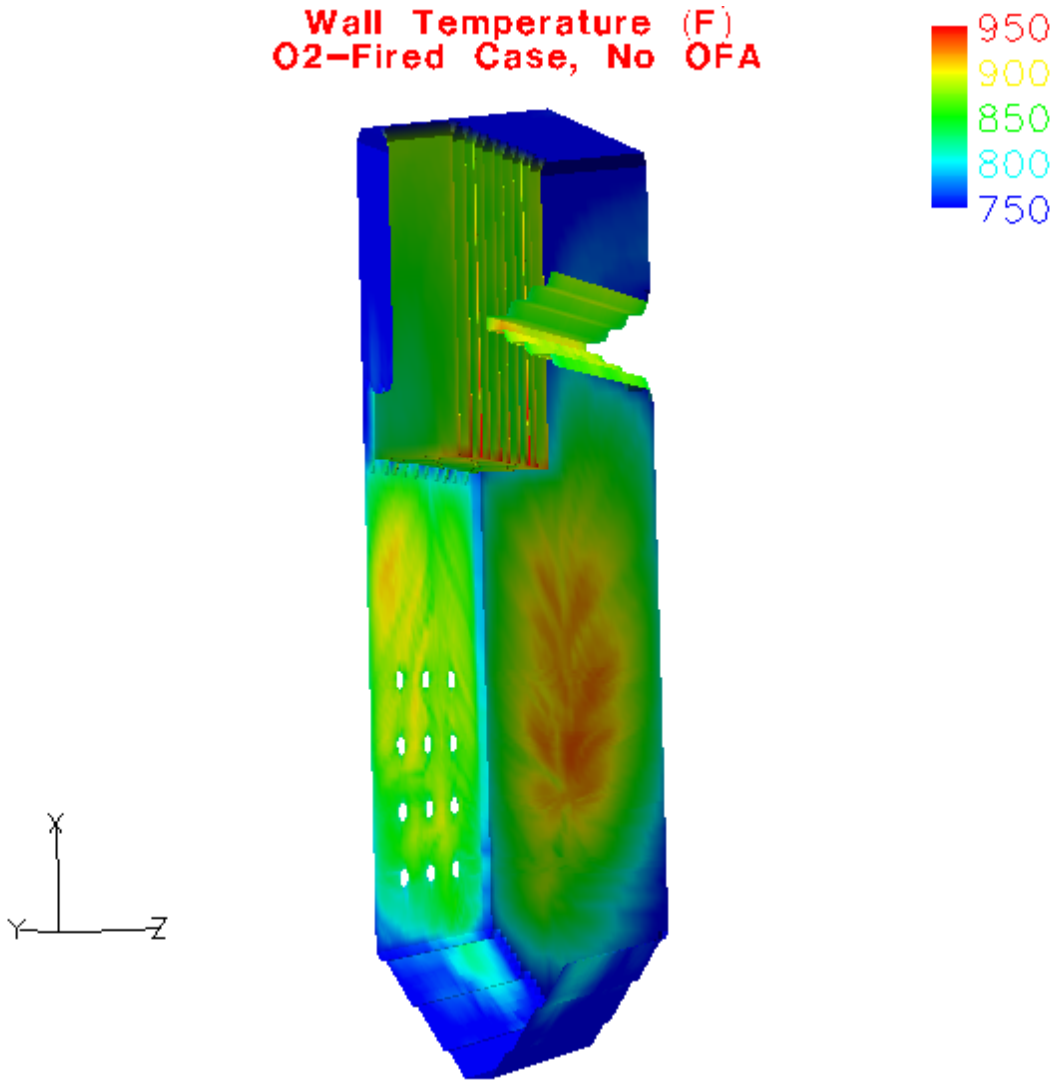

Figure 4.4.22 – Wall CO for O_2-Fired Case Without OFG

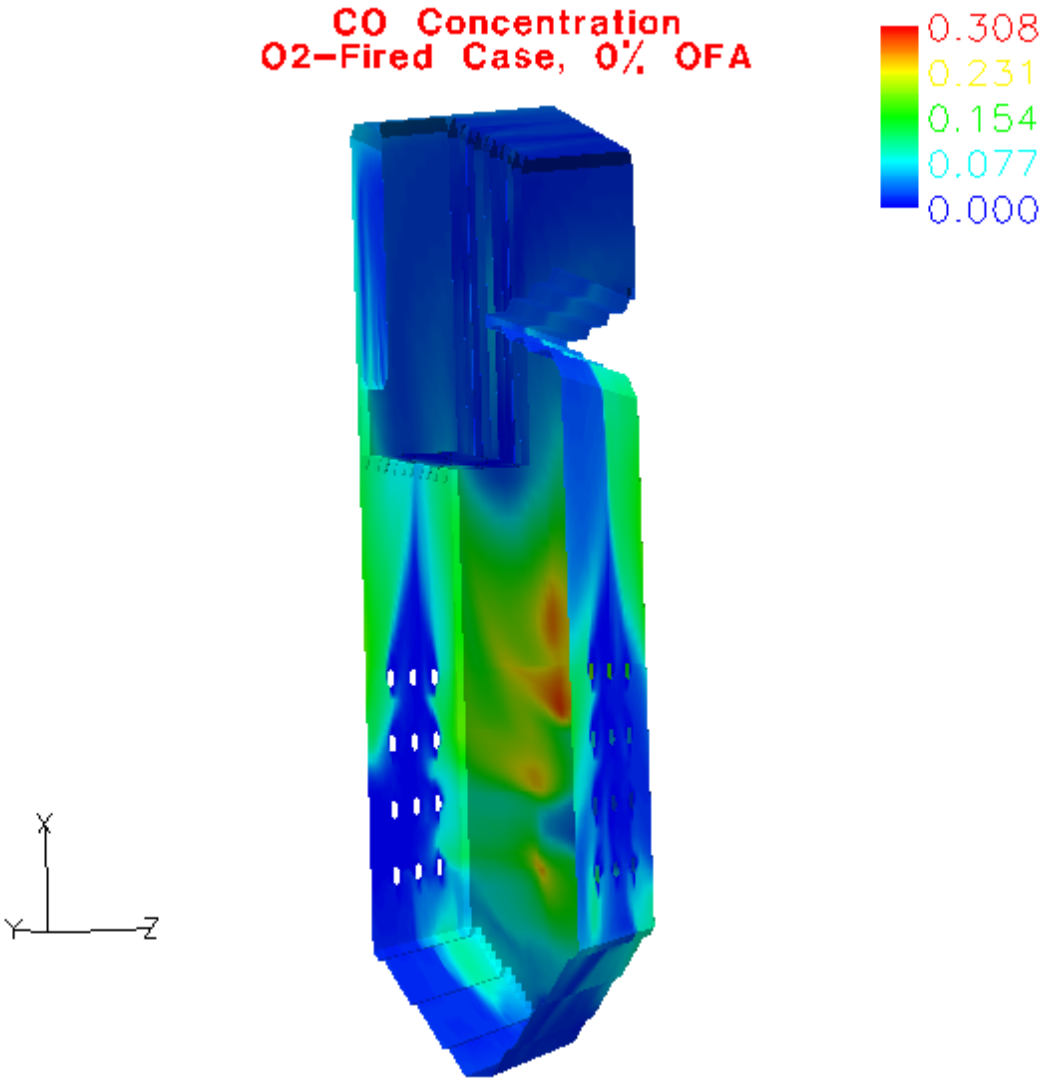

Figure 4.4.23 – Char Mass Fraction (69 micron) for O_2-Fired Case, No OFG

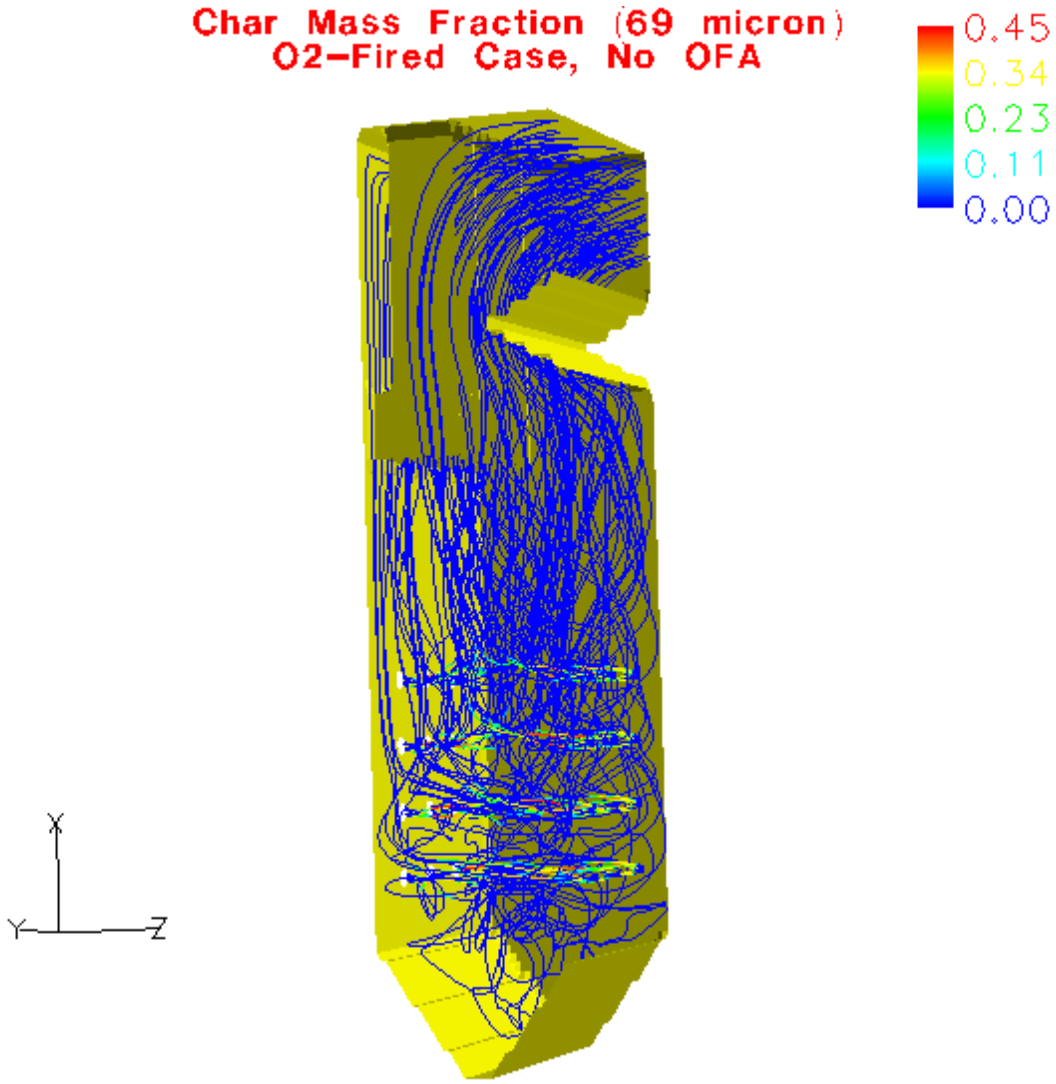

Figure 4.4.24 – Char Mass Fraction (169 micron) for O_2-Fired Case, No OFG

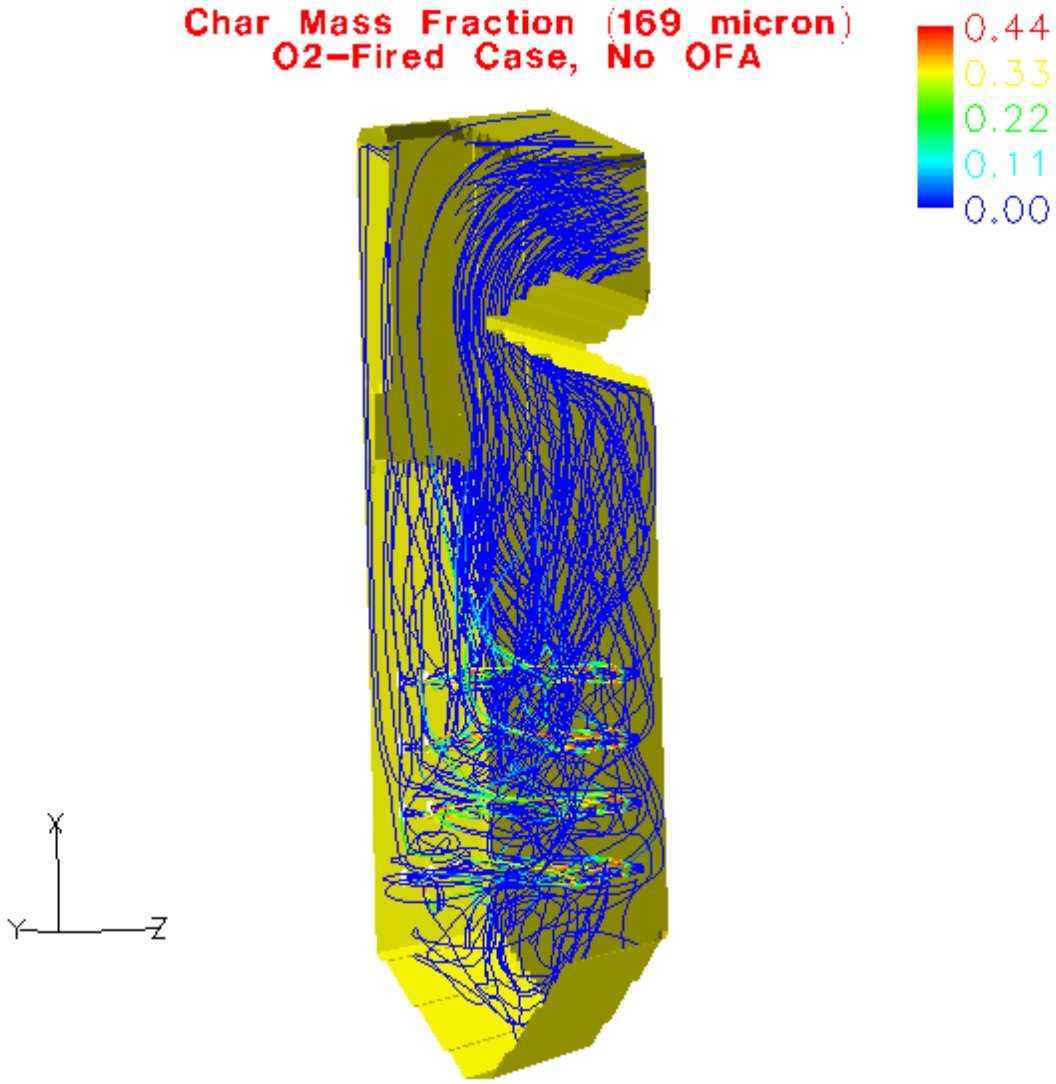

Figure 4.4.25 – Char Mass Fraction (169 micron) for O_2-Fired Case, No OFG, Without Primary gas Swirl

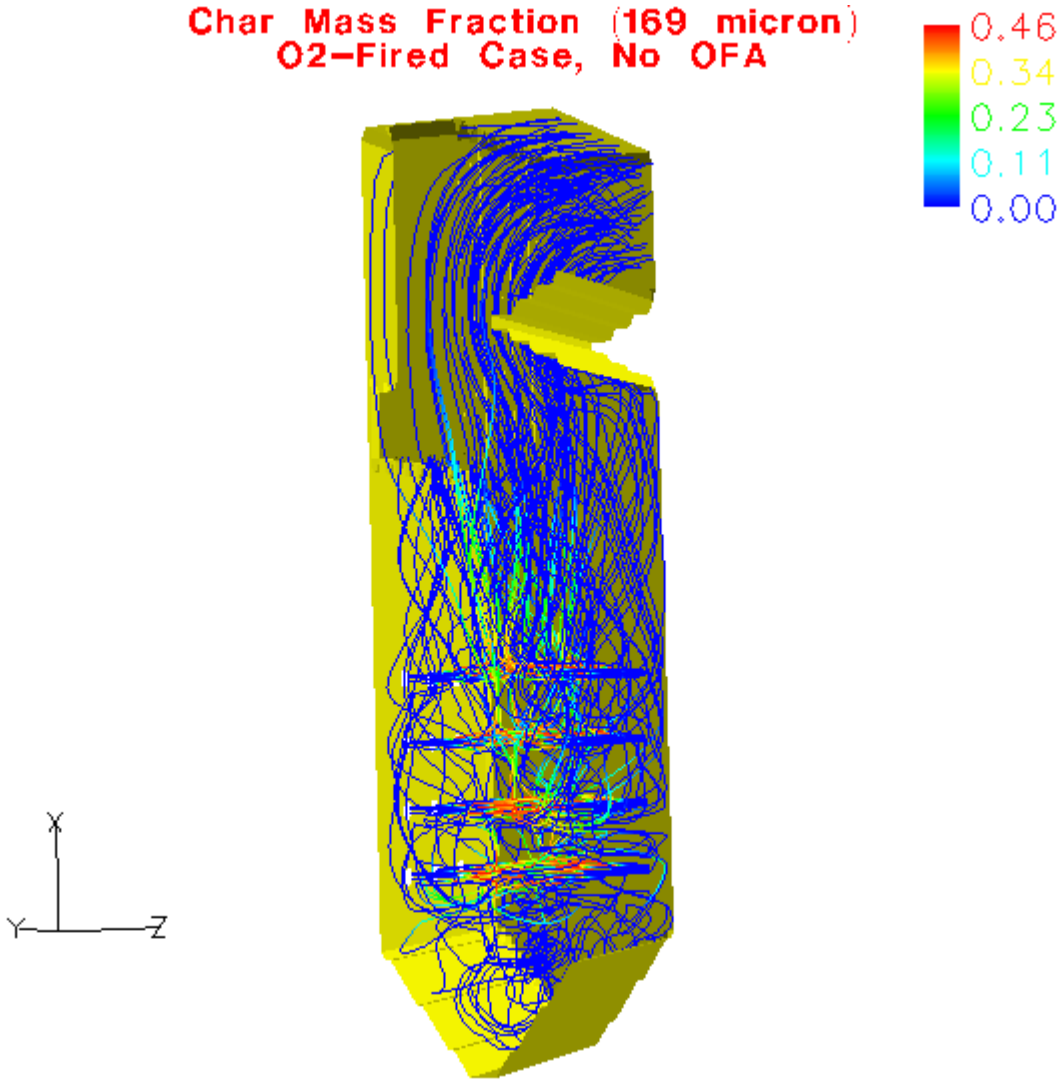

Figure 4.4.26 – Gas Velocity for O_2-Fired Case With 20% OFG

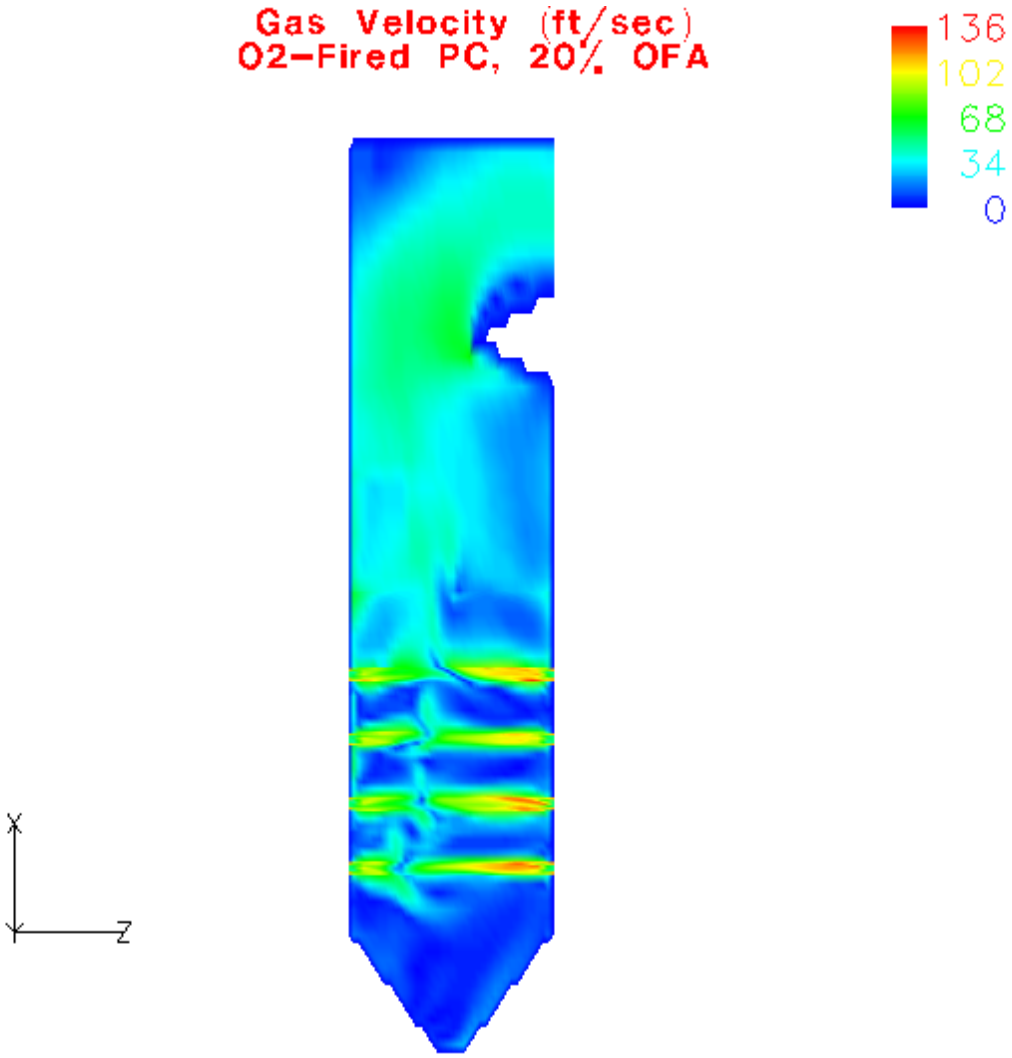

Figure 4.4.27 – Gas Temperature for O_2-Fired Case With 20% OFG

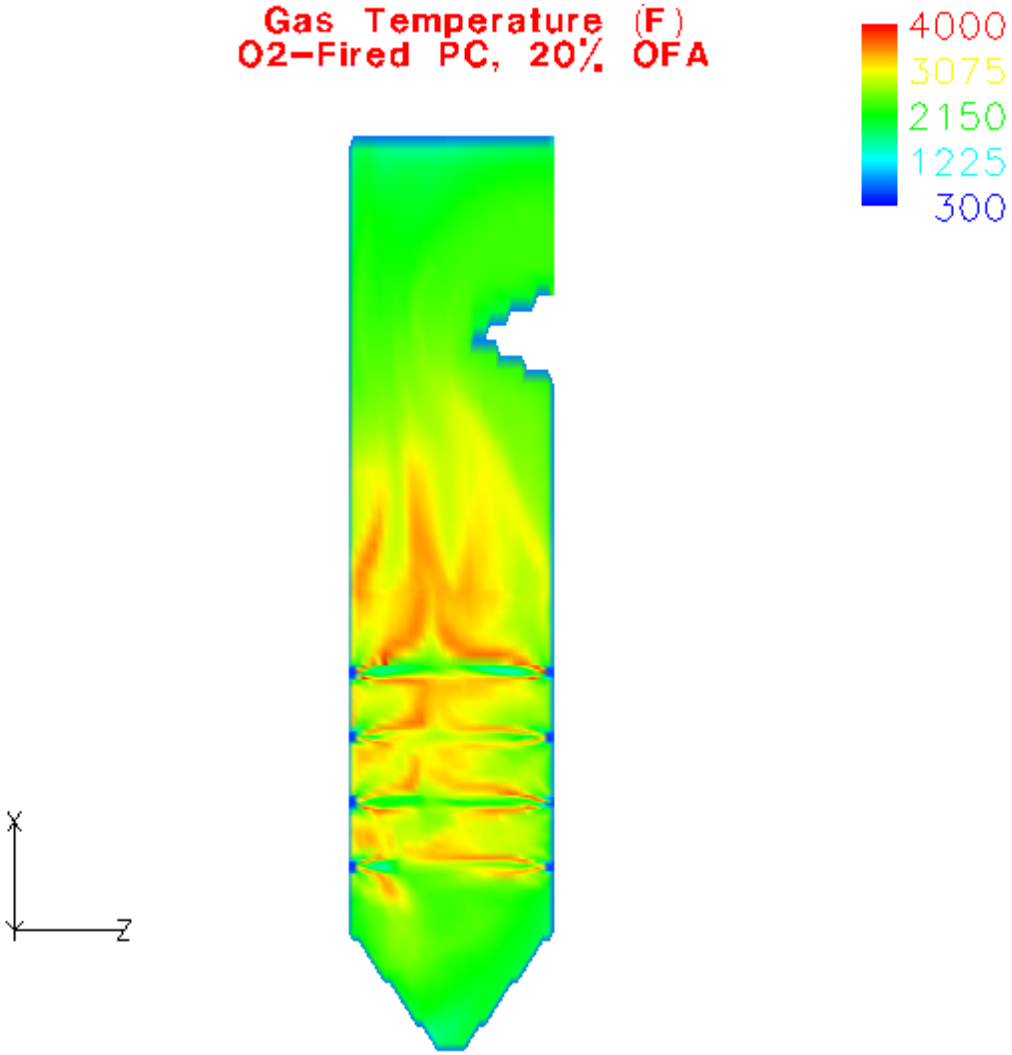

Figure 4.4.28 – O_2 Mole Fraction for O_2-Fired Case With 20% OFG

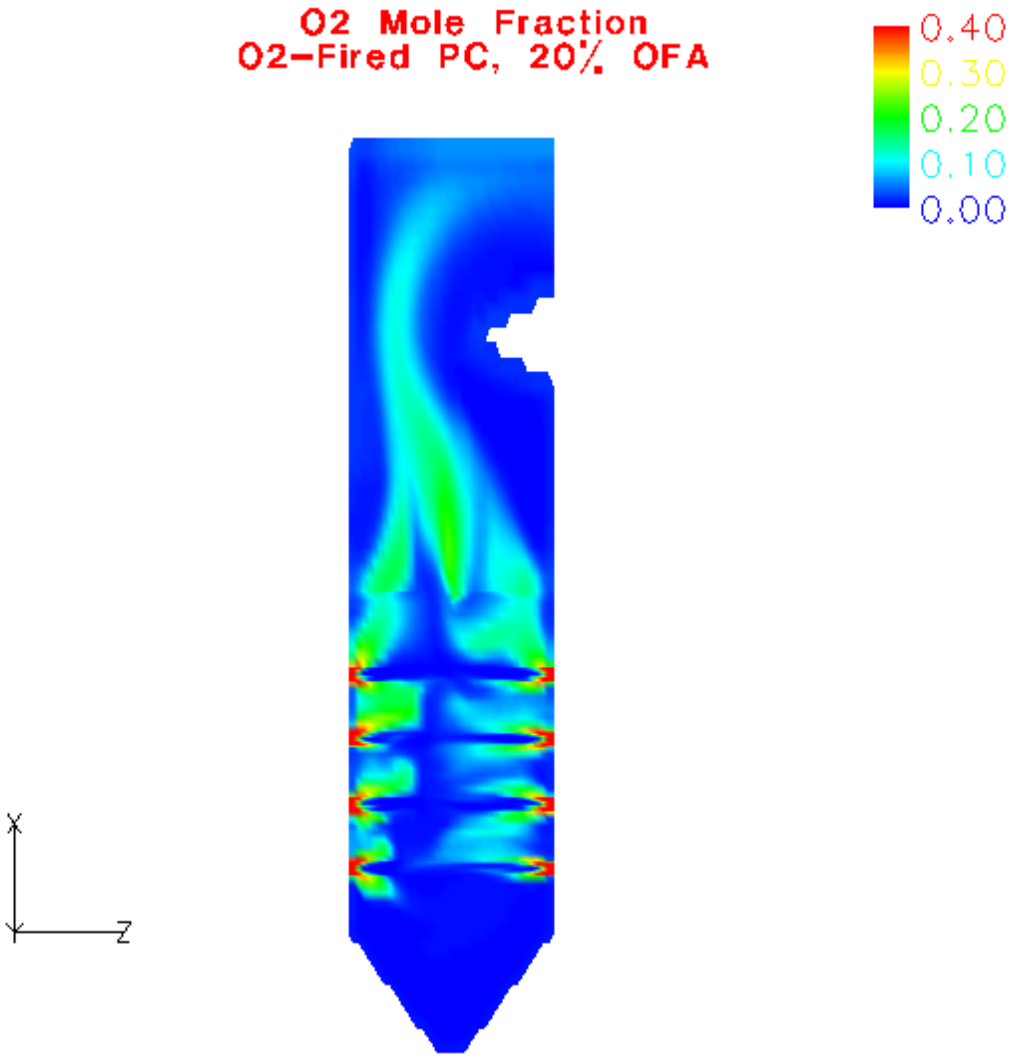

Figure 4.4.29 – Wall Heat Flux for O_2-Fired Case With 20% OFG

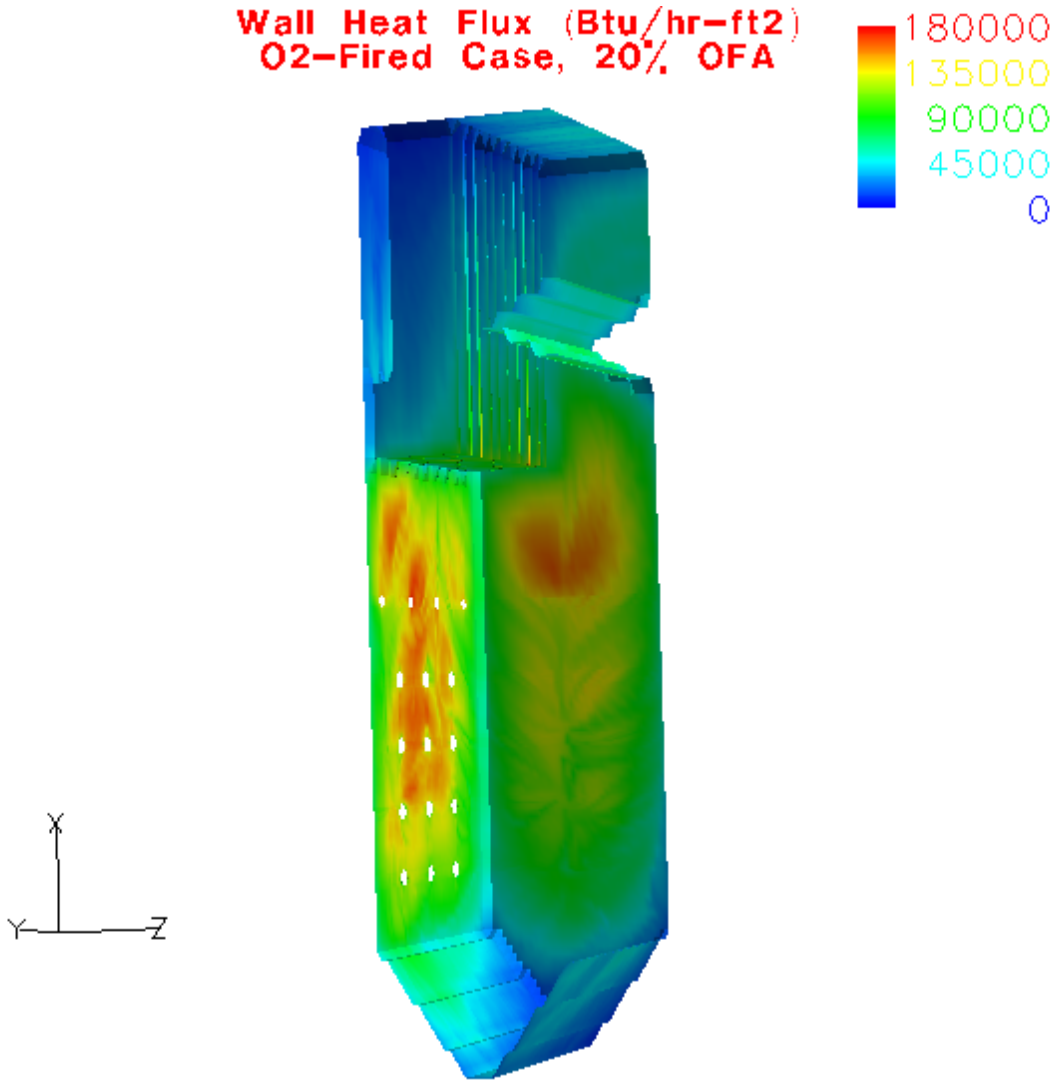

Figure 4.4.30 – Wall Temperature for O_2-Fired Case With 20% OFG

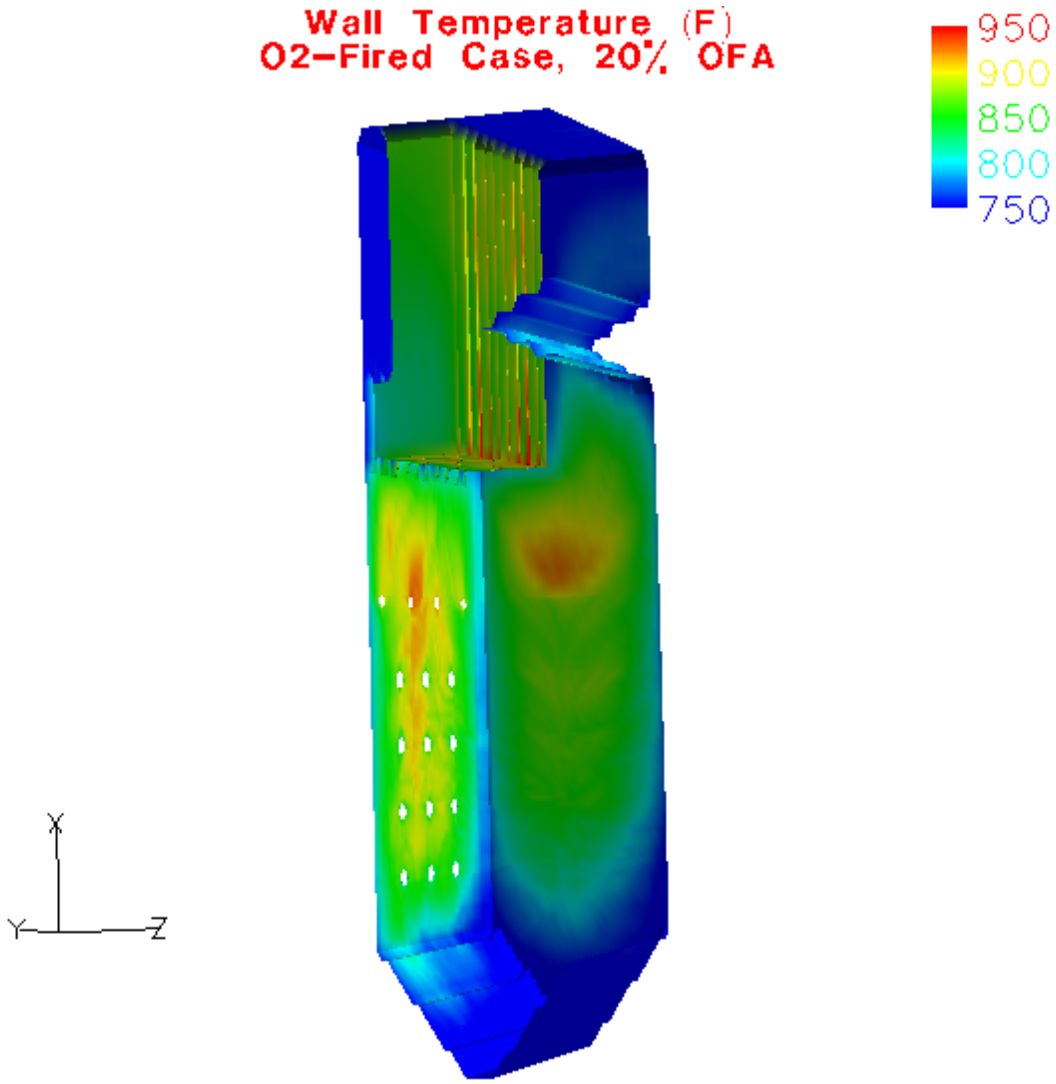

Figure 4.4.31 – Wall CO for O_2-Fired Case With 20% OFG

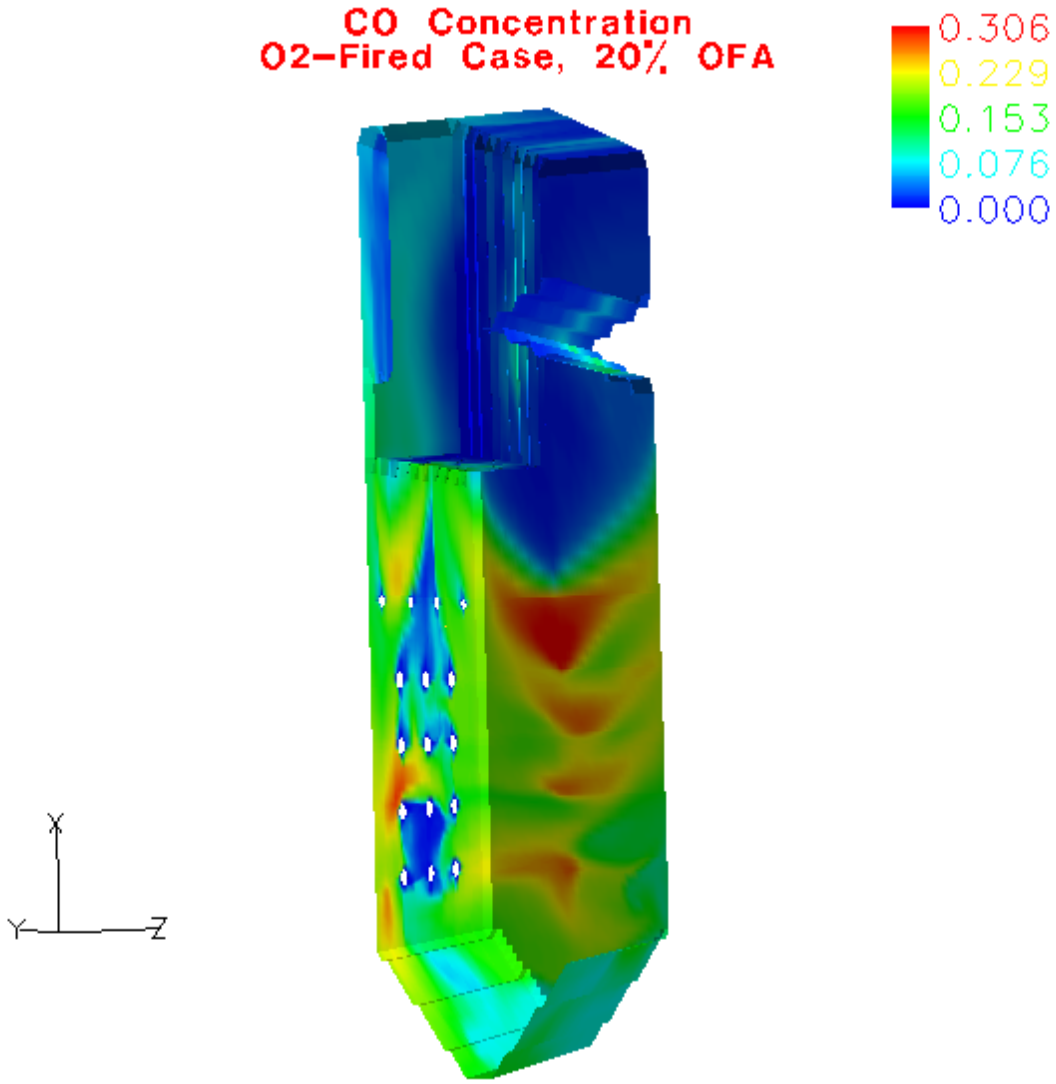

Figure 4.4.32 – Char Mass Fraction (69 micron) for O_2-Fired Case, 20% OFG

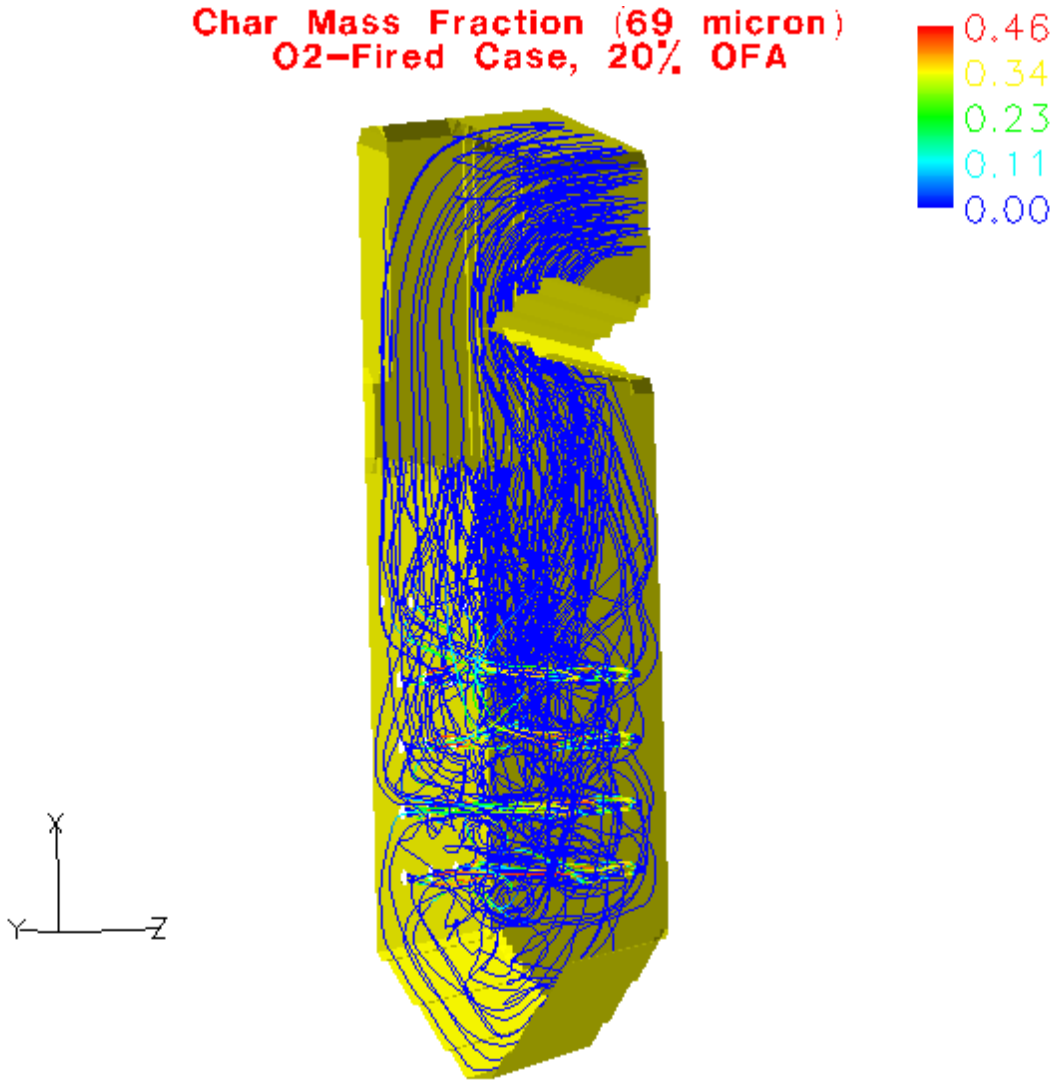

Figure 4.4.33 – Char Mass Fraction (169 micron) for O_2-Fired Case, 20% OFG

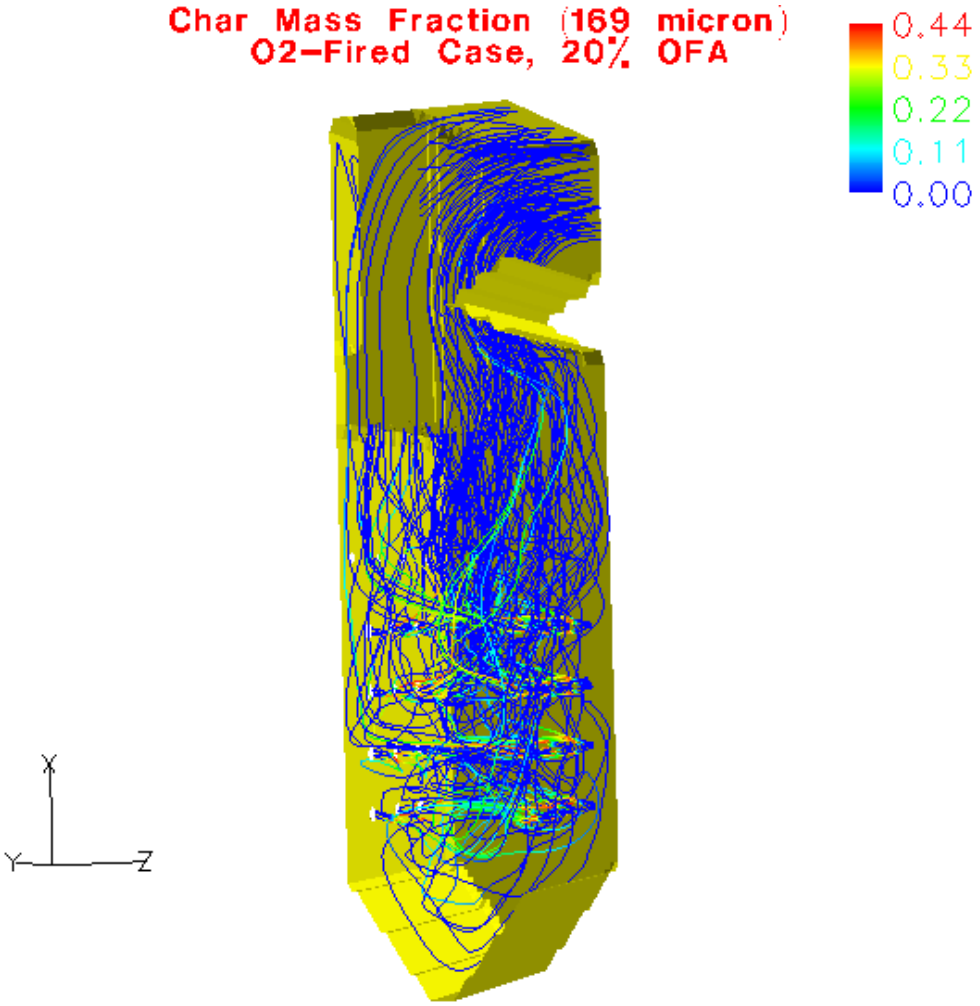

Figure 4.4.34 – Char Mass Fraction (169 micron) for O_2-Fired Case, 20% OFG, Without Primary gas Swirl

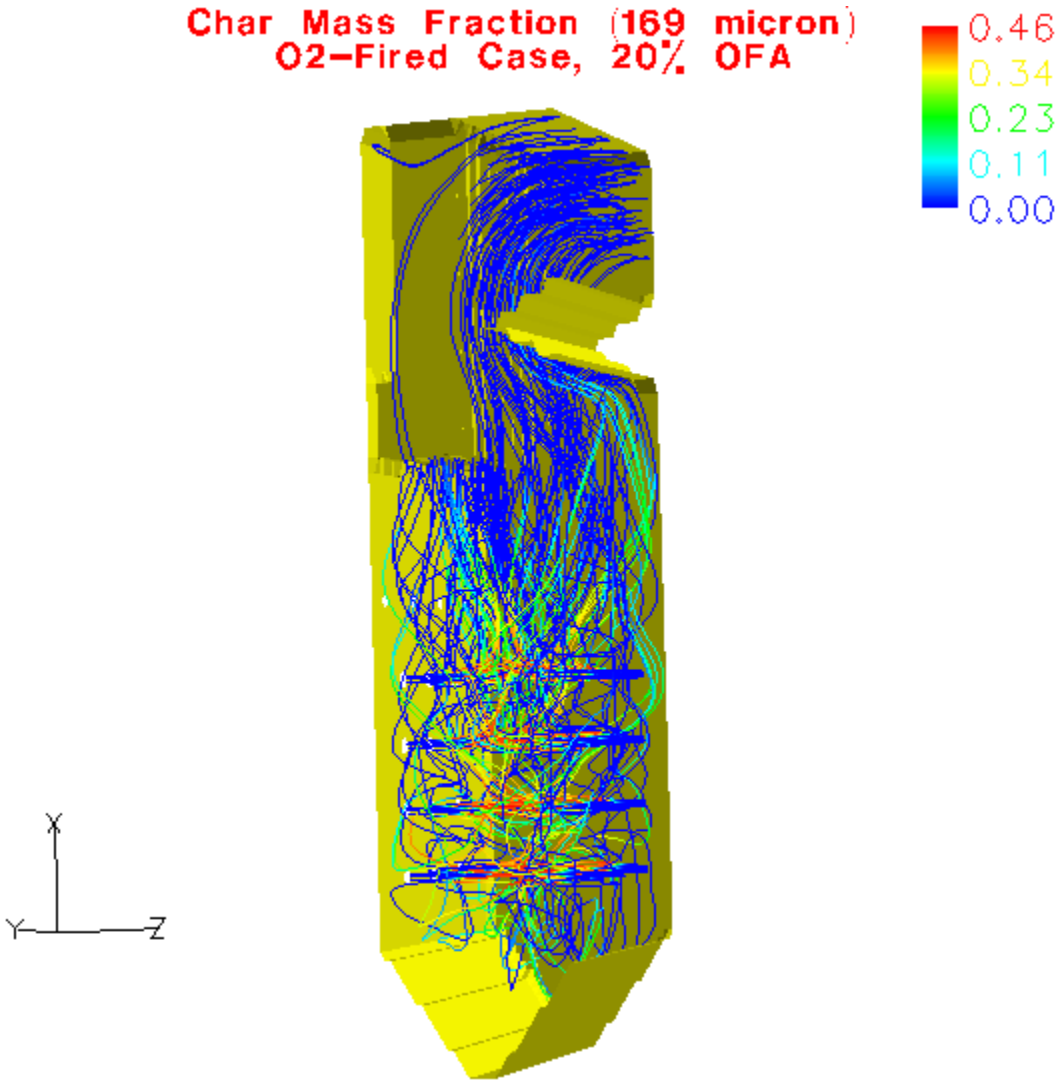

Table 4.4.4 – HRA Tube Bank Design

		Springerville	O2 PC
Finishing Superheater			
Length	ft	38.0	24.0
No. of Tubes Deep		48	48
No. of Tubes Wide		30	32
Total Number of Tubes		1,440	1,536
Tube Outside Diameter	in	2.000	2.000
Tube Thickness	in	0.266	0.266
Tube Material		SA-213-T91	SA-213-T91
Total Surface Area	ft2	28,839	20,587
Vertical Reheater			
Length	ft	30.5	20.0
No. of Tubes Deep		30	50
No. of Tubes Wide		63	51
Total Number of Tubes		1,890	2,550
Tube Outside Diameter	in	2.250	2.250
Tube Thickness	in	0.165	0.165
Tube Material		SA-213-T91	SA-213-T91
Total Surface Area	ft2	33,926	30,042
Primary Superheater			
Length	ft	18.0	9.0
No. of Tubes Deep		96	162
No. of Tubes Wide		63	54
Total Number of Tubes		6,048	8,748
Tube Outside Diameter	in	2.250	2.250
Tube Thickness	in	0.23	0.23
Tube Material		T12/T2/CS	T12/T2/CS
Total Surface Area	ft2	67,231	48,440
Horizontal Reheater			
Length	ft	16.0	15.0
No. of Tubes Deep		65	100
No. of Tubes Wide		126	90
Total Number of Tubes		8,190	9,000
Tube Outside Diameter	in	2.250	2.250
Tube Thickness	in	0.165	0.165
Tube Material		T91/T22/T2/CS	T91/T22/T2/CS
Total Surface Area	ft2	81,952	84,821
Upper Economizer			
Length	ft	18.0	
No. of Tubes Deep		24	
No. of Tubes Wide		126	
Total Number of Tubes		3,024	
Tube Outside Diameter	in	2.250	
Tube Thickness	in	0.205	
Tube Material		SA-210-A1	
Total Surface Area	ft2	32,064	0
Lower Economizer			
Length	ft	25.5	20.0
No. of Tubes Deep		27	30
No. of Tubes Wide		126	90
Total Number of Tubes		3,402	2,700
Tube Outside Diameter	in	2.250	2.250
Tube Thickness	in	0.205	0.205
Tube Material		SA-210-A1	SA-210-A1
Total Surface Area	ft2	50,099	31,810
Total HRA Surface Area	ft2	294,111	215,700

Table 4.4.5 – HRA Tube Bank Performance

	Bank	Surface Area (ft2)	Heat Trans. Coeff. (Btu/hr-ft2-F)	Mean Temp. Diff. (F)	Heat Transfer (MM Btu/hr)	Gas Press. Drop (in H2O)
Air PC	Finishing Superheater	28,839	11.7	1080	364	0.14
O2 PC	Finishing Superheater	20,587	14.6	1172	353	0.16
Air PC	Primary Superheater	67,231	10.1	437	295	0.69
O2 PC	Primary Superheater	48,438	10.1	294	144	0.69
Air PC	Finishing Reheater	33,926	10.6	785	281	0.29
O2 PC	Finishing Reheater	30,042	12.4	728	271	0.26
Air PC	Primary Reheater	81,952	8.3	403	274	0.48
O2 PC	Primary Reheater	84,821	10.5	296	264	0.63
Air PC	Upper Economizer	32,064	9.4	367	111	0.39
O2 PC	Upper Economizer	0				0.00
Air PC	Lower Economizer	50,099	10.7	261	140	0.46
O2 PC	Lower Economizer	31,810	10.6	192	64	0.30
Air PC	Total	294,111			1354	2.45
O2 PC	Total	215,698			1096	2.04

4.5 Economic Analysis

4.5.1 Main Assumptions

The economic analysis was carried out based on the EPRI Technical Assessment Guide (TAG) methodology. Plant capital costs were compiled under the Code of Accounts developed by EPRI and used in references [12] and [24].

The estimate basis and major assumptions are listed below:

- Total plant costs are estimated in January 2004 dollars.
- Plant book life is 20 years.
- The net power output for the reference PC plant (without CO_2 sequestration) is 450 MWe and for the O_2 PC plant (with sequestration) is 327 MWe.
- Capacity factor is 85%. The plant will operate at 100% load at 85% of the time.
- Cost of electricity (COE) was determined on a levelized constant dollar basis.
- Average annual ambient air conditions for material balances, thermal efficiencies and other performance related parameters are at a dry bulb temperature of 60 deg. F and an air pressure of 14.7 psia.
- The coal is Illinois #6 coal (see Table 4.2.1 for analysis).
- Terms used are consistent with the EPRI TAG.

4.5.2 Plant Cost Basis

The total plant cost (TPC), also referred to as the plant capital cost is comprised of the following elements:

1. Bare erected plant cost.
2. Overheads and fee for engineering and home office.
3. Project and process contingencies.

The O_2-fired PC plant capital costs were derived in comparison to a recently constructed Foster Wheeler reference plant, which is an existing subcritical pressure, natural circulation PC plant.

The major changes to the reference plant were:

- Redesigned boiler (boiler size, and heat transfer surface) (see Section 4.4)
- Removed air pre-heater
- Added new flue gas-to-recycle gas heat exchanger
- Reduced size of FD and ID boiler fans
- Reduced weight of primary and secondary oxidant ductwork
- Removed plant selective catalytic NOx reduction (SCR) system
- Removed plant flue gas desulfurization (FGD) system
- Replaced full size plant stack with start-up stack
- Added air separation unit
- Added CO_2 compression and dehydration unit

For the modified components, the plant capital costs were calculated as cost differentials by the Foster Wheeler estimating department. These cost differentials were then added to the base cost of the reference plant.

For the new components costs were either obtained from vendor quotes and/or determined by the Foster Wheeler estimating department as follows:

- The ASU cost was obtained from Air Products and Chemicals Inc.
- The CO_2 compression and de-hydration system costs were developed using internal data from a Foster Wheeler commercial project. This price was compared to a recent estimate by Nexant Inc. (Ref. 25) for confirmation.
- The flue gas-to-recycle gas heat exchanger cost was estimated by Foster Wheeler based on internal cost data for similar units.

Allowance for engineering and home office overheads and fee of 6% of the bare erected cost was added for the new components. The “bare erected cost” is the installed cost of the equipment and systems that make up the plant.

For the new plant items, project contingencies were added to account for the uncertainty based on the level of detail currently available (or lacking) in the design. Consistent with EPRI Technical Assessment Guide (TAG), a 15% (of bare erected cost) project contingency was used for the CO_2 compression and de-hydration system, and a 5% project contingency was used for the ASU. No process contingencies were applied, since the components of the new systems (e.g. compressors, knock-out pots, etc.) are well-developed technologies.

Table 4.5.1 shows the capital cost worksheet for the O_2 fired PC plant. As the table shows, a total plant cost of $668,673,700.00, or 2106 $/kW was calculated. A substantial part of the cost increase is caused by CO_2 compression equipment, which must be included for any CO_2 removal systems.

Table 4.5.1 – Oxygen-Fired PC Plant Capital Cost Estimate

Base Plant: Air-Fired subcritical pressure, natural circulation PC
Base Plant Output: 450 MWe, net
Base Plant "As bid" cost: $ 585,000,000.00 Includes contingencies and EPC costs

Cost differences in converting air-fired PC to the oxygen-fired PC configuration:

			Eng'g CM	Contingencies		Total Plant
Item	Description of change	Bare erected cost	HO & Fee	Process	Project	Cost
Boiler	Furnace panels change from carbon steel to alloy steel	$ 600,000.00	Incl. As bid	$ -	$ -	$ 600,000.00
	Less HRA surface needed	$ (306,000.00)	Incl. As bid	$ -	$ -	$ (306,000.00)
	Smaller economizer	$ (600,000.00)	Incl. As bid	$ -	$ -	$ (600,000.00)
	Air pre-heater not required	$ (4,600,000.00)	Incl. As bid	$ -	$ -	$ (4,600,000.00)
	New Flue-gas/recycle gas heat exchanger	$ 6,000,000.00	Incl. As bid	$ -	$ -	$ 6,000,000.00
	Less oxidant and gas ductwork	$ (1,000,000.00)	Incl. As bid	$ -	$ -	$ (1,000,000.00)
	SCR system not required	$ (6,400,000.00)	Incl. As bid	$ -	$ -	$ (6,400,000.00)
	Smaller FD and ID boiler fans	$ (2,200,000.00)	Incl. As bid	$ -	$ -	$ (2,200,000.00)
	Less boiler structural steel (smaller boiler)	$ (2,000,000.00)	Incl. As bid	$ -	$ -	$ (2,000,000.00)
BOP	FGD sytem not required	$ (56,000,000.00)	Incl. As bid	$ -	$ -	$ (56,000,000.00)
	Full size stack replaced by small, start-up stack	$ (6,000,000.00)	Incl. As bid	$ -	$ -	$ (6,000,000.00)
ASU	Air separation unit added	$ 116,970,000.00	$ 7,018,200.00	$ -	$ 5,848,500.00	$ 129,836,700.00
CO2 System	CO2 compression and dehydration unit added	$ 38,300,000.00	$ 2,298,000.00	$ -	$ 5,745,000.00	$ 46,343,000.00
	Total difference:	$ 82,764,000.00	$ 9,316,200.00	$ -	$ 11,593,500.00	***$ 103,673,700.00***

O2 PC Plant Cost: $ 688,673,700.00 2,106 $/kW

O2 PC Plant net output: 327 MW

4.5.3 Total Plant Investment (TPI)

To determine the total investment required at the date of start-up, the TPC is escalated by the average interest rate over the construction period. Unlike the TPC, which assumes instantaneous construction, TPI ensures that escalation of construction costs and allowance for funds used during construction is properly taken into account. The construction period was estimated to be 4 years. Assuming uniform cash flow over the construction period, the TPI was calculated as follows:

$$TPI = TPC\ [1+i_{avg}]$$

Where

i_{avg} = Average interest rate over construction period
= (Interest rate)(Construction Period in Years)/2 = 10%

The annual interest rate was taken as 5%.

4.5.4 Total Capital Requirement (TCR)

The TCR includes all capital required to complete the project. TCR is the sum of TPI, pre-paid royalties, pre-production (start-up) costs, inventory capital, and land cost:

- Royalties costs are assumed inapplicable to the CO_2 hybrid plant
- Pre-production costs cover operator training, equipment checkout, major changes in plant equipment, extra maintenance, and inefficient use of fuel and other materials during start-up. They are estimated as follows:
    - 1 month of fixed operating costs, operating and maintenance labor, administrative and support labor, and maintenance materials.
    - 1 month of variable operating costs at full capacity (excluding fuel) – includes chemicals, water, and other consumables and waste disposal charges.
    - 25% of full capacity fuel cost for 1 month – covers inefficient operation that occurs during the start-up period.
    - 2% of TPI – covers expected changes and modifications to equipment that will be needed to bring the plant up to full capacity.
- Inventory capital is the capital required for initial inventories of fuel and other consumables, which are capitalized and included in the inventory capital account. Fuel and other consumables inventory (except water) are based on full-capacity operation for 15 days. An allowance of ½ percent of the TPC equipment cost is included for spare parts.

- Initial catalyst and chemical charge covers the initial cost of any catalysts or chemicals that are contained in the process equipment, but not in storage. In this study, this small charge was included with the equipment capital costs and is a part of the TPC.
- Land cost is based on 60 acres at $10,000/acre.

The TPI and the TCR cost components are shown on Table 4.5.5 and Table 4.5.6.

4.5.5 Operating Costs And Expenses

Operating costs were expressed in terms of the following categories:

- Operating Labor
- Maintenance Cost
    - Maintenance labor
    - Maintenance materials
- Administrative and Support Labor
- Consumables
- Fuel Cost

These values were calculated in consistence with EPRI TAG methodology. All costs were based on a first year basis with January 2004 dollars. The first year costs do not include start-up expenses, which are included in the TCR.

The cost categories listed above are calculated, on a dollars per year basis, as follows:

- Operating labor is calculated by multiplying the number of operating personnel with the average annual (burdened) compensation per person.

- Maintenance costs are estimated to be 2% of the TPC and are divided into maintenance labor and maintenance materials

    - Maintenance labor is estimated to be 40% of the total maintenance cost
    - Maintenance materials are estimated to be 60% of the total maintenance cost

- Administrative and support labor is estimated to be equal to 25% of the sum of operating and maintenance labor.

- Consumables are feedstock and disposal costs calculated from the annual usage at 100% load and 85% capacity factor. The costs is expressed in year 2004 dollars and levelized over 20 years on constant dollar basis.

- Fuel cost is calculated based on the assumed net cost for delivered coal, which is $1.14/MMBtu [26]. Fuel cost is determined on a first year basis and levelized over 20 years on a constant dollar basis. The calculation of first year fuel costs is done as follows:

$$\text{Fuel (tons/day)} = \frac{\text{(Plant Heat Rate)x (net capacity in kW) x 24 hr/day}}{\text{HHV x 2000 lb/ton}}$$

$$\text{Fuel Unit Cost (\$/ton)} = \text{HHV x 2000 lb/ton x (Fuel Cost in \$/MMBtu) x } 10^6$$

$$\text{Fuel Cost (1}^{st}\text{ year)} = \text{Fuel (tons/day) x Fuel Unit Cost (\$/ton) x 365 day/yr x 0.85 (CF)}$$

The operating and maintenance costs, excluding fuel and consumables, are combined and divided into two components: 1) Fixed O&M, which is independent of power generation, and 2) Variable O&M, which is proportional to power generation. These are calculated as follows:

$$\text{Fixed O\&M (\$/yr)} = \text{Oper. Labor + Maint. Labor + Adm. and Support Labor}$$

$$\text{Fixed O\&M (\$/kW-yr)} = \frac{\text{Fixed O\&M(\$/year)}}{\text{Net Power (kW)}}$$

$$\text{Variable O\&M (\$/yr)} = \text{Maintenance Materials}$$

$$\text{Variable O\&M (¢/kWh)} = \frac{\text{Variable O\&M (\$/yr)}}{\text{Net Power (kW) x CF x 8760}}$$

Where, CF is the plant capacity factor and 8760 is the total number of hours in one year.

The operating and maintenance costs for the O_2-fired PC and the air-fired reference plant are shown on Table 4.5.2. The “total production cost” shown at the bottom of the table expresses the charge of operating and maintaining the baseline plant (including fuel and consumable costs) in terms of cents per kilowatt-hour.

4.5.6 Cost Of Electricity (COE)

The COE value is made up of contributions from the capital cost (called the carrying charge), operating and maintenance costs, consumables, and fuel costs. The following relationship is used to calculate COE from these cost components:

COE = LCC + LFOM x 100/(8760 x CF) + LVOM + LCM +LFC

LCC = Levelized carrying charge, ¢/kWh

LFOM = Levelized fixed O&M, $/kW-yr
LVOM = Levelized variable O&M, ¢/kWh
LCM = Levelized consumables, ¢/kWh
LFC = Levelized fuel costs, ¢/kWh
CF = plant capacity factor (0.85)

The basis for calculating the capital investment and revenue requirements for the reference plant and the O_2 PC are given in Table 4.5.3 and Table 4.5.4, respectively. The capital investment and revenue requirements summary is given in Table 4.5.5 for the reference plant without CO_2 sequestration and in Table 4.5.6 for the O_2 PC.

As Table 4.5.5 and Table 4.5.6 show, the levelized COE for 85% capacity factor was calculated at 4.61 ¢/kWh without CO_2 sequestration and at 6.41¢/kWh with CO_2 sequestration.

4.5.7 Comparison with Other Technologies

An economic comparison was performed between the O_2 PC and other competing CO_2 removal technologies. For comparison the following alternate technologies were chosen:

Air PC: Supercritical PC plant with post-combustion CO_2 mitigation (Ref [12] case 7A).
NGCC: Natural Gas Combined Cycle with post combustion (Ref. [12] case 1A).
IGCC: Integrated Gasification Combined Cycle with pre-combustion CO_2 mitigation (Ref. [24] case 3E).

The economics of these technologies were compared with the O_2 PC using both the levelized cost of electricity and the CO_2 mitigation cost as indexes. The CO_2 mitigation cost (MC) shows the cost impact, in dollars per tonne of CO_2 that would otherwise be emitted, of a configuration that allows CO_2 capture relative to the reference plant.

The MC is calculated as follows:

$$MC = \frac{COE_{with\ removal} - COE_{reference}}{E_{reference} - E_{with\ removal}} \times 0.01\ \$/¢$$

COE = Cost of electricity in ¢/kWh
E = CO_2 emission in tonnes/kWh

The COE and MC for the Air PC, NGCC, and IGCC were obtained from Ref. 12and Ref. 24. Since the economic analysis of Ref. 12 and Ref. 24 were made in

2000 two adjustments were necessary so that the values can be compared to the results of the current O_2 PC economic analysis:

1. A constant inflation rate of 2% was assumed between 2000 and 2004.
2. The 2000 natural gas fuel price was replaced with the 2004 natural gas fuel price (fuel price = 5.89 $/MM Btu, an increase of 118% above 2000 price).

Since the analyses of Ref. 12 and Ref. 24 were assumed at a 65% capacity factor, Figure 4.5.1 and Figure 4.5.2 present a comparison of the COE and MC using a 65% capacity factor for the O_2 PC. Compared to the COE of the O_2 PC, the COE for the other technologies is 17% higher for Air PC, 15% higher for NGCC, and 14% lower for IGCC. Compared to the MC of the O_2 PC, the MC for the other technologies is 170% higher for NGCC, 100% higher for Air PC, and 9% lower for IGCC.

Since the O_2 PC uses reliable long-proven technology it is expected that the capacity factor of the O_2 PC will be close to 85%. Consequently Figure 4.5.3 and Figure 4.5.4 present a comparison of the COE and MC using an 85% capacity factor for the O_2 PC. Compared to the COE of the O_2 PC, the COE for the other technologies is 45% higher for Air PC, 40% higher for NGCC, and 6% higher for IGCC. Compared to the MC of the O_2 PC, the MC for the other technologies is 250% higher for NGCC, 160% higher for Air PC, and 17% higher for IGCC.

Note that the air-fired post combustion capture PC plant data used in Figure 4.5.1 to Figure 4.5.4 is for a supercritical unit whereas the O_2 PC plant operates at subcritical pressure. It is expected that the economic cost (COE and MC) of a supercritical O_2 PC will be lower than a subcritical O_2 PC.

Table 4.5.2 - Operating, Maintenance and Fuel Costs for the O_2 PC and the Air-fired Reference

1) With CO2 Sequestration (O2 PC)

Plant Net Power =		326	MW			
Capacity Factor		85%				
Operating and Maintenance Costs						
				Unit Cost	**$/year**	**$/KW-yr**
Operating labor		60	people	$90,000.00	$5,400,000.00	$16.56
Maintenance Cost	2% of TPC					
Maintenance Labor (40%)					$5,509,389.60	$16.90
Maintenance Materials (60%)					$8,264,084.40	$25.35
Administrative Support and Labor	25 % of O&M Labor				$2,727,347.40	$8.37
Consumable Operating Costs (Except Fuel)				**Unit Cost**	**$/year**	**c/KWh**
Water		8080	kgals/day	$0.80	$2,005,411	0.070
Water Chemicals		19553	lbs/day	$0.16	$970,619	0.034
Limestone						
Start-up Fuel	5 starts/year				$50,000.00	0.002
Startup Electricity		6300	MWh/yr	$30	$189,000.00	0.007
Ash disposal		18.26	ton/hr	$10	$1,359,639.60	0.048
Other Chemicals					$330,000.00	0.012
						0.160
Fuel Cost (2004 Dollars)	Heat Rate =		11,411	Btu/kWh		
				Unit Cost	**$/year**	**c/KWh**
		3720.11	MMBtus/hr	$1.14	$31,577,905	1.301
Total Production Cost						2.36 c/kWh

2) Without CO2 Sequestration (Air-fired reference)

Plant Net Power =		417	MW			
Capacity Factor		85%				
Operating and Maintenance Costs						
				Unit Cost	**$/year**	**$/KW-yr**
Operating labor		56	people	$90,000.00	$5,040,000.00	$15.46
Maintenance Cost	2% of TPC					
Maintenance Labor (40%)					$4,680,000.00	$14.36
Maintenance Materials (60%)					$7,020,000.00	$21.53
Administrative Support and Labor	25 % of O&M Labor				$2,430,000.00	$7.45
Consumable Operating Costs (Except Fuel)				**Unit Cost**	**$/year**	**c/KWh**
Water		7906	kgals/day	$0.80	$1,962,269	0.054
Water Chemicals		19133	lbs/day	$0.16	$949,738	0.026
Limestone		432	tons/day	$15	$2,010,420	0.055
Start-up Fuel	5 starts/year				$50,000.00	0.001
Startup Electricity		6300	MWh/yr	$30	$189,000.00	0.005
Ash disposal		52.43	ton/hr	$10	$3,903,937.80	0.107
						0.248
Fuel Cost (2004 Dollars)	Heat Rate =		9,302	Btu/kWh		
				Unit Cost	**$/year**	**c/KWh**
		3878.96	MMBtus/hr	$1.14	$32,926,353	1.060
Total Production Cost						2.10 c/kWh

Table 4.5.3 - Estimate Basis/Financial Criteria for Revenue Requirement Calculations: Air-fired Reference Plant

GENERAL DATA/CHARACTERISTICS

Plant Type:	Air-fired Subcritical PC			
Plant Size:	450	MW, net		
Location:	Sea Level, Middletown USA			
Fuel: Primary/Secondary	Illinois #6		--	
Energy from Primary/Secondary Fuels:	9,302	Btu/kWh	--	Btu/kWh
Levelized Capacity Factor / Preproduction (equivalent months):	85%		1	months
Capital Cost Year Dollars (Reference Year Dollars):	2004 (January)			
Delivered Cost of Primary/Secondary Fuel:	1.14	$/MBtu	--	$/MBtu
Design/ Construction Period:	4	years		
Plant Start-up Date (1st year Dollars):	2008 (January)			
Land Area/Unit Cost:	60	acres	$10,000	/ Acre

FINANCIAL CRITERIA

Project Book Life:	20	years		
Book Salvage Value:	-	%		
Project Tax Life:	20	years		
Tax Depreciation Method:	Accel. Based on ACRS Class			
Inflation Rate	2.0	%		
Property Tax Rate:	1.0	%		
Insurance Tax Rate:	1.0	%		
Federal Income Tax Rate:	34.0	%		
State Income Tax Rate:	4.2	%		
Investment Tax Credit/% Eligible	-	%	-	%
Economic Basis:	Over Book	Constant Dollars		

Capital Structure	% of Total	Cost(%)
Common Equity	40	12
Preferred Stock	0	8.5
Debt	60	7
Weighted Cost of Capital: (after tax)	7.456%	

Table 4.5.4 - Estimate Basis/Financial Criteria for Revenue Requirement Calculations: O_2-fired Reference Plant

GENERAL DATA/CHARACTERISTICS

Plant Type:	Oxygen Fired Subcritical PC			
Plant Size:	327	MW, net		
Location:	Sea Level, Middletown USA			
Fuel: Primary/Secondary	Illinois #6		--	
Energy from Primary/Secondary Fuels:	11,411	Btu/kWh	--	Btu/kWh
Levelized Capacity Factor / Preproduction (equivalent months):	85%		1	months
Capital Cost Year Dollars (Reference Year Dollars):	2004 (January)			
Delivered Cost of Primary/Secondary Fuel:	1.14	$/MBtu	--	$/MBtu
Design/ Construction Period:	4	years		
Plant Start-up Date (1st year Dollars):	2008 (January)			
Land Area/Unit Cost:	60	acres	$10,000	/ Acre

FINANCIAL CRITERIA

Project Book Life:	20	years		
Book Salvage Value:	-	%		
Project Tax Life:	20	years		
Tax Depreciation Method:	Accel. Based on ACRS Class			
Inflation Rate:	2.0	%		
Property Tax Rate:	1.0	%		
Insurance Tax Rate:	1.0	%		
Federal Income Tax Rate:	34.0	%		
State Income Tax Rate:	4.2	%		
Investment Tax Credit/% Eligible	-	%	-	%
Economic Basis:	Over Book	Constant Dollars		

Capital Structure	% of Total	Cost(%)
Common Equity	40	12
Preferred Stock	0	8.5
Debt	60	7
Weighted Cost of Capital: (after tax)	7.456%	

Table 4.5.5 - Capital Investment and Revenue Requirement Summary: Air-fired Reference Plant

Case:	Subcritical PC Plant		
Plant size:	417 MW net	**Net Cycle Efficiency:**	36.68%
Primary/Secondary Fuel (type):	Illinois #6	**Net Plant Heat Rate (NPHR):**	9,302 (Btu/kWh)
Design/Construction:	4 (years)	**Cost:**	1.14 ($/MMBtu)
TPC (Plant Cost) Year:	2004 (July)	**Book Life:**	20 (years)
Capacity Factor:	85% (%)	**TPI Year:**	2004 (July)
		CO2 Removed:	(tons/year)

CAPITAL INVESTMENT		**$x1000**	**$/kW**
Process Capital and Facilities		585,000	1,402.9
Engineering Adder (Incl. C.M., H.O., and Fee)		-	-
Process Contingency Adder		-	-
Project Contingency Adder		-	-
TOTAL PLANT COST (TPC)		$ 585,000	1,402.9
TOTAL CASH EXPENDED	$ 585,000		
AFDC	$ 58,500		
TOTAL PLANT INVESTMENT (TPI)		$ 643,500	
Royalty Allowance			
Preproduction Cost		$16,012	
Inventory Capital		$3,544	
Initial Chemicals and Catalysts (w/equip)			
Land Cost		$600	
TOTAL CAPITAL REQUIREMENT (TCR)		$ 663,656	

OPERATING & MAINTENANCE COSTS (1999 DOLLARS)	**$x1000**	**$/kW-yr**
Operating Labor	5,040	12.1
Maintenance Labor	4,680	11.2
Maintenance Materials	7,020	16.8
Administrative Support and Labor	2,430	5.8
TOTAL OPERATION & MAINTENANCE	$ 19,170	46.0
FIXED O & M	29.14 $/kW-yr	
VARIABLE O & M	0.23 c/kWh	

CONSUMABLE OPERATING COSTS less Fuel (1999 DOLLARS)	**$x1000**	**c/kWh**
Water	1962	0.05
Chemicals	2960	0.08
Other Consumables	239	0.01
Waste Disposal	3904	0.11
TOTAL CONSUMABLE OPERATING COST	$ 9,065	0.25
FUEL COST (1999 Dollars)	$ 32,926	1.06

PRODUCTION COST SUMMARY	Levelized (Over Book Life $)	**c/kWh**
Fixed O&M		0.39
Variable O&M		0.23
Consumables		0.25
By-product Credit		0
Fuel		1.06
TOTAL PRODUCTION COST		1.93
LEVELIZED CARRYING CHARGES (Capital)		2.68
LEVELIZED (Over Book Life) BUSBAR COST OF POWER		4.61

Table 4.5.6 - Capital Investment and Revenue Requirement Summary: O_2-fired Plant

Case:	Oxygen Fired Subcritical PC Plant		
Plant size:	326 MW net	**Net Cycle Efficiency:**	29.90%
Primary/Secondary Fuel (type):	Illinois #6	**Net Plant Heat Rate (NPHR):**	11,411 (Btu/kWh)
Design/Construction:	4 (years)	**Cost:**	1.14 ($/MMBtu)
TPC (Plant Cost) Year:	2004 (July)	**Book Life:**	20 (years)
Capacity Factor:	85% (%)	**TPI Year:**	2004 (July)
		CO2 Removed:	3,652,640 (tons/year)

CAPITAL INVESTMENT		**$x1000**	**$/kW**
Process Capital and Facilities		667,764	2,048.4
Engineering Adder (Incl. C.M., H.O., and Fee)		9,316	28.6
Process Contingency Adder		-	-
Project Contingency Adder		11,594	35.6
TOTAL PLANT COST (TPC)		$ 688,674	2,112.5
TOTAL CASH EXPENDED	$ 688,674		
AFDC	$ 68,867		
TOTAL PLANT INVESTMENT (TPI)		$ 757,541	
Royalty Allowance			
Preproduction Cost		$18,268	
Inventory Capital		$3,718	
Initial Chemicals and Catalysts (w/equip)			
Land Cost		$600	
TOTAL CAPITAL REQUIREMENT (TCR)		$ 780,128	

OPERATING & MAINTENANCE COSTS (1999 DOLLARS)	**$x1000**	**$/kW-yr**
Operating Labor	5,400	16.6
Maintenance Labor	5,509	16.9
Maintenance Materials	8,264	25.3
Administrative Support and Labor	2,727	8.4
TOTAL OPERATION & MAINTENANCE	$ 21,901	67.2
FIXED O & M	41.83 $/kW-yr	
VARIABLE O & M	0.34 c/kWh	

CONSUMABLE OPERATING COSTS less Fuel (1999 DOLLARS)	**$x1000**	**c/kWh**
Water	2005	0.07
Chemicals	1301	0.05
Other Consumables	239	0.01
Waste Disposal	1360	0.05
TOTAL CONSUMABLE OPERATING COST	$ 4,905	0.17

FUEL COST (1999 Dollars)	$ 31,578	1.30

PRODUCTION COST SUMMARY	Levelized (Over Book Life $) **$/tonne CO2 avoided**	**c/kWh**
Fixed O&M	2.03	0.56
Variable O&M	1.36	0.34
Consumables	(0.91)	0.17
By-product Credit	-	-
Fuel	2.86	1.30
TOTAL PRODUCTION COST	5.34	2.37
LEVELIZED CARRYING CHARGES (Capital)	16.08	4.03
LEVELIZED (Over Book Life) BUSBAR COST OF POWER	21.42	6.41

Figure 4.5.1- Comparison of Levelized Cost of Electricity Among Alternative Technologies (O_2 PC with 65% CF)

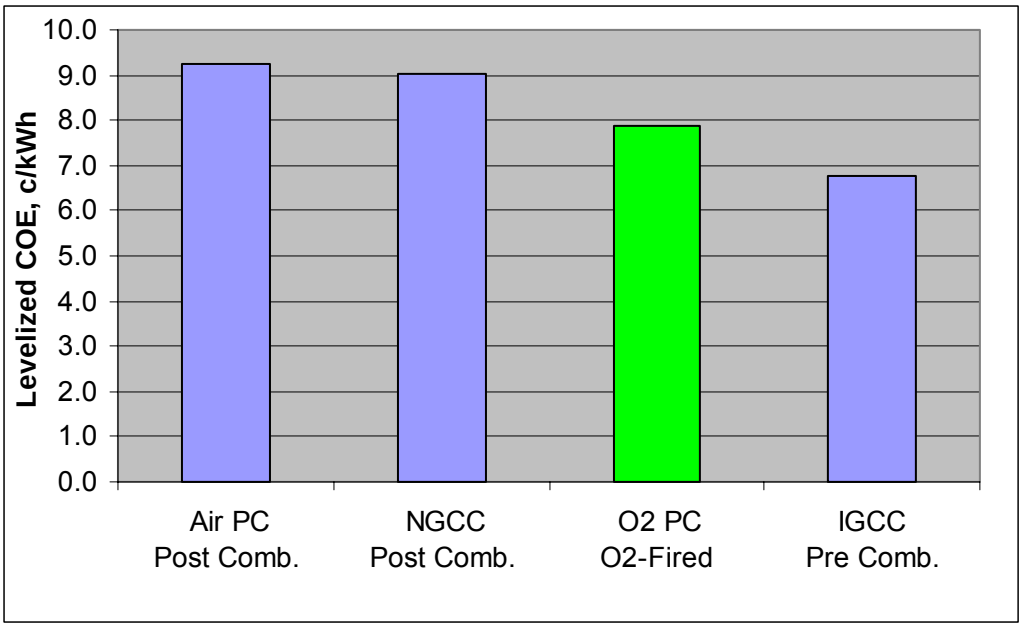

Figure 4.5.2 - Comparison of Mitigation Costs Among Alternative Technologies (O_2 PC with 65% CF)

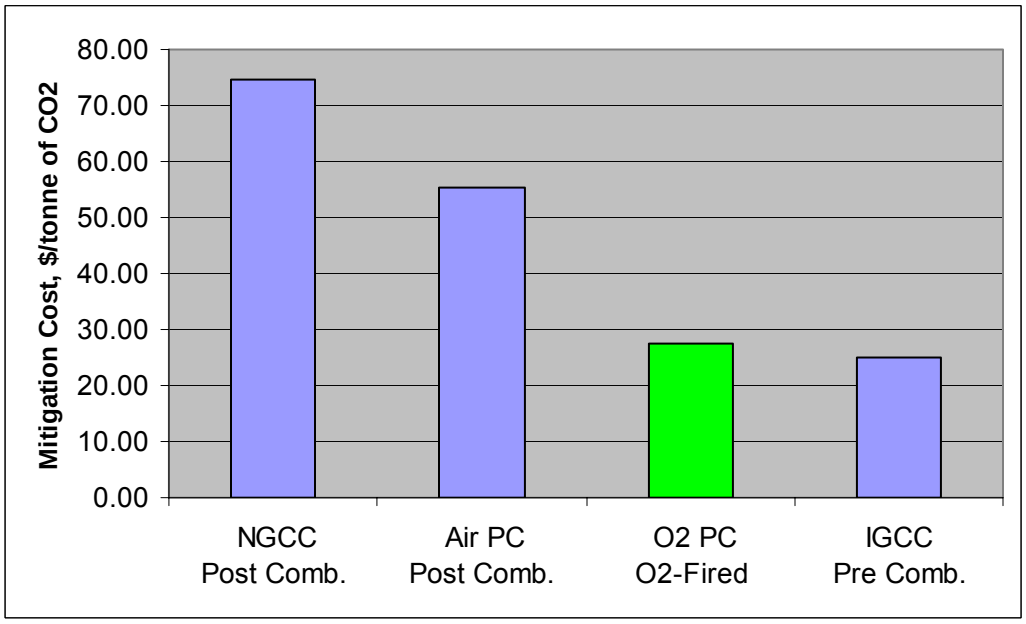

Figure 4.5.3 - Comparison of Levelized Cost of Electricity Among Alternative Technologies (O_2 PC with 85% CF)

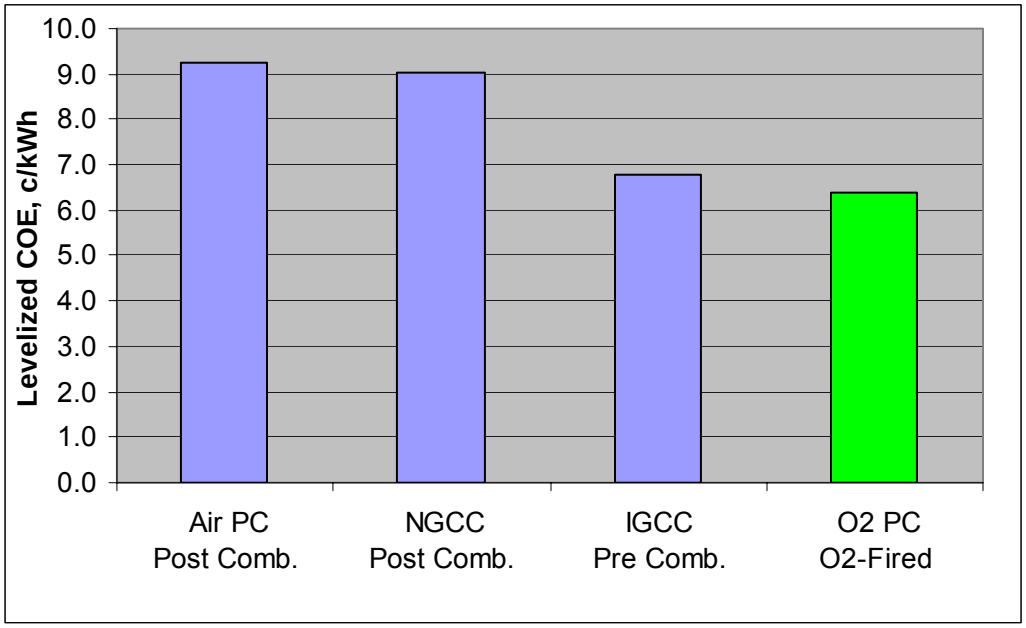

Figure 4.5.4 - Comparison of Mitigation Costs Among Alternative Technologies (O_2 PC with 85% CF)

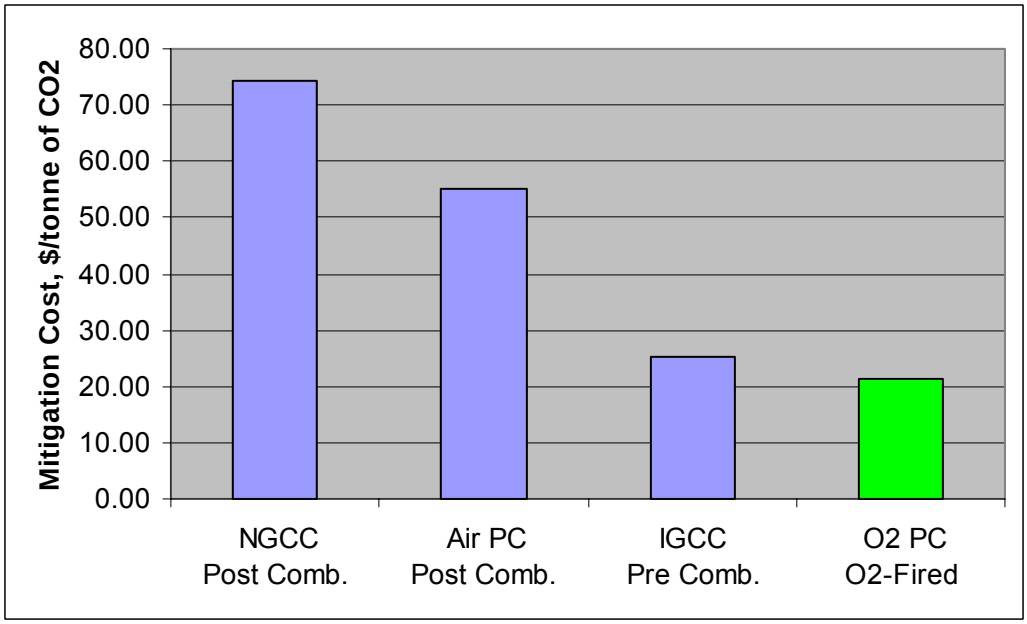

5.0 Conclusion

To assure continued U.S. power generation from its abundant domestic coal resources, new coal combustion technologies must be developed to meet future emissions standards, especially CO_2 sequestration. Current conventional coal-fired boiler plants burn coal using 15-20% excess air producing a flue gas, which is only approximately 15% CO_2. Consequently, CO_2 sequestration requires non-condensable gases stripping, which is both expensive and highly power-consumptive. Several different technologies for concentrating the CO_2 by removing the non-condensable gases have been proposed including amine-based absorption and membrane gas absorption. However, these techniques require substantial energy, typically from low-pressure steam.

A new boiler is presented where the combustion air is separated into O_2 and N_2 and the boiler uses the O_2, mixed with recycled flue gas, to combust the coal. The products of combustion are thus only CO_2 and water vapor. The water vapor is easily condensed, yielding a pure CO_2 stream ready for sequestration. The CO_2 effluent is in a liquid form and is piped from the plant to the sequestration site. The combustion facility is thus truly a zero emission stackless plant.

The efficiency and cost-effectiveness of carbon sequestration in oxygen-firing boilers can rival competing gasification plants by specifically tailoring boiler design by appropriate surface location, combustion system design, material selection, furnace layout, and water/steam circuitry. Boiler efficiencies of near 100% can be achieved by recovery of virtually all of the flue gas exhaust sensible and latent heat. Boiler size can be substantially reduced due to higher radiative properties of O_2-combustion versus air-combustion. Furthermore, a wider range of fuels can be burned due to the high oxygen content of the combustion gas and potential for high coal preheat.

A review of the published literature indicates that:

1.) It is possible to design a pulverized coal burner to operate with an oxygen-carbon dioxide gas mixture rather than air; a properly designed O_2 burner can yield flame temperatures and thermal profiles similar to those of an air–fired boiler while also providing improved flame stability, combustion efficiency; and NOx emissions.

2.) Plant conceptual designs and cost estimates, although differing in absolute values, indicate an O_2 combustion based plant are technically feasible and, when compared to alternative existing technologies, appear to be the lowest cost way of providing a concentrated CO_2 stream for sequestration. It is also expected that when for a new plant, O_2 combustion will result in a more compact, less expensive boiler. Depending upon the SO_2 and NOx levels that

can be recirculated back to the boiler, as well as tolerated at the sequestration site, O_2 can possibly result in reduced flue gas cleanup costs.

3.) Even though O_2 combustion is projected to be the least expensive way of providing a concentrated CO_2 stream for sequestration, significant increases in plant heat rates and costs will be experienced.

4.) Since O_2 combustion eliminates the need for large, back end amine based scrubbers and, in essence, saves the boiler, it is especially attractive for retrofit applications.

5.) O_2 based PC plants will require large amounts of oxygen and cryogenic air separation presently appears best suited for this application. Cryogenic units, however, are expensive and consume substantial amounts of power. It is noted that ceramic oxygen transport membranes are under development that are projected to be a lower cost, lower power consuming way to produce large quantities of oxygen. When commercial, these membranes should improve the performance and reduce the costs of the O_2 based plant.

A conceptual design of a CO_2 sequestration-ready oxygen-based 460 MWe (gross) PC boiler plant was developed. The selected O_2-fired design case has a system efficiency of 30.6% compared to the air-fired system efficiency of 36.7%. The design O_2-fired case requires T91 waterwall material and has a waterwall surface area of only 65% of the air-fired reference case.

A design and analysis of the Low NOx wall-fired burners for the proposed oxygen-fired boiler were performed. Burner designs were performed for 56% and 65% flue gas recycle for both 0% OFG and 20% OFG.

To achieve proper burnout (> 70% by the center of the furnace) and stable ignition, a primary gas swirl ratio of 0.5 was required for all four burner designs. To achieve optimal performance the following wall-fired burner design conditions were selected as optimal:

1. Primary gas exit conditions are an axial velocity of 100 ft/sec with a tangential swirl ratio of 0.5 to achieve proper burnout and stable ignition.

2. A low velocity (60-70 ft/sec) inner secondary gas exit velocity for combustion air staging to minimize NOx formation.

3. Outer secondary gas exit conditions are an axial velocity of 120-135 ft/sec with a tangential swirl ratio of 1.0 to induce hot flue gas recirculation to the flame ignition point.

A design and analysis of the reference air-fired boiler and the proposed oxygen-fired boiler were performed. The following conclusions are made comparing the air-fired furnace with the oxygen-fired furnace design and performance:

1. The oxygen furnace has only approximately 65% of the surface area and approximately 45% of the volume of the air-fired furnace due to the higher heat flux of the oxygen-fired furnace.

2. Due to the higher O_2 concentration of the oxygen-fired furnace versus the air-fired furnace (42% vs. 21%), the maximum flame temperature of the oxygen-fired furnace is approximately 500°F higher.

3. Maximum wall heat flux in the oxygen-fired furnace is more than double that of the air-fired furnace (165,000 Btu/hr-ft^2 vs. 75,000 Btu/hr-ft^2) due to the higher flame temperature and higher H_2O and CO_2 concentrations.

4. 100% coal burnout is achieved in the oxygen-fired furnace (compared to 99.7% burnout in the air-fired furnace) due to higher furnace temperature and higher concentration of oxygen. The burnout differential between the oxygen-fired boiler and the air-fired boiler is expected to be significantly greater when harder to burn fuels are fired.

5. The higher heat flux of the oxygen-fired furnace significantly increases the maximum waterwall temperature (from 800°F for the air-fired furnace to 935°F for the oxygen-fired furnace) requiring the material to be upgraded from carbon steel to T91.

6. The average NOx at the air-fired furnace outlet is reduced by 30% by injecting 20% OFA and by 45% by injecting 30% OFA. The average NOx at the oxygen-fired furnace outlet is reduced by 23% by injecting 20% OFG. Since it is unclear how much NOx can be tolerated by the oxygen-fired furnace liquid CO_2 piping system and sequestration site, the maximum permissible NOx of the oxygen-fired furnace is unknown.

7. The total heat transfer surface required in the oxygen-fired heat recovery area (HRA) is 25% less than the air-fired HRA due to more heat being absorbed in the oxygen-fired furnace and the greater molecular weight of the oxygen-fired flue gas.

8. The required HRA tube materials and wall thickness are virtually the same for the air-fired and oxygen-fired design since the flue gas and water/steam temperature profiles encountered by the heat transfer banks are very similar.

The levelized cost of electricity (COE) was calculated to be 4.61 ¢/kWh for the reference air-fired plant and to be 6.41¢/kWh for the O_2 PC plant. The CO_2 mitigation cost (MC) of the O_2-PC plant was calculated at 21.4 $/tonne.

Compared to the COE of the O_2 PC, the COE for the other technologies is 45% higher for Air PC, 40% higher for NGCC, and 6% higher for IGCC. Compared to the MC of the O_2 PC, the MC for the other technologies is 250% higher for NGCC, 160% higher for Air PC, and 17% higher for IGCC.

It is expected that the COE and MC of the O_2 PC will be reduced by the incorporation of new lower power-consuming air separation techniques, such as membrane separation and more advanced steam cycles such as supercritical and ultra-supercritical. In DOE contract, DE-FC26-04NT42207, FW will conduct a study to improve the efficiency and cost-effectiveness of the O_2-based PC power plant through the incorporation of a high-temperature supercritical steam cycle and advanced O_2 separation techniques.

Thus CO_2 sequestration with an oxygen-fired combustion plant can be performed in a proven reliable technology while maintaining a low-cost high-efficiency power plant. Of the CO_2 sequestration-ready technologies, the O_2-fired PC is the simplest, requires the least modification of existing proven designs, and requires no special chemicals for CO_2 separation. As new lower power-consuming air separation techniques, such as membrane separation, become commercially available for large-scale operation in O_2-fired plants, the CO_2 removal power consumption and efficiency reduction will continue to decline.

6.0 References

1. International Energy Agency Greenhouse Gas R&D Programme Web Site.

2. International Energy Agency, "Key world Energy Statistics", 2003.

3. Energy Information Administration of the U.S. Department of Energy, "Annual Energy Outlook 2004", January 2004.

4. Smith, D. and Danish, K., "The Heat is On", Public Utilities Fortnightly, January 2004.

5. Bradley, J., et. al., "NOx Reduction From A 125 MW Wall-Fired Boiler Utilizing Oxygen Enhanced Combustion", 29th International Technical Conference on Coal Utilization and Fuel Systems, April 18-22, 2004, Clearwater, FL.

6. Haeyang, P., et. al., "Bench Scale Experiment of Pure Oxygen Pulverized Coal Combustion in High Temperature", 9th Asian Pacific Conference on Chemical Engineering Congress, September 29, 2002, Christchurch, New Zealand.

7. Douglas, M., et. al., "Oxy-Fuel Combustion At The CANMET Vertical Combustor Research Facility", 1st National Conference on Carbon Sequestration, May 15-17, 2001,Washington, DC.

8. Thambimuthu, K. and Croiset, E., "Enriched Oxygen Coal-Fired Combustion", Advanced Coal-Based Power and Environmental Systems Conference, July 21-23, 1998, Morgantown, W. VA.

9. Varagani, R., et. al., "Oxycombustion in Pulverized Coal-Fired Boiler; A Promising Technology for CO_2 Capture", Third Annual Conference on Carbon Sequestration, May 3-6, 2004, Alexandria, VA.

10. "Greenhouse Gas Emissions from Power Stations", International Energy Agency Greenhouse Gas R&D Programme, Report No. ISBN 1 898373 10 8, June 1993.

11. "Carbon Dioxide Capture from Power Stations", International Energy Agency Greenhouse Gas R&D Programme, Report No. ISBN 1 898373 15G, February, 1994.

12. White, J.S., Buchanan, T.L., Schoff, R.L. (Parsons); Stiegel, G. (DOE); Holt, N.A., Booras G. (EPRI); Wolk, R. (WITS), "Evaluation of Innovative

Fossil Fuel Power Plants with CO_2 Removal", EPRI, Palo Alto, CA, U,S. Department of Energy—Office of Fossil Energy, Germantown, MD and U.S. Department of Energy/NETL, Pittsburgh, PA EPRI Report No. 1000316, December 2000.

13. Amick, A. et. al., "An Advanced IGCC Coal Power Plant", Twentieth Annual International Pittsburgh Coal Conference, Pittsburgh PA., September 15-19, 2001.

14. Holt, N. et. al., "Summary of Recent IGCC Studies of CO_2 Capture for Sequestration", Gasification Technologies 2003, San Francisco CA., October12-15, 2003.

15. Steigel, G., et. al., "DOE's Gasification Industry Interviews: Survey of Market Trends, Issues, and R&D Needs", Gasification Technologies 2001, San Francisco, CA, October 7-10, 2001.

16. Nsakala, Y., et. al., "Engineering Feasibility of CO_2 Capture On An Existing US Coal-Fired Power Plant", First National Conference on Carbon Sequestration, May 15-17, 2001, Washington, DC.

17. Simbeck, D., "Overview and Insights on the Three Basic CO2 Capture Options", Third Annual Conference on Carbon Sequestration, May 3-6, 2004, Alexandria, VA.

18. Armstrong, P., et. al., "ITM Oxygen: An Enabler for IGCC", Gasification Technologies 2003, San Francisco CA., October12-15, 2003.

19. Prasad, R., et. al., "Oxygen Transport Membranes for Future IGCC Power Plants", Twentieth Annual International Pittsburgh Coal Conference, Pittsburgh PA., September 15-19, 2001.

20. Wilkinson, M.,Boden, John (BP), Panesar, R. (Mitsui Babcock), Allam, R. (Air Products), "CO_2 Capture Via Oxygen Firing: Optimisation of a Retrofit Design Concept for a Refinery Power Station Boiler", First National Conference on Carbon Sequestration, May 15-17, 2001, Washington DC.

21. FW-FIRE, Fossil-fuel Water-walled Furnace Integrated Reaction Emission, Theory and User's Manual, Foster Wheeler Development Corp., 11/30/99.

22. HEATEX Computer Program, "A Program to Determine the Thermal/Hydraulic Performance of Gas-Cooled Heat Exchangers", Revision 24, Foster Wheeler Corporation.

23. EMISS Computer Program, “A Program to Determine Gaseous Emissivity”, Foster Wheeler Corporation.

24. Schoff, R.L., White, J.S., Buchanan, T.L. (Parsons); Holt, N.A., Booras G. (EPRI); Wolk, R. (WITS), “Updated Cost and Performance Estimates For Fossil Fuel Power Plants with CO_2 Removal”, EPRI, Palo Alto, CA, U.S. Department of Energy – Office of Fossil Energy, Germantown, MD and U.S. Department of Energy/NETL, Pittsburgh, PA: 2002. 1004483.

25. Gerard N. Choi, et al., “Cost Efficient Amine Plant Design for Post Combustion CO_2 Capture from Power Plant Flue Gas”, DOE/NETL 3rd Annual Conference on Carbon Sequestration, Alexandria, VA, May 3-6, 2004.

26. Energy Information Administration/Electric Power Monthly, October 2004.

7.0 Bibliography

N/A

8.0 List of Acronyms and Abbreviations

A	Absorptivity
σ	Stefan-Boltzmann constant
ε	Emissivity
ACI	Activated Carbon Injection
ASU	Air separation unit
CF	Capacity Factor
CFD	Computational fluid dynamics
CO_2	Carbon Dioxide
COE	Cost or Electricity
E	Emission of CO_2
EIA	Energy Information Agency
EOR	Enhanced Oil Recovery
EPRI	Electric Power Research Institute
ESP	Electrostatic Precipitator
FD	Forced draft
FEGT	Furnace exit gas temperature
FGD	Flue Gas Desulfurization
FW	Foster Wheeler
FW-FIRE	Fossil fuel, Water-walled Furnace Integrated Reaction and Emission Simulation
GE	General Electric Company
H_2S	Hydrogen Sulfide
HHV	Higher heating value
HRA	Heat recovery area
HRSG	Heat Recovery Steam Generator
ID	Induced draft
IEA	International Energy Agency
IGCC	Integrated Coal Gasification Combined Cycle
ITM	Ion Transport Membrane
LCC	Levelized Carrying Charge
LCM	Levelized Consumables
LFC	Levelized Fuel Costs
LFOM	Levelized Fixed O&M
LHV	Lower heating value
LOI	Loss on ignition
LSD	Limestone Spray Dryer
LVOM	Levelized Variable O&M
MC	Mitigation Cost (CO_2)
MEA	Monoethanolamine
N_2	Nitrogen
NGCC	Natural Gas Combined Cycle
NOx	Nitrogen oxides
O&M	Operation and Maintenance

O_2	Oxygen
OEC	Oxygen Enhanced Combustion
OFA	Over-fired air
OFG	Over-fire gas
OTM	Oxygen Transport Membrane
PA	Primary Air
PG	Primary Gas
PC	Pulverized coal
PDF	Probability density function
ppmv	Parts Per Million by Volume
PRB	Powder River Basin
Q/A	Heat Flux
SC	Super Critical Pressure
SCR	Selective catalytic reactor
SO_2	Sulfur Dioxide
SOx	Oxides of Sulfur
T	Temperature
TCR	Total Capital Requirement
TEG	Triethyleneglycol
TPC	Total Plant Cost
TPI	Total Plant Investment
U	Heat transfer coefficient
U.S.	United States
UBC	Unburned carbon loss
USC	Ultra Super Critical Pressure